UNIVERSITÉ DU QUÉBEC

THÈSE PRÉSENTÉE À
L'UNIVERSITÉ DU QUÉBEC À TROIS-RIVIÈRES

COMME EXIGENCE PARTIELLE
DU DOCTORAT EN PSYCHOLOGIE

PAR
IAN MASSÉ

LES CONNEXIONS DES CORTEX SENSORIELS PRIMAIRES POUR LE TRAITEMENT CONTEXTUEL ET MULTISENSORIEL DE L'INFORMATION

AOUT 2017

Université du Québec à Trois-Rivières

Service de la bibliothèque

Avertissement

L'auteur de ce mémoire ou de cette thèse a autorisé l'Université du Québec à Trois-Rivières à diffuser, à des fins non lucratives, une copie de son mémoire ou de sa thèse.

Cette diffusion n'entraîne pas une renonciation de la part de l'auteur à ses droits de propriété intellectuelle, incluant le droit d'auteur, sur ce mémoire ou cette thèse. Notamment, la reproduction ou la publication de la totalité ou d'une partie importante de ce mémoire ou de cette thèse requiert son autorisation.

UNIVERSITÉ DU QUÉBEC À TROIS-RIVIÈRES

Cette thèse a été dirigée par :

Gilles Bronchti, directeur de recherche, Ph.D.	Université du Québec à Trois-Rivières
Denis Boire, codirecteur de recherche, Ph.D.	Université du Québec à Trois-Rivières

Jury d'évaluation de la thèse :

Gilles Bronchti, Ph.D.	Université du Québec à Trois-Rivières
Johannes Frasnelli, Ph.D.	Université du Québec à Trois-Rivières
Mathieu Piché, Ph.D.	Université du Québec à Trois-Rivières
Patrice Voss, Ph.D.	Université McGill

Thèse soutenue le 21/04/2017

Ce document est rédigé sous la forme d'articles scientifiques, tel qu'il est stipulé dans les règlements des études de cycles supérieurs (Article 138) de l'Université du Québec à Trois-Rivières. Les articles ont été rédigés selon les normes de publication de revues reconnues et approuvées par le Comité d'études de cycles supérieurs en psychologie. Le nom du directeur de recherche pourrait donc apparaitre comme co-auteur de l'article soumis pour publication.

Sommaire

Notre perception de l'environnement dépend des interactions entre les différentes modalités sensorielles. Ces interactions sont possibles entre les cinq sens traditionnellement reconnus : la vision, l'audition, le toucher, l'odorat et le goût. Le cortex cérébral, qui est un ensemble d'aires corticales interreliées par un réseau de connexions, traite les informations provenant de chacun des sens. L'information sensorielle est acheminée à partir des voies ascendantes, depuis les récepteurs spécialisés, à des cortex sensoriels dédiés à des modalités spécifiques : le cortex visuel, somatosensoriel et auditif. L'information sensorielle est par la suite acheminée aux aires associatives qui assurent un traitement plus complexe de l'information. Bien que les interactions multisensorielles aient été clairement démontrées dans les aires corticales associatives multisensorielles du cortex temporal supérieur, pariétal et frontal, de nombreuses études chez les humains, les primates et les rongeurs ont démontré que les cortex sensoriels primaires sont également impliqués dans les interactions multisensorielles. Les informations des autres modalités sensorielles peuvent atteindre les cortex sensoriels primaires à partir de trois sources : les voies descendantes provenant des aires corticales associatives multisensorielles, les connexions thalamocorticales provenant du thalamus et les connexions corticocorticales directes entre les cortex sensoriels primaires. Par conséquent, le concept des cortex sensoriels primaires purement unisensoriels ne peut être maintenu.

Le traitement effectué dans les cortex sensoriels primaires inclurait donc l'information sensorielle provenant des autres modalités, et l'information associative et motrice. Leur position au premier niveau dans la hiérarchie corticale du traitement de l'information sensorielle et à l'interface entre les voies sensorielles ascendantes provenant du thalamus et les voies descendantes provenant des aires corticales associatives multisensorielles suggérerait que les cortex sensoriels primaires ont un rôle clé dans le traitement de l'information axé sur le stimulus et le traitement de l'information axé sur la tâche. Pour comprendre comment ces aires contribuent au traitement de l'information sensorielle, associative et motrice, il est important de connaitre l'ensemble des afférences des cortex sensoriels primaires, tant corticales que sous-corticales. Des études démontrent l'étendue des afférences corticales et sous-corticales vers le cortex visuel primaire et le cortex auditif primaire afin d'avoir un inventaire complet des projections vers ces cortex. Un tel inventaire a été réalisé pour le cortex somatosensoriel primaire. Un projet de grande envergure a cartographié le connectôme des afférences et des efférences du cortex somatosensoriel primaire de la souris. Cette analyse des projections du cortex somatosensoriel primaire est cependant qualitative et ne fournit pas d'informations sur leur distribution laminaire et leur poids relatif, qui sont des caractéristiques importantes de la connectivité corticale. L'évaluation quantitative de la distribution laminaire des neurones permet la classification des projections en tant que « *feedforward* », « *feedback* » ou latérale. Notre premier objectif était donc de faire l'évaluation quantitative des afférences du cortex somatosensoriel primaire de la souris.

Les résultats de notre première étude démontrent que le cortex somatosensoriel primaire de la souris possède des connexions avec les cortex moteurs, les aires corticales associatives et des noyaux thalamiques propices aux interactions multisensorielles. Ces résultats confirment que les cortex sensoriels primaires ne sont pas seulement limités au traitement unisensoriel et incluent l'information sensorielle provenant des autres modalités. Un résultat important est la démonstration que la partie caudale du champ de tonneaux du cortex somatosensoriel primaire possède plus de connexions qui ciblent des aires corticales et sous-corticales sensorielles propices à l'exploration. Ces aires incluent des aires visuelles, auditives, olfactives et associatives, dont le cortex auditif et visuel, en plus du cortex perirhinal et ectorhinal qui sont impliqué dans le traitement sensoriel. Certaines régions sous-corticales sont également impliquées, telles que le noyau thalamique ventral latéral qui module les processus nociceptifs. En comparaison, les connexions de la partie rostrale du champ de tonneaux et de la partie du cortex somatosensoriel primaire à l'extérieur du champ de tonneaux ciblent davantage des aires somatosensorielles et motrices. S1 reçoit aussi des afférences de plusieurs sources différentes par le biais des voies descendantes. De plus, la distribution laminaire des neurones rétrogradement marqués suggère que S1 chez la souris, reçoit des projections de type *feedback* de ces aires. Ces différentes aires pourraient avoir un rôle de modulation, mais à différent degré étant donné que les indices laminaires, même si dans l'ensemble négatifs, l'étaient à différents degrés. Ces projections de type *feedback* pourraient moduler l'information dans le cortex somatosensoriel primaire, de sorte que les signaux ascendants deviennent consciemment accessibles. En effet, S1 aurait un rôle

clé dans le codage prédictif qui est le processus d'appariement du système nerveux entre l'information sensorielle des stimuli tactiles acheminée par les signaux ascendants et les attentes envers l'environnement généré à l'interne par les signaux descendants. Le champ de tonneaux comprend une représentation corticale des vibrisses chez les rongeurs. Les vibrisses servent à l'exploration. Chez l'humain, la représentation des mains occupe une grande surface du cortex somatosensoriel et est aussi surreprésentée que les vibrisses dans le cortex. L'interaction des vibrisses avec la vision serait importante dans la représentation de l'espace péripersonnel, soit l'espace à la portée de n'importe quel membre d'un individu. Chez l'humain, cet espace est centré sur les mains tandis que chez les rongeurs, cet espace serait centré sur les vibrisses. Des connexions corticocorticales directes entre le champ de tonneaux et le cortex visuel primaire seraient avantageuses pour favoriser des interactions multisensorielles rapides. Une étude plus poussée de la structure de ces connexions permettrait de mieux comprendre comment ces deux modalités sensorielles s'influencent mutuellement au niveau des cortex sensoriels primaires. L'étude de la morphologie des axones et de leurs terminaux permettrait aussi d'en apprendre davantage sur leurs fonctions. Notre deuxième objectif était donc d'étudier la microcircuiterie des connexions corticocorticales directes et réciproques entre les cortex visuel et somatosensoriel primaires de la souris. Chez les primates, très peu de neurones projettent directement d'un cortex sensoriel primaire vers un autre. Cependant, les projections directes entre les cortex sensoriels primaires sont abondantes chez les rongeurs. La souris est donc un meilleur modèle pour l'étude des connexions corticocorticales directes entre les cortex sensoriels primaires.

Les résultats de notre deuxième étude démontrent que la projection du champ de tonneaux vers le cortex visuel primaire est de type *feedback* et aurait une influence modulatrice prédominante alors que la projection réciproque est de type latéral et aurait plutôt une influence inductrice. Ce résultat est important, car il démontre que ces connexions corticocorticales entre deux cortex sensoriels primaires, bien que réciproques, ne sont certainement pas symétriques. De plus, la présence de gros boutons terminaux dans le champ de tonneaux du cortex somatosensoriel primaire et leur absence dans le cortex visuel primaire suggère que chez la souris, la vision aurait une influence inductrice sur l'exploration tactile et l'information tactile aurait une influence modulatrice prédominante sur l'information visuelle. Ces deux modalités sensorielles ne s'influencent donc pas mutuellement de la même manière au niveau des cortex sensoriels primaires. À la lumière de ces résultats, nous nous sommes interrogés sur l'influence de l'expérience visuelle pendant la période de vie postnatale sur le développement des connexions corticocorticales entre les cortex visuel et somatosensoriel primaires. L'activité provenant des récepteurs sensoriels peut considérablement influencer le développement de la connectivité corticale. La plasticité intermodale implique des changements anatomiques importants dans le néocortex, mais les effets de la cécité sur les connexions corticocorticales entre les cortex sensoriels primaires ne sont pas encore bien documentés. Plusieurs études ont démontré chez des modèles de cécité animale énucléée que le cortex visuel reçoit des afférences auditives et somatosensorielles, mais peu d'études se sont consacrées aux efférences du cortex visuel vers les aires des autres modalités sensorielles. Une étude plus poussée de la structure

des connexions entre les cortex visuel et somatosensoriel primaires permettrait de mieux comprendre comment les connexions entre deux cortex sensoriels primaires sont altérées par la perte d'un sens. Notre troisième objectif était donc d'étudier l'impact de la perte de la vision sur la microcircuiterie de ces connexions à l'aide d'un échantillon de souris énucléées à la naissance. Enfin, la discussion générale est consacrée à la signification de nos résultats dans le contexte des connaissances actuelles sur les interactions multisensorielles, la hiérarchie des sens et nous spéculons sur leurs implications cliniques en termes de la recherche sur les prothèses.

Mots clés : microcircuiterie, neuroanatomie, connectivité, cortex visuel primaire, cortex somatosensoriel primaire, champ de tonneaux, afférence, efférence, interaction multisensorielle, convergence multisensorielle, vision, acuité tactile, perception sensorielle, morphologie, cécité.

Table des matières

Sommaire iv

Liste des tableaux xvii

Liste des figures xix

Liste des symboles et abréviations xxiii

Remerciements xxvii

Introduction 1

Les voies sensorielles ascendantes et descendantes 2

L'apprentissage perceptif 5

Les connexions corticocorticales 6

La distribution laminaire des connexions corticocorticales 7

Le connectome et la connectomique 8

Les différentes échelles de connectome 8

Le modèle de recherche animal 9

Comparaison entre humain et rongeur 10

Le connectome du cerveau de souris 11

Les modules somatosensoriels de la souris 12

Objectif 1 : Projections afférentes corticales et sous-corticales du cortex somatosensoriel primaire de la souris 13

L'espace péripersonnel 14

Comparaison entre humain et rongeur 15

Les interactions multisensorielles 16

Les interactions visuotactiles 17

Les modes de transmission glutamatergique 18

Les réponses postsynaptiques de Classe 1 20

Les réponses postsynaptiques de Classe 2 21

Les corrélations anatomiques des réponses postsynaptiques 22

Les implications fonctionnelles des réponses postsynaptiques 23

Objectif 2 : Les connexions corticocorticales directes et réciproques entre le cortex visuel et somatosensoriel primaire de la souris 26

La cécité et les connexions corticocorticales 28

Les effets de la cécité sur les connexions corticales 29

Objectif 3 : Effets de l'énucléation sur les connexions corticocorticales directes et réciproques entre le cortex visuel et somatosensoriel primaire de la souris 30

Résumé des objectifs de recherche 31

Méthode 32

Souris C57Bl/6 énucléée à la naissance 33

Énucléation néonatale 34

Traçage neuronal 34

Transports antérograde et rétrograde 34

Sous-unité B de la toxine du choléra 37

Dextran-biotine aminé 39

Chapitre I. Cortical and subcortical afferent connections of the primary somatosensory cortex of the mouse 41

Abstract 43

Introduction 45

Methods 48

Animals and experiment groups 48

Tracing procedures 49

Perfusion 49

Staining procedures 50

Data analysis 51

Data comparison to the Mouse Connectome Project 52

Antibody characterization 53

Statistical analysis 53

Results 54

CTb labeling 54

Cortical projections to S1 57

Subcortical projections to S1 82

Discussion 92

Summary 92

Connectomes and modules in the somatosensory barrel field vs. non-barrel field 93

Multimodality of primary sensory cortices 98

Possible functions of non-somatosensory sensory and multisensory inputs to S1 100

Top-down cortical projections and conscious sensory perception in S1 101

Top-down and multisensory thalamocortical connections to S1 105

Conclusions 107

References 109

Chapitre II. Asymmetric direct reciprocal connections between primary visual and somatosensory cortices of the mouse 119

Abstract 121

Introduction 122

Methods 124

Tracing procedures 125

Charting of retrogradely labeled neurons 127

Single axon reconstructions 129

Stereological sampling of laminar distribution of axonal swellings 130

Sampling of axonal diameters 133

Statistical analysis 134

Results 135

Labeling of cortical visuotactile connections with CTb 135

Laminar distribution of Cholera toxin b labeled neurons 141

Anterograde BDA labeling of visuotactile connections 143

Single axon branching morphology 145

Axonal thickness 152

Number of anterogradely labeled axonal swellings 153

Laminar distribution of axonal swellings 156

Size distribution of axonal swellings in cortical layers 158

Discussion 160

Direct reciprocal projection between visual and somatosensory cortices 161

Hierarchical order of primary sensory cortices 162

Asymmetry of the strength of the reciprocal projections between V1 and S1BF 165

Size of axonal swellings 166

Single axon morphology 170

Conclusions 172

References 173

Chapitre III. Effects of enucleation on the direct reciprocal corticocortical connections between primary visual and somatosensory cortices of the mouse 180

Abstract 182

Introduction 184

Methods 186

Neonatal enucleation 186

Tracing procedures 187

Charting of retrogradely labeled neurons 189

Stereological sampling of laminar distribution of axonal swellings 191

Sampling of axonal diameters 197

Statistical analysis 199

Results 199

Labeling of cortical visuotactile connections with CTb 199

Laminar distribution of Cholera toxin b labeled neurons 206

Laminar distribution of axonal swellings 210

Size distribution of axonal swellings in cortical layers 212

Axonal thickness 215

Discussion 217

The effects of enucleation on V1 afferent projections 217

The effects of enucleation on the structure of the projections between V1 and S1 221

The effects of enucleation on the thickness of axons and size axonal swellings 221

Conclusions 225

References 226

Discussion 236

Objectif 1 : Projections afférentes corticales et sous-corticales du cortex somatosensoriel primaire de la souris 238

La multimodalité du cortex somatosensoriel primaire 240

Les voies les plus rapides vers S1 242

Les voies descendantes des aires associatives vers S1 243

Spécificité des espèces aux niveaux des connexions entre aires primaires : rongeurs vs non-rongeurs 244

Objectif 2 : Les connexions corticocorticales directes et réciproques entre le cortex visuel et somatosensoriel primaire de la souris 245

La position hiérarchique des cortex sensoriels primaires 246

L'asymétrie du poids des projections 248

L'asymétrie de la taille des boutons terminaux 248

L'asymétrie du diamètre des axones 249

L'hypothèse de la précision des modalités sensorielles 250

Les prothèses 252

Les interfaces humain-robot 255

Objectif 3 : Effets de l'énucléation sur les connexions corticocorticales directes et réciproques entre le cortex visuel et somatosensoriel primaire de la souris 257

Les effets de la cécité sur le poids des projections 259

Les effets de la cécité sur la nature des projections 261

Les effets de la cécité sur la taille des boutons et des axones 263

Conclusion 267

Références générales 273

Liste des tableaux

Tableau

1 Résumé des caractéristiques anatomiques et synaptiques 19

2 List of our cases that received CTb injections in the primary somatosensory cortex (S1) outside the barrel field, in the rostral (rS1BF) and caudal (cS1Bf) barrel field and the cases used from the MCP corticocortical connectivity atlas that received CTb or Fluorogold (FG) injections in the primary somatosensory barrel field (SSp-bfd), lower limb (SSp-ll), and upper limb (SSp-ul) areas 60

3 Number and percentage (in parentheses) of retrogradely labeled neurons in sensory and non-sensory cortical areas in the ipsilateral hemisphere after injections of CTb into the primary somatosensory cortex (S1) of intact C57Bl/6 mice 61

4 Number and percentage (in parentheses) of retrogradely labeled neurons in sensory and non-sensory cortical areas in the contralateral hemisphere after injections of CTb into the primary somatosensory cortex (S1) of intact C57Bl/6 mice 65

5 Numbers of retrogradely labeled neurons in supragranular/infragranular layers and layer indices (below) in non-somatosensory sensory and non-sensory neocortical areas in the ipsilateral hemisphere after injections of CTb into S1, S1BF (rostral part) and S1BF (caudal part) of C57Bl/6 mice 73

6 Numbers of retrogradely labeled neurons in supragranular/infragranular layers and layer indices (below) in non-somatosensory sensory and non-sensory neocortical areas in the contralateral hemisphere after injections of CTb into S1, S1BF (rostral part) and S1BF (caudal part) of C57Bl/6 mice 76

7 Number and percentage (in parentheses) of retrogradely labeled neurons in sensory and non-sensory subcortical areas after injections of CTb into the primary somatosensory cortex (S1) of intact C57Bl/6 mice 84

8 Stereological sampling parameters for the estimation of the number of anterogradely labeled axonal swellings in each layers in S1BF after injections of BDA into V1 of C57Bl/6 mice 132

9 Sampling parameters for the estimation of the number of anterogradely labeled axons as they enter the gray matter in S1BF and V1 after injections of BDA into V1 and S1BF respectively of C57Bl/6 mice 134

Tableau

10 Numbers and percentage (in parentheses) of retrogradely labeled neurons in supragranular / granular / infragranular layers and layer indices (below) in S1, S1BF and V1 after injections of CTb into V1 and S1BF of C57Bl/6 mice 138

11 Stereological sampling parameters for the estimation of the number of anterogradely labeled axonal swellings in each layers in V1 after injections of BDA into S1BF of C57Bl/6 mice 155

12 Stereological sampling parameters for the estimation of the number of anterogradely labeled axonal swellings in each layers in S1BF after injections of BDA into V1 of intact C57Bl/6 mice 193

13 Stereological sampling parameters for the estimation of the number of anterogradely labeled axonal swellings in each layers in S1BF after injections of BDA into V1 of enucleated C57Bl/6 mice 194

14 Stereological sampling parameters for the estimation of the number of anterogradely labeled axonal swellings in each layers in V1 after injections of BDA into S1BF of intact C57Bl/6 mice 195

15 Stereological sampling parameters for the estimation of the number of anterogradely labeled axonal swellings in each layers in V1 after injections of BDA into S1BF of enucleated C57Bl/6 mice 196

16 Sampling parameters for the estimation of the diameter of anterogradely labeled axons as they enter the gray matter in S1BF and V1 after injections of BDA into V1 and S1BF respectively of intact and enucleated at birth C57Bl/6 mice 198

17 Number and percentage (in parentheses) of retrogradely labeled neurons in neocortical areas after injections of CTb into the primary visual cortex (V1) and the primary somatosensory cortex (S1) of intact and enucleated C57Bl/6 mice 203

18 Numbers of retrogradely labeled neurons in layers I-III/IV/V/VI and layer indices (below) in neocortical areas after injections of CTb into the primary visual cortex (V1) and the primary somatosensory cortex (S1) of intact and enucleated C57Bl/6 mice 208

19 Résumé des caractéristiques des projections entre V1 et S1 266

Liste des figures

Figure

1 Représentation schématique des voies sensorielles 4

2 L'apprentissage perceptif 5

3 Connexions feedforward, feedback et latérale d'après la distribution laminaire des neurones (Inspiré de Vezoli et al. 2004) 7

4 Vue latérale du cortex cérébral chez l'humain et le rat 9

5 Parallèles entre humains et rongeurs. Homoncule et souricule (Bear et al., 2007; Zembrzycki et al., 2013) 10

6 Les quatre modules de connectivités somatosensoriels de la souris tel que démontré sur la base des données disponibles dans le *Mouse Brain Connectome Project* (Zingg et al., 2014) 12

7 Parallèles entre humains et rongeurs. Espace péripersonnel (Cardinali et al., 2009; Rizzolatti et al., 1981b; Rizzolatti et al., 1981a) 16

8 Les boutons terminaux inducteurs et modulateurs 19

9 Connexions corticothalamiques 26

10 Transport axonal antérograde en rouge et transport axonal rétrograde en bleu 35

11 Tracer injection sites and distribution of retrogradely labeled neurons in the somatosensory thalamus 55

12 CTb-labeled neurons in the cortex after an injection into the posterior part of the barrel field of S1 55

13 Diagram of the afferent connections of the primary somatosensory cortex (S1) of the C57Bl/6 mouse 56

14 Percentage of retrogradely labeled neurons in cortical areas in the ipsilateral (A) and contralateral hemispheres (B) 70

15 Layer indices for neocortical areas in the ipsilateral (A) and contralateral hemispheres (B) 78

Figure

16 Layer indices matching between the ipsilateral hemisphere (X axis) and the contralateral hemisphere (Y axis) 80

17 Percentage of retrogradely labeled neurons (Y axis) depending on their distance (X axis) from one of the three different injection sites in S1 81

18 CTb-labeled neurons in the subcortex after an injection into the posterior part of the barrel field of S1. Scale: 250 µm 83

19 Percentage of retrogradely labeled neurons in different subcortical areas 89

20 Diagram showing the input ratios of different modalities into the primary somatosensory cortex of the C57Bl/6 mouse 91

21 A: An injection of CTb in V1 produced in B: Anterograde and retrograde labeling in S1BF. Note the more abundant retrogradely labeled neurons in layer 5 than in supragranular layers and the intense anterograde labeling in layers 2/3 and 5. C: An injection of CTb in S1BF produced in D: Retrogradely labeled neurons in supragranular and infragranular layers, a typical distribution of lateral connections 136

22 A: Number of retrogradely labeled neurons in cortical areas following an injection of CTb in V1 and S1BF of C57Bl/6 mice. B: Percentage of retrogradely labeled neurons in cortical areas following an injection of CTb in V1 and S1BF of C57Bl/6 mice. C: Layer indices for neocortical areas following an injection of CTb in V1 and S1BF of C57Bl/6 mice 140

23 A: An injection of BDA in S1BF produced in B: Anterograde labeling of axons in the supragranular and infragranular layers in V1. C: An injection of BDA in V1 produced in D: Anterograde labeling of axons in the supragranular and infragranular layers in S1BF 145

24 Single axons in S1BF following an injection of BDA in V1 of C57Bl/6J mice 148

25 Single axons in V1 following an injection of BDA in S1BF of C57Bl/6J mice 150

26 Size distribution of axonal diameters in S1BF (solid line) following BDA injections in V1 and in V1 following injections in S1BF (dotted line) 153

Figure

27 Laminar and size distribution of axonal swellings in S1BF and V1 following an injection of BDA in V1 cortex and S1BF respectively of C57Bl/6J mice from the sample of reconstructed single axons (A and C resp) and from the stereological sampling of these cortical areas following columnar BDA cortical injections (B and D resp)....157

28 A: An injection of CTb in V1 of intact C57Bl/6 mice produced in B: Anterograde and retrograde labeling in S1BF. C: An injection of CTb in V1 of enucleated C57Bl/6 mice produced in D: Anterograde and retrograde labeling in S1BF....200

29 A: An injection of CTb in S1BF of intact C57Bl/6 mice produced in B: Anterograde and retrograde labeling in V1. C: An injection of CTb in S1BF of enucleated C57Bl/6 mice produced in D: Anterograde and retrograde labeling in V1 200

30 A: Percentage of retrogradely labeled neurons in cortical areas following an injection of CTb in V1 and S1BF. Percentage of retrogradely labeled neurons in each cortical layer following an injection of CTb in V1 (B) and in S1BF (C).....205

31 Layer indices for neocortical areas following an injection of CTb in V1 and S1BF 206

32 High power photomicrographs of swellings in S1BF of intact and enucleated mice (A and B resp)....211

33 Laminar distribution of the number of axonal swellings in S1BF (A) and V1 (B) following and injection of BDA in V1 and S1BF respectively of intact and enucleated mice 212

34 Size distribution (A and C) and box plot representation (B and D) of axonal swelling size in S1BF (A and B) and V1 (C and D) following injections of BDA in V1 and S1BF respectively of intact and enucleated mice. The box plots depict the minimum and maximum values, the upper (Q3) and lower (Q1) quartiles and the median 214

35 Size distribution (A and B) and box plot representation (C) of the diameters of randomly sampled axons as they enter the gray matter in S1BF (A and C) and V1 (B and C) following an injection of BDA in V1 and S1BF respectively of intact and enucleated mice....216

36 Asymétrie fonctionnelle entre les cortex sensoriels primaires de la souris (Iurilli et al., 2012)....241

Figure

37 L'illusion de la main en caoutchouc (Botvinick & Cohen, 1998) 253

Liste des symboles et abréviations

A1	Cortex auditif primaire
AD	Noyau thalamique antérodorsal
AM	Noyau thalamique antéromédial
Amyg	Noyaux amygdalaires
Au	Cortex auditif
AuD	Cortex auditif, aire dorsale
AuV	Cortex auditif, aire ventrale
AV	Noyau thalamique antéroventral
B	Noyau basal de Meynert
Cg	Cortex cingulaire
CGLd	Corps géniculé latéral dorsal
CGM	Corps géniculé médial
CGMd	Corps géniculé médial dorsal
CGMm	Corps géniculé médio médial
CGMv	Corps géniculé médial ventral
CI	Collicule inférieur
Cl	Claustrum
CL	Noyau thalamique centrolatéral
CM	Noyau thalamique centromédian
CS	Collicule supérieur
CTb	Sous-unité B de la toxine du choléra

DAB	3,3-diaminobenzidine
DBA	Dextran-biotine aminé
E	Jour embryonnaire
Ect	Cortex ectorhinal
Ent	Cortex entorhinal
Fr2	Cortex agranulaire médial
HDB	Segment horizontal de la bande diagonale de Broca
Hyp	Hypothalamus
IAM	Noyau thalamique interantéromédial
iGluR	Récepteur glutamatergique ionotropique
Ins	Cortex insulaire
IRMf	Imagerie par résonance magnétique fonctionnelle
LD	Noyau thalamique latérodorsal
LP	Noyau latéral postérieur
LPO	Aire latérale préoptique
LSI	Noyau septal latéral, partie intermédiaire
M	Cortex moteur
Ml	Cortex moteur primaire
M2	Cortex moteur secondaire
Mam	Noyaux mamillaires
MDL	Noyau thalamique médiodorsal, partie latérale
mGluR	Récepteur glutamatergique métabotropique

NDS	Normal donkey serum
Orb	Cortex orbital
P	Jour postnatal
PC	Noyau thalamique paracentral
PF	Noyau thalamique parafasciculaire
Pir	Cortex piriforme
Pli	Noyau thalamique postérieur limitans
Po	Noyau postérieur
PPC	Cortex pariétal postérieur
PPSE	Potentiels postsynaptiques excitateurs initiaux élevés
PPSI	Potentiels postsynaptiques inhibiteurs initiaux élevés
PRh	Cortex périrhinal
PtA	Cortex pariétal associatif
PV	Noyau thalamique paraventriculaire
Re	Noyau thalamique réuniens
Rh	Noyau thalamique rhomboïde
RS	Cortex rétrosplénial
RSA	Cortex rétrosplénial agranulaire
RSG	Cortex rétrosplénial granulaire
Rt	Noyau thalamique réticulaire
S1	Cortex somatosensoriel primaire
S1Sh	Cortex somatosensoriel primaire, épaules

S1J	Cortex somatosensoriel primaire, mâchoire
S1FL	Cortex somatosensoriel primaire, membres antérieurs
S1HL	Cortex somatosensoriel primaire, membres postérieurs
S1Tr	Cortex somatosensoriel primaire, tronc
S2	Cortex somatosensoriel secondaire
SG	Noyau supragéniculé
SIP	Sillon intrapariétal
Som	Cortex somatosensoriel
STS	Sillon temporal supérieur
Sub	Noyau thalamique submedius
TeA	Cortex temporal associatif
V1	Cortex visuel primaire
V2	Cortex visuel secondaire
V2L	Cortex visuel secondaire, aire latérale
V2M	Cortex visuel secondaire, aire médiale
VA	Noyau thalamique ventral antérieur
VDB	Segment vertical de la bande diagonale de Broca
VL	Noyau thalamique ventral latéral
VM	Noyau thalamique ventral médial
VP	Noyau thalamique ventral postérieur
VPL	Noyau thalamique ventral postérolatéral
VPM	Noyau thalamique ventral postéromédial
ZI	Zona incerta

Remerciements

J'aimerais premièrement remercier mon directeur de recherche principal, Monsieur Gilles Bronchti, Ph.D., professeur au Département d'anatomie de l'Université du Québec à Trois-Rivières, pour m'avoir donné la chance de travailler dans son laboratoire alors que je finissais ma première année d'étude au baccalauréat et que j'hésitais entre la clinique et la recherche. J'ai découvert un univers fascinant où la persévérance est de mise, mais où les efforts sont toujours récompensés. Je voudrais aussi le remercier pour son soutien, son souci du travail bien fait, ses conseils pratiques tout au long de ce projet ainsi que pour son appui technique dans la réalisation de la présente recherche.

J'aimerais aussi remercier mon codirecteur de recherche, Monsieur Denis Boire, Ph.D., professeur au Département d'anatomie de l'Université du Québec à Trois-Rivières, pour ses commentaires constructifs et ses conseils. Je voudrais aussi le remercier pour les discussions, les critiques constructives, la disponibilité, la patience, l'intégrité et le dévouement. Merci d'avoir eu confiance en moi et de m'avoir transmis votre passion pour la recherche. Grâce à vous, mon passage au laboratoire aura été très enrichissant, tant sur le plan scientifique que personnel. Je voudrais aussi le remercier pour m'avoir donné l'opportunité de voyager et de présenter mes travaux dans des congrès où j'ai pu rencontrer de grands chercheurs, élargir mes connaissances et aviver ma passion pour la neuroscience. Merci aussi de m'avoir donné la chance de faire ce doctorat en sachant que la courbe d'apprentissage pour un étudiant en psychologie serait abrupte. Vous m'avez supporté et encouragé tout au long de ces études.

Merci aux nombreux collègues que j'ai eu la chance de côtoyer au fil des ans. Ils ont été une deuxième famille et ils ont su rendre agréables les longues journées passées au laboratoire. Merci à Marie-Eve Laramée et Sonia Guillemette de m'avoir enseigné la méthodologie qui m'a servi tout au long de mon doctorat et de toujours avoir pris le temps de répondre à mes nombreuses questions. Merci à Joshua Cloutier-Beaupré et Jonathan Pommainville d'avoir su faire du laboratoire un endroit dynamique et convivial. Merci finalement à Robert Tremblay-Laliberté et Samuel Stromei-Cléroux, pour leur patience et leur bonne humeur, malgré les heures passées au microscope. Je voudrais aussi remercier le Réseau de Recherche en Science de la Vision pour m'avoir permis de présenter mes résultats dans un cadre valorisant et pour les prix qui ont été beaucoup plus qu'un simple support financier, ils ont été un tremplin pour ma carrière scientifique.

Je remercie finalement ma famille et mes amis, qui m'ont toujours encouragé. Merci d'avoir accepté que le travail à accomplir limitait parfois le temps passé avec vous. Sachez par contre que chaque instant en votre compagnie a d'autant plus compté. Merci finalement pour les tapes dans le dos. Ce sont ces gestes qui m'ont donné la force de continuer. Mes derniers remerciements et non les moindres s'adressent à ma femme Jessica, qui pour mon plus grand bonheur partage ma vie et mes expériences professionnelles depuis leurs origines. Elle a su, tout au long de cette thèse m'encourager dans ma voie. Son soutien a été sans faille et je lui serai éternellement reconnaissant d'avoir été à mes côtés et d'être la clé de ma réussite.

- Je dédie cette thèse à mes parents.

Introduction

Dans les prochaines sections, les différentes voies sensorielles ascendantes et descendantes seront présentées, depuis les récepteurs spécialisés, jusqu'au cortex cérébral. Une attention particulière sera portée sur le système visuel, somatosensoriel et auditif, principaux sujets à l'étude. Pour la description des systèmes, différents ouvrages de référence en neuroanatomie ont été utilisés (Bear, Connors, & Paradiso, 2007; Brodal, 2010; Moller, 2003; Nieuwenhuys, Voogd, & Van Juijzen, 2008), mais ne sont pas cités de manière exhaustive dans ce texte. Bien que ces principes aient surtout été étudiés chez les primates, un parallèle sera par la suite fait avec la souris, le modèle utilisé pour la réalisation de cette thèse.

Les voies sensorielles ascendantes et descendantes

Notre perception cohérente de l'environnement dépend de l'information sensorielle que les cinq sens traditionnellement reconnus nous livrent. Le cortex cérébral, qui est un ensemble d'aires corticales interreliées par un réseau de connexions, traite et analyse les informations provenant de chacun des sens. Pour comprendre comment le cortex cérébral traite les informations provenant de chacun des sens, il est important de comprendre d'où proviennent les projections afférentes. Le cortex visuel reçoit des afférences visuelles de l'organe visuel principal, l'œil, le cortex auditif reçoit des afférences auditives de l'oreille et le cortex somatosensoriel reçoit des afférences somatosensorielles des récepteurs cutanés.

L'information sensorielle est par la suite acheminée aux noyaux thalamiques spécifiques par les voies sensorielles ascendantes. Le corps géniculé latéral dorsal pour la vision, le noyau ventral postérieur pour le toucher et le corps géniculé médial ventral pour l'audition. Dans les voies sensorielles ascendantes, la perception est axée sur le stimulus et le signal se déplace du bas vers le haut. L'information arrive ensuite aux cortex sensoriels primaires dédiés à chacune des modalités. Le cortex visuel primaire pour la vision, le cortex somatosensoriel primaire pour le toucher et le cortex auditif primaire pour l'audition. Le terme primaire provient du fait que ces aires corticales représentent le premier niveau de traitement de l'information sensorielle. Elles traitent les informations sensorielles de base comme les formes, les textures et les sons.

Les cortex sensoriels primaires relaient ensuite l'information à partir des voies ascendantes vers des cortex sensoriels secondaires qui traitent les informations plus complexes comme la perception spatiale, la reconnaissance et la vitesse de mouvement. Les connexions à partir d'aires corticales de différentes modalités sensorielles vont ensuite converger vers les aires associatives multisensorielles au sommet qui sont impliquées dans les fonctions supérieures. Ces dernières retournent l'information sensorielle vers les cortex sensoriels primaires à partir des voies descendantes. Dans les voies sensorielles descendantes, la perception est axée sur le contexte et le signal se déplace du haut vers le bas. La communication ente les aires corticales peut également se faire par les connexions indirectes des boucles cortico-thalamo-corticales qui passent par des noyaux thalamiques d'ordre supérieur.

Les cortex sensoriels primaires ne seraient donc pas seulement impliqués dans le traitement de l'information sensorielle de leur propre modalité acheminée par les voies ascendantes provenant des noyaux thalamiques spécifiques. Les cortex sensoriels primaires reçoivent également des informations contextuelles des voies descendantes provenant des aires associatives, et des boucles cortico-thalamo-corticales indirectes provenant des noyaux thalamiques d'ordre supérieur (Kaas & Collins, 2013; Scheich, Brechmann, Brosch, Budinger, & Ohl, 2007). Les cortex sensoriels primaires sont ainsi situés à l'interface des voies ascendantes et descendantes et auraient un rôle clé dans le traitement de l'information axé sur le stimulus et axé sur le contexte. La Figure 1 est une représentation schématique des voies sensorielles.

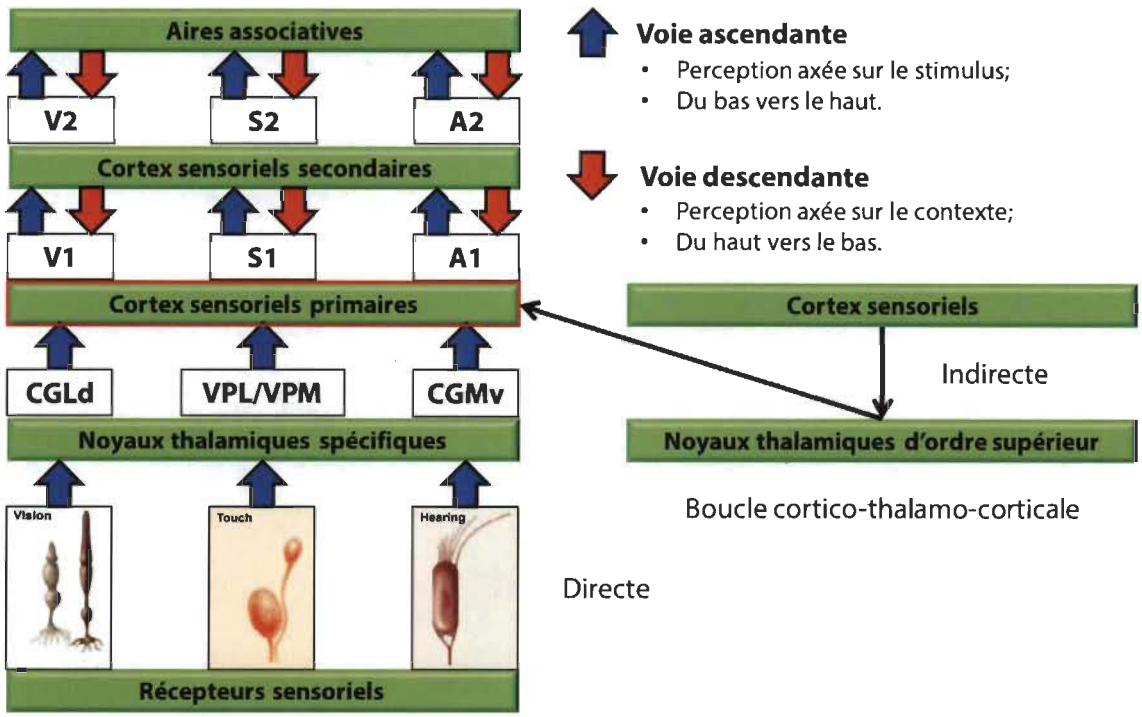

Figure 1. Représentation schématique des voies sensorielles.

L'apprentissage perceptif

Un exemple qui valide le rôle clé des cortex sensoriels primaires dans le traitement de l'information axé sur le stimulus et axé sur le contexte est l'apprentissage perceptif. L'apprentissage perceptif reflète un processus d'appariement du système nerveux entre l'information sensorielle des stimuli externes acheminée par les voies ascendantes et les attentes envers l'environnement généré à l'interne par les voies descendantes (Grossberg, 1980; Lee & Mumford, 2003; Llinas & Pare, 1991). Dans la Figure 2 par exemple, le traitement de l'information sensorielle axé sur le stimulus des voies ascendantes permet de percevoir des taches noires disposées sur un fond blanc. Pour un observateur naïf, il est difficile de percevoir l'image cachée dans cet amas de taches. Si cet observateur prend conscience de l'image et qu'il regarde à nouveau la première figure, le traitement de l'information sensorielle axé sur le contexte des voies descendantes fait que l'image de grenouille cachée devient perceptible.

Figure 2. L'apprentissage perceptif. Les voies ascendantes permettent de percevoir les taches, mais pas l'image qui devient perceptible si on la connait (Gregory, 1970).

Les connexions corticocorticales

Les axones sont les prolongements uniques des neurones qui transmettent les influx nerveux vers une cible. En 1979, les chercheurs Kathleen Rockland et Deepak Pandya ont démontré que les connexions corticocorticales, c'est-à-dire d'un cortex vers un autre cortex, auraient des caractéristiques différentes selon leur direction. Les connexions rostro-caudales, désignées comme les connexions « *feedforward* », sont dirigées de l'avant vers l'arrière du cortex. Les connexions caudo-rostrales, désignées comme les connexions « *feedback* », sont dirigées de l'arrière vers l'avant du cortex. Ces directions pourraient correspondre aux voies ascendantes et descendantes. La réciprocité est aussi un important principe des connexions corticocorticales. Ils ont démontré que les voies ont tendance à être bidirectionnelles, de sorte que si l'aire A projette vers l'aire B, l'aire B risque de projeter aussi vers l'aire A.

En 1991, ces notions ont été utilisées par les chercheurs Daniel Felleman et David Van Essen pour former la base de leur modèle de la hiérarchie corticale du cortex visuel chez le primate. Dans leur analyse des connexions corticocorticales, ils ont présenté un modèle dans lequel 32 aires corticales sont réparties sur 10 niveaux hiérarchiques. Dans ce modèle, les connexions *feedforward* projettent vers une aire de plus haut niveau et les connexions *feedback* vers une aire de plus bas niveau. Un troisième type, les connexions latérales, lie des aires corticales de niveau similaire (Bullier, 2001). Les motifs de connectivité asymétrique entre des aires réciproquement connectés permettent de déterminer la position des aires corticales dans la hiérarchie.

La distribution laminaire des connexions corticocorticales

Les neurones d'origine des connexions corticocorticales auraient une distribution laminaire différente dans les six couches du cortex (voir Figure 3) (Felleman & Van Essen, 1991). Les connexions *feedforward* proviennent des neurones situés dans les couches supragranulaires deux et trois, au-dessus de la couche quatre, la couche granulaire. Les connexions *feedback* proviennent des neurones situés dans les couches infragranulaires cinq et six, en dessous de la couche quatre. Les connexions latérales proviennent également des couches infragranulaires et supragranulaires. Ces connexions latérales forment entre autres des connexions locales intracorticales (Bullier, 2001). Ceci prend en considération l'aspect structurel des connexions corticocorticales, mais ces connexions peuvent aussi être décrites selon leur aspect fonctionnel avec comme critères le métabolisme cellulaire, la mesure des potentiels d'action, les changements de potentiel électrique et des techniques de lésion ou de désactivation (Reid, 2009).

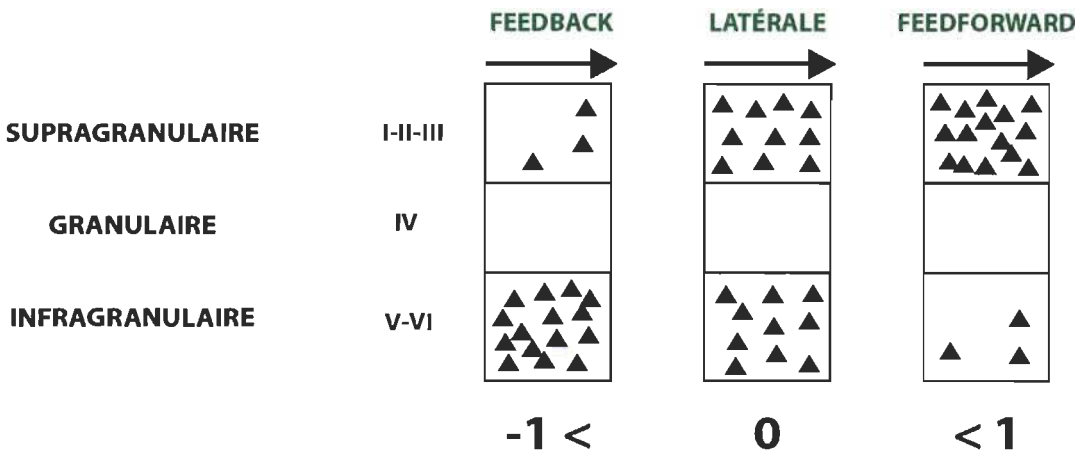

Figure 3. Connexions *feedforward*, *feedback* et latérale d'après la distribution laminaire des neurones (Inspiré de Vezoli et al. 2004).

Le connectome et la connectomique

L'analyse des connexions corticocorticales a été réalisée au-delà du cortex visuel du primate sous forme de connectome. Un connectome est un plan complet des connexions neuronales dans un cerveau. La production et l'étude des connectomes sont connue sous le nom de connectomique. Le *Human Connectome Project* a construit le connectome d'un cerveau humain à l'échelle macroscopique.

Les différentes échelles de connectome

Les réseaux de connexions du cerveau peuvent être définis à différentes échelles comme l'échelle macroscopique, l'échelle mésoscopique ou l'échelle microscopique. L'échelle macroscopique décrit l'organisation générale des réseaux de connexions. Le *Human Connectome Project* est un exemple de connectome à l'échelle macroscopique et l'imagerie par résonance magnétique de diffusion est un exemple de technique employé. L'échelle mésoscopique décrit la structure des connexions d'une aire à l'autre dans l'ensemble du cerveau. Le *Mouse Brain Connectome Project* et le *Allen Mouse Brain Connectivity Atlas* sont des exemples de connectome à l'échelle mésoscopique et l'injection de traceurs antérogrades et rétrogrades est un exemple de technique employé. L'échelle microscopique décrit le détail des synapses, c'est-à-dire comment les axones et les dendrites se connectent. La microscopie électronique est un exemple de technique employé. Cette thèse porte sur les connexions des cortex sensoriels primaires pour le traitement contextuel et multisensoriel de l'information, ce que l'on a étudié à l'échelle mésoscopique avec l'injection de traceurs.

Le modèle de recherche animal

La souris est le modèle animal employé dans cette thèse étant donné que les études effectuées chez l'humain sont restreintes à des techniques peu invasives. Il est donc nécessaire d'utiliser un modèle animal, chez qui des méthodes plus invasives comme les injections de traceurs peuvent être employées. La souris C57Bl/6 est la souche de souris la plus utilisée et la plus vendue en recherche, en raison de son élevage facile et de sa robustesse. Le cerveau des rongeurs possède moins d'aires corticales que celui des primates, mais les deux espèces ont les mêmes systèmes sensoriels avec les mêmes relais pour traiter l'information provenant des récepteurs spécialisés (Huberman & Niell, 2011). Même si le néocortex des rongeurs est plus petit que celui des primates, on associe les différentes aires corticales aux mêmes endroits. Contrairement à l'humain où les aires associatives occupent une grande place, la majorité du cortex des rongeurs est constituée d'aires sensorielles et motrices primaires (voir Figure 4).

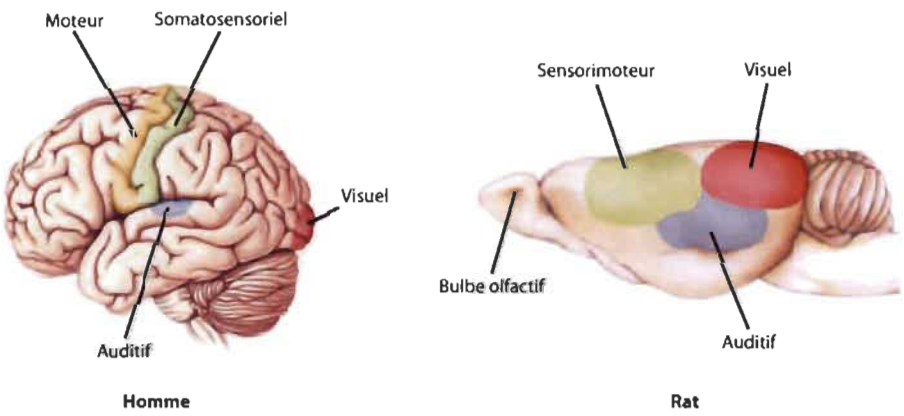

Figure 4. Vue latérale du cortex cérébral chez l'humain et le rat. Les aires visuelles (rouge), somatosensorielles (vert) et auditives (bleu) sont conservées entre les espèces et ont une topographie semblable (Bear et al., 2007).

Comparaison entre humain et rongeur

La proportion que représentent les différentes parties du corps au niveau cortical est illustrée par l'homoncule pour l'humain et par le souricule pour la souris (voir Figure 5) (Blumenfeld, 2010; Zembrzycki, Chou, Ashery-Padan, Stoykova, & O'Leary, 2013). Chez la souris, les vibrisses du museau, utilisées pour l'exploration de l'environnement sont surreprésentées dans le cortex somatosensoriel. Chez l'humain, c'est la représentation des mains qui est aussi surreprésentée que les vibrisses du museau.

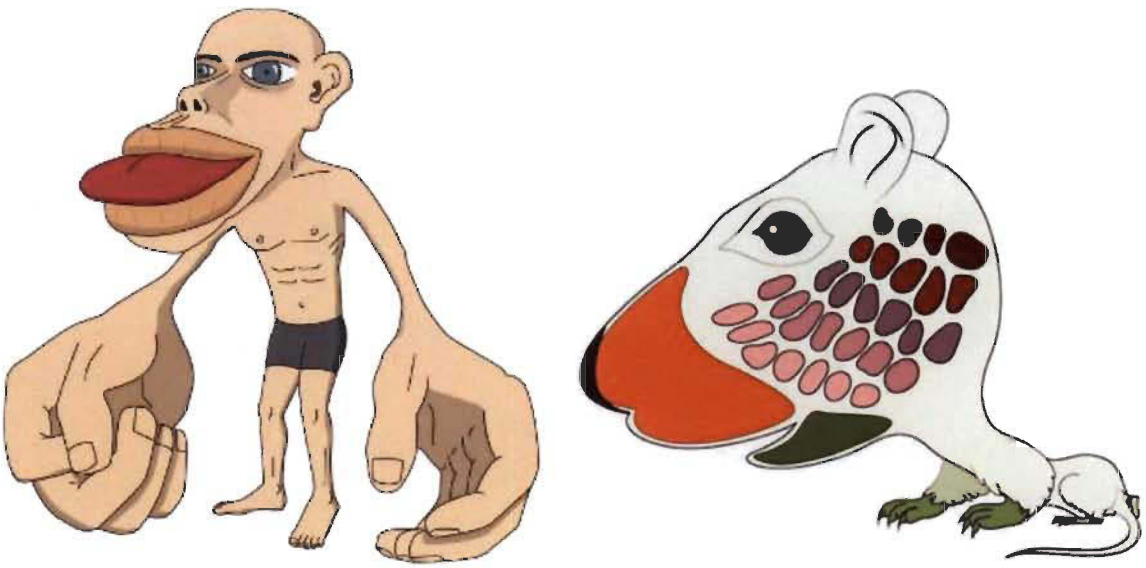

Figure 5. Parallèles entre humains et rongeurs. Homoncule et souricule (Bear et al., 2007; Zembrzycki et al., 2013).

Chez la souris, on retrouve une région du cortex somatosensoriel primaire dédiée à la représentation corticale des différentes parties du corps, le champ de tonneaux, qui est composé de plusieurs sous-régions associées à ces différentes parties. La partie postéromédiale du champ de tonneaux contient les corrélats corticaux des vibrisses du

museau. Chez ces animaux, les vibrisses du museau sont utilisées pour l'exploration de l'environnement et leur représentation corticale est très développée. On retrouve en effet au niveau du cortex somatosensoriel primaire une représentation exacte de la disposition des vibrisses sur le museau de l'animal (Woolsey & Van der Loos, 1970). La souris est un rongeur nocturne et elle dépend grandement de ses vibrisses pour la localisation des objets et pour la discrimination des textures (Kleinfeld, Ahissar, & Diamond, 2006). Chez cet animal, la voie trigéminale est donc très importante. Chez l'humain, la représentation des mains occupe une grande surface du cortex somatosensoriel et est aussi surreprésentée que les vibrisses du museau dans le cortex (Blumenfeld, 2010; Zembrzycki et al., 2013).

En plus de recevoir des informations des sources mentionnées précédemment, les cortex sensoriels primaires chez les rongeurs reçoivent également des informations des autres cortex sensoriels primaires par des connexions corticocorticales directes.

Le connectome du cerveau de souris

On s'est intéressé au cortex somatosensoriel primaire (S1) de la souris qui est l'aire qui occupe la plus grande superficie. Les projets de grande envergure comme le *Mouse Brain Connectome Project* et le *Allen Mouse Brain Connectivity Atlas* ont également cartographié le connectome des connexions du cortex de la souris. Ces projets de connectomes présentent des quantités impressionnantes de données à l'échelle

macroscopique, mais ne fournissent pas de données sur la structure des connexions corticales et ne prennent pas en considération les connexions sous-corticales.

Les modules somatosensoriels de la souris

Une étude précédente a démontré sur la base des données disponibles dans le *Mouse Brain Connectome Project*, que S1 chez la souris possède quatre modules de connectivités différentes : le module orofaciopharyngé, les membres supérieurs, les membres inférieurs, le tronc, et les vibrisses du museau (voir Figure 6) (Zingg et al., 2014). Les parties plus caudales de S1 comme les vibrisses du museau sont les seules à posséder des connexions avec des aires visuelles et auditives comparativement aux parties plus rostrales. Cette évaluation démontre que les sous-régions de S1 associées à différentes parties du corps n'ont pas toutes les mêmes connexions.

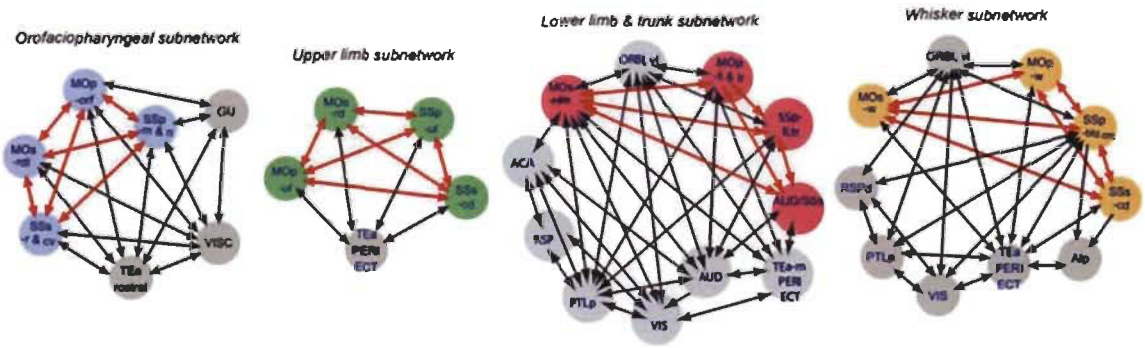

Figure 6. Les quatre modules de connectivités somatosensoriels de la souris tel que démontré sur la base des données disponibles dans le *Mouse Brain Connectome Project* (Zingg et al., 2014).

Objectif 1 : Projections afférentes corticales et sous-corticales du cortex somatosensoriel primaire de la souris

Pour comprendre comment les cortex sensoriels primaires contribuent au traitement de l'information sensorielle, associative et motrice, il est important de connaitre l'ensemble des afférences vers ces aires, tant corticales que sous-corticales. L'évaluation quantitative de la distribution laminaire des neurones permet la classification des projections en tant que *feedforward*, *feedback* ou latérale. Notre premier objectif était donc de faire l'évaluation quantitative des afférences du cortex somatosensoriel primaire chez la souris. Pour cartographier l'ensemble des afférences, corticales et sous-corticales, vers le cortex somatosensoriel primaire, des injections d'un traceur rétrograde ont été faites dans la partie rostrale et caudale du champ de tonneaux ainsi que dans S1, à l'extérieur du champ de tonneaux. La partie caudale du champ de tonneaux devrait être la seule à posséder des connexions avec le cortex visuel.

Les résultats de notre étude démontrent que le cortex somatosensoriel primaire de la souris possède des connexions avec les cortex moteurs, les aires corticales associatives multisensorielles et des noyaux thalamiques propices aux interactions multisensorielles, ce qui soutient clairement l'hypothèse selon laquelle les cortex sensoriels primaires ne sont pas limités au traitement unisensoriel. Un résultat important est la démonstration que les trois parties du cortex somatosensoriel primaire ont des projections différentes. La partie caudale du champ de tonneaux du cortex somatosensoriel primaire possède plus de connexions qui ciblent des aires corticales et sous-corticales sensorielles telles que des aires visuelles, auditives, somatosensorielles, olfactives et associatives en plus

des connexions qui ciblent des aires motrices comparativement à la partie rostrale du champ de tonneaux et à la partie de S1, à l'extérieur du champ de tonneaux dont les connexions ciblent davantage des aires somatosensorielles et motrices. La partie caudale du champ de tonneaux est la seule partie de S1 à recevoir des projections de V1.

L'évaluation quantitative de la distribution laminaire des neurones nous a permis de classifier les projections en tant que *feedforward*, *feedback* ou latérale. Les connexions *feedforward* servent au transfert de l'information à traiter vers une aire de plus haut niveau, les connexions *feedback* ont comme fonction le transfert de l'information vers une aire de plus bas niveau, et les connexions latérales permettent de lier des neurones d'aires corticales de niveau similaire (Bullier, 2001; Felleman & Van Essen, 1991). Les projections vers le cortex somatosensoriel primaire seraient en majorité de nature *feedback*. Dans le cas des cortex sensoriels primaires, les projections auditives seraient de nature *feedback* alors que les projections visuelles vers la partie caudale du champ de tonneaux seraient de nature latérale, ce qui démontre que les différents cortex sensoriels primaires n'occupent pas la même position dans la hiérarchie corticale.

L'espace péripersonnel

Comme on l'a vu dans la section précédente, le champ de tonneaux se démarque du reste du cortex somatosensoriel primaire en ayant plus de connexions qui ciblent des aires corticales et sous-corticales sensorielles telles que des aires visuelles, auditives, olfactives et associatives. De manière plus spécifique, la partie caudale du champ de

tonneaux est la seule partie du cortex somatosensoriel primaire à recevoir des projections du cortex visuel primaire. Cette connexion entre le cortex visuel et le champ de tonneaux pourrait être le substrat anatomique de l'influence de la vision sur les sensations tactiles et la navigation par les vibrisses chez la souris.

L'interaction des vibrisses avec la vision serait importante dans la représentation de l'espace péripersonnel, soit l'espace à la portée des membres d'un individu, plus particulièrement la tête et les bras dans le cas des humains (Rizzolatti, Scandolara, Matelli, & Gentilucci, 1981a, 1981b), d'une part dans la spécification de la position d'une cible et d'autre part dans la transformation de cette position en une commande motrice appropriée pour l'atteindre. Pour que le cortex cérébral soit en mesure d'encoder l'espace péripersonnel, les informations provenant de la modalité visuelle et tactile doivent converger ensemble (Allman, Keniston, & Meredith, 2009; Horn & Hill, 1966).

Comparaison entre humain et rongeur

Comme on l'a vu précédemment avec l'illustration de l'homoncule et du souricule, la représentation des mains chez l'humain (Blumenfeld, 2010) et des vibrisses chez la souris (Zembrzycki et al., 2013) possèdent un facteur de grossissement similaire dans le cortex. De manière similaire, l'espace péripersonnel serait centré sur les mains chez l'humain (Rizzolatti et al., 1981a, 1981b) tandis que chez les rongeurs, cet espace serait centré sur les vibrisses (Cardinali, Brozzoli, & Farne, 2009) (voir Figure 7). L'espace péripersonnel revêt une importance particulière pour la vie des humains autant que chez

les autres animaux. Lorsque les objets entrent dans l'espace péripersonnel, ils peuvent être liés à la saisie et la manipulation (Rizzolatti, Fadiga, Fogassi, & Gallese, 1997) ou être une menace, évoquant par exemple une réaction d'évitement (Graziano, Cooke, & Taylor, 2000).

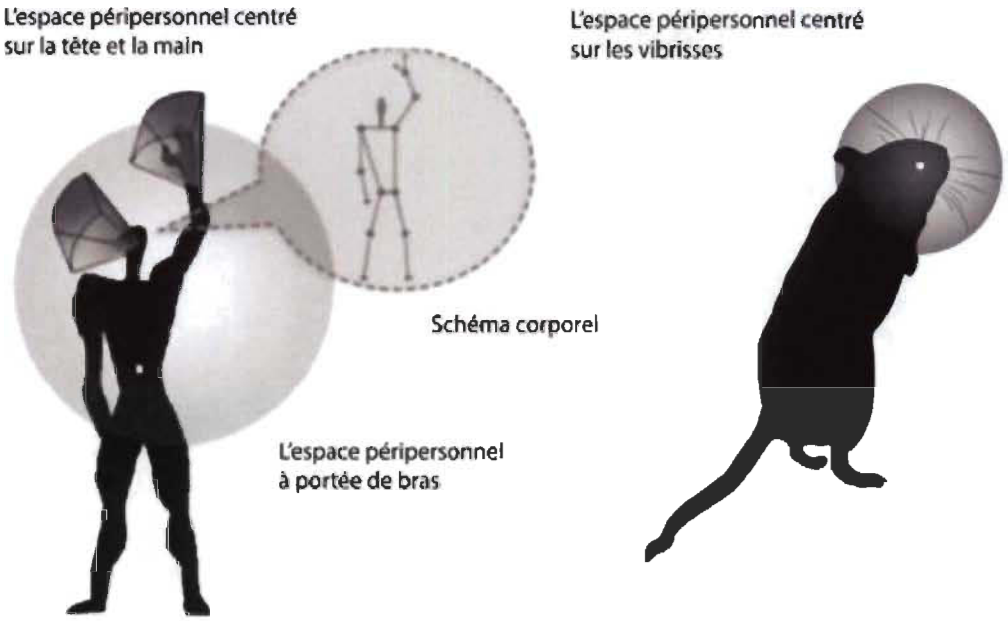

Figure 7. Parallèles entre humains et rongeurs. Espace péripersonnel (Cardinali et al., 2009; Rizzolatti et al., 1981a, 1981b).

Les interactions multisensorielles

La nature multisensorielle d'une aire est définie sur la base de (1) la convergence de projections à partir d'aires corticales de différentes modalités sensorielles (Jones & Powell, 1970) et (2) la présence des neurones qui peuvent répondre à des stimuli qui proviennent de plus d'une modalité sensorielle mentionnée dans la section précédente (Bruce, Desimone, & Gross, 1981). Nos résultats démontrent que des projections d'aires

corticales visuelles et auditives convergent sur S1 et bien que nous ne pouvons pas démontrer avec certitude la présence de ces neurones multisensoriels dans ce cortex sur la base de nos résultats anatomiques, l'existence de ces neurones a été démontrée à l'intérieur des cortex sensoriels primaires chez le rat (Wallace, Ramachandran, & Stein, 2004) et le furet (Bizley & King, 2008; Bizley, Nodal, Bajo, Nelken, & King, 2007).

L'interaction entre les modalités sensorielles facilite la localisation et l'identification (Stein, Huneycutt, & Meredith, 1988; Stein, Meredith, Huneycutt, & McDade, 1989), la détection (Frassinetti, Bolognini, & Ladavas, 2002; Lovelace, Stein, & Wallace, 2003) et le temps de réaction aux stimuli externes (Amlot, Walker, Driver, & Spence, 2003; Calvert & Thesen, 2004; Corneil, Van, Munoz, & Van Opstal, 2002; Diederich, Colonius, Bockhorst, & Tabeling, 2003; Forster, Cavina-Pratesi, Aglioti, & Berlucchi, 2002; Frens, Van Opstal, & Van der Willigen, 1995; Harrington & Peck, 1998; Hughes, Reuter-Lorenz, Nozawa, & Fendrich, 1994; Molholm et al., 2002).

Les interactions visuotactiles

Notre deuxième étude porte sur les connexions entre V1 et S1, et il est donc pertinent de connaitre les aspects comportementaux liés aux influences réciproques entre la vision et le toucher. Une étude chez l'humain a démontré que la vision peut améliorer l'acuité tactile (Kennett, Taylor-Clarke, & Haggard, 2001). Une autre a démontré que la vision peut diminuer la perception de la douleur (Longo, Schuur, Kammers, Tsakiris, & Haggard, 2008). Des connexions corticocorticales directes entre le champ de tonneaux et

V1 comme celles que nous avons observées seraient avantageuses pour ces interactions visuotactiles (Giard & Peronnet, 1999). Une étude plus poussée de la structure de ces connexions permettrait de mieux comprendre comment ces deux modalités s'influencent au niveau des cortex sensoriels primaires. L'étude de la morphologie des axones et de leurs terminaux permettrait d'en apprendre davantage sur la fonction de ces connexions et les propriétés fonctionnelles de leurs modes de transmission glutamatergiques.

Les modes de transmission glutamatergique

Les voies glutamatergiques comportent deux modes de transmission glutamatergique, les réponses postsynaptiques inductrices de Classe 1 et les réponses postsynaptiques modulatrices de Classe 2 (Petrof & Sherman, 2013). Le Tableau 1 et la Figure 8 résument les caractéristiques anatomiques et synaptiques qui différencient les réponses de Classe 1 et de Classe 2.

Tableau 1

Résumé des caractéristiques anatomiques et synaptiques

	Classe 1 - Inducteur	Classe 2 - Modulateur
Caractéristiques anatomiques	Gros boutons terminaux	Petits boutons terminaux
	Contacte des dendrites proximales	Contacte des dendrites distales
	Axones avec un gros diamètre	Axones avec un petit diamètre
	Moins de convergence	Plus de convergence
Caractéristiques synaptiques	PPSE de grande amplitude	PPSE de petite amplitude
	Dépression lors d'un test paired-pulse	Facilitation lors d'un test paired-pulse
	Active les récepteurs glutamatergiques ionotropiques seulement	Active les récepteurs glutamatergiques ionotropiques et métabotropiques

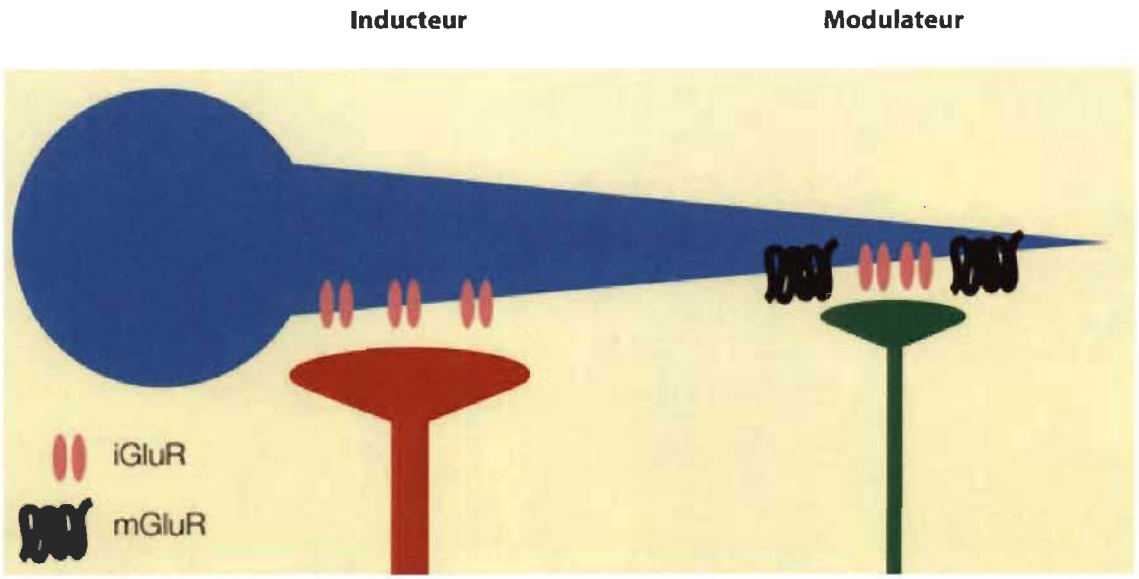

Figure 8. Les boutons terminaux inducteurs et modulateurs.

Les réponses postsynaptiques de Classe 1

Les différences dans les propriétés synaptiques des deux types de réponses postsynaptiques ont été examinées principalement in vitro, où l'activation de diverses voies glutamatergiques a produit des effets postsynaptiques radicalement différents. Par exemple, une stimulation électrique de plus de 10 Hz des voies glutamatergiques de Classe 1 a produit des potentiels postsynaptiques excitateurs initiaux de plus forte amplitude (PPSE), une dépression lors d'un test paired-pulse et une activation liée exclusivement aux récepteurs glutamatergiques ionotropiques (iGluR). Des exemples typiques de réponses postsynaptiques de Classe 1 sont trouvés dans les voies qui véhiculent l'information sensorielle des organes sensoriels de la périphérie vers le thalamus, voies désignées collectivement comme lemniscales, telles que la voie lemniscale médiale vers le noyau ventral postérieur médial et latéral (VPM et VPL) (Castro-Alamancos, 2002), la voie visuelle vers le corps géniculé latéral dorsal (CGLd) (Reichova & Sherman, 2004) et la voie auditive vers le corps géniculé médian ventral (CGMv) (Bartlett & Smith, 2002; Lee & Sherman, 2010). De manière similaire, les réponses postsynaptiques des voies corticothalamiques *feedforward* originaires de la couche 5 sont semblables à celle des réponses postsynaptiques de Classe 1 des voies lemniscales vers le thalamus (Li, Guido, & Bickford, 2003; Reichova & Sherman, 2004). Des réponses de Classe 1 ont également été identifiées à l'extérieur du thalamus, comme dans certaines voies thalamocorticales (Li, Guido et al., 2003; Reichova & Sherman, 2004; Viaene, Petrof, & Sherman, 2011a, 2011b), certaines voies

corticorticales (Covic & Sherman, 2011; De Pasquale & Sherman, 2011), et quelques voies corticales locales (De Pasquale & Sherman, 2012).

Les réponses postsynaptiques de Classe 2

Les propriétés synaptiques des Classe 2 diffèrent substantiellement de celles des Classe 1. Par exemple, une stimulation électrique des projections locales de la couche 6 vers la couche 4 dans le cortex auditif et somatosensoriel primaire a produit des PPSE faibles et une facilitation lors d'un test paired-pulse (Lee & Sherman, 2008; Lee & Sherman, 2009a). Des effets similaires ont été mis en évidence dans des projections corticothalamiques originaires des cellules de la couche 6 (Bartlett & Smith, 2002; Li, Guido et al., 2003), des afférences thalamocorticales (Viaene, Petrof, & Sherman, 2011a, 2011c), et des voies corticocorticales (Covic & Sherman, 2011; De Pasquale & Sherman, 2011), ainsi que dans certaines voies corticales locales (De Pasquale & Sherman, 2012; Lee & Sherman, 2008; Lee & Sherman, 2009a). Ces réponses de Classe 2 sont capables d'activer les récepteurs métabotropiques (mGluR) (Covic & Sherman, 2011; De Pasquale & Sherman, 2011; Lee & Sherman, 2008, 2009b; Reichova & Sherman, 2004; Viaene et al., 2011a, 2011c). Pour terminer, les voies contenant des réponses de Classe 2 sont constituées d'axones avec une plus grande tendance à converger sur des cellules individuelles par rapport à leurs homologues de la Classe 1 qui produisent des réponses postsynaptiques qui sont largement insensibles aux augmentations d'intensité des stimulations indiquant peu ou pas de convergence des axones.

Les corrélations anatomiques des réponses postsynaptiques

En plus des différences dans leurs propriétés synaptiques, les réponses de Classe 1 et de Classe 2 sont associées à des corrélations anatomiques différentes. Par exemple, les réponses de Classe 1 dans les voies vers le thalamus sont caractérisées par des axones de gros diamètre, qui se terminent en arborisation dense qui contient beaucoup de gros boutons terminaux. Des exemples établis d'afférences contenant des réponses de Classe 1, pour lesquels des données sur la taille de leurs boutons terminaux sont disponibles, comprennent les afférences de la rétine vers le CGLd (Colonnier & Guillery, 1964; Guillery, 1969; Hajdu, Hassler, & Somogyi, 1982; Li, Wang, & Bickford, 2003; Peters & Palay, 1966; So, Campbell, & Lieberman, 1985; Szentagothai, 1963; Van Horn, Erisir, & Sherman, 2000), les voies lemniscales vers VPM et VPL (Ralston, III, 1969), les afférences du collicule inférieur vers le CGMv (Bartlett et al., 2000; Morest, 1975), et les voies corticothalamiques originaires de la couche 5 (Bourassa, Pinault, & Deschenes, 1995; Feig & Harting, 1998; Hoogland, Wouterlood, Welker, & Van der Loos, 1991; Li, Guido et al., 2003; Rouiller & Welker, 1991; Rouiller & Welker, 2000; Vidnyanszky, Borostyankoi, Gorcs, & Hamori, 1996). Les voies thalamiques avec des réponses de Classe 1 ont tendance à contacter les dendrites proximales (Sherman & Guillery, 2006). De plus, les réponses de Classe 1 sont corrélées aux gros boutons terminaux. Ces gros boutons terminaux ont été démontrés dans un certain nombre de voies thalamocorticales vers les aires corticales auditives, visuelles et somatosensorielles, en particulier sur celles qui se terminent dans la couche 4 du cortex (Ahmed, Anderson, Douglas, Martin, & Nelson, 1994; Lee & Sherman, 2008; Viaene et

al., 2011a, 2011c), et quelques voies corticocorticales entre le cortex auditif primaire et secondaire de la souris (Covic & Sherman, 2011).

Contrairement aux réponses de Classe 1 dans les voies vers le thalamus, celles de Classe 2 provenant des afférences corticothalamiques de la couche 6 sont constituées d'axones avec un petit diamètre qui comprennent des petits boutons terminaux (Bartlett et al., 2000; Hoogland et al., 1991; Ichida & Casagrande, 2002; Li, Guido et al., 2003). Les voies thalamiques avec des réponses de Classe 2 ont tendance à contacter les dendrites distales (Sherman & Guillery, 2006). De plus, les réponses de Classe 2 sont corrélées aux petits boutons terminaux. Des exemples de petits boutons terminaux ont été démontrés dans certaines voies corticocorticales (Covic & Sherman, 2011), et la plupart des voies thalamocorticales vers les couches 2 et 3 du cortex somatosensoriel et auditif primaire (Viaene et al., 2011a, 2011a). La majeure partie des projections du noyau postérieur (Po) vers toutes les couches de S1 comprennent des réponses de Classe 2 et sont corrélées à des petits terminaux. (Viaene et al., 2011c).

Les implications fonctionnelles des réponses postsynaptiques

Les réponses postsynaptiques de Classe 1 produisent des grands PPSE et elles ne ciblent que les récepteurs glutamatergiques ionotropiques. Ces caractéristiques permettent aux réponses de Classe 1 d'exercer des effets importants sur leurs cibles postsynaptiques et d'avoir une vitesse de transmission synaptique plus rapide. De plus, la dépression lors d'un test paired-pulse est une propriété qui agit comme un mécanisme

de contrôle sur le traitement synaptique (Chung, Li, & Nelson, 2002), ce qui les rend idéales et fiables pour le relais de l'information sensorielle. Pour ces raisons, les réponses postsynaptiques de Classe 1 sont souvent désignées comme les influx inducteurs, étant donné qu'elles sont les principaux déterminants dans l'activité d'une cellule postsynaptique en vertu de la définition de son champ récepteur (Sherman & Guillery, 2006).

D'un autre côté, les réponses postsynaptiques de Classe 2 ne possèdent pas les caractéristiques synaptiques nécessaires pour permettre un relais efficace et fiable de l'information sensorielle. Au lieu de cela, leurs effets postsynaptiques relativement faibles, leur convergence extensive, et leur composante métabotropique lente et prolongée sont mieux adaptés au rôle de modulateur. La réponse prolongée serait plutôt utile pour le contrôle du voltage et de la conductance, et le temps de réaction de cette réponse dépasse l'influx d'environ 100 millisecondes à plusieurs secondes, des caractéristiques qui sont incohérentes avec un flux d'information efficace. Pour ces raisons, les réponses postsynaptiques de Classe 2 sont souvent désignées comme les influx modulateurs (Sherman & Guillery, 2006).

Un autre point qui mérite d'être mentionné est que même si les réponses postsynaptiques de Classe 1 sont les principaux transporteurs d'information sensorielle dans les circuits thalamiques et corticaux, les réponses postsynaptiques de Classe 2 sont beaucoup plus nombreuses, celles de Classe 1 ne représentant que de 2 à 10 % du

nombre total de synapses dans le thalamus et le cortex, selon les estimations (Van Horn & Sherman, 2004; Wang, Eisenback, & Bickford, 2002). Même si ces chiffres sous-estiment en quelque sorte le nombre total de réponses postsynaptiques de Classe 1, étant donné qu'ils prennent surtout en compte les plus gros boutons, il est évident que les effets synaptiques inducteurs plus importants des réponses postsynaptiques de Classe 1 ne sont pas dus à leur supériorité numérique par rapport aux réponses postsynaptiques de Classe 2 (Van Horn et al., 2000).

Une question intéressante qui n'a pas été abordée est de savoir si un axone unique peut posséder un large éventail de taille de boutons et par le fait même, différentes propriétés synaptiques ou non (Reyes et al., 1998). Dans les projections corticothalamiques, les terminaux associés aux deux types de réponses se trouvent sur deux types d'axones distincts (voir Figure 9). Les terminaux corrélés avec les réponses postsynaptiques de Classe 1 sont sur des axones avec un diamètre plus important qui proviennent des neurones pyramidaux de la couche 5 (Bourassa et al., 1995), alors que les terminaux corrélés avec les réponses postsynaptiques de Classe 2 sont sur des axones avec un diamètre moins important qui proviennent des neurones de la couche 6 (Bourassa et al., 1995).

Répondre à cette question pour les projections corticocorticales nous apporterait une meilleure compréhension des mécanismes exacts derrière la fonction des réponses

postsynaptiques de Classe 1 et de Classe 2 dans une connexion entre deux aires de modalités sensorielles différentes et au niveau des cortex sensoriels primaires.

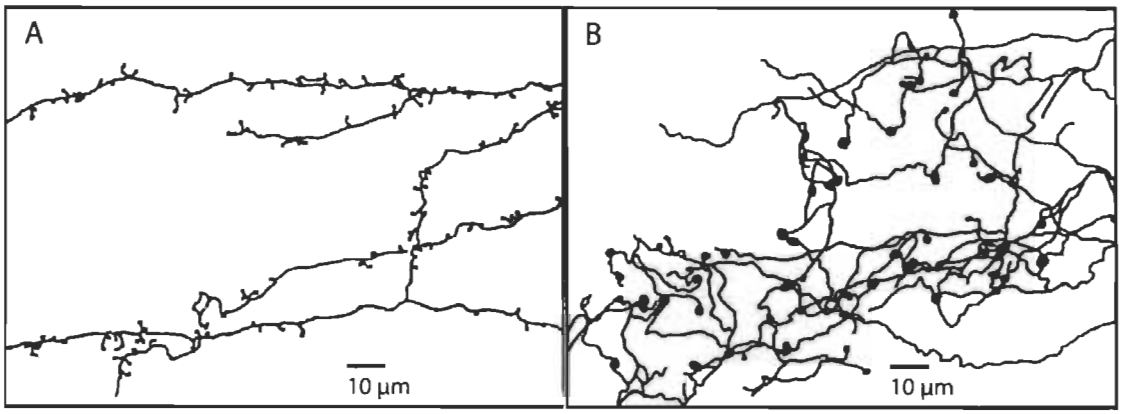

Figure 9. Connexions corticothalamiques. Terminaisons modulatrices, possèdent des boutons terminaux plus petits (A). Terminaisons inductrices, possèdent des boutons terminaux plus grands (B) (Bourassa et al., 1995).

Objectif 2 : Les connexions corticocorticales directes et réciproques entre le cortex visuel et somatosensoriel primaire de la souris

Une étude plus poussée de la structure des connexions corticocorticales directes et réciproques entre le champ de tonneaux de S1 et V1 permettrait de mieux comprendre comment la modalité sensorielle somatosensorielle et la modalité sensorielle visuelle s'influencent mutuellement au niveau des cortex sensoriels primaires. L'étude de la morphologie des axones et de leurs terminaux permettrait aussi d'en apprendre davantage sur leurs fonctions. Notre deuxième objectif était donc d'étudier la microcircuiterie des connexions corticocorticales directes et réciproques entre les cortex visuel et somatosensoriel primaires de la souris. La quantité et la distribution laminaire des corps cellulaires rétrogradement marqués ont été étudiées dans les cortex visuel et

somatosensoriel primaires afin de déterminer le poids et la nature de ces projections. Pour rétrogradement marquer les corps cellulaires, des injections d'un traceur rétrograde, la sous-unité B de la toxine du choléra, ont été faites dans les cortex visuel et somatosensoriel primaires. Afin d'obtenir une distribution de taille du diamètre des axones et de leurs boutons terminaux antérogradement marqués dans chaque couche corticale des projections entre V1 et S1, un échantillonnage stéréologique de ces axones et de leurs boutons terminaux a été réalisé pour chaque cas ayant reçu une injection en colonne d'un traceur antérograde, le dextran-biotine aminé. Des axones uniques ont été reconstruits dans les projections entre les cortex visuel et somatosensoriel primaires afin de déterminer si un axone unique peut contenir un large éventail de taille de boutons terminaux. Si l'on s'appuie sur les résultats de notre première étude, nous devrions observer une asymétrie dans les connexions entre ces deux aires primaires.

Les résultats de notre deuxième étude démontrent que la connexion du champ de tonneaux (S1BF) vers le cortex visuel primaire (V1) est de type *feedback* et a une influence modulatrice prédominante alors que la projection réciproque est de type latéral et a plutôt une influence inductrice. En effet, l'évaluation quantitative de la distribution laminaire des neurones a permis de classifier les projections en tant que *feedforward*, *feedback* ou latérale. Les résultats démontrent que la projection de S1BF vers V1 est de type *feedback* alors que la projection réciproque de V1 vers S1BF est de type latéral. De plus, la plus grande incidence de gros axones et de gros boutons terminaux dans la projection de V1 vers S1BF suggère fortement que V1 exerce une influence inductrice

sur S1BF alors que la plus grande incidence de petits axones et de petits boutons terminaux dans la projection de S1BF vers V1 suggère fortement que S1BF exerce une influence modulatrice prédominante sur V1. Les axones reconstruits dans la projection de S1BF vers V1 n'avaient que de petits boutons terminaux tandis que les axones reconstruits dans la projection de V1 vers S1BF avaient parfois un large éventail de taille de boutons terminaux. Cela pourrait suggérer qu'il y a deux types d'axones distincts sur la base de la présence ou de l'absence de gros boutons terminaux. Ce résultat est important, car il démontre que ces connexions entre deux cortex sensoriels primaires, bien que réciproques, ne sont certainement pas symétriques.

La cécité et les connexions corticocorticales

La projection de S1BF vers V1 est de type *feedback* (Charbonneau, Laramee, Boucher, Bronchti, & Boire, 2012) et pourrait avoir une influence modulatrice prédominante alors que la projection réciproque est de type latéral (Masse, Ross, Bronchti, & Boire, 2016) et pourrait plutôt avoir une influence inductrice. Ceci, ajouté aux résultats de la deuxième étude que nous venons de voir confirme que la modalité visuelle et la modalité somatosensorielle ne s'influencent pas de la même manière au niveau des cortex sensoriels primaires. À la lumière de ce résultat, nous nous sommes interrogés sur l'influence de l'expérience visuelle pendant la période de vie postnatale sur le développement des connexions corticocorticales entre V1 et S1. On sait que l'activité provenant des récepteurs sensoriels peut considérablement influencer le développement de la connectivité corticale (Katz & Shatz, 1996; Price et al., 2006). La

plasticité intermodale implique des changements anatomiques importants dans le néocortex, mais les effets de la cécité sur les connexions corticocorticales entre les cortex sensoriels primaires ne sont pas encore entièrement compris. Plusieurs études portent sur les afférences du cortex visuel lors de la perte de vision, mais peu se sont consacrées aux efférences du cortex visuel. L'étude de la structure des connexions entre le cortex visuel primaire et le cortex somatosensoriel primaire chez des souris énucléées à la naissance permettrait de mieux comprendre comment les connexions entre deux cortex sensoriels primaires sont altérées par la perte d'un sens.

Les effets de la cécité sur les connexions corticales

À l'heure actuelle, on ne sait pas si les connexions corticocorticales entre les cortex sensoriels primaires sont amplifiées ou diminuées dans les interactions multisensorielles. Bien que certaines études fonctionnelles rapportent une connectivité corticale intermodale entre les cortex sensoriels primaires améliorée chez les aveugles (Fujii, Tanabe, Kochiyama, & Sadato, 2009; Klinge, Eippert, Roder, & Buchel, 2010), d'autres rapportent plutôt une de diminution de la connectivité du cortex visuel avec les autres cortex sensoriels primaires chez les sujets aveugles (Liu et al., 2007; Yu et al., 2008). Cela pourrait dépendre de la modalité sensorielle, car comme il a été précédemment démontré, le pourcentage de neurones marqués projetant du cortex auditif vers le cortex visuel primaire n'était pas significativement différent entre des souris intactes et énuclées à la naissance (Charbonneau et al., 2012), contrairement au pourcentage de neurones projetant de S1 vers V1 qui diminue. De plus, une étude chez le rat a démontré

que l'absence d'expérience unisensorielle tactile suivant l'ablation des vibrisses durant les cinq premiers jours suivants la naissance diminue significativement la quantité de neurones projetant de V1 vers S1 (Sieben, Bieler, Roder, & Hanganu-Opatz, 2015). Ainsi, l'absence de stimuli visuels pourrait entrainer une perte généralisée en empêchant l'établissement d'un certain pourcentage de projections du cortex somatosensoriel vers le cortex visuel. Alors que la maturation des mécanismes d'interactions multisensoriels dans les neurones multisensoriels des collicules supérieurs semble véritablement dépendre des expériences unisensorielles (Stein, Stanford, & Rowland, 2014), on ne sait pas encore à quel point les réseaux de connexions corticocorticales entre les cortex sensoriels primaires en dépendent.

Objectif 3 : Effets de l'énucléation sur les connexions corticocorticales directes et réciproques entre le cortex visuel et somatosensoriel primaire de la souris

Notre troisième objectif était donc d'étudier, avec les méthodes utilisées lors de la 2^{e} étude, l'impact de la perte de la vision sur la microcircuiterie de ces connexions chez la souris énucléée à la naissance. On s'attend à ce que l'absence d'activité visuelle diminue la taille des boutons terminaux dans la projection de V1 vers S1. Les résultats de notre troisième étude démontrent que l'énucléation réduit le nombre de neurones afférents de S1 vers V1. L'énucléation réduit l'étendue de la taille des boutons terminaux et la taille des axones dans le cortex somatosensoriel primaire observés suite aux injections de dextran-biotine aminé dans le cortex visuel primaire. L'énucléation n'a pas d'effet sur la taille des axones et des boutons terminaux dans le cortex visuel primaire observés suite aux injections de dextran-biotine aminé dans S1. L'absence de gros boutons terminaux

dans la projection de V1 vers S1 chez les souris énucléées suggère que S1 ne reçoit plus les réponses postsynaptiques inductrices de Classe 1 de V1 et que V1 exerce alors une influence modulatrice prédominante sur S1. Notre troisième étude démontre que la cécité entraine des modifications anatomiques dans les connexions corticocorticales intermodales entre les cortex sensoriels primaires.

Résumé des objectifs de recherche

Le premier objectif de cette thèse était de faire l'évaluation quantitative et la cartographie de l'ensemble des afférences, corticales et sous-corticales, vers S1, à l'extérieur du champ de tonneaux, ainsi que la partie rostrale et caudale du champ de tonneaux, chez la souris. Le deuxième objectif de cette thèse était d'étudier la microcircuiterie des connexions corticocorticales directes et réciproques entre le cortex visuel primaire et le cortex somatosensoriel primaire chez la souris. Le troisième et dernier objectif de cette thèse était d'étudier l'impact de la perte de la vision sur la microcircuiterie des connexions entre le cortex visuel primaire et le cortex somatosensoriel primaire à l'aide d'un échantillon de souris énucléées à la naissance. Pour étudier les différences quantitatives dans le poids et la distribution laminaire des neurones et des terminaux dans les projections entre V1 et S1 chez les souris intactes et énucléées à la naissance, des injections de la sous-unité B de la toxine du choléra et de dextran-biotine aminé ont été réalisé dans V1 et S1 de ces deux groupes de souris.

Méthode

Dans cette thèse, l'organisation de la microcircuiterie des connexions corticocorticale entre les cortex visuel et somatosensoriel primaires sera étudiée dans l'optique d'améliorer la compréhension des réseaux corticaux impliqués dans la convergence multisensorielle. Il est donc nécessaire d'utiliser des modèles animaux, chez qui des méthodes plus invasives peuvent être employées.

Souris C57Bl/6 énucléée à la naissance

Énucléée à la naissance, la C57Bl/6 est un modèle de cécité permettant l'étude comparée des aspects anatomique de la réorganisation sensorielle chez les rongeurs aveugles. En effet, cette souris aura un développement normal des voies visuelles pendant la période embryonnaire, et c'est à la naissance, lors de l'énucléation, qu'elles seront coupées (Clancy, Darlington, & Finlay, 2001). Le thalamus visuel aura donc été innervé pendant une courte durée par les afférences rétiniennes. En effet, les connexions entre la rétine et le CGLd ont pu s'établir vers le 14^{ième} jour embryonnaire (E14), mais ont été détruites brusquement 6 jours plus tard. De plus, cette déafférentation survient avant la mise en place définitive de la couche 4 et avant l'arrivée des fibres thalamocorticales. Cependant, les neuroblastes ont été influencés dans la sous-plaque pendant environ 2 jours par l'activité spontanée présente dans les fibres rétiniennes atteignant le CGLd. Suite à l'énucléation, les nerfs optiques, le chiasma et les tractus optiques régressent. Il y a alors mort et dégénérescence des voies rétiniennes.

Énucléation néonatale

Les énucléations bilatérales des souriceaux C57Bl/6 ont été effectuées dans les 24h suivant la naissance sous anesthésie profonde par hypothermie. La fente palpébrale a été ouverte avec un scalpel, le globe oculaire a été doucement retiré et le nerf optique a été sectionné. Les orbites oculaires ont été remplies avec du Gelfoam (Upjohn, Kalamazoo, MI, USA) et les nouveau-nés ont été réchauffés jusqu'à leur éveil complet avant d'être remis dans leur cage.

Traçage neuronal

Puisque le traçage de connexions neuronales est central aux trois études effectuées dans cette thèse, il est nécessaire d'aborder plus en profondeur ce sujet et de définir les notions de transport antérograde et rétrograde, et de donner les particularités des deux traceurs qui ont été choisis pour les expériences : la sous-unité B de la toxine du choléra (CTb) et le dextran-biotine aminé (DBA).

Transports antérograde et rétrograde

Le neurone a besoin d'une quantité importante de protéines (neurotransmetteurs, neuropeptides, protéines du cytosquelette, etc.) pour subvenir à ses besoins et assurer ses fonctions. Puisque les ribosomes, structures impliquées dans leur biosynthèse, sont presque absents du cytoplasme des axones et de la partie terminale synaptique, la synthèse des protéines s'effectue principalement dans le corps cellulaire (Bear et al., 2007). Pour acheminer les protéines nouvellement synthétisées jusqu'à l'extrémité de

l'axone, le neurone utilise le transport axonal. Lorsque le transport de molécules dans un axone s'effectue du corps cellulaire vers les terminaisons synaptiques, on parle de transport antérograde (voir Figure 10). Par exemple, les neurotransmetteurs synthétisés dans le corps cellulaire sont transportés antérogradement dans des vésicules et libérés dans la fente synaptique par le neurone présynaptique (Bear et al., 2007). En plus du transport antérograde, le transport rétrograde permet de faire remonter des molécules de la partie terminale vers le corps cellulaire (voir Figure 10). Ce transport est utilisé lorsque la partie terminale du neurone envoie des signaux au corps cellulaire pour l'informer des modifications dans les besoins métaboliques des terminaisons (Bear et al., 2007). Dans d'autres cas, il peut être utilisé pour rapatrier diverses molécules vers le corps cellulaires dans le but de les dégrader, les recycler ou les réparer (Guénard, 1996).

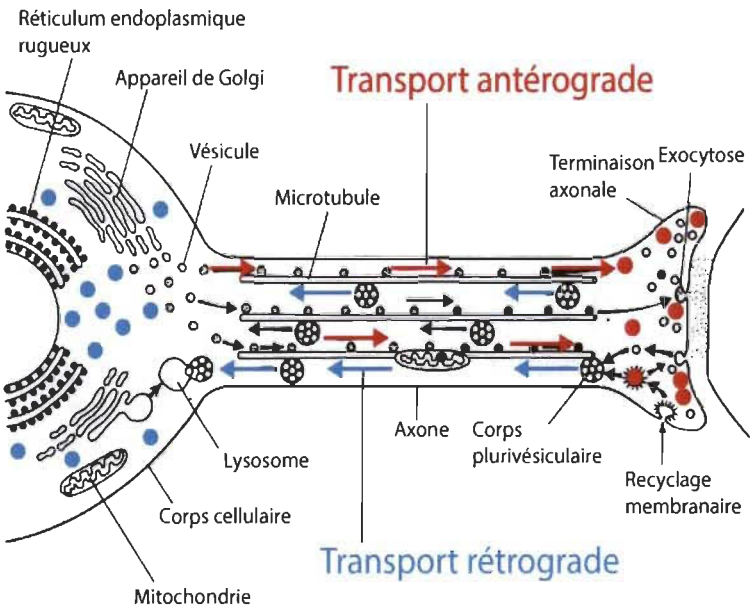

Figure 10. Transport axonal antérograde en rouge et transport axonal rétrograde en bleu. http://schwann.free.fr/neurobiologie_cellulaire03.html Université Montpellier.

Les éléments transportés, telles les protéines, sont stockés la plupart du temps dans des vésicules synaptiques. Ce sont ces vésicules qui sont transportées le long de l'axone. Le transport des vésicules est en partie assuré par des éléments du cytosquelette : les microtubules, les neurofilaments et les microfilaments (Guénard, 1996). De plus, pour chaque type de transport, une protéine spécifique sert de transporteur en se déplaçant le long du cytosquelette par un processus dépendant de l'ATP et du calcium. Il s'agit de la kinésine pour le transport antérograde et il s'agit de la dynéine pour le transport rétrograde (Oztas, 2003).

Une grande majorité de traceurs neuronaux utilise le transport neuronal de l'axone pour voyager. Lorsque le traceur a les caractéristiques nécessaires pour utiliser le transport rétrograde, il est incorporé au niveau des terminaisons axonales et remonte vers le corps cellulaire. Sur une coupe histologique, on pourra y remarquer le corps cellulaire et parfois même les dendrites remplies de traceur. Puisque le traceur remonte le long de l'axone pour revenir à la source des influx nerveux, il indique donc les afférences du site d'injection, c.-à-d. ce qui projette vers le site d'injection. Contrairement au traceur rétrograde, un traceur antérograde est incorporé au niveau du corps cellulaire ou de l'axone et migre vers la partie terminale. Il indique donc, en marquant les axones, les terminaisons axonales et parfois même les boutons synaptiques, les efférences du site d'injection, c.-à-d. les cibles des neurones qui ont incorporés le traceur au site d'injection. Le transport axonal rétrograde et antérograde n'a pas la même vitesse de déplacement. Le transport rétrograde s'effectue à une vitesse de 100 à 200 mm/jour et le

transport antérograde à une vitesse allant de 0.1 à 400 mm/jour (Oztas, 2003). Ce dernier est souvent classé selon 2 sous-types de transport, un lent (0.1 à 6 mm/jour) et un rapide (200 à 400 mm/jour). Le transport lent serait utilisé par la cellule pour véhiculer des éléments servant à la réparation graduelle et constante de sa structure et remplacer des sous-unités du cytosquelette neuronal. Le transport rapide servirait plutôt à transporter des vésicules synaptiques et des neurotransmetteurs (Oztas, 2003). Il serait aussi responsable du transport des traceurs neuronaux. Néanmoins, la vitesse de déplacement des traceurs neuronaux à l'intérieur des cellules dépend surtout de la composition moléculaire du traceur et du mécanisme de capture du traceur par le neurone. Les traceurs utilisés dans ces études seront discutés dans les prochaines sections.

Sous-unité B de la toxine du choléra. La sous-unité B de la toxine du choléra (CTb) a été introduite comme traceur rétrograde durant l'année 1977 (Sawchenko & Gerfen, 1985; Stoeckel, Schwab, & Thoenen, 1977). La toxine du choléra provient de la bactérie Vibrio choléra et sa sous-unité B est non-toxique et est la molécule responsable du transport du marqueur dans les neurones (Sawchenko & Gerfen, 1985). La CTb fait partie de la même classe de traceur que les lectines à cause de sa capacité à se fixer aux surfaces glycoconjuguées. En effet, la CTb se lie spécifiquement aux monosialoganglioside (Sawchenko & Gerfen, 1985). La CTb est un traceur rétrograde très sensible (Luppi, Fort, & Jouvet, 1990; Luppi, Sakai, Salvert, Fort, & Jouvet, 1987). C'est pour cette raison que nous l'avons choisi. C'est aussi un excellent traceur antérograde. La CTb est incorporée activement dans les vésicules des axones lésés et

celles-ci seraient transportées le long du cytosquelette des axones et des dendrites (Angelucci, Clasca, & Sur, 1996; Luppi et al., 1990). Le traceur reste dans les vésicules tout au long de son cheminement dans le neurone. Par la suite, les vésicules s'accumulent dans le corps cellulaire ce qui lui confère une apparence granulaire, et conséquemment, ne montre pas toute la morphologie du neurone (Kobbert et al., 2000). Pour visualiser les axones et les boutons lors des injections dans le cortex visuel primaire et le champ de tonneaux du cortex somatosensoriel primaire dans le deuxième et le troisième article, nous avons préféré utiliser le DBA (Luppi et al., 1990).

Le temps de survie chez l'animal peut varier entre 1 à 10 jours (Vercelli, Repici, Garbossa, & Grimaldi, 2000), mais étant donné que la sous-unité B de la toxine du choléra voyage rapidement dans les axones (Luppi et al., 1990) et que le cerveau de la souris est petit, le temps de survie dans ces travaux se situait entre 2 et 3 jours. Au-delà de ce temps, il y avait plus de chance que le traceur soit incorporé dans les fibres de passages lésées (Vercelli et al., 2000) ou qu'il voyage au-delà des synapses par le passage transsynaptique. La sous-unité B de la toxine du choléra peut être injectée par pression ou par iontophorèse (Luppi et al., 1990). Lorsqu'injectée par pression, les cellules au site d'injection sont souvent nécrosées, surtout si l'injection est massive, et cela peut venir interférer avec le captage du traceur dans les axones lésés. Injectée par iontophorèse, le site d'injection est généralement plus petit et la nécrose cellulaire est faible (Luppi et al., 1990) la sous-unité B de la toxine du choléra peut être révélée par immunohistochimie.

Dextran-biotine aminé. Le dextran-biotine aminé (DBA) est un traceur neuronal très utilisé depuis le début des années 1990. Sa structure moléculaire est constituée de sucres couplés à une biotine. L'affinité de la biotine pour l'avidine permet de révéler ce traceur par une histochimie du complexe avidine-biotine (système ABC). Il peut être injecté par pression ou par iontophorèse étant donné la charge anionique qu'il porte (Reiner et al., 2000). Son poids moléculaire peut varier entre 3 000 et 20 000 D. Les DBA de faible poids moléculaire (3kD) sont préférentiellement transportés rétrogradement, alors que ceux du plus haut poids moléculaire (10kD) sont surtout transportés antérogradement (Reiner et al., 2000). Les DBA sont facilement incorporés dans les axones endommagés et moins bien par les terminaisons nerveuses (Jiang, Johnson, & Burkhalter, 1993; Kobbert et al., 2000). L'incorporation des DBA dans les axones endommagés s'effectue par diffusion, alors que le transport du traceur par les neurones intacts, ce qui est plus rare, s'effectuerait par endocytose (Reiner et al., 2000). Le temps de survie chez l'animal suite à l'injection peut varier entre 2 et 21 jours dépendamment de la distance que le traceur doit parcourir pour marquer la cible d'intérêt (Vercelli et al., 2000). Dans ces travaux, le temps de survie chez la souris était de 7 jours. Lorsque le temps de survie de l'animal est long, le risque de transport transynaptique est très faible (Brandt & Apkarian, 1992).

Les DBA comportent plusieurs avantages. Ils sont parmi les meilleurs traceurs neuronaux puisqu'ils marquent les fins détails neuronaux (Brandt & Apkarian, 1992; Kobbert et al., 2000; Reiner et al., 2000). La méthode de détection est rapide et facile

d'exécution comparativement à bien d'autres traceurs (Brandt & Apkarian, 1992; Veenman, Reiner, & Honig, 1992). La stabilité de sa structure moléculaire est propice à l'observation et l'entreposage à long terme (Brandt & Apkarian, 1992). Il est aisé, lorsqu'injecté par iontophorèse, de restreindre la taille du site d'injection, ce qui permet de faire des études topographiques (Reiner et al., 2000). Ce traceur est intéressant puisqu'il offre un marquage homogène le long des axones et de leurs terminaisons (Lanciego & Wouterlood, 2011). Toutes ces raisons en ont fait un traceur de choix dans le cadre de deux des articles publiés.

Par contre, il existe quelques désavantages à l'utilisation des DBA. D'abord, il est possible que les fibres de passage qui ont été endommagées durant l'injection soient marquées (Brandt & Apkarian, 1992; Vercelli et al., 2000), ce qui pourrait fausser la validité des résultats en marquant une plus grande proportion de cellules qui ne seraient pas originaires du site d'injection. Puis, lors de l'utilisation du DBA 3kD, le traçage rétrograde est capricieux, c.-à-d. qu'une partie seulement des corps neuronaux sont marqués, ce qui ne facilite pas les études quantitatives (Vercelli et al., 2000). C'est principalement pour cette raison que nous avons décidé d'utiliser un autre traceur pour le marquage rétrograde, la sous-unité B de la toxine du choléra.

Chapitre I

Cortical and subcortical afferent connections of the primary somatosensory cortex of the mouse[1]

[1] Le contenu de ce chapitre est présenté sous forme de manuscrit qui sera dans la revue Journal of Comparative Neurology: Massé, I.O., Blanchet-Godbout, S., Bronchti, G. et Boire, D.

Title: Cortical and subcortical afferent connections of the primary somatosensory cortex of the mouse.

Authors: Ian O. Massé, Sohen Blanchet-Godbout, Gilles Bronchti, Denis Boire

Affiliations:

Département d'anatomie
Université du Québec à Trois-Rivières
Canada, G9A 2W7

Running title: Primary somatosensory cortex connections.

Abstract: Sensory information in conveyed from peripheral receptors through specific thalamic relays to primary areas of the cerebral cortex. Information is then routed to specialized areas for the treatment of specific aspects of the sensory signals and to multisensory associative areas. Information processing in primary sensory cortices is influenced by contextual information from top-down projections of multiple cortical motor and associative areas as well as areas of other sensory modalities and higher order thalamic nuclei. The primary sensory cortices are thus located at the interface of the ascending and descending pathways. The theory of predictive coding implies that the primary areas are the site of comparison between the sensory information expected as a function of the context and the sensory information that comes from the environment. In order to better understand the anatomical basis of this model of sensory systems we have charted the cortical and subcortical afferent inputs in the ipsilateral and contralateral hemispheres of the primary somatosensory cortex of adult C57Bl/6 mice. Iontophoretic injections of the b-fragment of cholera toxin were performed inside the mystacial caudal barrel field, more rostral barrel field and somatosensory cortex outside the barrel field to test the hypothesis that differences exist between these three parts and to compare their projections to the subnetworks built from the Mouse Connectome Project data. The laminar distribution of retrogradely labeled cell bodies was used to classify the projections as feedback, feedforward or lateral. Layer indices range between -1 and 1, indicating feedback and feedforward connections respectively. The primary

somatosensory cortex and the barrel field have afferent connections with somatosensory areas, non-somatosensory primary sensory areas, multisensory, motor, associative, and neuromodulatory areas. The caudal part of the barrel field displays different and more abundant cortical and subcortical connections compared to the rest of the primary somatosensory cortex. Layer indices of cortical projections to the primary somatosensory cortex and the barrel field were mainly negative and very similar for ipsilateral and contralateral projections. These data demonstrate that the primary somatosensory cortex receives sensory and non-sensory information from cortical and subcortical sources.

Keywords: Cross-modal, corticocortical connections, subcortical connections, feedforward, feedback, top-down, bottom-up.

Introduction

Sensory processing is based on countercurrent feedforward and feedback flow of information and the processing in the primary sensory cortices involves an interaction between these bottom-up thalamocortical and top-down direct corticocortical (Gilbert and Li, 2013; Makino and Komiyama, 2015; Mumford, 1992; Rao and Ballard, 1999; Zhang et al., 2014) and indirect cortico-thalamo-cortical pathways (Roth et al., 2016; Sherman, 2005; Sherman and Guillery, 2002; Theyel et al., 2010).

Recent evidence considers cortical areas as adaptive processors. Instead of making stereotypical processing of incoming sensory information, different analysis is performed as a function of both sensory and behavioral context. This contextual information can be provided to primary sensory cortices by varied top-down cortical projections and also by higher order thalamic nuclei (Budinger et al., 2006; Budinger & Scheich, 2009; Charbonneau et al., 2012; Miller & Vogt, 1984; Paperna & Malach, 1991; Zingg et al., 2014). It has been proposed that perception results from a reverberation between feedforward and feedback information and that neurons in early stages of sensory processing are adaptive processors multiplexing between functions as instructed by feedback projections from higher cortical areas (Gilbert and Li, 2013; Gilbert and Sigman, 2007).

Top-down processing in the visual system has been studied in many aspects showing the influence of cortical feedback onto the primary visual cortex and even back

to the thalamic lateral geniculate nucleus (Bullier, 2001a, 2001b; Lamme and Roelfsema, 2000; Sillito et al., 2006). Top-down modulation by feedback projections to early sensory processing is thought to achieve an integration of local and global levels of analysis (see Gilbert and Li, 2013; Teufel and Nanay, 2016 for review). Top-down modulation is also provided by non-sensory sources such as attention, expectation and stimulus context (Ito and Gilbert, 1999; Jiang et al., 2013; McManus et al., 2011; Roelfsema et al., 1998; Summerfield and de Lange, 2014; Summerfield and Egner, 2009) and memory (Moore and Cavanagh, 1998).

Moreover, several studies suggest conscious perception might depend on top-down inputs from higher order cortices to primary sensory cortices (Meyer, 2011). Indeed, early activity in primary sensory cortices is stimulus-bound whereas later activity thought to represent top-down incoming information from higher order cortical areas is correlated with conscious perception (Gutschalk et al., 2008; Hudetz et al., 2009; Meador et al., 2002; Super et al., 2001; see Meyer, 2011 for review).

Extensive inventories of cortical afferent have been drawn for the primary visual (Charbonneau et al., 2012), auditory (Budinger et al., 2006, 2008; Budinger and Scheich, 2009) and somatosensory cortices (Zingg et al., 2014) in rodents. Such extensive inventories are not available for other widely studied mammals such as primates and carnivores. In agreement with the wide range of processes that can modulate early sensory processing, these studies have shown a host of top-down cortical projections to

primary sensory cortices that comes from very diverse motor, association and also from cortices devoted to other sensory modalities supporting the particular position of primary cortices at the interface of ascending and descending pathways. Moreover, the laminar distribution of the cortical neurons projecting to primary visual and auditory cortices shows a wide range of structure, some projections arising almost exclusively from infragranular layers whereas other projections arise from all cortical layers (Budinger et al., 2006, 2008; Budinger and Scheich, 2009; Charbonneau et al., 2012).

Ascending and descending cortical projections have different morphological and functional features. Specifically, feedforward connections originate from neurons mainly located in supragranular layers 1 to 3 and terminate in the granular layer, whereas feedback connections originate mainly from neurons located in infragranular layers 5 and 6 and avoid the granular layer (Felleman and Van Essen, 1991; Rockland and Pandya, 1979). Lateral connections originate equally from infragranular and supragranular layers. A similar hierarchical organization of visual cortices based on feedback and feedforward corticocortical connections has been suggested for the rat (Coogan and Burkhalter, 1990, 1993; Sieben et al., 2013) and mouse (Berezovskii et al., 2011; Dong et al., 2004; Godement et al., 1979; Yamashita et al., 2003). In rodents however, feedforward projections terminate in all cortical layers, not only in granular layer 4 as in primates (Coogan and Burkhalter, 1990).

The somatosensory cortex of the mouse also has widespread cortical afferents (Zingg et al., 2014) as those of the visual and auditory cortices. There is evidence for four somatic sensorimotor subnetworks: orofaciopharyngeal, upper limb, lower limb and trunk, and whisker subnetworks (Zingg et al., 2014). This evaluation demonstrates that S1 subregions associated with different parts of the body do not all have the same connections. Our study extends this knowledge in providing a quantitative evaluation of afferent cortical and thalamic projections to the primary somatosensory cortex and a laminar distribution of cortical neurons in order to compare the structure of these numerous corticothalamic top-down connections. Moreover, these features were compared between afferent connections to the mystacial caudal barrel field, more rostral barrel field and somatosensory cortex outside the barrel field to see if the different somatosensory subnetworks follow similar patterns of cortical connectivity.

Methods

Animals and experiment groups

Animals were treated in accordance with the regulations of the Canadian Council for the Protection of Animals and the study was approved by the Comité de bons soins aux animaux de l'Université du Québec à Trois-Rivières. C57Bl/6 mice ($n = 15$) (Charles River, Montreal, QC, Canada) from our colonies were used. All animals were kept under a light/dark cycle of 14/10 hours and were adults (60 days) when sacrificed.

Tracing procedures

Surgical anesthesia was achieved and maintained with inhalation of 1.5-2.5% isoflurane and vital signs were monitored throughout the procedures. The animals were mounted on a stereotaxic apparatus. A scalp incision was made along the midline to expose the skull. For injections in the primary somatosensory cortex (S1), a small craniotomy was performed 1.5 mm caudal to Bregma and 1.5 mm from the midline or, for injections in the rostral and caudal parts of the barrel field of the primary somatosensory cortex (S1BF), 0.9 mm caudal to Bregma and 2.9 mm from the midline, and 1.5 mm caudal to Bregma and 2.9 mm from the midline respectively. The dura was incised and a glass micropipette (20 μm tip diameter) filled with 1% solution of the b-fragment of cholera toxin (CTb) (Lists Biological Laboratories, CA) in phosphate-buffered saline (PBS) was inserted into the cortex into S1 of 5 animals and S1BF of 10 animals. A 1.5 μA positive current with a 7-s duty cycle was applied for 10 min at depths ranging between 100 and 500 μm from the pial surface. Starting at a depth of 500 μm and ending at 100 μm from the pial surface, 2 min at each 100 μm. The mice were kept warm until they recovered from anesthesia. Postoperative pain was managed with buprenorphine (Temgesic, Schering-Plough, Hertfordshire, UK; i.p.; 0.009 mg/kg) injected at the beginning of the procedure.

Perfusion

After a 2-day survival, mice received an intraperitoneal injection of 120 mg/kg sodium pentobarbital (Euthanyl; Bimeda-MTC, Cambridge, ON, Canada) and were

perfused through the heart with 0.1 m 0.9% PBS (pH 7.4) followed by phosphate-buffered 4% paraformaldehyde. Brains were harvested, postfixed for 1-2 hours, cryoprotected with 30% sucrose and frozen prior to sectioning for CTb immunohistochemistry processing.

Staining procedures

Serial 50-μm-thick coronal sections were taken using a freezing microtome. One series was processed for CTb immunohistochemistry and the other series was mounted on slides and stained with cresyl violet to identify the cortical areas of interest and to differentiate the cortical layers. To visualize CTb labeled neurons, free-floating sections were treated for 45 min with 0.15% H2O2 and 70% methanol to quench endogenous peroxidase, and thoroughly rinsed in 0.05 M Tris-HCl-buffered 0.9% saline solution (TBS, pH 8.0) containing 0.5% Triton X-100 (TBS-Tx). Sections were then incubated in 2% normal donkey serum (NDS) for 2 hours and transferred to a solution of primary antibody (goat polyclonal anti-CTb 1:4 000; Molecular Probes) with 1% NDS in PBS-Tx for 2 days at 4°C. Subsequently, sections were rinsed in PBS-Tx and incubated in a secondary antibody (biotinylated donkey anti-goat; 1:500; Molecular Probes) solution with 1% NDS in PBS-Tx for 2 hours at room temperature. Following further rinsing, the sections were then incubated for 90 min in an avidin-biotin complex solution (Elite Vectastain, Vector Laboratories, PK4000 Standard kit) in TBS-Tx, pH 8.0, rinsed in TBS, and then incubated in a 0.015% '3-diaminobenzidine (DBA) solution. Labeled neurons were revealed by the addition of 0.005% H2O2. Sections were washed and

mounted on gelatin-subbed slides, air-dried, dehydrated and cover-slipped with Permount mounting media (Fisher Scientific, Ottawa, ON, Canada).

Data analysis

All retrogradely labeled neurons found on one of every two sections immunostained for CTb labeling, distributed throughout the whole rostro-caudal extent of the brain, were plotted using an Olympus BX51WI microscope (20 x 0.75 NA objective) equipped with a three-axis computer-controlled stepping motor system (0.05 μm resolution) coupled to a personal computer and to a color Optronix CCD camera and driven by the Neurolucida software (MBF Biosciences, Williston, VT, USA). In this way, the whole cortex was systematically and randomly sampled on sections 200 μm apart. Cortical and subcortical areas were delineated at lower magnification (4 x 0.16 NA objective) on adjacent Nissl-stained sections. Borders between cortical and subcortical areas were delineated according to the cytoarchitectonic descriptions provided by Caviness (1975) and the mouse brain atlas of Franklin and Paxinos (2008). Contours of each cortical and subcortical area in which retrogradely labeled cells were located were traced with Neurolucida and the limits of each cortical layer were traced. These contours were superimposed on the images of CTb-reacted sections and resized for shrinkage differences between the Nissl and CTb sections. This allowed plotted neurons in each cortical area to be assigned to supragranular, granular or infragranular layers for the calculation of layer indices. These indices provide a quantitative assessment of the laminar distribution of retrogradely labeled neurons and are instrumental in the

classification of corticocortical feedback, feedforward and lateral connections (Felleman and Van Essen, 1991). Layer indices (L) were calculated using the formula where S and I are the numbers of labeled neurons in supragranular and infragranular layers respectively (Budinger et al., 2006, 2008; Budinger and Scheich, 2009):

$$L = (S - I) / (S + I)$$

The indices range between -1 and 1. Negative values indicate feedback connections mostly originating in infragranular layers and positive values indicate feedforward connections mostly originating in supragranular layers. Values near zero indicate lateral connections. The relationship between the abundance of labeled neurons in the ipsilateral cortex and the distance for all three injection sites was evaluated by measuring the shortest physical distance between the center of the injection sites and each labeled neuron in each area with Neurolucida.

All photomicrographs were cropped and luminosity and contrast were adjusted with Adobe Photoshop software. Localization of injections sites was illustrated from sections charts extracted from Neurolucida Explorer software (MBF Biosciences).

Data comparison to the Mouse Connectome Project

The afferent cortical and subcortical projections to S1 from our animals were compared to those reported for S1 injection cases made public on the website of the corticocortical connectivity atlas of Mouse Connectome Project (MCP,

www.MouseConnectome.org) through an interactive visualization tool, the iConnectome. In these cases, double co-injections of tracers were made into the barrel field and the lower and upper limb region of S1 of 8 week old male C57Bl/6 mice ($n = 10$). Retrograde labeling was achieved through injections of either CTb or Fluorogold. All retrogradely labeled neurons were noted to obtain a qualitative assessment of their presence.

Antibody characterization

The Anti-Cholera B Subunit antibody (Product # 703, Lists Biological Laboratories) was raised in goat using Cholera B Subunit (Product #104) as the immunogen. The antibody was tested in an immuno-diffusion assay. A 1:4 dilution of the Anti-Cholera B Subunit sera formed an immunoprecipitation during interaction with a 0.5mg/ml solution of Cholera B Subunit (Product #104). The sera showed no reaction in a similar assay against diphtheria toxin (Product #150) or Pertussis Toxin (Product #180).

Statistical analysis

Statistical analyses were performed using SPSS v 16.0 software (SPSS, Chicago, IL, USA). To test for significance of the differences in the relative abundance of labeled neurons, and the layer indices in each cortical area between injection sites, Kruskal-Wallis and Tukey HSD tests were performed with a significance level of $p < 0.05$.

Results

CTb labeling

Representative CTb injection sites in the somatosensory cortex are illustrated in Figure 11A (S1), in the rostral part of the somatosensory barrel field in Figure 11B (S1BF) and in the caudal part of the somatosensory barrel field in Figure 11C (S1BF). None of the injections involved the underlying white matter. Cases were considered valid only if injections in S1 retrogradely labeled neurons in the ventral posterior lateral thalamic nucleus (VPL) (see Figure 11D) and if injections in the rostral and caudal parts of S1BF, retrogradely labeled neurons in the ventral posterior medial nucleus (VPM) (see Figures 11E and 11F). In all cases, CTb injections in S1 and S1BF retrogradely labeled numerous neuronal cell bodies in cortical and subcortical structures in all experiments for all the three animal groups. CTb-labeled neurons in the cortex after an injection into the caudal part of the barrel field of S1 are represented in Figure 12. All the telencephalic and thalamic afferent connections of S1 were mapped and are represented in Figure 13.

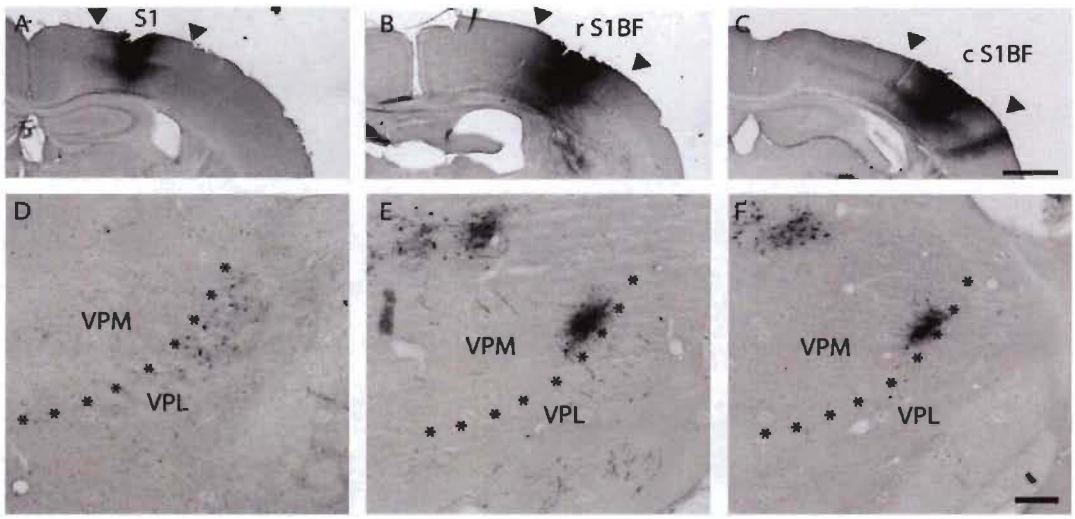

Figure 11. Tracer injection sites and distribution of retrogradely labeled neurons in the somatosensory thalamus. Photomicrographs of coronal sections from representative cases, showing CTb injection site in S1 (A), the rostral (B) and caudal (C) parts of the barrel field of S1 with retrogradely labeled neurons in VPL (D) and VPM (E/F) respectively. Scale: 1000 μm (A/B/C) and 200 μm (D/E/F).

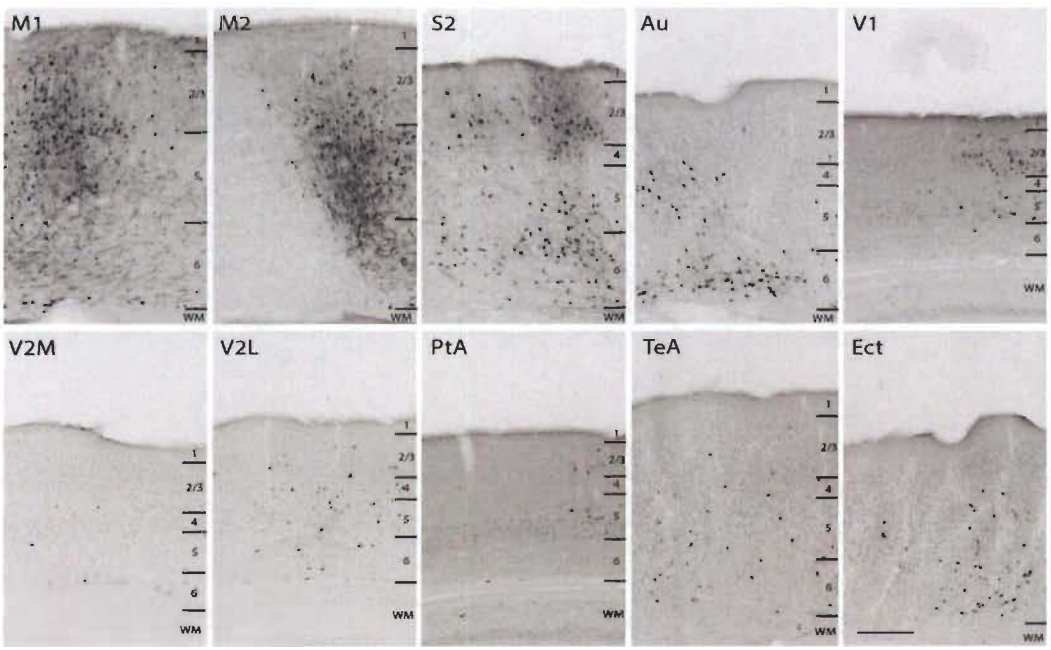

Figure 12. CTb-labeled neurons in the cortex after an injection into the posterior part of the barrel field of S1. Scale: 250 μm.

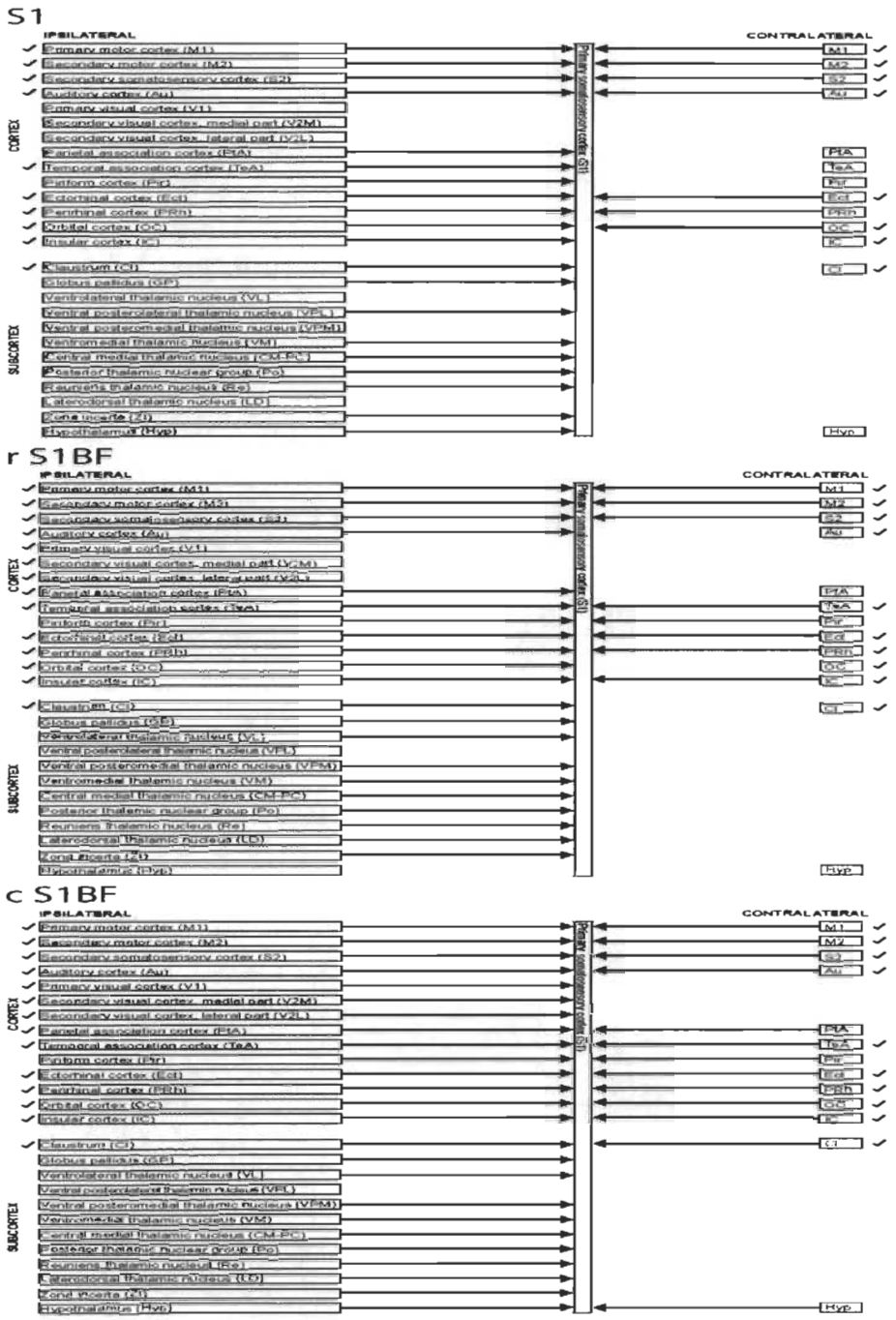

Figure 13. Diagram of the afferent connections of the primary somatosensory cortex (S1) of the C57Bl/6 mouse. Each box represents a brain structure which is connected with S1 or the rostral or caudal parts of S1BF. The target of a projection is represented by an arrow. Checkmarks next to the boxes represent a brain structure which is connected with the barrel field or the lower or upper limb regions of S1 that was presented in the Mouse Connectome Project.

Cortical projections to S1

Following injections in S1, many labeled neurons were observed within the somatosensory cortex surrounding the injection sites. These local intra-areal projections were not included in our connectivity charts and were not quantified. In addition, many retrogradely labeled neurons were found in the ipsilateral primary (M1) and secondary (M2) motor cortices and in the secondary somatosensory cortex (S2). Neurons were also found in cortices dedicated to other sensory modalities such as the primary auditory (Au), and in the olfactory piriform (Pir) cortex. Neurons were also observed in association cortices such as the parietal (PtA) and temporal association (TeA), ectorhinal (Ect), perirhinal (PRh), orbital (OC) and insular (IC) cortices. Most of these connections were also observed in the mouse connectome material except the projections to S1, outside the barrel field, from the parietal association and piriform cortex which were not charted. We did not observe projections from the claustrum to this portion of S1 whereas these projections were reported in the mouse connectome. Labeled neurons were also found in retrosplenial granular and dysgranular (RSG and RSD respectively), prelimbic (PrL), infralimbic (IL), dorsal peduncular (DP) and cingulate (Cg) cortices and in the dentate gyrus (DG) but because of the very low number of labeled neurons and inconsistent occurrence of labeled neurons between our cases, these areas were not included in the statistical analysis. The same ipsilateral cortical projections were observed following injections in the rostral somatosensory barrel field. However injections in the more caudal aspect of the barrel field produced retrograde labeling of neurons in the primary visual (V1) cortex and in the medial and lateral extrastriate visual

areas (V2M and V2L). Injections in both rostral and caudal barrel field produced retrogradely labeled neurones in the claustrum.

Callosal projections to the somatosensory cortex were more restricted than ipsilateral projections (see Figure 13). Injections in the three parts of the somatosensory cortex labeled homospecific callosal neurons in the somatosensory cortex and neurons in contralateral motor cortices, M1 and M2, secondary somatosensory cortex and auditory cortices and from ectorhinal, perirhinal and orbital cortices. These were also charted in the mouse connectome database along with other projections from infralimbic cortex and claustrum. The injections in the rostral and caudal barrel field labeled similar ipsi- and contralateral cortical areas with the exception of the three visual areas, V1, V2M and V2L. The absence of heterospecific visual callosal projections to the caudal barrel field was also found in the mouse connectome database.

Comparing our results with the Mouse Connectome Project (MCP), we find that many of the ipsilateral and contralateral corticocortical projections observed in our analysis are registered in the MCP and that the MCP contains reports of some additional retrograde projections from the ipsilateral Cl and contralateral IC and Cl to the lower limb and upper limb representations of S1, outside of the barrel field, as seen by the checkmarks next to the corresponding boxes in Figure 13. Our injections outside of the barrel field cover both the forelimb and hindlimb representations of S1 which correspond to both the upper limb and lower limb representations of S1 in the MCP

respectively. The MCP also contains reports of retrograde projections to the barrel field but precise information on the injection coordinates for each individual case is not available on the iConnectome tool. This means that each individual case available on the MCP website could not be related to either the rostral or the caudal part of S1BF from our own material. A list of our cases that received CTb injections in the primary somatosensory cortex (S1) outside the barrel field, in the rostral (rS1BF) and caudal (cS1Bf) barrel field and the cases used from the MCP corticocortical connectivity atlas that received CTb or Fluorogold (FG) injections in the primary somatosensory barrel field (SSp-bfd), lower limb (SSp-ll), and upper limb (SSp-ul) areas is given in Table 2.

The relative weight of ipsilateral (see Table 3) and contralateral (see Table 4) cortical connections to S1 and the rostral; and caudal parts of S1BF were quantified in each experimental case. All the injection sites in the somatosensory cortex labeled many neurons in the ipsilateral motor cortices M1 and M2, in the secondary somatosensory cortex and in other ipsilateral cortical fields. More robust projections arose from the auditory and visual cortices as well as from parietal and temporal association cortices. As observed in other studies, the percentage of labeled neurons in each cortex was quite variable making strong statistical decisions on group differences less powerful. Several cortices such as RSG, RSD, PrL, IL, DP, Cg and DG comprised less than 1% of the total number of labeled cortical neurons.

Table 2

List of our cases that received CTb injections in the primary somatosensory cortex (S1) outside the barrel field, in the rostral (rS1BF) and caudal (cS1Bf) barrel field and the cases used from the MCP corticocortical connectivity atlas that received CTb or Fluorogold (FG) injections in the primary somatosensory barrel field (SSp-bfd), lower limb (SSp-ll), and upper limb (SSp-ul) areas

Our cases CTB injections			MCP cases			
Injection site	Case	Coordinates (mm) AP/ML/depth	Injection site	Case	Tracer	Coordinates (mm) AP/ML/depth
S1	02-03a4	1.5/1.5/0.1-0.5	SSp-bfd	SW110420-01	CTB	4.0/-0.08/1.12
	02-03a5	1.5/1.5/0.1-0.5		SW110322-04	NA	NA
	02-03a3	1.5/1.5/0.1-0.5		SW110419-03	CTB	3.1/-0.88/0.9
	02-03a6	1.5/1.5/0.1-0.5		SW110419-01	NA	NA
	02-03a7	1.5/1.5/0.1-0.5		SW110322-01	NA	NA
				SW110418-01	NA	NA
r S1BF	03-02b2	0.9/2.9/0.1-0.5		SW110420-03	NA	NA
	03-04a6	0.9/2.9/0.1-0.5				
	03-04a7	0.9/2.9/0.1-0.5	SSp-ll	SW110419-04	NA	NA
	03-04b4	0.9/2.9/0.1-0.5				
	03-04b5	0.9/2.9/0.1-0.5	SSp-ul	SW110419-02	CTB	2.3/0.75/0.8
				SW110516-01	NA	NA
c S1BF	03-02b7	1.5/2.9/0.1-0.5				
	04-01b2	1.5/2.9/0.1-0.5				
	03-02b4	1.5/2.9/0.1-0.5				
	03-02b5	1.5/2.9/0.1-0.5				
	03-02b6	1.5/2.9/0.1-0.5				

Table 3

Number and percentage (in parentheses) of retrogradely labeled neurons in sensory and non-sensory cortical areas in the ipsilateral hemisphere after injections of CTb into the primary somatosensory cortex (S1) of intact C57Bl/6 mice

Injection site	Case	Cortical area (ipsi)					
		M1	M2	S2	Au	V1	V2M
S1	02-03a4	638 (24.13)	148 (5.60)	720 (27.23)	584 (22.09)	0 (0)	0 (0)
	02-03a5	832 (22.75)	438 (11.97)	1736 (47.46)	140 (3.83)	0 (0)	0 (0)
	02-03a3	688 (22.21)	222 (7.17)	974 (31.44)	474 (15.30)	0 (0)	0 (0)
	02-03a6	368 (19.73)	147 (7.88)	614 (32.92)	181 (9.71)	0 (0)	0 (0)
	02-03a7	1176 (22.24)	549 (10.38)	2223 (42.05)	378 (7.15)	0 (0)	0 (0)
	Mean ± SEM	740.40 ± 147.91 (22.21 ± 0.80)	300.80 ± 91.39 (8.60 ± 1.28)	1253.4 ± 348.61 (36.22 ± 4.14)	351.40 ± 94.73 (11.61 ± 3.60)	0 ± 0 (0 ± 0)	0 ± 0 (0 ± 0)
r S1BF	03-02b2	170 (9.65)	832 (47.22)	296 (16.80)	0 (0)	0 (0)	0 (0)
	03-04a6	1376 (60.09)	122 (5.33)	492 (21.49)	6 (0.26)	0 (0)	0 (0)
	03-04a7	1650 (36.85)	1324 (29.57)	404 (9.02)	200 (4.47)	0 (0)	0 (0)
	03-04b4	1364 (30.41)	1416 (31.57)	736 (16.41)	50 (1.12)	0 (0)	0 (0)
	03-04b5	1060 (29.66)	1190 (33.30)	478 (13.37)	84 (2.35)	0 (0)	0 (0)
	Mean ± SEM	1124.0 ± 286.36 (33.33 ± 9.05)	976.80 ± 263.46 (29.40 ± 7.57)	481.20 ± 81.13 (15.42 ± 2.30)	68.00 ± 40.68 (1.64 ± 0.91)	0 ± 0 (0 ± 0)	0 ± 0 (0 ± 0)
c S1BF	03-02b7	148 (7.18)	209 (10.14)	415 (20.14)	151 (7.33)	546 (26.49)	10 (0.46)
	04-01b2	726 (23.61)	573 (18.63)	582 (18.93)	365 (11.87)	76 (2.47)	8 (0.26)
	03-02b4	800 (13.69)	1510 (25.85)	600 (10.27)	409 (7.00)	400 (6.85)	69 (1.18)
	03-02b5	929 (14.88)	1197 (19.16)	1181 (18.91)	1063 (17.02)	154 (2.47)	93 (1.49)
	03-02b6	450 (16.43)	323 (11.79)	1117 (40.78)	121 (4.42)	33 (1.21)	3 (0.11)
	Mean ± SEM	610.60 ± 156.20 (15.16 ± 2.95)	762.40 ± 283.17 (17.12 ± 3.16)	779.00 ± 173.06 (21.80 ± 5.67)	421.80 ± 190.12 (9.53 ± 2.49)	241.80 ± 110.78 (7.90 ± 5.31)	36.60 ± 20.74 (0.71 ± 0.30)

Table 3

Number and percentage (in parentheses) of retrogradely labeled neurons in sensory and non-sensory cortical areas in the ipsilateral hemisphere after injections of CTb into the primary somatosensory cortex (S1) of intact C57Bl/6 mice (continued)

Injection site	Case	Cortical area (ipsi)					
		V2L	PtA	TeA	RSGc	RSD	Ect
S1	02-03a4	0 (0)	218 (8.25)	108 (4.09)	0 (0)	0 (0)	194 (7.34)
	02-03a5	0 (0)	236 (6.45)	12 (0.33)	6 (0.16)	32 (0.88)	104 (2.84)
	02-03a3	0 (0)	224 (7.23)	84 (2.71)	8 (0.26)	36 (1.16)	172 (5.55)
	02-03a6	0 (0)	114 (6.11)	30 (1.61)	8 (0.43)	26 (1.39)	75 (4.02)
	02-03a7	0 (0)	348 (6.58)	57 (1.08)	9 (0.17)	37 (0.70)	192 (3.63)
	Mean ± SEM	0 ± 0 (0 ± 0)	228.00 ± 41.52 (6.92 ± 0.42)	58.20 ± 19.49 (1.96 ± 0.74)	6.20 ± 1.82 (0.20 ± 0.08)	26.20 ± 7.64 (0.83 ± 0.27)	147.40 ± 27.26 (4.68 ± 0.89)
r S1BF	03-02b2	0 (0)	0 (0)	0 (0)	0 (0)	0 (0)	36 (2.04)
	03-04a6	0 (0)	0 (0)	2 (0.09)	0 (0)	2 (0.09)	80 (3.49)
	03-04a7	0 (0)	92 (2.05)	18 (0.40)	10 (0.22)	40 (0.89)	418 (9.34)
	03-04b4	0 (0)	0 (0)	10 (0.22)	12 (0.27)	36 (0.80)	230 (5.13)
	03-04b5	0 (0)	30 (0.84)	10 (0.28)	8 (0.22)	26 (0.73)	228 (6.38)
	Mean ± SEM	0 ± 0 (0 ± 0)	24.40 ± 19.98 (0.58 ± 0.45)	8.00 ± 3.61 (0.20 ± 0.08)	6.00 ± 2.83 (0.14 ± 0.07)	20.80 ± 9.40 (0.50 ± 0.21)	198.40 ± 75.20 (5.28 ± 1.40)
c S1BF	03-02b7	100 (4.85)	13 (0.63)	42 (2.04)	8 (0.39)	14 (0.68)	215 (10.43)
	04-01b2	37 (1.20)	185 (6.02)	88 (2.86)	4 (0.13)	24 (0.78)	245 (7.97)
	03-02b4	230 (3.94)	168 (2.88)	145 (2.48)	37 (0.63)	146 (2.50)	274 (4.69)
	03-02b5	115 (1.84)	352 (5.64)	234 (3.75)	70 (1.12)	163 (2.61)	231 (3.70)
	03-02b6	20 (0.73)	166 (6.06)	17 (0.62)	4 (0.15)	23 (0.84)	235 (8.58)
	Mean ± SEM	100.40 ± 41.45 (2.51 ± 0.90)	176.80 ± 60.10 (4.24 ± 1.21)	105.20 ± 43.48 (2.35 ± 0.58)	24.60 ± 14.45 (0.48 ± 0.21)	74.00 ± 36.92 (1.48 ± 0.49)	240.00 ± 10.93 (7.07 ± 1.40)

Table 3

Number and percentage (in parentheses) of retrogradely labeled neurons in sensory and non-sensory cortical areas in the ipsilateral hemisphere after injections of CTb into the primary somatosensory cortex (S1) of intact C57Bl/6 mice (continued)

Injection site	Case	Cortical area (ipsi)					
		PRh	Pir	Amyg	PrL	IL	Orbital Cx
S1	02-03a4	0 (0)	0 (0)	2 (0.08)	0 (0)	0 (0)	0 (0)
	02-03a5	22 (0.60)	6 (0.16)	4 (0.11)	0 (0)	16 (0.44)	6 (0.16)
	02-03a3	114 (3.68)	19 (0.61)	6 (0.19)	0 (0)	8 (0.26)	3 (0.10)
	02-03a6	42 (2.25)	7 (0.38)	14 (0.75)	0 (0)	4 (0.22)	192 (10.30)
	02-03a7	67 (1.27)	16 (0.30)	12 (0.23)	0 (0)	12 (0.23)	87 (1.65)
	Mean ± SEM	49.00 ± 21.98 (1.56 ± 0.73)	9.60 ± 3.88 (0.29 ± 0.12)	7.60 ± 2.59 (0.27 ± 0.14)	0 ± 0 (0 ± 0)	8.00 ± 3.16 (0.23 ± 0.08)	57.60 ± 41.75 (2.44 ± 2.22)
r S1BF	03-02b2	44 (2.50)	26 (1.48)	22 (1.25)	0 (0)	0 (0)	112 (6.36)
	03-04a6	78 (4.41)	4 (0.18)	4 (0.18)	0 (0)	0 (0)	32 (1.40)
	03-04a7	186 (4.15)	32 (0.72)	8 (0.18)	0 (0)	0 (0)	0 (0)
	03-04b4	72 (1.61)	10 (0.22)	26 (0.58)	0 (0)	0 (0)	380 (8.47)
	03-04b5	100 (2.80)	22 (0.62)	18 (0.50)	0 (0)	0 (0)	164 (4.59)
	Mean ± SEM	96.00 ± 27.07 (2.89 ± 0.48)	18.80 ± 5.77 (0.64 ± 0.26)	15.60 ± 4.66 (0.54 ± 0.22)	0 ± 0 (0 ± 0)	0 ± 0 (0 ± 0)	137.60 ± 75.08 (4.16 ± 1.74)
c S1BF	03-02b7	42 (2.04)	77 (3.74)	2 (0.10)	0 (0)	0 (0)	39 (1.89)
	04-01b2	36 (1.17)	65 (2.11)	1 (0.03)	0 (0)	0 (0)	26 (0.85)
	03-02b4	48 (0.82)	111 (1.90)	42 (0.72)	1 (0.02)	6 (0.10)	623 (10.66)
	03-02b5	67 (1.07)	189 (3.03)	5 (0.08)	5 (0.08)	11 (0.18)	72 (1.15)
	03-02b6	92 (3.36)	56 (2.04)	1 (0.04)	0 (0)	0 (0)	20 (0.73)
	Mean ± SEM	57.00 ± 11.38 (1.69 ± 0.52)	99.60 ± 27.08 (2.56 ± 0.40)	10.20 ± 8.93 (0.19 ± 0.15)	1.20 ± 1.08 (0.02 ± 0.02)	3.40 ± 2.49 (0.06 ± 0.04)	156.00 ± 130.92 (3.06 ± 2.14)

Table 3

Number and percentage (in parentheses) of retrogradely labeled neurons in sensory and non-sensory cortical areas in the ipsilateral hemisphere after injections of CTb into the primary somatosensory cortex (S1) of intact C57Bl/6 mice (continued)

Injection site	Case	Cortical area (ipsi)			
		Insular Cx	Cl	DP	Cg
S1	02-03a4	0 (0)	8 (0.30)	0 (0)	0 (0)
	02-03a5	4 (0.11)	46 (1.26)	0 (0)	18 (0.49)
	02-03a3	9 (0.29)	18 (0.58)	0 (0)	27 (0.87)
	02-03a6	18 (0.97)	14 (0.75)	0 (0)	5 (0.27)
	02-03a7	32 (0.61)	57 (1.08)	0 (0)	17 (0.32)
	Mean ± SEM	12.60 ± 6.38	28.60 ± 10.78	0 ± 0	13.40 ± 5.42
		(0.39 ± 0.20)	(0.79 ± 0.19)	(0 ± 0)	(0.39 ± 0.16)
r S1BF	03-02b2	124 (7.04)	100 (5.68)	0 (0)	0 (0)
	03-04a6	34 (1.49)	58 (2.53)	0 (0)	0 (0)
	03-04a7	14 (0.31)	30 (0.67)	16 (0.36)	36 (0.80)
	03-04b4	34 (0.76)	110 (2.45)	0 (0)	0 (0)
	03-04b5	58 (1.62)	80 (2.24)	3 (0.17)	6 (0.34)
	Mean ± SEM	52.80 ± 21.37	75.60 ± 16.18	4.40 ± 3.49	9.60 ± 7.82
		(2.24 ± 1.37)	(2.71 ± 0.91)	(0.11 ± 0.08)	(0.23 ± 0.18)
c S1BF	03-02b7	9 (0.44)	21 (1.02)	0 (0)	0 (0)
	04-01b2	1 (0.03)	33 (1.07)	0 (0)	0 (0)
	03-02b4	39 (0.67)	143 (2.45)	8 (0.14)	33 (0.57)
	03-02b5	0 (0)	84 (1.35)	1 (0.02)	31 (0.50)
	03-02b6	4 (0.15)	48 (1.75)	6 (0.22)	0 (0)
	Mean ± SEM	10.60 ± 8.13	65.80 ± 24.61	3.00 ± 1.87	12.80 ± 8.77
		(0.26 ± 0.14)	(1.53 ± 0.30)	(0.07 ± 0.05)	(0.21 ± 0.15)

Table 4

Number and percentage (in parentheses) of retrogradely labeled neurons in sensory and non-sensory cortical areas in the contralateral hemisphere after injections of CTb into the primary somatosensory cortex (S1) of intact C57Bl/6 mice

Injection site	Case	Cortical area (con)					
		S1	S1BF	M1	M2	S2	Au
S1	02-03a4	244 (61.93)	6 (1.52)	70 (17.77)	60 (15.23)	8 (2.03)	4 (1.02)
	02-03a5	364 (46.13)	7 (0.89)	206 (26.11)	132 (16.73)	10 (1.27)	0 (0)
	02-03a3	287 (36.89)	7 (0.90)	104 (13.37)	78 (10.03)	10 (1.29)	4 (0.51)
	02-03a6	165 (42.20)	4 (1.02)	69 (17.65)	48 (12.28)	5 (1.28)	2 (0.51)
	02-03a7	521 (44.08)	11 (0.93)	258 (21.83)	171 (14.47)	15 (1.27)	6 (0.51)
	Mean ± SEM	316.20 ± 67.62 (46.25 ± 4.71)	7.00 ± 1.28 (1.05 ± 0.13)	141.40 ± 42.94 (19.34 ± 2.41)	97.80 ± 26.02 (13.75 ± 1.31)	9.60 ± 1.82 (1.43 ± 0.17)	3.20 ± 1.14 (0.51 ± 0.18)
r S1BF	03-02b2	42 (6.09)	272 (39.42)	8 (1.16)	0 (0)	162 (23.48)	0 (0)
	03-04a6	173 (13.58)	637 (50.00)	132 (10.36)	8 (0.63)	110 (8.63)	0 (0)
	03-04a7	90 (7.65)	53 (4.50)	162 (13.76)	100 (8.50)	20 (1.70)	0 (0)
	03-04b4	385 (13.57)	1350 (47.59)	324 (11.42)	114 (4.02)	304 (10.72)	0 (0)
	03-04b5	177 (11.12)	579 (36.37)	164 (10.30)	72 (4.52)	162 (10.18)	0 (0)
	Mean ± SEM	173.40 ± 65.67 (10.40 ± 1.71)	578.20 ± 246.06 (35.58 ± 9.13)	158.00 ± 56.34 (9.40 ± 2.41)	58.80 ± 26.17 (3.53 ± 1.71)	151.60 ± 51.53 (10.94 ± 3.94)	0 ± 0 (0 ± 0)
c S1BF	03-02b7	36 (9.65)	62 (16.62)	19 (5.09)	183 (49.06)	17 (4.56)	0 (0)
	04-01b2	44 (0)	59 (0)	43 (20.38)	14 (6.64)	16 (7.58)	4 (1.90)
	03-02b4	244 (0)	427 (0)	129 (16.69)	124 (16.04)	117 (15.14)	25 (3.23)
	03-02b5	64 (0)	103 (0)	42 (11.35)	36 (9.73)	28 (7.57)	24 (6.49)
	03-02b6	21 (0)	22 (0)	24 (14.46)	13 (7.83)	6 (3.62)	0 (0)
	Mean ± SEM	81.80 ± 46.00 (12.51 ± 1.50)	134.6 ± 82.98 (18.94 ± 3.44)	51.40 ± 22.33 (9.41 ± 1.66)	74.00 ± 38.04 (15.01 ± 9.55)	36.80 ± 22.75 (5.17 ± 0.94)	10.60 ± 6.40 (1.50 ± 0.92)

Table 4

Number and percentage (in parentheses) of retrogradely labeled neurons in sensory and non-sensory cortical areas in the contralateral hemisphere after injections of CTb into the primary somatosensory cortex (S1) of intact C57Bl/6 mice (continued)

Injection site	Case	Cortical area (con)					
		V1	V2M	V2L	PtA	TeA	RSGc
S1	02-03a4	0 (0)	0 (0)	0 (0)	0 (0)	0 (0)	0 (0)
	02-03a5	0 (0)	0 (0)	0 (0)	0 (0)	0 (0)	0 (0)
	02-03a3	0 (0)	0 (0)	0 (0)	0 (0)	0 (0)	0 (0)
	02-03a6	0 (0)	0 (0)	0 (0)	0 (0)	0 (0)	0 (0)
	02-03a7	0 (0)	0 (0)	0 (0)	0 (0)	0 (0)	0 (0)
	Mean ± SEM	0 ± 0	0 ± 0	0 ± 0	0 ± 0	0 ± 0	0 ± 0
		(0 ± 0)	(0 ± 0)	(0 ± 0)	(0 ± 0)	(0 ± 0)	(0 ± 0)
r S1BF	03-02b2	0 (0)	0 (0)	0 (0)	0 (0)	0 (0)	0 (0)
	03-04a6	0 (0)	0 (0)	0 (0)	0 (0)	4 (0.31)	0 (0)
	03-04a7	0 (0)	0 (0)	0 (0)	0 (0)	0 (0)	0 (0)
	03-04b4	0 (0)	0 (0)	0 (0)	0 (0)	6 (0.21)	0 (0)
	03-04b5	0 (0)	0 (0)	0 (0)	0 (0)	2 (0.13)	0 (0)
	Mean ± SEM	0 ± 0	0 ± 0	0 ± 0	0 ± 0	2.40 ± 1.30	0 ± 0
		(0 ± 0)	(0 ± 0)	(0 ± 0)	(0 ± 0)	(0.13 ± 0.07)	(0 ± 0)
c S1BF	03-02b7	0 (0)	0 (0)	0 (0)	1 (0.27)	1 (0.27)	0 (0)
	04-01b2	0 (0)	0 (0)	0 (0)	0 (0)	3 (1.42)	2 (0.95)
	03-02b4	0 (0)	0 (0)	0 (0)	15 (1.94)	4 (0.52)	2 (0.26)
	03-02b5	0 (0)	0 (0)	0 (0)	9 (2.43)	13 (3.51)	0 (0)
	03-02b6	0 (0)	0 (0)	0 (0)	0 (0)	0 (0)	0 (0)
	Mean ± SEM	0 ± 0	0 ± 0	0 ± 0	5.00 ± 3.37	4.20 ± 2.58	0.80 ± 0.55
		(0 ± 0)	(0 ± 0)	(0 ± 0)	(0.60 ± 0.37)	(0.78 ± 0.49)	(0.16 ± 0.14)

Table 4

Number and percentage (in parentheses) of retrogradely labeled neurons in sensory and non-sensory cortical areas in the contralateral hemisphere after injections of CTb into the primary somatosensory cortex (S1) of intact C57Bl/6 mice (continued)

Injection site	Case	Cortical area (con)					
		RSD	Ect	PRh	Pir	Amyg	PrL
S1	02-03a4	0 (0)	2 (0.51)	0 (0)	0 (0)	0 (0)	0 (0)
	02-03a5	16 (2.03)	14 (1.77)	32 (4.06)	0 (0)	0 (0)	0 (0)
	02-03a3	8 (1.03)	6 (0.77)	270 (34.70)	0 (0)	0 (0)	0 (0)
	02-03a6	4 (1.02)	4 (1.02)	67 (17.14)	0 (0)	0 (0)	0 (0)
	02-03a7	12 (1.02)	18 (1.52)	157 (13.28)	0 (0)	0 (0)	0 (0)
	Mean ± SEM	8.00 ± 3.16	8.80 ± 3.44	105.20 ± 54.62	0 ± 0	0 ± 0	0 ± 0
		(1.02 ± 0.36)	(1.12 ± 0.26)	(13.84 ± 6.77)	(0 ± 0)	(0 ± 0)	(0 ± 0)
r S1BF	03-02b2	0 (0)	26 (3.77)	174 (25.22)	0 (0)	4 (0.58)	0 (0)
	03-04a6	0 (0)	80 (6.28)	90 (7.06)	2 (0.16)	2 (0.16)	0 (0)
	03-04a7	0 (0)	116 (9.86)	508 (43.16)	12 (1.02)	8 (0.68)	0 (0)
	03-04b4	0 (0)	86 (3.03)	118 (4.16)	20 (0.71)	10 (0.35)	2 (0.07)
	03-04b5	0 (0)	76 (4.77)	266 (16.71)	10 (0.63)	8 (0.50)	0 (0)
	Mean ± SEM	0 ± 0	76.80 ± 16.23	231.20 ± 84.36	8.80 ± 4.04	6.40 ± 1.64	0.40 ± 0.45
		(0 ± 0)	(5.54 ± 1.35)	(19.26 ± 7.87)	(0.50 ± 0.21)	(0.45 ± 0.10)	(0.01 ± 0.02)
c S1BF	03-02b7	1 (0.27)	44 (11.80)	4 (1.07)	2 (0.54)	1 (0.27)	1 (0.27)
	04-01b2	6 (2.84)	43 (20.38)	17 (8.06)	4 (1.90)	0 (0)	0 (0)
	03-02b4	14 (1.81)	149 (19.28)	101 (13.07)	2 (0.26)	0 (0)	0 (0)
	03-02b5	1 (0.27)	55 (14.87)	106 (28.65)	36 (9.73)	0 (0)	0 (0)
	03-02b6	1 (0.60)	8 (4.82)	34 (20.48)	7 (4.22)	0 (0)	0 (0)
	Mean ± SEM	4.60 ± 2.84	59.80 ± 26.45	52.40 ± 23.94	10.20 ± 7.28	0.20 ± 0.22	0.20 ± 0.22
		(0.76 ± 0.36)	(9.98 ± 1.86)	(9.90 ± 3.90)	(2.40 ± 1.35)	(0.05 ± 0.06)	(0.05 ± 0.06)

Table 4

Number and percentage (in parentheses) of retrogradely labeled neurons in sensory and non-sensory cortical areas in the contralateral hemisphere after injections of CTb into the primary somatosensory cortex (S1) of intact C57Bl/6 mice (continued)

Injection site	Case	Cortical area (con)					
		Insular Cx	IL	Orbital Cx	Cl	DP	Cg
S1	02-03a4	0 (0)	0 (0)	0 (0)	0 (0)	0 (0)	0 (0)
	02-03a5	0 (0)	0 (0)	8 (1.01)	0 (0)	0 (0)	0 (0)
	02-03a3	0 (0)	0 (0)	4 (0.51)	0 (0)	0 (0)	0 (0)
	02-03a6	0 (0)	0 (0)	23 (5.88)	0 (0)	0 (0)	0 (0)
	02-03a7	0 (0)	0 (0)	13 (1.10)	0 (0)	0 (0)	0 (0)
	Mean ± SEM	0 ± 0 (0 ± 0)	0 ± 0 (0 ± 0)	9.60 ± 4.45 (1.70 ± 1.19)	0 ± 0 (0 ± 0)	0 ± 0 (0 ± 0)	0 ± 0 (0 ± 0)
r S1BF	03-02b2	0 (0)	0 (0)	0 (0)	2 (0.29)	0 (0)	0 (0)
	03-04a6	34 (2.67)	0 (0)	0 (0)	0 (0)	0 (0)	2 (0.16)
	03-04a7	108 (9.18)	0 (0)	0 (0)	0 (0)	0 (0)	0 (0)
	03-04b4	70 (2.47)	0 (0)	42 (1.48)	6 (0.21)	0 (0)	0 (0)
	03-04b5	60 (3.77)	0 (0)	14 (0.88)	2 (0.13)	0 (0)	0 (0)
	Mean ± SEM	54.40 ± 20.19 (3.62 ± 1.70)	0 ± 0 (0 ± 0)	11.20 ± 9.13 (0.47 ± 0.34)	2.00 ± 1.23 (0.13 ± 0.06)	0 ± 0 (0 ± 0)	0.40 ± 0.45 (0.03 ± 0.04)
c S1BF	03-02b7	0 (0)	1 (0.27)	0 (0)	0 (0)	0 (0)	0 (0)
	04-01b2	12 (5.69)	0 (0)	15 (7.11)	32 (15.17)	0 (0)	0 (0)
	03-02b4	12 (1.55)	0 (0)	55 (7.12)	24 (3.11)	0 (0)	0 (0)
	03-02b5	0 (0)	0 (0)	18 (4.87)	2 (0.54)	0 (0)	0 (0)
	03-02b6	62 (4.82)	0 (0)	10 (6.02)	1 (20.48)	0 (0)	0 (0)
	Mean ± SEM	17.20 ± 12.88 (6.86 ± 6.42)	0.20 ± 0.22 (0.05 ± 0.06)	19.60 ± 10.47 (3.35 ± 0.99)	11.80 ± 7.54 (2.54 ± 2.16)	0 ± 0 (0 ± 0)	0 ± 0 (0 ± 0)

The relative abundance of labeled neurons in each cortical area was compared between injection sites (see Figure 14). This quantitative analysis demonstrates that the three sites of the somatosensory cortex have many similar cortical connections that have often different relative weights. The proportion of labeled cortical neurons in the different cortical areas was quite variable between cases, and only quite large differences reached levels of statistical significance. Indeed, the rostral portion of the barrel field had more robust projections from the motor cortices, M1 and M2 than the non-barrel field portion and the caudal barrel field. Only the difference in the proportion of neurons labeled in M2 between S1 and rostral S1BF reached statistical significance (Tukey-HSD, $p = 0.013$). Conversely the projections of S1 with S2 and Au were more robust than the other injection sites but only the difference between the rostral S1BF and S1 reaches statistical significance (S2 Tukey-HSD, $p = 0.006$; Au Tukey-HSD, $p = 0.025$). Only the caudal barrel field received projections from striate and extrastriate visual cortices (V2M Tukey-HSD, $p = 0.019$; V2L Tukey-HSD, $p = 0.006$). Several differences between fields were detected in the lesser projections. Projection from the association areas PtA and TeA were less important in the caudal barrel field than in the other areas. Also the projection from the piriform cortex was more important in the caudal barrel field.

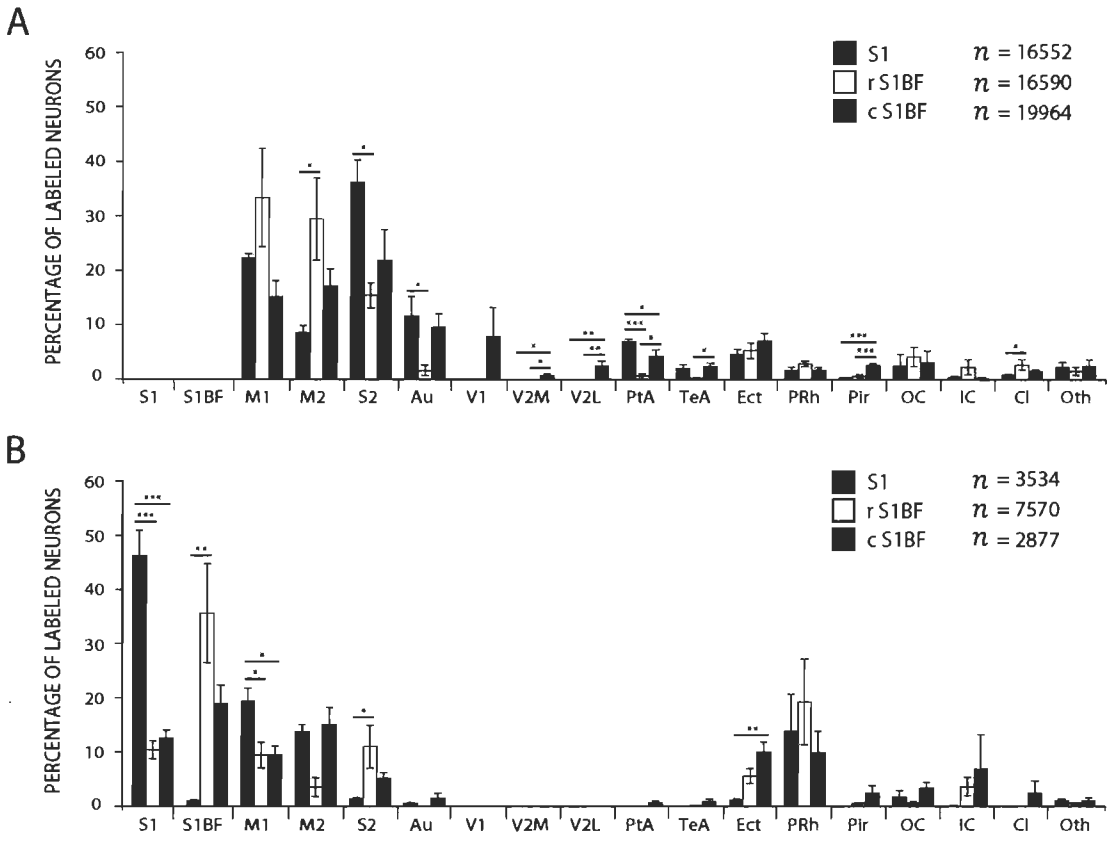

Figure 14. Percentage of retrogradely labeled neurons in cortical areas in the ipsilateral (A) and contralateral hemispheres (B).

Callosal projections also demonstrate the heterogeneity of the mouse somatosensory cortex. Homospecific callosal connections seem predominant. Indeed, S1 receives a robust projection from its contralateral homolog and much reduced projections from the contralateral rostral (Tukey-HSD, $p < 0.001$), and caudal (Tukey-HSD, $p < 0.001$) barrel field. Similarly, the rostral barrel field injections produced more labeled neurones in the contralateral barrel field than in the non-barrel field somatosensory cortex (Tukey-HSD, $p = 0.001$).

Callosal projections from the motor cortices and secondary somatosensory cortex also show differences between injection sites. Moreover, these differences do not mirror the heterogeneities in the ipsilateral projections. The somatosensory cortex outside the barrel field had a more important projection from the contralateral M1 than the rostral and caudal barrel field (Tukey-HSD, $p = 0.010$). Although the rostral barrel field had more important projections from the ipsilateral M2, the somatosensory areas received a relatively smaller callosal projection form this area than the other injection sites. This difference however does not reach statistical significance. A similar inverted pattern of callosal projection is seen with S2 that contributes a relatively stronger projection to the contralateral rostral barrel field compared to the other injection sites.

Contrary to ipsilateral projections, the somatosensory cortex received very few heteromodal callosal projections. The projections from the contralateral auditory cortex were very small and in all cases, no labeled neurons were observed in the primary and extrastriate visual cortices. The callosal projections from the ectorhinal and perirhinal cortices were of similar weight as M1, M2 and S2. The other callosal projections were relatively small and did not show significant differences between injection sites. No significant differences in the percentage of labeled neurons were observed in the contralateral hemisphere between the group which received injections in the rostral part of S1BF and the group which received injections in the caudal part of S1BF.

Layer indices were calculated in order to scale projections in the feedforward and feedback continuum (see Tables 5 and 6 respectively and Figure 15). In all the cases and for the three injections sites, all the layer indices of ipsilateral projections had negative values. For the injections in S1 the layer indices ranged between -0.27 in M1 and -0.94 in TeA. Injections in the rostral S1BF produced layer indices ranging between -0.43 in M1 and -0.87 in TeA, and the injections in the caudal S1BF between -0.27 in M1 and -0.91 in TeA. They also show heterogeneities between the three injection sites of the mouse somatosensory cortex. Injections sites in the rostral S1BF produced more negative layer indices for the projections from the motor cortices M1 and M2 and from the secondary somatosensory cortex. Only the difference between rostral and caudal S1BF of the projection from M2 (Tukey-HSD, $p = 0.038$), and the difference between S1 and rostral S1BF of the projection from S2 (Tukey-HSD, $p = 0.023$) reached statistical significance. In all the ipsilateral projections, the layer indices of the projections from the temporal cortices Au and TeA were the most negative and of the same magnitude for all three injection sites. This contrasts with the heteromodal connections with the primary visual cortex, V1, and the medial extrastriate visual cortex, V2M, which were close to zero. The layer index of the projection from the ipsilateral parietal association cortex, PtA to the rostral S1BF is also very close to zero whereas it is more strongly negative for the projection to S1 and caudal S1BF.

Table 5

Numbers of retrogradely labeled neurons in supragranular/infragranular layers and layer indices (below) in non-somatosensory sensory and non-sensory neocortical areas in the ipsilateral hemisphere after injections of CTb into S1, S1BF (rostral part) and S1BF (caudal part) of C57Bl/6 mice

Injection site	Case	Cortical area (ipsi)		
		M1	M2	S2
S1	02-03a4	242 / 396	36 / 112	98 / 456
		-0.24	-0.51	-0.65
	02-03a5	291 / 541	154 / 284	506 / 858
		-0.30	-0.30	-0.26
	02-03a3	255 / 433	66 / 156	200 / 558
		-0.26	-0.41	-0.47
	02-03a6	133 / 235	48 / 99	151 / 329
		-0.28	-0.35	-0.37
	02-03a7	419 / 757	187 / 362	606 / 1140
		-0.29	-0.32	-0.31
	Mean ± SEM	268 ± 52/472 ± 97	98 ± 34/203 ± 58	312 ± 114/668 ± 167
		-0.28 ± 0.01	-0.35 ± 0.04	-0.37 ± 0.08
r S1BF	03-02b2	44 / 126	280 / 552	30 / 138
		-0.48	-0.33	-0.64
	03-04a6	416 / 960	24 / 98	88 / 342
		-0.40	-0.61	-0.59
	03-04a7	563 / 1087	386 / 938	20 / 324
		-0.32	-0.42	-0.88
	03-04b4	263 / 1101	194 / 1222	86 / 474
		-0.61	-0.73	-0.69
	03-04b5	289 / 771	286 / 904	46 / 312
		-0.46	-0.52	-0.74
	Mean ± SEM	315 ± 96/809 ± 205	234 ± 24/743 ± 224	54 ± 16/318 ± 60
		-0.44 ± 0.06	-0.52 ± 0.09	-0.71 ± 0.06
c S1BF	03-02b7	81 / 67	103 / 106	38 / 351
		0.10	-0.01	-0.80
	04-01b2	332 / 394	340 / 233	122 / 413
		-0.09	0.19	-0.54
	03-02b4	127 / 673	259 / 1251	124 / 436
		-0.68	-0.66	-0.56
	03-02b5	405 / 524	551 / 646	373 / 733
		-0.13	-0.08	-0.33
	03-02b6	167 / 283	133 / 178	169 / 888
		-0.26	-0.18	-0.68
	Mean ± SEM	222 ± 70/388 ± 130	277 ± 90/485 ± 239	165 ± 63/564 ± 134
		-0.27 ± 0.15	-0.27 ± 0.16	-0.55 ± 0.09

Table 5

Numbers of retrogradely labeled neurons in supragranular/infragranular layers and layer indices (below) in non-somatosensory sensory and non-sensory neocortical areas in the ipsilateral hemisphere after injections of CTb into S1, S1BF (rostral part) and S1BF (caudal part) of C57Bl/6 mice (continued)

Injection site	Case	Cortical area (ipsi)		
		Au	V1	V2M
S1	02-03a4	74 / 470 -0.73		
	02-03a5	6 / 98 -0.89		
	02-03a3	58 / 378 -0.73		
	02-03a6	20 / 143 -0.76		
	02-03a7	36 / 291 -0.78		
	Mean ± SEM	39 ± 14/276 ± 82 -0.75 ± 0.03		
r S1BF	03-02b2			
	03-04a6	0 / 6 -1.00		
	03-04a7	8 / 144 -0.90		
	03-04b4	8 / 30 -0.58		
	03-04b5	6 / 58 -0.81		
	Mean ± SEM	6 ± 2/60 ± 29 -0.83 ± 0.09		
c S1BF	03-02b7	1 / 127 -0.98	216 / 236 -0.04	3 / 3 0.00
	04-01b2	19 / 247 -0.86	34 / 39 -0.07	6 / 1 0.71
	03-02b4	14 / 295 -0.91	157 / 203 -0.13	11 / 43 -0.59
	03-02b5	119 / 675 -0.70	79 / 60 0.14	34 / 28 0.10
	03-02b6	3 / 94 -0.94	16 / 12 0.14	1 / 2 -0.33
	Mean ± SEM	31 ± 25/288 ± 119 -0.80 ± 0.06	100 ± 42/110 ± 51 -0.05 ± 0.06	11 ± 7/15 ± 10 -0.17 ± 0.25

Table 5

Numbers of retrogradely labeled neurons in supragranular/infragranular layers and layer indices (below) in non-somatosensory sensory and non-sensory neocortical areas in the ipsilateral hemisphere after injections of CTb into S1, S1BF (rostral part) and S1BF (caudal part) of C57Bl/6 mice (continued)

Injection site	Case	Cortical area (ipsi)		
		V2L	PtA	TeA
S1	02-03a4		58 / 116	2 / 98
			-0.33	-0.96
	02-03a5		42 / 124	0 / 12
			-0.49	-1.00
	02-03a3		54 / 118	2 / 78
			-0.37	-0.95
	02-03a6		25 / 60	1 / 28
			-0.41	-0.93
	02-03a7		69 / 183	3 / 54
			-0.45	-0.90
	Mean ± SEM		50 ± 8/120 ± 23	2 ± 1/54 ± 18
			-0.41 ± 0.03	-0.94 ± 0.02
r S1BF	03-02b2			
	03-04a6			
	03-04a7		34 / 40	2 / 16
			-0.08	-0.78
	03-04b4			0 / 6
				-1.00
	03-04b5		12 / 12	0 / 6
			0.00	-1.00
	Mean ± SEM		23 ± 7/26 ± 9	1 ± 0/7 ± 4
			-0.06 ± 0.02	-0.87 ± 0.24
c S1BF	03-02b7	14 / 42	4 / 7	0 / 33
		-0.50	-0.27	-1.00
	04-01b2	2 / 26	51 / 72	0 / 77
		-0.86	-0.17	-1.00
	03-02b4	30 / 150	29 / 114	12 / 103
		-0.67	-0.59	-0.79
	03-02b5	51 / 45	39 / 237	7 / 192
		0.06	-0.72	-0.93
	03-02b6	3 / 12	69 / 75	0 / 14
		-0.6	-0.04	-1.00
	Mean ± SEM	20 ± 10/55 ± 27	38 ± 12/101 ± 44	4 ± 3/84 ± 36
		-0.47 ± 0.17	-0.45 ± 0.14	-0.91 ± 0.05

Table 6

Numbers of retrogradely labeled neurons in supragranular/infragranular layers and layer indices (below) in non-somatosensory sensory and non-sensory neocortical areas in the contralateral hemisphere after injections of CTb into S1, S1BF (rostral part) and S1BF (caudal part) of C57Bl/6 mice

Injection site	Case	Cortical area (con)			
		S1	S1BF	M1	M2
S1	02-03a4	141 / 58	1 / 4	52 / 18	23 / 37
		0.42	-0.60	0.49	-0.23
	02-03a5	199 / 99	2 / 3	113 / 93	36 / 96
		0.34	-0.20	0.10	-0.46
	02-03a3	167 / 72	2 / 3	67 / 37	26 / 52
		0.40	-0.20	0.29	-0.33
	02-03a6	93 / 43	1 / 1	41 / 28	15 / 33
		0.37	0.00	0.19	-0.38
	02-03a7	289 / 140	4 / 6	147 / 111	50 / 121
		0.35	-0.20	0.14	-0.42
	Mean ± SEM	178 ± 37/83 ± 19	2 ± 1/3 ± 1	84 ± 22/57 ± 21	30 ± 7/68 ± 21
		0.37 ± 0.02	-0.26 ± 0.11	0.19 ± 0.08	-0.39 ± 0.04
r S1BF	03-02b2	14 / 24	56 / 200	0 / 8	
		-0.26	-0.56	-1.00	
	03-04a6	20 / 131	69 / 547	14 / 118	2 / 6
		-0.74	-0.78	-0.79	-0.50
	03-04a7	12 / 60	12 / 36	28 / 134	13 / 87
		-0.67	-0.50	-0.65	-0.74
	03-04b4	57 / 299	187 / 1099	23 / 301	6 / 108
		-0.68	-0.71	-0.86	-0.90
	03-04b5	33 / 128	102 / 445	18 / 146	6 / 66
		-0.59	-0.63	-0.78	-0.83
	Mean ± SEM	27 ± 9/128 ± 54	85 ± 33/465 ± 201	17 ± 5/141 ± 54	7 ± 3/67 ± 26
		-0.65 ± 0.09	-0.69 ± 0.06	-0.79 ± 0.06	-0.82 ± 0.09
c S1BF	03-02b7	20 / 13	15 / 42	5 / 14	101 / 82
		0.21	-0.47	-0.48	0.10
	04-01b2	18 / 26	14 / 38	3 / 40	12 / 2
		-0.18	-0.46	-0.86	0.71
	03-02b4	121 / 110	108 / 288	5 / 124	16 / 108
		0.05	-0.46	-0.92	-0.74
	03-02b5	33 / 23	29 / 63	12 / 30	17 / 19
		0.18	-0.37	-0.43	-0.06
	03-02b6	10 / 9	5 / 15	9 / 15	5 / 8
		0.05	-0.50	-0.25	-0.23
	Mean ± SEM	40 ± 23/36 ± 21	171 ± 21/446 ± 56	7 ± 2/45 ± 23	30 ± 20/44 ± 25
		0.06 ± 0.08	-0.45 ± 0.03	-0.74 ± 0.15	-0.18 ± 0.27

Table 6

Numbers of retrogradely labeled neurons in supragranular/infragranular layers and layer indices (below) in non-somatosensory sensory and non-sensory neocortical areas in the contralateral hemisphere after injections of CTb into S1, S1BF (rostral part) and S1BF (caudal part) of C57Bl/6 mice (continued)

Injection site	Case	Cortical area (con)			
		S2	Au	PtA	TeA
S1	02-03a4	2 / 6	0 / 4		
		-0.50	-1.00		
	02-03a5	4 / 6			
		-0.20			
	02-03a3	4 / 6	0 / 4		
		-0.20	-1.00		
	02-03a6	2 / 3	0 / 2		
		-0.20	-1.00		
	02-03a7	6 / 9	0 / 6		
		-0.20	-1.00		
	Mean ± SEM	4 ± 1/6 ± 1	0 ± 0/4 ± 1		
		-0.25 ± 0.07	-1.00 ± 0.00		
r S1BF	03-02b2	12 / 146			
		-0.85			
	03-04a6	0 / 108			
		-1.00			
	03-04a7	0 / 20			
		-1.00			
	03-04b4	0 / 284			0 / 2
		-1.00			-1.00
	03-04b5	4 / 150			
		-0.95			
	Mean ± SEM	3 ± 3/142 ± 56			0 ± 0/2 ± 0
		-0.96 ± 0.03			-1.00 ± 0.00
c S1BF	03-02b7	1 / 16		1 / 0	1 / 0
		-0.88		1.00	1.00
	04-01b2	0 / 12	0 / 4		1 / 2
		-1.00	-1.00		-0.33
	03-02b4	11 / 95	1 / 24	5 / 8	0 / 3
		-0.79	-0.92	-0.23	-1.00
	03-02b5	8 / 12	1 / 23	0 / 6	0 / 10
		-0.20	-0.92	-1.00	-1.00
	03-02b6	0 / 5			
		-1.00			
	Mean ± SEM	4 ± 3/28 ± 19	1 ± 0/17 ± 7	2 ± 1/5 ± 3	1 ± 0/4 ± 2
		-0.75 ± 0.17	-0.93 ± 0.02	-0.40 ± 0.50	-0.77 ± 0.47

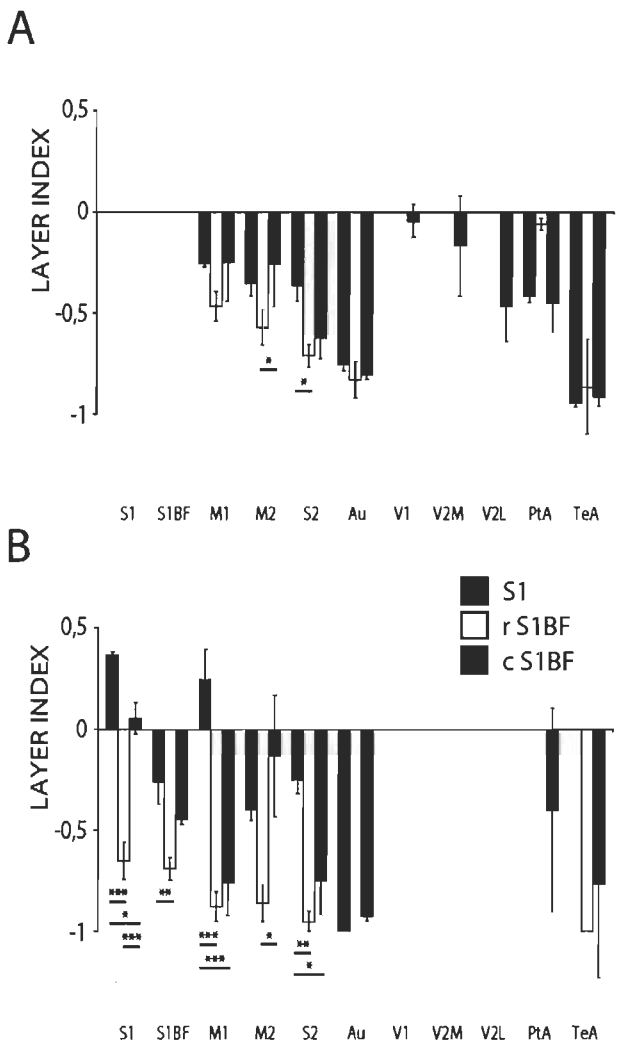

Figure 15. Layer indices for neocortical areas in the ipsilateral (A) and contralateral hemispheres (B).

The layer indices of the callosal projections were also mostly negative. There is a similar pattern in the layer indices of the callosal projections from somatosensory (S1 and S1BF) motor (M1 and M2) and secondary somatosensory cortices in the projections from these cortices to the rostral S1BF were more strongly negative than the projections to the other sites. Not all these differences reach statistical significance however. This is

most evident for the projections from S1. The layer indices for this projection to S1 and caudal S1BF were either positive or close to zero whereas the projection to the rostral S1BF was less than -0.7. The projections from M2 also followed a similar pattern but differences do not reach statistical significance. Layer indices of the projection from M1 to S1 were positive whereas the layer indices of the projections to rostral and caudal S1BF were very similar and significantly different. The layer indices of the quite weak projection from the auditory cortex to all portions of the somatosensory cortex had very strongly negative values similar to the other temporal cortical field TeA. There were no visual heteromodal callosal projections to the mouse somatosensory cortices.

To further visualise the relationship between the structure of ipsilateral and callosal projections, the values of layer indices for each projection in each case were plotted in a scatter diagram (see Figure 16). This shows that in most cases both the ipsilateral and contralateral projections have negative layer indices. In all cases the layers indices were positive for the callosal and slightly negative for the ipsilateral projection from M1 to S1. The projection from M2 to the caudal S1BF had highly variable and inconsistent layer indices values for the ipsi- and contralateral projections. In one case both values are strongly negative and in one case, both are strongly positive. Three cases have intermediate values.

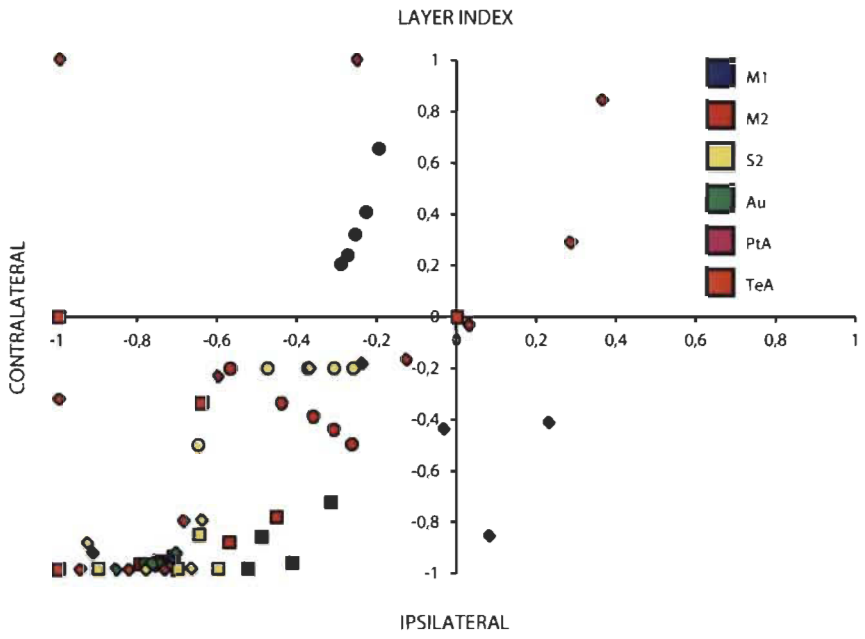

Figure 16. Layer indices matching between the ipsilateral hemisphere (X axis) and the contralateral hemisphere (Y axis). Each circle (S1), square (r S1BF) and diamond (c S1BF) represents the layer index of a cortical area for a single case in which retrogradely labeled neurons were plotted in both hemispheres.

There was a clear inverse relationship between the abundance of labeled neurons in the ipsilateral cortex and the distance for all three injection sites (see Figure 17). Since the neurons labeled in the somatosensory cortex were not quantified, very few neurons were charted in close proximity of the injections sites. This explains the increasing number of neurons in a radius up to 2500 μm from the injection sites. For greater distances, the decrease in the abundance of labeled neurons with distance from the injection sites is quite evident, showing that in corticocortical connections, shorter connections are more abundant than longer ones.

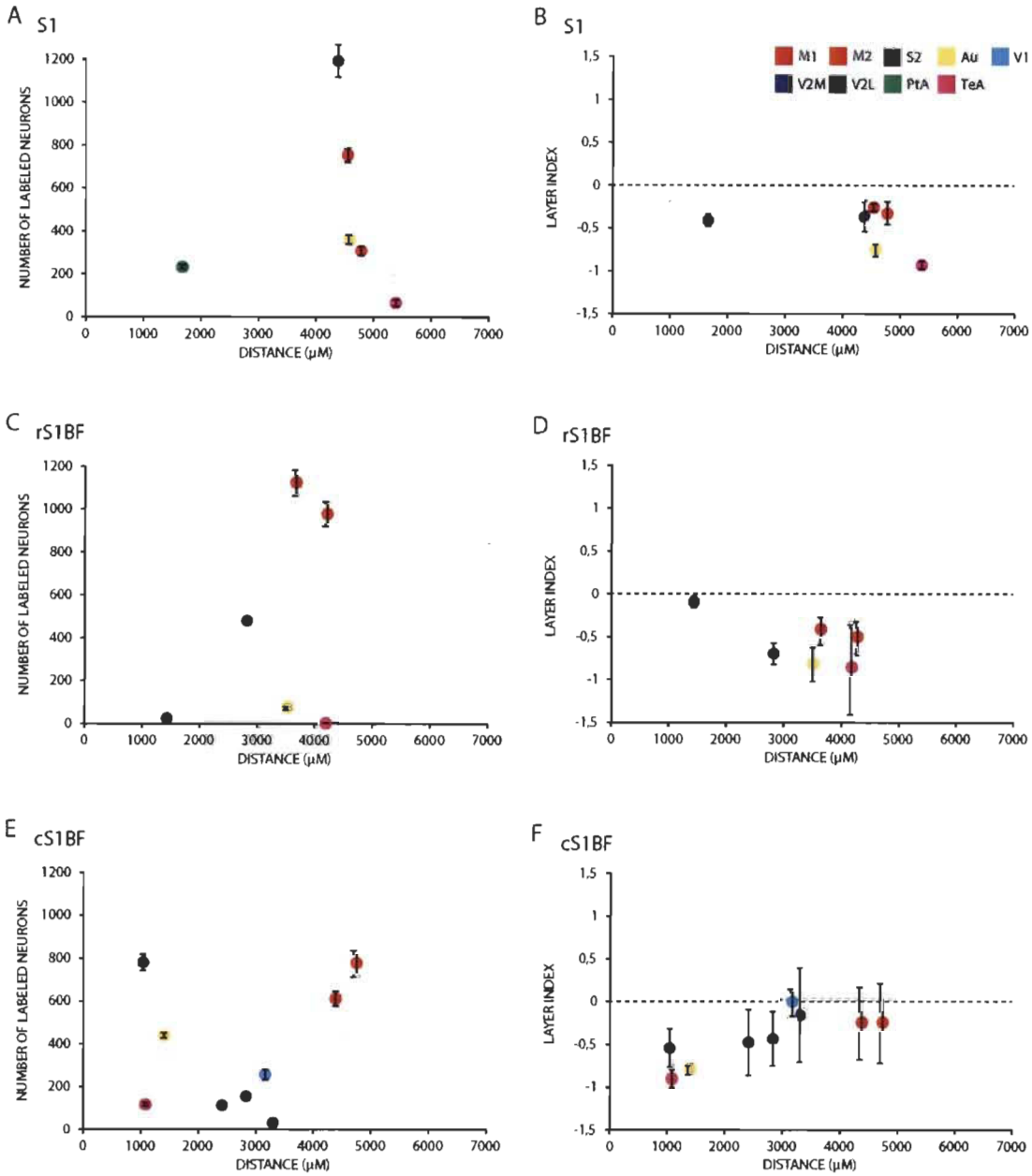

Figure 17. Percentage of retrogradely labeled neurons (Y axis) depending on their distance (X axis) from one of the three different injection sites in S1.

Subcortical projections to S1

Following injections of CTb into S1 and the rostral and caudal parts of S1BF, retrogradely labeled neurons were found in several subcortical structures of all three animal groups (see Table 6). The main sources of thalamic inputs to S1 and S1BF were VPL and VPM respectively, but due to the high density of labeled neurons therein (see Figure 11), these areas were not included in the statistical analysis. Labeled neurons were found mainly in the posterior thalamic nuclear group (Po), the ventrolateral thalamic nucleus (VL), the ventromedial thalamic nucleus (VM), the reuniens thalamic nucleus (Re), the globus pallidus (GP), the zona incerta (ZI), the central medial thalamic nucleus (CM-PC), the hypothalamus (Hyp) and the laterodorsal thalamic nucleus (LD) (see Figure 18). In addition, some labeled neurons were found in several other thalamic nuclei and subcortical structures. Quantification of the labeled cells is detailed in Table 7. Statistical analysis was performed for the nine subcortical structures that consistently contained labeled neurons.

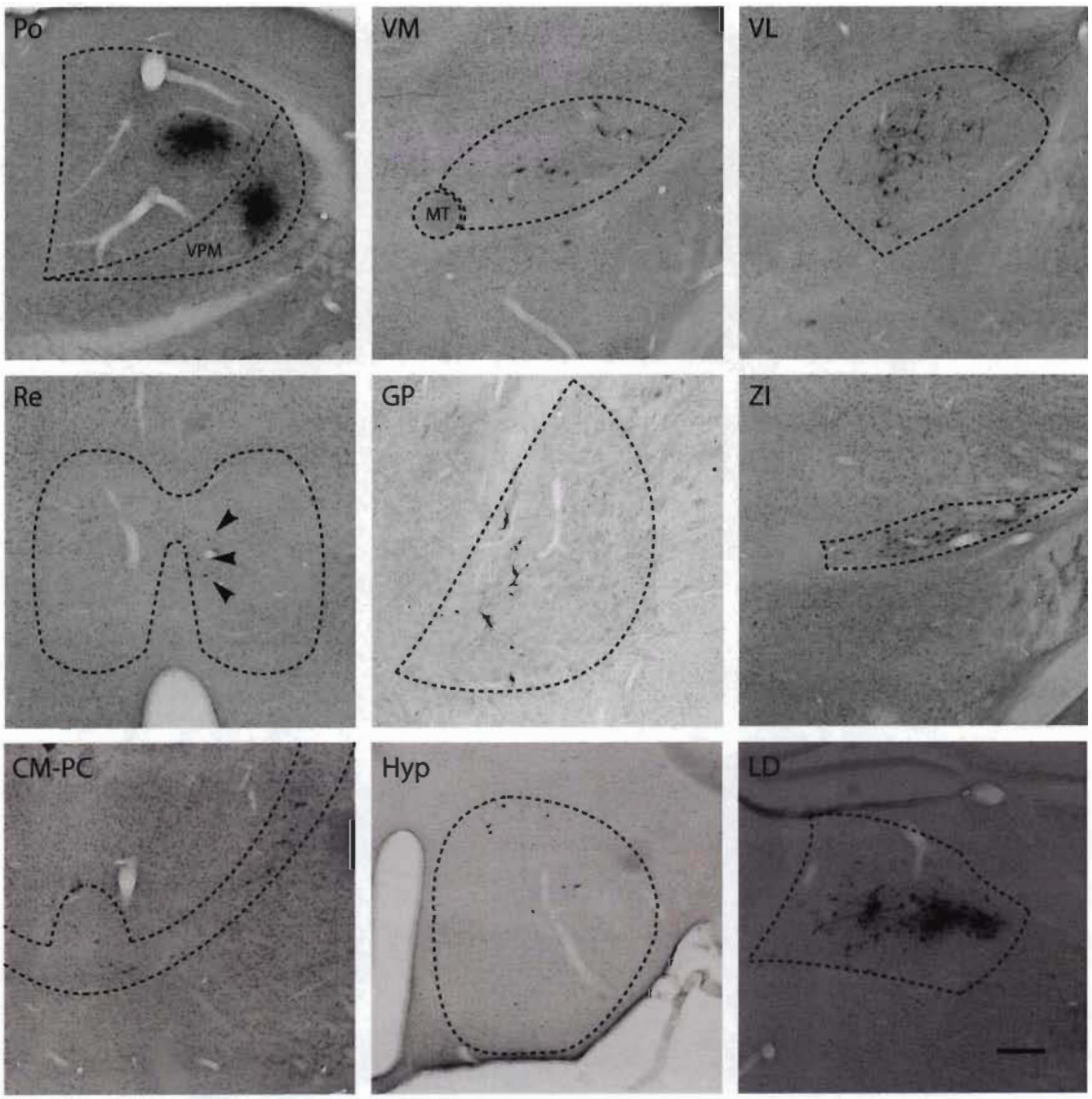

Figure 18. CTb-labeled neurons in the subcortex after an injection into the posterior part of the barrel field of S1. Scale: 250 μm.

Table 7

Number and percentage (in parentheses) of retrogradely labeled neurons in sensory and non-sensory subcortical areas after injections of CTb into the primary somatosensory cortex (S1) of intact C57Bl/6 mice

Injection site	Case	Subcortical area					
		Po	VPL	VPM	AM	VL	VM
S1	02-03a4	64 (10.06)	510 (80.19)	0 (0)	0 (0)	0 (0)	0 (0)
	02-03a5	88 (12.61)	478 (68.48)	0 (0)	0 (0)	0 (0)	56 (8.02)
	02-03a3	70 (8.90)	502 (63.79)	0 (0)	0 (0)	0 (0)	85 (10.80)
	02-03a6	38 (8.56)	247 (55.63)	0 (0)	0 (0)	0 (0)	31 (6.98)
	02-03a7	123 (11.38)	729 (67.44)	0 (0)	0 (0)	0 (0)	68 (6.29)
	Mean ± SEM	76.60 ± 15.76	493.20 ± 85.44	0 ± 0	0 ± 0	0 ± 0	48.00 ± 16.63
		(10.30 ± 0.85)	(67.11 ± 4.44)	(0 ± 0)	(0 ± 0)	(0 ± 0)	(6.42 ± 1.99)
r S1BF	03-02b2	294 (39.95)	0 (0)	258 (35.05)	0 (0)	0 (0)	8 (1.09)
	03-04a6	198 (30.18)	0 (0)	258 (39.33)	0 (0)	36 (5.49)	16 (2.44)
	03-04a7	434 (48.22)	0 (0)	162 (18)	0 (0)	68 (7.56)	114 (12.67)
	03-04b4	402 (31.31)	0 (0)	258 (20.09)	26 (2.03)	258 (20.09)	34 (2.65)
	03-04b5	376 (38.76)	0 (0)	226 (23.30)	8 (0.83)	108 (11.13)	52 (5.36)
	Mean ± SEM	340.80 ± 47.60	0 ± 0	232.40 ± 20.86	6.80 ± 5.64	94.00 ± 49.98	44.80 ± 21.13
		(37.68 ± 3.66)	(0 ± 0)	(27.16 ± 4.74)	(0.57 ± 0.44)	(8.85 ± 3.73)	(4.84 ± 2.32)
c S1BF	03-02b7	263 (50.19)	0 (0)	165 (31.49)	10 (1.91)	19 (3.63)	3 (0.57)
	04-01b2	264 (36.72)	0 (0)	232 (32.27)	0 (0)	26 (3.62)	112 (15.58)
	03-02b4	580 (37.69)	0 (0)	111 (7.21)	12 (0.78)	59 (3.83)	61 (3.96)
	03-02b5	362 (30.17)	0 (0)	357 (29.75)	44 (3.67)	162 (13.5)	1 (0.08)
	03-02b6	215 (38.19)	0 (0)	200 (35.52)	11 (1.95)	48 (8.53)	2 (0.36)
	Mean ± SEM	336.80 ± 73.04	0 ± 0	15.40 ± 46.08	15.40 ± 8.35	62.80 ± 28.88	35.80 ± 24.84
		(38.59 ± 3.62)	(0 ± 0)	(27.25 ± 5.70)	(1.66 ± 0.69)	(6.62 ± 2.19)	(4.11 ± 3.30)

Table 7

Number and percentage (in parentheses) of retrogradely labeled neurons in sensory and non-sensory subcortical areas after injections of CTb into the primary somatosensory cortex (S1) of intact C57Bl/6 mice (continued)

Injection site	Case	Subcortical area						
		Re	GP	PT	AHA	ZI	CM-PC	Hyp
S1	02-03a4	0 (0)	0 (0)	0 (0)	0 (0)	62 (9.75)	0 (0)	0 (0)
	02-03a5	38 (5.44)	0 (0)	0 (0)	0 (0)	26 (3.73)	2 (0.29)	2 (0.29)
	02-03a3	43 (5.46)	0 (0)	0 (0)	0 (0)	54 (6.86)	18 (2.29)	11 (1.40)
	02-03a6	12 (2.70)	0 (0)	0 (0)	0 (0)	22 (4.96)	87 (19.60)	5 (1.13)
	02-03a7	38 (3.52)	0 (0)	0 (0)	0 (0)	54 (5.00)	54 (5.00)	9 (0.83)
	Mean ± SEM	26.20 ± 9.52 (3.43 ± 1.13)	0 ± 0 (0 ± 0)	0 ± 0 (0 ± 0)	0 ± 0 (0 ± 0)	43.60 ± 9.12 (6.06 ± 1.17)	32.20 ± 18.76 (5.43 ± 4.08)	5.40 ± 2.31 (0.73 ± 0.29)
r S1BF	03-02b2	0 (0)	28 (3.80)	0 (0)	0 (0)	22 (2.99)	108 (14.67)	16 (2.17)
	03-04a6	8 (1.22)	18 (2.74)	0 (0)	0 (0)	0 (0)	112 (17.07)	6 (0.92)
	03-04a7	48 (5.33)	8 (0.89)	0 (0)	0 (0)	2 (0.22)	34 (3.78)	20 (2.22)
	03-04b4	4 (0.31)	38 (2.96)	0 (0)	0 (0)	66 (5.14)	172 (13.40)	8 (0.62)
	03-04b5	18 (1.86)	24 (2.47)	0 (0)	0 (0)	30 (3.09)	104 (10.72)	14 (1.44)
	Mean ± SEM	15.60 ± 9.65 (1.74 ± 1.07)	23.20 ± 5.60 (2.57 ± 0.53)	0 ± 0 (0 ± 0)	0 ± 0 (0 ± 0)	24.00 ± 13.38 (2.29 ± 1.08)	106.00 ± 24.48 (11.93 ± 2.55)	12.80 ± 2.88 (1.48 ± 0.36)
c S1BF	03-02b7	2 (0.38)	16 (3.05)	1 (0.19)	2 (0.38)	6 (1.15)	24 (4.58)	13 (2.48)
	04-01b2	0 (0)	29 (4.03)	0 (0)	0 (0)	19 (2.64)	7 (0.97)	29 (4.03)
	03-02b4	16 (1.04)	25 (1.62)	0 (0)	0 (0)	38 (2.47)	143 (9.29)	49 (3.18)
	03-02b5	23 (1.92)	15 (1.25)	0 (0)	0 (0)	51 (4.25)	26 (2.17)	25 (2.08)
	03-02b6	6 (1.07)	17 (3.02)	0 (0)	0 (0)	15 (2.66)	24 (4.26)	10 (1.78)
	Mean ± SEM	9.40 ± 4.89 (0.88 ± 0.37)	20.40 ± 3.12 (2.60 ± 0.57)	0.20 ± 0.22 (0.04 ± 0.04)	0.40 ± 0.45 (0.08 ± 0.09)	25.80 ± 9.15 (2.63 ± 0.55)	44.80 ± 27.72 (4.26 ± 1.59)	25.20 ± 7.75 (2.71 ± 0.45)

Table 7

Number and percentage (in parentheses) of retrogradely labeled neurons in sensory and non-sensory subcortical areas after injections of CTb into the primary somatosensory cortex (S1) of intact C57Bl/6 mice (continued)

Injection site	Case	Subcortical area						
		CPu	Acb	AVVL	Rt	MD	LD	Rh
S1	02-03a4	0 (0)	0 (0)	0 (0)	0 (0)	0 (0)	0 (0)	0 (0)
	02-03a5	0 (0)	0 (0)	0 (0)	0 (0)	0 (0)	0 (0)	0 (0)
	02-03a3	0 (0)	0 (0)	0 (0)	0 (0)	0 (0)	0 (0)	0 (0)
	02-03a6	0 (0)	0 (0)	0 (0)	0 (0)	0 (0)	0 (0)	0 (0)
	02-03a7	0 (0)	0 (0)	0 (0)	0 (0)	0 (0)	0 (0)	0 (0)
	Mean ± SEM	0 ± 0	0 ± 0	0 ± 0	0 ± 0	0 ± 0	0 ± 0	0 ± 0
		(0 ± 0)	(0 ± 0)	(0 ± 0)	(0 ± 0)	(0 ± 0)	(0 ± 0)	(0 ± 0)
r S1BF	03-02b2	0 (0)	0 (0)	0 (0)	0 (0)	0 (0)	0 (0)	0 (0)
	03-04a6	2 (0.31)	0 (0)	0 (0)	0 (0)	0 (0)	0 (0)	0 (0)
	03-04a7	10 (1.11)	0 (0)	0 (0)	0 (0)	0 (0)	0 (0)	0 (0)
	03-04b4	2 (0.16)	0 (0)	0 (0)	16 (1.25)	0 (0)	0 (0)	0 (0)
	03-04b5	4 (0.41)	0 (0)	0 (0)	6 (0.62)	0 (0)	0 (0)	0 (0)
	Mean ± SEM	3.60 ± 1.92	0 ± 0	0 ± 0	4.40 ± 3.49	0 ± 0	0 ± 0	0 ± 0
		(0.40 ± 0.21)	(0 ± 0)	(0 ± 0)	(0.37 ± 0.28)	(0 ± 0)	(0 ± 0)	(0 ± 0)
c S1BF	03-02b7	0 (0)	0 (0)	0 (0)	0 (0)	0 (0)	0 (0)	0 (0)
	04-01b2	1 (0.14)	0 (0)	0 (0)	0 (0)	0 (0)	0 (0)	0 (0)
	03-02b4	61 (3.96)	5 (0.33)	1 (0.07)	99 (6.43)	70 (4.55)	149 (9.68)	6 (0.39)
	03-02b5	0 (0)	0 (0)	0 (0)	3 (0.25)	0 (0)	120 (10)	0 (0)
	03-02b6	0 (0)	0 (0)	0 (0)	0 (0)	0 (0)	3 (0.53)	0 (0)
	Mean ± SEM	12.40 ± 13.59	1.00 ± 1.12	0.20 ± 0.22	20.40 ± 21.98	14.00 ± 15.65	54.40 ± 36.92	1.20 ± 1.34
		(0.82 ± 0.88)	(0.07 ± 0.07)	(0.01 ± 0.02)	(1.34 ± 1.43)	(0.91 ± 1.02)	(4.04 ± 2.65)	(0.08 ± 0.09)

Table 7

Number and percentage (in parentheses) of retrogradely labeled neurons in sensory and non-sensory subcortical areas after injections of CTb into the primary somatosensory cortex (S1) of intact C57Bl/6 mice (continued)

Injection site	Case	Subcortical area					
		LP	LH	PVP	APTD	PM	mfb
S1	02-03a4	0 (0)	0 (0)	0 (0)	0 (0)	0 (0)	0 (0)
	02-03a5	0 (0)	0 (0)	0 (0)	0 (0)	0 (0)	8 (1.15)
	02-03a3	0 (0)	0 (0)	0 (0)	0 (0)	0 (0)	4 (0.51)
	02-03a6	0 (0)	0 (0)	0 (0)	0 (0)	0 (0)	2 (0.45)
	02-03a7	0 (0)	0 (0)	0 (0)	0 (0)	0 (0)	6 (0.56)
	Mean ± SEM	0 ± 0	0 ± 0	0 ± 0	0 ± 0	0 ± 0	4.00 ± 1.58
		(0 ± 0)	(0 ± 0)	(0 ± 0)	(0 ± 0)	(0 ± 0)	(0.53 ± 0.20)
r S1BF	03-02b2	0 (0)	0 (0)	0 (0)	0 (0)	0 (0)	2 (0.27)
	03-04a6	0 (0)	0 (0)	0 (0)	0 (0)	0 (0)	2 (0.31)
	03-04a7	0 (0)	0 (0)	0 (0)	0 (0)	0 (0)	0 (0)
	03-04b4	0 (0)	0 (0)	0 (0)	0 (0)	0 (0)	0 (0)
	03-04b5	0 (0)	0 (0)	0 (0)	0 (0)	0 (0)	0 (0)
	Mean ± SEM	0 ± 0	0 ± 0	0 ± 0	0 ± 0	0 ± 0	0.80 ± 0.55
		(0 ± 0)	(0 ± 0)	(0 ± 0)	(0 ± 0)	(0 ± 0)	(0.12 ± 0.08)
c S1BF	03-02b7	0 (0)	0 (0)	0 (0)	0 (0)	0 (0)	0 (0)
	04-01b2	0 (0)	0 (0)	0 (0)	0 (0)	0 (0)	0 (0)
	03-02b4	2 (0.13)	3 (0.20)	10 (0.65)	32 (2.08)	7 (0.46)	0 (0)
	03-02b5	0 (0)	0 (0)	0 (0)	0 (0)	0 (0)	11 (0.92)
	03-02b6	0 (0)	0 (0)	0 (0)	0 (0)	0 (0)	5 (0.89)
	Mean ± SEM	0.40 ± 0.45	0.60 ± 0.67	2.00 ± 2.24	6.40 ± 7.16	1.40 ± 1.57	3.20 ± 2.43
		(0.03 ± 0.03)	(0.04 ± 0.04)	(0.13 ± 0.15)	(0.42 ± 0.47)	(0.09 ± 0.10)	(0.36 ± 0.25)

Table 7

Number and percentage (in parentheses) of retrogradely labeled neurons in sensory and non-sensory subcortical areas after injections of CTb into the primary somatosensory cortex (S1) of intact C57Bl/6 mice (continued)

Injection site	Case	Subcortical area					
		VA	LSI	STLP	AV	EP	VP
S1	02-03a4	0 (0)	0 (0)	0 (0)	0 (0)	0 (0)	0 (0)
	02-03a5	0 (0)	0 (0)	0 (0)	0 (0)	0 (0)	0 (0)
	02-03a3	0 (0)	0 (0)	0 (0)	0 (0)	0 (0)	0 (0)
	02-03a6	0 (0)	0 (0)	0 (0)	0 (0)	0 (0)	0 (0)
	02-03a7	0 (0)	0 (0)	0 (0)	0 (0)	0 (0)	0 (0)
	Mean ± SEM	0 ± 0	0 ± 0	0 ± 0	0 ± 0	0 ± 0	0 ± 0
		(0 ± 0)	(0 ± 0)	(0 ± 0)	(0 ± 0)	(0 ± 0)	(0 ± 0)
r S1BF	03-02b2	0 (0)	2 (0.27)	0 (0)	0 (0)	0 (0)	0 (0)
	03-04a6	0 (0)	0 (0)	0 (0)	0 (0)	2 (0.31)	0 (0)
	03-04a7	0 (0)	2 (0.22)	2 (0.22)	2 (0.22)	2 (0.22)	0 (0)
	03-04b4	0 (0)	0 (0)	0 (0)	4 (0.31)	0 (0)	4 (0.31)
	03-04b5	0 (0)	2 (0.21)	0 (0)	0 (0)	0 (0)	2 (0.21)
	Mean ± SEM	0 ± 0	1.20 ± 0.55	0.40 ± 0.45	1.60 ± 0.84	0.80 ± 0.55	1.20 ± 0.89
		(0 ± 0)	(0.04 ± 0.04)	(0.04 ± 0.04)	(0.07 ± 0.07)	(0.03 ± 0.03)	(0.04 ± 0.04)
c S1BF	03-02b7	0 (0)	0 (0)	0 (0)	0 (0)	0 (0)	0 (0)
	04-01b2	0 (0)	0 (0)	0 (0)	0 (0)	0 (0)	0 (0)
	03-02b4	0 (0)	0 (0)	0 (0)	0 (0)	0 (0)	0 (0)
	03-02b5	0 (0)	0 (0)	0 (0)	0 (0)	0 (0)	0 (0)
	03-02b6	7 (1.24)	0 (0)	0 (0)	0 (0)	0 (0)	0 (0)
	Mean ± SEM	1.40 ± 1.57	0 ± 0	0 ± 0	0 ± 0	0 ± 0	0 ± 0
		(0.25 ± 0.28)	(0 ± 0)	(0 ± 0)	(0 ± 0)	(0 ± 0)	(0 ± 0)

Significant differences in the percentage of labeled neurons in Po, VL, GP and ZI were observed between the group which received injections in S1 and the group which received injections in the anterior part of S1BF (see Figure 19). Post-hoc tests revealed that a greater proportion of labeled neurons was found in ZI (Tukey-HSD, $p = 0.025$) of the group which received injections in S1 compared with the group which received injections in the rostral part of S1BF. Also, a greater proportion of labeled neurons was found in Po (Tukey-HSD, $p < 0.001$), VL (Tukey-HSD, $p = 0.039$) and GP (Tukey-HSD, $p = 0.002$) of the group which received injections in the rostral part of S1BF compared with the group which received injections in S1.

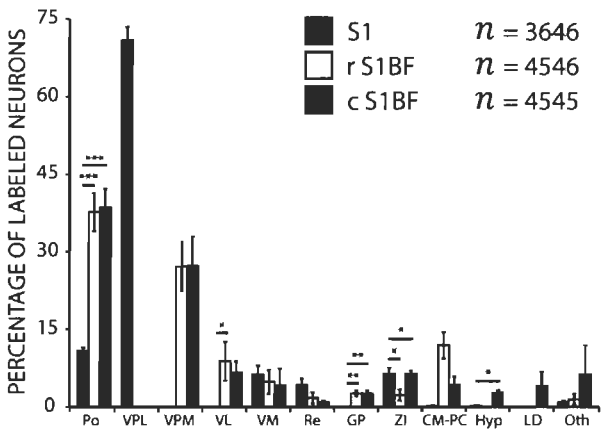

Figure 19. Percentage of retrogradely labeled neurons in different subcortical areas.

Significant differences in the percentage of labeled neurons in Po, GP, ZI and Hyp were observed between the group which received injections in S1 and the group which received injections in the caudal part of S1BF. Post-hoc tests revealed that a greater proportion of labeled neurons was found in Po (Tukey-HSD, $p < 0.001$), GP

(Tukey-HSD, $p = 0.002$), ZI (Tukey-HSD, $p = 0.041$) and Hyp (Tukey-HSD, $p = 0.003$) of the group which received injections in the caudal part of S1BF compared with the group which received injections in S1. No significant differences in the percentage of labeled neurons were observed in the subcortical structures between the group which received injections in the rostral part of S1BF and the group which received injections in the caudal part of S1BF.

In order to assess and compare the multimodality of the different portions of the mouse somatosensory cortex, the relative importance of cortical projections were grouped according to sensory modality, motor and in functional domains such as multisensory areas and modulatory areas (see Figure 20). This classification was the same as used by Budinger and Scheich (2009) for the sake of comparison between studies. This analysis shows that S1 and the rostral barrel field receive less multisensory input and input from other sensory modalities, than the caudal portion of the somatosensory barrel field. Indeed, both the ipsilateral and callosal cortical inputs of these areas come mainly from somatosensory and motor cortices. The caudal portion of the barrel field receives an important contingent of projections from somatosensory and motor cortices but received a greater proportion of ipsilateral projections from cortices dedicated to other sensory modalities and also from multisensory association cortices. Callosal projections convey less heteromodal and multisensory projections than the ipsilateral cortical projections. A similar pattern was shown for subcortical projections to the somatosensory cortex. Indeed, the non-barrel field received mainly modality specific

afferents from the thalamus whereas the barrel field areas received more multisensory thalamic inputs.

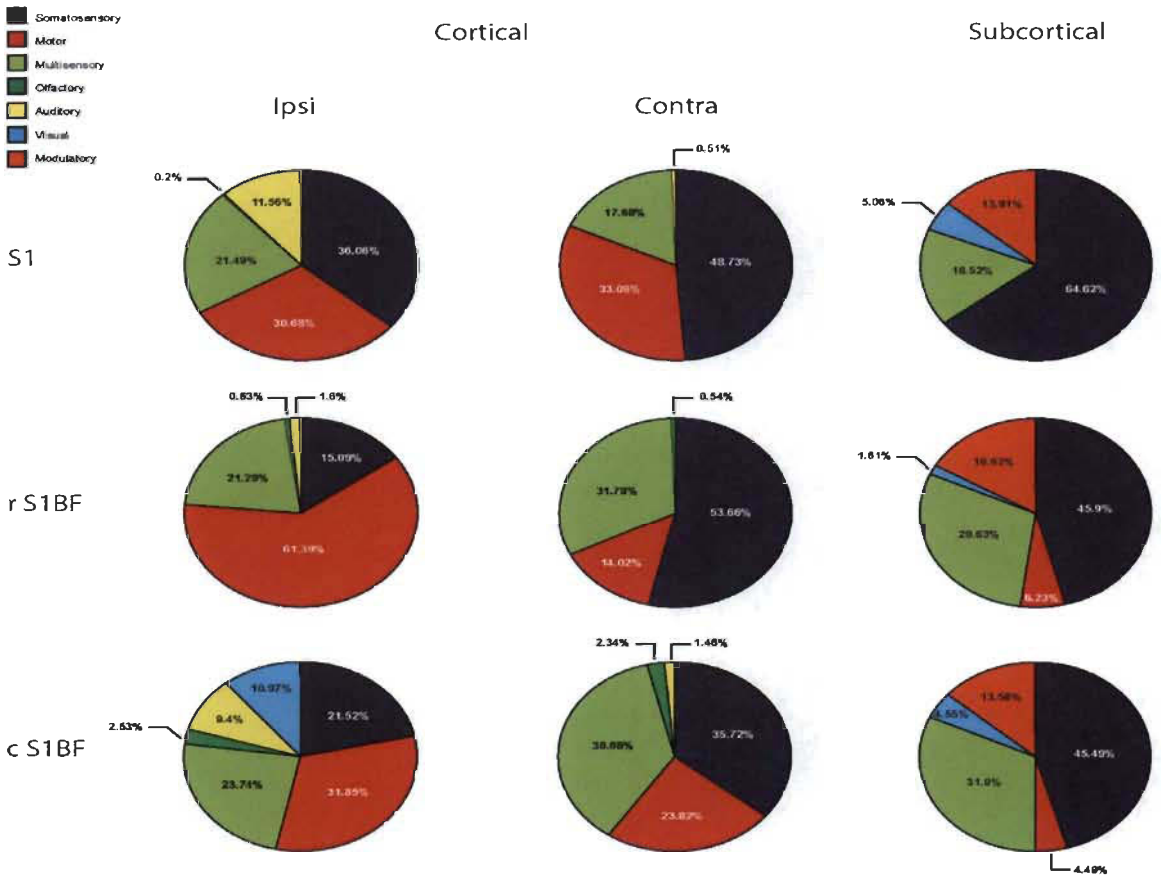

Figure 20. Diagram showing the input ratios of different modalities into the primary somatosensory cortex of the C57Bl/6 mouse. Ratios were calculated from the relative numbers of retrogradely labeled neurons found in the respective structures.

CORTEX:
Somatosensory = S2 (S1 & S1BF only for the contralateral hemisphere); Motor = M1, M2; Multisensory = , TeA, Cl, RSGc, RSD, Ect, PRh, PrL, IL, Orbital Cx, Insular Cx, DP, Cg.; Olfactory = Pir.; Auditory = Au.; Visual = V1, V2M, V2L.; Modulatory = No area.

SUBCORTEX:
Somatosensory = Po, VPL, VPM, APTD.; Motor = VL, VM, GP, ZI, CPu.; Multisensory = PT, Rt, Re, CPu, Rh.; Olfactory = No area.; Auditory = No area.; Visual = LD, LP.; Modulatory = AM, AHA, CM-PC, Hyp, Acb, AVVL, MD, LH, PVP, PM, mfb, VA.

Discussion

Summary

The aim of this study was to identify the top-down connections as well as the networks of the mouse involved in multisensory integration, and to test the hypothesis that differences exist in the quantity and/or structure of projections found in S1, and the rostral and caudal parts of S1BF. The present study has shown, by use of the sensitive neuronal tracer CTb, that these three different parts of S1 have afferent connections with somatosensory areas, non-somatosensory primary sensory areas, multisensory, motor, associative, and neuromodulatory areas. The retrograde tracer used here made it possible to quantitatively analyze the retrogradely labeled cells of origin and their laminar distribution to classify the projections as feedback, feedforward or lateral.

Top-down influences on early cortical sensory processing contribute to several aspects such as perceptual grouping, constancies and shape recognitions but most importantly they provide contextual information from sensory, motor and association areas of the brain (see Gilbert and Li, 2013; Gilbert and Sigman, 2007 for review). The diversity of afferent projections to the somatosensory cortex shown here are commensurate with the afferent projections shown for the visual cortex in the mouse (Charbonneau et al., 2012) and the auditory cortex of the gerbil (Budinger et al., 2008). The present results and these previous studies illustrate the important functional diversity of top-down influences on primary sensory cortices in rodents. Whether this

diversity is also present in primates is not known emphasizing the need for brain wide connectivity of the cortex in mammals with more highly developed cerebral cortex.

Connectomes and modules in the somatosensory barrel field vs. non-barrel field

Compared to precedent anatomical studies (Henschke et al., 2014; Zakiewicz et al., 2014), our brain-wide analysis contributes more complete and detailed information about S1 afferent projections, both regarding the differences between cortical and subcortical projections to the different parts of S1 and their structure. The presented results are of relevance for ongoing large-scale efforts to systematically map connections in the rodent brain, such as the Mouse Brain Connectome Project and the Allen Mouse Brain Connectivity Atlas. A connectomics analysis of the mouse cortex has demonstrated four subnetworks of the somatosensory cortex (Zingg et al., 2014), the orofaciopharyngeal, upper limb, lower limb and trunk, and whisker subnetworks.

Our study extends this knowledge on the widespread cortical afferents of S1 of the mouse by providing a quantitative rather than qualitative evaluation and also by taking into account the thalamic afferents. Moreover, these quantifications were compared between afferent connections to the mystacial caudal barrel field, more rostral barrel field and somatosensory cortex outside the barrel field to see if the different somatosensory subnetworks follow similar patterns of cortical connectivity. Our injections outside of the barrel field cover both the forelimb and hindlimb representations of S1 which correspond to both the upper limb and lower limb

representations of S1 respectively in the MCP data used to build the four subnetworks. The MCP also contains reports of retrograde projections to the barrel field but this data could not be specifically related to either the rostral or the caudal part of S1BF from our own material.

Each of the four somatic sensorimotor subnetworks displayed connections with other somatic sensorimotor areas like M1, M2 and S2 (Zingg et al., 2014), which also represented the overall majority of the connections displayed in our results for all three injection sites of S1. Each of the four somatic sensorimotor subnetworks is also composed of major nodes. The orofaciopharyngeal subnetwork is composed of five major nodes: M1, M2, S1, including the barrel field, and S2. The gustatory, visceral, and dorsal agranular areas, grouped together as the insular cortex in our material, are also connected with this subnetwork, which could contribute relevant information on gustation and food safety (Carleton et al., 2010; Maffei et al., 2012). We did not perform CTb injections directly into the mouth and nose regions of the primary somatosensory cortex but we did observe afferent connections from the insular cortex to all three injection sites of S1 without any significant differences between the three in both hemispheres.

The upper limb subnetwork is composed of four major nodes: M1, M2, S1 and S2. The upper limb subnetwork also shares connections with the temporal association, perirhinal, and ectorhinal cortices. We also observed afferent connections with the

temporal association, perirhinal and ectorhinal cortices to the primary somatosensory cortex, outside of the barrel field and both parts of the barrel field.

The lower limb and trunk subnetwork is composed of three major nodes: M1, M2 and S1. Relevant information for the lower limb and trunk subnetwork is also provided by inputs from the temporal association, perirhinal and ectorhinal cortices as well as from visual and auditory areas, and several other areas such as the parietal association cortex and ventral orbital cortex. We also observed afferent connections with the temporal association, perirhinal and ectorhinal cortices to the primary somatosensory cortex, outside of the barrel field and both parts of the barrel field. We observed afferent connections from auditory areas to S1, outside of the barrel field, but no projections from visual areas were observed to this part of S1. The afferent connections from the parietal association cortex and the ventral orbital cortex were observed as well in S1, outside of the barrel field, with the former being more prominent in this part of S1 compared to the two parts of the barrel field.

The whisker subnetwork is composed of three major nodes: M1, S2 and the barrel field. The whisker subnetwork also shares connections with the temporal and parietal association cortices, the perirhinal and ectorhinal cortices as well as visual and insular areas. These connections, including the ones from visual areas, were also observed in the caudal barrel field, and to a lesser extent in the cases which received injections in the rostral barrel field, excluding the ones from visual areas.

The most caudal part of S1 was also reported to be highly connected with the primary visual and auditory cortices to form major components of the medial network, another big network which mediate transduction of information between these sensory areas and higher order association areas of the neocortex. Interestingly, this medial network provides an interface for direct interactions between different sensory modalities though reciprocal connections among the visual and auditory cortices and the barrel field.

The unique topological organization of the many subnetworks would reflect different information processing strategies for each. The heavy and reciprocal connections between the somatosensory and motor areas of the somatic sensorimotor network could enable rapid integration of tactile information for dynamically regulating motor actions. For example, the orofaciopharyngeal subnetwork could enable the integration of tactile information in the oral cavity and proprioception of the jaw for initiation, maintenance, or termination of rhythmic jaw movements throughout the masticatory period (Yamada et al., 2005). Heavy connections with somatosensory and motor areas were also observed in afferent inputs to the rostral part of the barrel field, which could reflect such processes more centered on somatosensory and motor information.

Unlike the interactions that occur within the somatic sensorimotor network, the medial network primarily mediates interactions between the sensory and higher order

association areas. The medial network serves to transmit sensory information from the primary visual and auditory cortices as well as the caudal barrel field to the retrosplenial, parietal, anterior cingulate, and orbital areas which have been implicated in orientating and coordinating movements of the eyes, head, and body in object searching tasks and spatial navigation (Bucci, 2009; Feierstein et al., 2006; Vann et al., 2009; Weible, 2013).

The projections to the caudal part of the barrel field in our material support the implication of this area in such a medial network and concretizes its position at the interface between ascending bottom-up and descending top-down pathways. Our comparison of the projections indeed shows that the barrel field of S1, particularly the caudal part, displays different and more abundant cortical and subcortical connections compared to the rest of S1, by targeting more sensory related cortical areas relevant to exploration such as the auditory and visual cortex along the perirhinal and ectorhinal cortex which are implicated in sensory integration and gating (Naber et al., 2000; Rodgers et al., 2008), as well as some additional subcortical brain regions, such as the ventrolateral nucleus of the thalamus which modulates nociceptive processes (Blomqvist et al., 1992; Craig, Jr. and Burton, 1981; Miletic and Coffield, 1989). This suggests that somatosensory processing in whisker representations of S1 could be directly influenced by other sensory information.

Multimodality of primary sensory cortices

In traditional models of sensory cortex organization, sensory information processing for each modality is initially segregated in modality-specific sensory areas before subsequent integration in higher-order association areas. This organizational scheme has been challenged by the demonstration of multimodal responses in primary sensory cortices (Driver and Noesselt, 2008; Ghazanfar et al., 2005). Indeed, our data suggests that somatosensory processing in whisker representations of S1 is directly influenced by other sensory information. In particular, the caudal part of the barrel field of S1 receives afferents from more sensory related cortical areas dedicated to other modalities compared to the rest of S1.

Other studies on corticocortical connectivity in rodents show that the primary visual cortex of the mouse receives direct inputs from somatosensory, auditory, olfactory as well as multisensory and associative cortical areas such as the RSD, RSG, Cg, M, PtA, TeA, Ect, Ent, PRh, Cl, IC and OC (Charbonneau et al., 2012), and that the primary auditory cortex of the gerbil also receives direct inputs from somatosensory, visual, olfactory, multisensory and associative areas (Budinger et al., 2009). Moreover, the existence of direct and reciprocal connections has been demonstrated among the primary sensory cortices (Budinger et al., 2006; Campi et al., 2010; Charbonneau et al., 2012; Laramée et al., 2013; Larsen et al., 2009; Sieben et al., 2013; Wang and Burkhalter, 2007;). As in the present study, retrogradely labeled neurons were quantified following injections of CTb in the primary visual cortex of the mouse (Charbonneau et al., 2012).

It appears that 6.57% of the labeled cell bodies providing inputs to V1 come from somatosensory areas and 28.47% of them come from auditory areas. Retrogradely labeled cell bodies were also quantified following tracer injections in the primary auditory cortex of the gerbil (Budinger and Scheich, 2009). It appears that only 0.5% of the labeled cell bodies providing inputs to A1 come from somatosensory areas and 1.7% of them come from visual areas. Our data indicates that 9.4% of the inputs to the caudal part of the barrel field come from auditory areas and 10.97% of them come from visual areas. This part of the primary somatosensory cortex would benefit the most from heteromodal connections and be the most multimodal part of the primary somatosensory cortex. Similarly, the caudal-most barrel field is part of the medial network built from the MCP data (Zingg et al., 2014), which also shares connections with many sensory related cortical areas dedicated to other modalities.

These results suggest that in rodents, the highest input ratio for "non-preferred" modalities is for V1. This suggests that the visual modality in rodents would benefit the most from heteromodal connections and be the most multimodal of the primary sensory cortices. On the other hand, A1 receives only faint inputs from the other primary sensory cortices (Budinger and Scheich, 2009; Henschke et al., 2014). These observations suggest that the mutual influences between the senses are not equivalent in strength. The influence of the auditory areas on the visual cortex would be the stronger one.

Possible functions of non-somatosensory sensory and multisensory inputs to S1

The functional role of integration of non-somatosensory sensory and multisensory information at early somatosensory cortical stage has been demonstrated in previous studies. Studies in humans demonstrated how vision influences somatosensory perception. Visually modulated improvement of tactile perception is known as the visual enhancement of touch (Cardini et al., 2011; Kennett et al., 2001; Serino et al., 2007, 2009; Taylor-Clarke et al., 2004; Tipper et al., 1998). Vision can also modulate pain perception (Longo et al., 2009). Moreover binding of visual and tactile information is important in the sensory representation of the peripersonal space (Rizzolatti et al., 1981a, 1981b). A study has shown that congruent haptic stimulation can improve performance on a simple visual grating detection task compared to incongruent haptic stimulation (van der Groen et al., 2013). Visual information adds to the perception of surface texture and indicates a crossmodal interaction of sensory information already at an early cortical processing stage (Eck et al., 2013). Visual information exerts substantial influences on torque perception even when participants know that visual information is unreliable (Xu et al., 2012).

Object manipulation produces characteristic sounds and causes specific haptic sensations that facilitate the recognition of the manipulated object (Kassuba et al., 2013). Combining information across the sensory modalities improves sensory performance, for example, by decreasing reaction times (Hoefer et al., 2013; Molholm et al., 2002; Noesselt et al., 2010; Teder-Salejarvi et al., 2002), which in turn can be crucial for the

survival of the individual. Our results suggest that there are indeed direct connections between S1 and both Au and V1 and that the fastest, and thus most efficient, way to convey information about S1 and both modalities could be such connections (Bizley and King, 2008; Bizley, Nodal, Bajo, Nelken, & King, 2007; Wallace et al., 2004). Likewise, audiotactile (Hoefer et al., 2013) and visuotactile information (Macaluso, 2006) can be rapidly processed in the respective crossmodal networks.

Top-down cortical projections and conscious sensory perception in S1

The three parts of S1 receive afferent projections from several associative areas of higher order, such as the parietal and temporal association cortices, agranular and dysgranular retrosplenial cortices, and the ectorhinal, perirhinal, orbital and insular cortices. Moreover, the laminar distribution of labeled neurons suggests that S1 in mice receives feedback-type projections from these areas. These projections have different structures and could also have different functions since the layer indices, although on the whole negative, were different in degree. These projections could modulate information in S1 (Bullier, 2001b), so that bottom-up signals become consciously perceptible (Tononi and Koch, 2008). Indeed, S1 would have a key role in predictive coding, which is the matching process of the nervous system between the sensory information conveyed by the bottom-up signals and the expectations towards the environment generated by the top-down signals (Grossberg, 1980; Lee and Mumford, 2003; Llinas and Pare, 1991).

The top-down projections not only serve to modulate the bottom-up signals, they are capable of constructing a conscious sensory perception in the primary sensory cortices even in the absence of external stimuli from the sensory organs of their respective modalities (Meyer, 2011). Top-down projections to V1 (Charbonneau et al., 2012) and A1 (Budinger et al., 2006, 2008; Budinger and Scheich, 2009) are also present and very diverse in rodents. These studies along with our results therefore support a model where top-down connections are necessary for conscious sensory perception and where the primary sensory cortices are at the top of an inverted cortical hierarchy (Lamme and Roelfsema, 2000).

Top-down influences in cortical circuits are not homogeneous in function. In the visual system top-down influences can sharpen tuning, provide contextual information, and modulate plasticity, etc (see Gilbert and Sigman, 2007 for review). The present study more specifically emphasises the structural diversity of top-down influences on the somatosensory cortex subfields. The layer indices calculated here demonstrate that top-down influences were provided by projections with mainly negative values. This indicates that these projections are provided by more neurons in infragranular than supragranular layers. The layer indices range however between values close to 0 and -1, and are therefore not homogeneous. This diversity of size indices of top-down projections to the somatosensory cortex was greater than those to the visual cortex of the mouse (Charbonneau et al., 2012) and in the auditory cortex of the gerbil (Budinger et al., 2008). Only a few layer indices are given for the mouse afferents to the visual cortex

but they were mostly quite strongly negative, as for those shown for the gerbil cortical afferents of the auditory cortex.

The most striking differences in layer index values are between the auditory and visual projections to the caudal barrel field. Indeed, the layer index of the auditory cortex is strongly negative whereas that of the visual cortices V1 and V2M were close to 0. Although negative layer indices seem to be most prevalent in cortical afferent projections to somatosensory, visual and auditory cortices in these rodents, the interconnections between them appear quite different. Lateral type projections with layer indices close to 0 were found here from the projections from the visual cortex and this was also the case in the gerbil (Henschke et al., 2014). This contrasts further with the positive layer index reported in the projections from the visual cortex to the auditory cortex of the gerbil (Henschke et al., 2014).

There are significant functional differences between supra- and infragranular cortical connections. Electrophysiological studies have shown that gamma band oscillations are more prevalent in supragranular neurons (Bollimunta et al., 2011; Buffalo et al., 2011; Xing et al., 2012), whereas beta-band oscillations are more important in infragranular neurons (Buffalo et al., 2011; Xing et al., 2012). It has been suggested that feedback cortical projections might promote beta synchronization between cortical areas and that feedforward projections could promote gamma band interareal synchronizations (Markov et al., 2014). Further studies demonstrated that

feedforward processing in the visual system increased activity in the gamma band and that feedback processing increased activity in the theta and beta frequencies (Bastos et al., 2015; Michalareas et al., 2016; van Kerkoerle et al., 2014). Moreover there is a significant correlation between anatomically determined indices of neuron distributions in cortical layers, and beta/gamma band activity in feedback and feedforward projections in monkeys (Bastos et al., 2015).

The predominant negative values in the cortical afferent projections to the somatosensory cortex of the mouse shown here suggest that top-down influences act most importantly in the beta range oscillations. However we can hypothesize that the is a range in the intensity of synchronization in the beta and gamma frequencies exerted by namely visual and auditory cortices upon the caudal barrel field and also coming from the contralateral cortices in which a wider range of layer indices values were found.

We show here that the strength of corticocortical connections of the somatosensory decreases with distance from the injection sites in all three subfields of the somatosensory cortex of the mouse. This demonstrates that the interareal connectivity rules demonstrated for the monkey cortex (Ercsey-Ravasz et al., 2013) might also apply to mouse. This also suggest that the mouse cortex interareal connections also develops under the same constraint of wire minimization (Cherniak, 1994, 2012; Cherniak et al., 1999, 2004; Chklovskii, 2000; Chklovskii and Koulakov, 2004; Chklovskii et al., 2002;

Klyachko and Stevens, 2003; Koulakov and Chklovskii, 2001; Mitchison, 1991) notwithstanding it small brain size.

Top-down and multisensory thalamocortical connections to S1

Subcortical projections can also provide important top-down recurrent inputs. Indeed, cortical connectivity also takes place through higher order thalamic nuclei such as the pulvinar through which cortico-thalamo-cortical loops are established (Saalmann et al., 2012; Sherman, 2005; Sherman and Guillery, 2002, 2011; Theyel et al., 2010). The Po is such a higher order thalamic nucleus of the somatosensory system in the mouse (Bourassa et al., 1995; Diamond et al., 1992; Hoogland et al., 1987; Sherman and Guillery, 2006). The Po projections to the rostral and caudal barrel field were much stronger than to the non-barrel field somatosensory cortex. This could indicate that the barrel field might require more abundant indirect cortical information than the cortical representations of the rest of the body. The barrel field also receives more abundant projections from cortices dedicated to other sensory modalities and association cortices.

We also show here that the somatosensory cortex receives projections from both the Po and the visual higher-order thalamic lateral posterior nucleus which contrasts with the visual cortex that receives projections from the LP only (Charbonneau et al., 2012). The visual LP in the mouse has been shown to provide contextual information on the speed of locomotion to the visual cortex (Roth et al., 2016). This information would be

also conveyed to the somatosensory cortex and could be useful contextual information in whisking behavior.

Among the nuclei of the ventral thalamic group, VL sends a good number of projections to S1BF. It is well established that VL provides somatotopic motor information to the motor cortex (Schmahmann, 2003; Strick, 1973; Tlamsa and Brumberg, 2010), however, there is a small number of neurons in VL that projects to S1 (Donoghue and Parham, 1983; Spreafico et al., 1981). As we show here, this projection could target specifically S1BF. VL could be part of anatomical motor loops for eye blink conditioning (Sears et al., 1996), eye positioning (Werner-Reiss et al., 2003), and sensory motor task performance (Brosch et al., 2005).

LD is a nucleus with major projections to the visual cortex (Towns et al., 1982; van der Groen T. and Wyss, 1992), which in addition to its visual connections, contains neurons projecting to the caudal part of the barrel field in our study on the mouse as well as the rat (Kamishina et al., 2009) and the gerbil (Henschke et al., 2014). These could represent the fraction of LD neurons that already respond to somatosensory stimulation (Bezdudnaya and Keller, 2008). Alternatively, they may transmit visual information to the somatosensory cortex (Shires et al., 2013; van der Groen T. and Wyss, 1992) or could be involved in rapid spatial processing of multisensory information for turning behavior (Fabre-Thorpe et al., 1986).

Altogether, the mystacial caudal barrel field stands out from the rest of the primary somatosensory cortex by having more connections with cortical and subcortical visual structures such as V1 and LD. These projections could be the anatomical substrate of the influence of vision on the vibrissae tactile sensations and navigation in mice. The interaction of the vibrissae with vision could be important in the representation of the peripersonal space (Rizzolatti et al., 1981a, 1981b), and which is specifically centered on the vibrissae in mice (Cardinali et al., 2009).

Conclusions

In conclusion, this study demonstrates the multitude and diversity of top-down and heteromodal cortical and subcortical projections to S1. This study confirms the hypothesis that differences exist between the projections of the mystacial caudal barrel field, more rostral barrel field and somatosensory cortex outside the barrel field. S1 and the barrel field have afferent connections with somatosensory areas, non-somatosensory primary sensory areas, multisensory, motor, associative, and neuromodulatory areas but the caudal part of the barrel field displays different and more abundant cortical and subcortical connections compared to the rest of S1. Indeed, when compared to the networks built from the Mouse Connectome Project data, a more caudal area such as the mystacial barrel field is a major component of the medial network which mediates transduction of information between the primary sensory areas and higher order association areas of the neocortex compared to the more rostral areas whose processes are more centered on somatosensory and motor information in the somatic sensorimotor

network. The projections to S1 are mostly of a feedback nature, but would still have a different structure since the laminar indices, albeit negative overall, were of varying degrees. In the case of the primary sensory cortices, the auditory projections would be of feedback nature whereas the visual projections towards the caudal part of the barrel field would be of lateral nature, demonstrating that the different primary sensory cortices do not occupy the same position in the cortical hierarchy. Along the previous studies on V1 and A1 in the mouse, this study demonstrates that associative and multisensory projections are present in all primary sensory cortices of the mouse and that these areas are not only dedicated to the processing of information of their own sensory modality.

Acknowledgements

We are grateful to Nadia Desnoyers for animal care and maintenance. This work was supported by discovery grants from the Natural Sciences and Engineering Research Council of Canada (NSERC) to DB and GB, and the Canadian Foundation for Innovation to DB. SBG was supported by a Réseau de Recherche en Santé de la Vision (RRSV) undergraduate student award.

References

Bastos AM, Vezoli J, Bosman CA, Schoffelen JM, Oostenveld R, Dowdall JR, De WP, Kennedy H, Fries P. 2015. Visual areas exert feedforward and feedback influences through distinct frequency channels. Neuron 85:390-401.

Berezovskii VK, Nassi JJ, Born RT. 2011. Segregation of feedforward and feedback projections in mouse visual cortex. J Comp Neurol 519:3672-3683.

Bezdudnaya T, Keller A. 2008. Laterodorsal nucleus of the thalamus: A processor of somatosensory inputs. J Comp Neurol 507:1979-1989.

Bizley JK, King AJ. 2008. Visual-auditory spatial processing in auditory cortical neurons. Brain Res 1242:24-36.

Bizley JK, Nodal FR, Bajo VM, Nelken I, King AJ. 2007. Physiological and anatomical evidence for multisensory interactions in auditory cortex. Cereb Cortex 17:2172-2189.

Blomqvist A, Ericson AC, Broman J, Craig AD. 1992. Electron microscopic identification of lamina I axon terminations in the nucleus submedius of the cat thalamus. Brain Res 585:425-430.

Bollimunta A, Mo J, Schroeder CE, Ding M. 2011. Neuronal mechanisms and attentional modulation of corticothalamic alpha oscillations. J Neurosci 31:4935-4943.

Bourassa J, Pinault D, Deschenes M. 1995. Corticothalamic projections from the cortical barrel field to the somatosensory thalamus in rats: A single-fibre study using biocytin as an anterograde tracer. Eur J Neurosci 7:19-30.

Brosch M, Selezneva E, Scheich H. 2005. Nonauditory events of a behavioral procedure activate auditory cortex of highly trained monkeys. J Neurosci 25:6797-6806.

Bucci DJ. 2009. Posterior parietal cortex: An interface between attention and learning? Neurobiol Learn Mem 91:114-120.

Budinger E, Heil P, Hess A, Scheich H. 2006. Multisensory processing via early cortical stages: Connections of the primary auditory cortical field with other sensory systems. Nsci 143:1065-1083.

Budinger E, Laszcz A, Lison H, Scheich H, Ohl FW. 2008. Non-sensory cortical and subcortical connections of the primary auditory cortex in Mongolian gerbils: Bottom-up and top-down processing of neuronal information via field AI. Brain Res 1220:2-32.

Budinger E, Scheich H. 2009. Anatomical connections suitable for the direct processing of neuronal information of different modalities via the rodent primary auditory cortex. Hear Res 258:16-27.

Buffalo EA, Fries P, Landman R, Buschman TJ, Desimone R. 2011. Laminar differences in gamma and alpha coherence in the ventral stream. Proc Natl Acad Sci U S A 108:11262-11267.

Bullier J. 2001a. Feedback connections and conscious vision. Trends Cogn Sci 5:369-370.

Bullier J. 2001b. Integrated model of visual processing. Brain Res Brain Res Rev 36:96-107.

Campi KL, Bales KL, Grunewald R, Krubitzer L. 2010. Connections of auditory and visual cortex in the prairie vole (Microtus ochrogaster): Evidence for multisensory processing in primary sensory areas. Cereb Cortex 20:89-108.

Cardinali L, Brozzoli C, Farne A. 2009. Peripersonal space and body schema: Two labels for the same concept? Brain Topogr 21:252-260.

Cardini F, Longo MR, Haggard P. 2011. Vision of the body modulates somatosensory intracortical inhibition. Cereb Cortex 21:2014-2022.

Carleton A, Accolla R, Simon SA. 2010. Coding in the mammalian gustatory system. Trends Neurosci 33:326-334.

Caviness VS. 1975. Architectonic map of neocortex of the normal mouse. J Comp Neurol 164:247-263.

Charbonneau V, Laramée ME, Boucher V, Bronchti G, Boire D. 2012. Cortical and subcortical projections to primary visual cortex in anophthalmic, enucleated and sighted mice. Eur J Neurosci 36:2949-2963.

Cherniak C. 1994. Component placement optimization in the brain. J Neurosci 14:2418-2427.

Cherniak C. 2012. Neural wiring optimization. Prog Brain Res 195:361-371.

Cherniak C, Changizi M, Kang D. 1999. Large-scale optimization of neuron arbors. Phys Rev E Stat Phys Plasmas Fluids Relat Interdiscip Topics 59:6001-6009.

Cherniak C, Mokhtarzada Z, Rodriguez-Esteban R, Changizi K. 2004. Global optimization of cerebral cortex layout. Proc Natl Acad Sci U S A 101:1081-1086.

Chklovskii DB. 2000. Optimal sizes of dendritic and axonal arbors in a topographic projection. J Neurophysiol 83:2113-2119.

Chklovskii DB, Koulakov AA. 2004. Maps in the brain: What can we learn from them? Annu Rev Neurosci 27:369-392.

Chklovskii DB, Schikorski T, Stevens CF. 2002. Wiring optimization in cortical circuits. Neuron 34:341-347.

Coogan TA, Burkhalter A. 1990. Conserved patterns of cortico-cortical connections define areal hierarchy in rat visual cortex. Exp Brain Res 80:49-53.

Coogan TA, Burkhalter A. 1993. Hierarchical organization of areas in rat visual cortex. J Neurosci 13:3749-3772.

Craig AD, Jr., Burton H. 1981. Spinal and medullary lamina I projection to nucleus submedius in medial thalamus: A possible pain center. J Neurophysiol 45:443-466.

Diamond ME, Armstrong-James M, Budway MJ, Ebner FF. 1992. Somatic sensory responses in the rostral sector of the posterior group (POm) and in the ventral posterior medial nucleus (VPM) of the rat thalamus: Dependence on the barrel field cortex. J Comp Neurol 319:66-84.

Dong H, Shao Z, Nerbonne JM, Burkhalter A. 2004. Differential depression of inhibitory synaptic responses in feedforward and feedback circuits between different areas of mouse visual cortex. J Comp Neurol 475:361-373.

Donoghue JP, Parham C. 1983. Afferent connections of the lateral agranular field of the rat motor cortex. J Comp Neurol 217:390-404.

Driver J, Noesselt T. 2008. Multisensory interplay reveals crossmodal influences on 'sensory-specific' brain regions, neural responses, and judgments. Neuron 57:11-23.

Eck J, Kaas AL, Goebel R. 2013. Crossmodal interactions of haptic and visual texture information in early sensory cortex. Neuroimage 75:123-135.

Ercsey-Ravasz M, Markov NT, Lamy C, Van Essen DC, Knoblauch K, Toroczkai Z, Kennedy H. 2013. A predictive network model of cerebral cortical connectivity based on a distance rule. Neuron 80:184-197.

Fabre-Thorpe M, Vievard A, Buser P. 1986. Role of the extra-geniculate pathway in visual guidance. II. Effects of lesioning the pulvinar-lateral posterior thalamic complex in the cat. Exp Brain Res 62:596-606.

Feierstein CE, Quirk MC, Uchida N, Sosulski DL, Mainen ZF. 2006. Representation of spatial goals in rat orbitofrontal cortex. Neuron 51:495-507.

Felleman DJ, Van Essen DC. 1991. Distributed hierarchical processing in the primate cerebral cortex. Cereb Cortex 1:1-47.

Franklin BJ, Paxinos G. 2008. The Mouse Brain in Stereotaxic Coordinates. San Diego: Academic Press.

Ghazanfar AA, Maier JX, Hoffman KL, Logothetis NK. 2005. Multisensory integration of dynamic faces and voices in rhesus monkey auditory cortex. J Neurosci 25:5004-5012.

Gilbert CD, Li W. 2013. Top-down influences on visual processing. Nat Rev Neurosci 14:350-363.

Gilbert CD, Sigman M. 2007. Brain states: Top-down influences in sensory processing. Neuron 54:677-696.

Godement P, Saillour P, Imbert M. 1979. Thalamic afferents to the visual cortex in congenitally anophthalmic mice. Neurosci Lett 13:271-278.

Grossberg S. 1980. How does a brain build a cognitive code? Psychol Rev 87:1-51.

Gutschalk A, Micheyl C, Oxenham AJ. 2008. Neural correlates of auditory perceptual awareness under informational masking. PLoS Biol 6:1-10.

Henschke JU, Noesselt T, Scheich H, Budinger E. 2014. Possible anatomical pathways for short-latency multisensory integration processes in primary sensory cortices. Brain Struct Funct 10:1007-1030.

Hoefer M, Tyll S, Kanowski M, Brosch M, Schoenfeld MA, Heinze HJ, Noesselt T. 2013. Tactile stimulation and hemispheric asymmetries modulate auditory perception and neural responses in primary auditory cortex. Neuroimage 79:371-382.

Hoogland PV, Welker E, Van der Loos H. 1987. Organization of the projections from barrel cortex to thalamus in mice studied with Phaseolus vulgaris-leucoagglutinin and HRP. Exp Brain Res 68:73-87.

Hudetz AG, Vizuete JA, Imas OA. 2009. Desflurane selectively suppresses long-latency cortical neuronal response to flash in the rat. Anesthesiology 111:231-239.

Ito M, Gilbert CD. 1999. Attention modulates contextual influences in the primary visual cortex of alert monkeys. Neuron 22:593-604.

Jiang J, Summerfield C, Egner T. 2013. Attention sharpens the distinction between expected and unexpected percepts in the visual brain. J Neurosci 33:18438-18447.

Kamishina H, Conte WL, Patel SS, Tai RJ, Corwin JV, Reep RL. 2009. Cortical connections of the rat lateral posterior thalamic nucleus. Brain Res 1264:39-56.

Kassuba T, Menz MM, Roder B, Siebner HR. 2013. Multisensory interactions between auditory and haptic object recognition. Cereb Cortex 23:1097-1107.

Kennett S, Taylor-Clarke M, Haggard P. 2001. Noninformative vision improves the spatial resolution of touch in humans. Curr Biol 11:1188-1191.

Klyachko VA, Stevens CF. 2003. Connectivity optimization and the positioning of cortical areas. Proc Natl Acad Sci U S A 100:7937-7941.

Koulakov AA, Chklovskii DB. 2001. Orientation preference patterns in mammalian visual cortex: A wire length minimization approach. Neuron 29:519-527.

Lamme VA, Roelfsema PR. 2000. The distinct modes of vision offered by feedforward and recurrent processing. Trends Neurosci 23:571-579.

Laramée ME, Rockland KS, Prince S, Bronchti G, Boire D. 2013. Principal component and cluster analysis of layer V pyramidal cells in visual and non-visual cortical areas projecting to the primary visual cortex of the mouse. Cereb Cortex 23:714-728.

Larsen DD, Luu JD, Burns ME, Krubitzer L. 2009. What are the Effects of Severe Visual Impairment on the Cortical Organization and Connectivity of Primary Visual Cortex? Front Neuroanat 3:1-16.

Lee TS, Mumford D. 2003. Hierarchical Bayesian inference in the visual cortex. J Opt Soc Am A Opt Image Sci Vis 20:1434-1448.

Llinas RR, Pare D. 1991. Of dreaming and wakefulness. Neuroscience 44:521-535.

Longo MR, Betti V, Aglioti SM, Haggard P. 2009. Visually induced analgesia: Seeing the body reduces pain. J Neurosci 29:12125-12130.

Macaluso E. 2006. Multisensory processing in sensory-specific cortical areas. Neuroscientist 12:327-338.

Maffei A, Haley M, Fontanini A. 2012. Neural processing of gustatory information in insular circuits. Curr Opin Neurobiol 22:709-716.

Makino H, Komiyama T. 2015. Learning enhances the relative impact of top-down processing in the visual cortex. Nat Neurosci 18:1116-1122.

Markov NT, Vezoli J, Chameau P, Falchier A, Quilodran R, Huissoud C, Lamy C, Misery P, Giroud P, Ullman S, Barone P, Dehay C, Knoblauch K, Kennedy H. 2014. Anatomy of hierarchy: Feedforward and feedback pathways in macaque visual cortex. J Comp Neurol 522:225-259.

McManus JN, Li W, Gilbert CD. 2011. Adaptive shape processing in primary visual cortex. Proc Natl Acad Sci U S A 108:9739-9746.

Meador KJ, Ray PG, Echauz JR, Loring DW, Vachtsevanos GJ. 2002. Gamma coherence and conscious perception. Neurology 59:847-854.

Meyer K. 2011. Primary sensory cortices, top-down projections and conscious experience. Prog Neurobiol 94:408-417.

Michalareas G, Vezoli J, van PS, Schoffelen JM, Kennedy H, Fries P. 2016. Alpha-Beta and Gamma Rhythms Subserve Feedback and Feedforward Influences among Human Visual Cortical Areas. Neuron: 89:384-397.

Miletic V, Coffield JA. 1989. Responses of neurons in the rat nucleus submedius to noxious and innocuous mechanical cutaneous stimulation. Somatosens Mot Res 6:567-587.

Miller MW, Vogt BA. 1984. Direct connections of rat visual cortex with sensory, motor, and association cortices. J Comp Neurol: 226:184-202.

Mitchison G. 1991. Neuronal branching patterns and the economy of cortical wiring. Proc Biol Sci 245:151-158.

Molholm S, Ritter W, Murray MM, Javitt DC, Schroeder CE, Foxe JJ. 2002. Multisensory auditory-visual interactions during early sensory processing in humans: A high-density electrical mapping study. Brain Res Cogn Brain Res 14:115-128.

Moore C, Cavanagh P. 1998. Recovery of 3D volume from 2-tone images of novel objects. Cognition 67:45-71.

Mumford D. 1992. On the computational architecture of the neocortex. II. The role of cortico-cortical loops. Biol Cybern 66:241-251.

Naber PA, Witter MP, Lopes da Silva FH. 2000. Differential distribution of barrel or visual cortex. Evoked responses along the rostro-caudal axis of the peri- and postrhinal cortices. Brain Res 877:298-305.

Noesselt T, Tyll S, Boehler CN, Budinger E, Heinze HJ, Driver J. 2010. Sound-induced enhancement of low-intensity vision: Multisensory influences on human sensory-specific cortices and thalamic bodies relate to perceptual enhancement of visual detection sensitivity. J Neurosci 30:13609-13623.

Paperna T, Malach R. 1991. Patterns of sensory intermodality relationships in the cerebral cortex of the rat. J Comp Neurol: 308:432-456.

Rao RP, Ballard DH. 1999. Predictive coding in the visual cortex: A functional interpretation of some extra-classical receptive-field effects. Nat Neurosci 2:79-87.

Rizzolatti G, Scandolara C, Matelli M, Gentilucci M. 1981a. Afferent properties of periarcuate neurons in macaque monkeys. I. Somatosensory responses. Behav Brain Res 2:125-146.

Rizzolatti G, Scandolara C, Matelli M, Gentilucci M. 1981b. Afferent properties of periarcuate neurons in macaque monkeys. II. Visual responses. Behav Brain Res 2:147-163.

Rockland KS, Pandya DN. 1979. Laminar origins and terminations of cortical connections of the occipital lobe in the rhesus monkey. Brain Res 179:3-20.

Rodgers KM, Benison AM, Klein A, Barth DS. 2008. Auditory, somatosensory, and multisensory insular cortex in the rat. Cereb Cortex 18:2941-2951.

Roelfsema PR, Lamme VA, Spekreijse H. 1998. Object-based attention in the primary visual cortex of the macaque monkey. Nature 395:376-381.

Roth MM, Dahmen JC, Muir DR, Imhof F, Martini FJ, Hofer SB. 2016. Thalamic nuclei convey diverse contextual information to layer 1 of visual cortex. Nat Neurosci 19:299-307.

Saalmann YB, Pinsk MA, Wang L, Li X, Kastner S. 2012. The pulvinar regulates information transmission between cortical areas based on attention demands. Science 337:753-756.

Schmahmann JD. 2003. Vascular syndromes of the thalamus. Stroke 34:2264-2278.

Sears LL, Logue SF, Steinmetz JE. 1996. Involvement of the ventrolateral thalamic nucleus in rabbit classical eyeblink conditioning. Behav Brain Res 74:105-117.

Serino A, Farne A, Rinaldesi ML, Haggard P, Ladavas E. 2007. Can vision of the body ameliorate impaired somatosensory function? Neuropsychologia 45:1101-1107.

Serino A, Padiglioni S, Haggard P, Ladavas E. 2009. Seeing the hand boosts feeling on the cheek. Cortex 45:602-609.

Sherman SM. 2005. Thalamic relays and cortical functioning. Prog Brain Res 149:107-126.

Sherman SM, Guillery RW. 2002. The role of the thalamus in the flow of information to the cortex. Philos Trans R Soc Lond B Biol Sci 357:1695-1708.

Sherman SM, Guillery RW. 2006. Exploring the thalamus and its role in cortical function. 2 ed. Cambridge, Mass.: MIT Press.

Sherman SM, Guillery RW. 2011. Distinct functions for direct and transthalamic corticocortical connections. J Neurophysiol 106:1068-1077.

Shires KL, Hawthorne JP, Hope AM, Dudchenko PA, Wood ER, Martin SJ. 2013. Functional connectivity between the thalamus and postsubiculum: Analysis of evoked responses elicited by stimulation of the laterodorsal thalamic nucleus in anesthetized rats. Hippocampus 23:559-569.

Sieben K, Roder B, Hanganu-Opatz IL. 2013. Oscillatory entrainment of primary somatosensory cortex encodes visual control of tactile processing. J Neurosci 33:5736-5749.

Sillito AM, Cudeiro J, Jones HE. 2006. Always returning: Feedback and sensory processing in visual cortex and thalamus. Trends Neurosci 29:307-316.

Spreafico R, Hayes NL, Rustioni A. 1981. Thalamic projections to the primary and secondary somatosensory cortices in cat: Single and double retrograde tracer studies. J Comp Neurol 203:67-90.

Strick PL. 1973. Light microscopic analysis of the cortical projection of the thalamic ventrolateral nucleus in the cat. Brain Res 55:1-24.

Summerfield C, de Lange FP. 2014. Expectation in perceptual decision making: Neural and computational mechanisms. Nat Rev Neurosci 15:745-756.

Summerfield C, Egner T. 2009. Expectation (and attention) in visual cognition. Trends Cogn Sci 13:403-409.

Super H, Spekreijse H, Lamme VA. 2001. Two distinct modes of sensory processing observed in monkey primary visual cortex (V1). Nat Neurosci 4:304-310.

Taylor-Clarke M, Kennett S, Haggard P. 2004. Persistence of visual-tactile enhancement in humans. Neurosci Lett 354:22-25.

Teder-Salejarvi WA, McDonald JJ, Di RF, Hillyard SA. 2002. An analysis of audio-visual crossmodal integration by means of event-related potential (ERP) recordings. Brain Res Cogn Brain Res 14:106-114.

Teufel C, Nanay B. 2016. How to (and how not to) think about top-down influences on visual perception. Conscious Cogn.

Theyel BB, Llano DA, Sherman SM. 2010. The corticothalamocortical circuit drives higher-order cortex in the mouse. Nat Neurosci 13:84-88.

Tipper SP, Lloyd D, Shorland B, Dancer C, Howard LA, McGlone F. 1998. Vision influences tactile perception without proprioceptive orienting. Neuroreport 9:1741-1744.

Tlamsa AP, Brumberg JC. 2010. Organization and morphology of thalamocortical neurons of mouse ventral lateral thalamus. Somatosens Mot Res 27:34-43.

Tononi G, Koch C. 2008. The neural correlates of consciousness: An update. Ann N Y Acad Sci 1124:239-261.

Towns LC, Burton SL, Kimberly CJ, Fetterman MR. 1982. Projections of the dorsal lateral geniculate and lateral posterior nuclei to visual cortex in the rabbit. J Comp Neurol 210:87-98.

van der Groen O, van der Burg E, Lunghi C, Alais D. 2013. Touch influences visual perception with a tight orientation-tuning. PLoS One 8:1-9.

van der Groen T., Wyss JM. 1992. Projections from the laterodorsal nucleus of the thalamus to the limbic and visual cortices in the rat. J Comp Neurol 324:427-448.

van Kerkoerle T, Self MW, Dagnino B, Gariel-Mathis MA, Poort J, van der Togt C, Roelfsema PR. 2014. Alpha and gamma oscillations characterize feedback and feedforward processing in monkey visual cortex. Proc Natl Acad Sci U S A 111:14332-14341.

Vann SD, Aggleton JP, Maguire EA. 2009. What does the retrosplenial cortex do? Nat Rev Neurosci 10:792-802.

Wallace M.T., Ramachandran R. Stein, B.E. 2004. A revised view of sensory cortical parcellation. Proc.Natl.Acad.Sci.U.S.A 101:2167-2172.

Wang Q, Burkhalter A. 2007. Area map of mouse visual cortex. J Comp Neurol 502:339-357.

Weible AP. 2013. Remembering to attend: The anterior cingulate cortex and remote memory. Behav Brain Res 245:63-75.

Werner-Reiss U, Kelly KA, Trause AS, Underhill AM, Groh JM. 2003. Eye position affects activity in primary auditory cortex of primates. Curr Biol 13:554-562.

Xing D, Yeh CI, Burns S, Shapley RM. 2012. Laminar analysis of visually evoked activity in the primary visual cortex. Proc Natl Acad Sci U S A 109:13871-13876.

Xu Y, O'Keefe S, Suzuki S, Franconeri SL. 2012. Visual influence on haptic torque perception. Perception 41:862-870.

Yamada Y, Yamamura K, Inoue M. 2005. Coordination of cranial motoneurons during mastication. Respir Physiol Neurobiol 147:177-189.

Yamashita A, Valkova K, Gonchar Y, Burkhalter A. 2003. Rearrangement of synaptic connections with inhibitory neurons in developing mouse visual cortex. J Comp Neurol 464:426-437.

Zakiewicz IM, Bjaalie JG, Leergaard TB. 2014. Brain-wide map of efferent projections from rat barrel cortex. Front Neuroinform 8:1-15.

Zhang S, Xu M, Kamigaki T, Hoang Do JP, Chang WC, Jenvay S, Miyamichi K, Luo L, Dan Y. 2014. Selective attention. Long-range and local circuits for top-down modulation of visual cortex processing. Science 345:660-665.

Zingg B, Hintiryan H, Gou L, Song MY, Bay M, Bienkowski MS, Foster NN, Yamashita S, Bowman I, Toga AW, Dong HW. 2014. Neural networks of the mouse neocortex. Cell 156:1096-1111.

Chapitre II

Asymmetric direct reciprocal connections between primary visual and somatosensory cortices of the mouse[1]

[1] Le contenu de ce chapitre est présenté sous forme de manuscrit qui a été publié durant l'été 2016 dans la revue Cerebral Cortex: Massé, I.O., Ross, S., Bronchti, G. et Boire, D.

Title: Asymmetric direct reciprocal connections between primary visual and somatosensory cortices of the mouse.

Authors: Ian O. Massé, Stéphanie Ross, Gilles Bronchti, Denis Boire

Affiliations:

Département d'anatomie
Université du Québec à Trois-Rivières
Canada, G9A 2W7

Running title: Visuo-tactile cortical connections.

Abstract: Several studies show direct connections between primary sensory cortices involved in multisensory integration. The purpose of this study is to understand the microcircuitry of the reciprocal connections between visual and somatosensory cortices. The laminar distribution of retrogradely labeled cell bodies in V1 and in the somatosensory cortex both in (S1BF) and outside (S1) the barrel field was studied to provide layer indices in order to determine whether the connections are of feedforward, feedback or lateral type. Single axons were reconstructed and the size of their swellings was stereologically sampled. The negative layer indices in S1 and S1BF and the layer index near zero in V1 indicate that the connection from S1BF to V1 is of feedback type while the opposite is of lateral type. The greater incidence of larger axonal swellings in the projection from V1 to S1BF strongly suggests that S1BF receives a stronger driver input from V1 and that S1BF inputs to V1 have a predominant modulatory influence.

Keywords: cross-modal, corticocortical connections, visuo-haptic interaction, feedforward, feedback.

Introduction

Multisensory integration is important for the formation of a coherent percept, to enhance the salience of biologically meaningful events and for the facilitation of adaptive behaviors (Ernst and Bulthoff 2004; Stein and Meredith 1993; Stein and Stanford 2008). Although it is clearly established that multisensory convergence occurs in higher order temporal, parietal and frontal cortices (Kaas and Collins 2013), numerous studies in primates, carnivores and rodents demonstrate that early sensory cortices are also involved in multisensory processing (Bizley and King 2009; Bizley et al. 2007; Brosch et al. 2005; Cappe and Barone 2005; Clavagnier et al. 2004; Driver and Noesselt 2008; Falchier et al. 2013; Foxe et al. 2000; Ghazanfar and Schroeder 2006; Giard and Peronnet 1999; Hishida et al. 2014; Iurilli et al. 2012; Laurienti et al. 2002; Macaluso 2006; Schroeder et al. 2003; Sieben et al. 2013; Yoshitake et al. 2013).

In contrast to primates (Cappe and Barone 2005; Clavagnier et al. 2004; Falchier et al. 2002; Rockland and Ojima 2003), there are significant direct connections between primary sensory cortices in rodents (Budinger et al. 2006; Budinger and Scheich 2009; Campi et al. 2010; Charbonneau et al. 2012; Henschke et al. 2014; Iurilli et al. 2012; Miller and Vogt 1984; Paperna and Malach 1991; Sieben et al. 2013; Stehberg et al. 2014; Wang and Burkhalter 2007; Zingg et al. 2014). The mouse is therefore an interesting model for the study of multisensory integration at the level of primary sensory cortices.

The hierarchical organization of cortical connectivity has been defined by feedforward and feedback pathways (Felleman and Van Essen 1991; Rockland and Pandya 1979). Although there are some differences in the morphological features of these connections, this classification also seems to apply to rodents (Berezovskii et al. 2011; Coogan and Burkhalter 1990, 1993; Godement et al. 1979; Gonchar and Burkhalter 1999; Gonchar and Burkhalter 2003; Yamashita et al. 2003). Although primary sensory cortices might be expected to be at the same basal level of the cortical hierarchy and linked by symmetrical reciprocal connections, this is not always the case. Retrograde tracing studies have shown that the primary auditory and somatosensory cortices project in a feedback manner to the primary visual cortex (Charbonneau et al. 2012; Henschke et al. 2014), the primary visual cortex projects in a feedforward manner to the primary auditory cortex and in a lateral manner to the primary somatosensory cortex, and the primary auditory and somatosensory cortices are linked by reciprocal feedback projections (Henschke et al. 2014). This suggests that primary sensory cortices might be at different levels of the cortical hierarchy. Moreover these projection patterns have not been corroborated by the laminar distribution of anterogradely labeled terminals.

There is evidence for two types of glutamatergic synaptic contacts in corticocortical connections (Covic and Sherman 2011; De Pasquale and Sherman 2011; Petrof and Sherman 2013). Class 1B synapses have larger initial excitatory postsynaptic potentials, exhibit paired-pulse depression, are limited to ionotropic glutamate receptor activation

and are anatomically correlated with larger synaptic terminals. Class 2 synapses have smaller initial excitatory postsynaptic potentials, exhibit paired-pulse facilitation, are limited to metabotropic glutamate receptor activation and are anatomically correlated with smaller synaptic terminals (see Sherman and Guillery 2013a). Class 1 and 2 are respectively considered drivers and modulators (Lee and Sherman 2008; Lee and Sherman 2009a, 2009b; Petrof and Sherman 2013; Reichova and Sherman 2004; Sherman and Guillery 1996, 1998; Sherman and Guillery 2013a; Viaene et al. 2011). We might expect that direct connections between primary sensory cortices comprise mainly Class 2 synapses.

The reciprocal projections between the primary visual cortex and the somatosensory cortex in mouse will be studied in order to quantify the relative strengths of the connections with both retrograde and anterograde neuronal tracers. The size and laminar density of axonal swellings will be studied in order to see whether these direct projections between primary sensory cortices fit in the classification criteria provided by the distribution of retrogradely labeled neurons and if they present features of driving or modulatory corticocortical inputs.

Methods

Animals were treated in accordance with the regulations of the Canadian Council for the Protection of Animals and the study was approved by the Animal Care committee of the Université du Québec à Trois-Rivières. C57Bl/6J mice ($n = 20$)

(Charles River, Montréal, QC, Canada) from our colonies were used. All animals were kept under a light/dark cycle of 14/10 hours and were adults when sacrificed.

Tracing procedures

Surgical anesthesia was achieved and maintained with inhalation of 1.5-2.5% isoflurane and vital signs were monitored throughout the procedures. The animals were mounted on a stereotaxic apparatus. Mice were protected from ocular dryness by applying ophthalmic ointment (Polysporin; Pfizer, Toronto, ON, Canada). A scalp incision was made along the midline to expose the skull. For injections in the primary visual cortex (V1), a small craniotomy was performed 3.7 mm caudal and 2.5 mm lateral to Bregma or, for injections in the barrel field of the primary somatosensory cortex (S1BF), 1.5 mm caudal to Bregma and 2.9 mm from the midline. The dura was incised and a glass micropipette filled with a solution of the b-fragment of cholera toxin (CTb) or biotinylated dextran amine (BDA) was inserted into the cortex. Retrograde and anterograde neuronal tracing was achieved with iontophoretic injections of 1% solution of CTb and of a 10% solution of high molecular weight BDA (10 kDa) respectively in phosphate-buffered saline (PBS) (Molecular Probes, Cedarlane Laboratories, Ontario, Canada) through glass micropipettes (20 μm tip diameter) into V1 for 5 animals and S1BF for 5 animals for each tracer. A 1.5 μA positive current with a 7-s duty cycle was applied for 10 min, starting at a depth of 500 μm and ending at 100 μm from the pial surface, 2 min at each 100 μm. The mice were kept warm until they recovered from anesthesia and postoperative pain was managed with buprenorphine Temgesic,

Schering-Plough, Hertfordshire, UK; (i.p.; 0.009 mg/kg) injected before anesthesia was induced.

After a 2-day survival period following CTb injections and a 7-day survival period following BDA injections, mice received an intraperitoneal injection of 120 mg/kg sodium pentobarbital (Euthanyl; Bimeda-MTC, Cambridge, ON, Canada) and were perfused through the heart with PBS (pH 7.4) followed by phosphate-buffered 4% paraformaldehyde. Brains were harvested, postfixed for 1-2 hours, cryoprotected with 30% sucrose and frozen prior to sectioning and CTb or BDA processing.

Serial 50-µm-thick coronal sections were taken using a freezing microtome. One series was processed for CTb immunohistochemistry and the other was mounted on slides and stained with cresyl violet to identify the cortical areas and layers. Sections processed for BDA histochemisty were counterstained with bisbenzimide to identify the cortical areas and layers.

To visualize CTb labeled neurons, free-floating sections were treated for 45 min with 0.15% H2O2 and 70% methanol to quench endogenous peroxidase and thoroughly rinsed in 0.05 M Tris-HCl-buffered 0.9% saline solution (TBS, pH 8.0) containing 0.5% Triton X-100 (TBSTx). Sections were then incubated in 2% normal donkey serum (NDS) for 2 hours and transferred to a solution of primary antibody (goat polyclonal anti-CTb 1:40 000; Molecular Probes) with 1% NDS in PBS-Tx for 2 days at 4°C.

Subsequently, sections were rinsed in PBS-Tx and incubated in a secondary antibody (biotinylated donkey anti-goat; 1:500; Molecular Probes) solution with 1% NDS in PBS-Tx for 2 hours at room temperature. Following further rinsing, the sections were then incubated for 90 min in an avidin-biotin complex solution (Elite Vectastain, Vector Laboratories, PK4000 Standard kit) in TBS-Tx, pH 8.0, rinsed in TBS, and then incubated in a 0.015% '3- diaminobenzidine (DBA) solution. Labeled neurons were revealed by the addition of 0.005% H2O2. Sections were washed and mounted on gelatin-subbed slides, air-dried, dehydrated and cover-slipped with Permount mounting media (Fisher Scientific, Ottawa, ON, Canada).

For BDA staining, after quenching endogenous peroxidase, sections were incubated for 90 min in an avidin-biotin complex solution (ABC Vectastain elite), washed and BDA was revealed using nickel-intensified DAB (Sigma-Aldrich, St-Louis, MO, USA) as a chromogen. Sections were pre-incubated for 30 min in Tris-buffered (TB) (0.05 m) - nickel ammonium sulfate 0.4%, pH 8.0, followed by 10 min in TB-nickel ammonium containing 0.015% DAB and 0.005% H2O2. Sections were dehydrated in ethanol, cleared in xylenes and cover-slipped with Eukitt mounting media.

Charting of retrogradely labeled neurons

All CTb retrogradely labeled neurons on one of every two sections of S1, S1BF and of V1 were plotted using an Olympus BX51WI microscope (20X, 0.75 NA objective) equipped with a three-axis computer-controlled stepping motor system coupled to a

personal computer and to a color Optronix CCD camera and driven by the Neurolucida software (MBF Biosciences, Williston, VT, USA).

The whole primary somatosensory and visual cortices were systematically and randomly sampled on sections spaced 200 μm apart. Cortical areas were delineated at lower magnification (4X, 0.16 NA objectives) on adjacent Nissl-stained sections. Borders between cortical areas were delineated according to the cytoarchitectonic descriptions provided by Caviness (1975) and the mouse brain atlas of Franklin and Paxinos (2008). Contours of each cortical area in which retrogradely labeled cells were located were traced with Neurolucida and the limits of each cortical layer were traced. These contours were superimposed on the images of CTb-reacted sections and resized for shrinkage differences between the Nissl and CTb sections. This allowed plotted neurons in each cortical area to be assigned to either supragranular, granular or infragranular layers for the calculation of layer indices. These indices provide a quantitative assessment of the laminar distribution of retrogradely labeled neurons and are instrumental in the classification of corticocortical feedback, feedforward and lateral connections (Felleman and Van Essen 1991). Layer indices (L) were calculated using the formula where S and I are the numbers of labeled neurons in supragranular and infragranular layers respectively (Budinger et al. 2006, 2008; Budinger and Scheich 2009):

$$L = (S - I) / (S + I)$$

The indices range between -1 and 1. Negative values indicate feedback connections mostly originating in infragranular layers and positive values indicate feedforward connections mostly originating in supragranular layers. Values near zero indicate lateral connections. All photomicrographs were cropped, and luminosity and contrast were adjusted with Adobe Photoshop software.

Single axon reconstructions

Six anterogradely labeled axons projecting from V1 to the barrel field of S1 and six axons projecting from the barrel field of S1 to V1 were reconstructed at higher magnification (100X, 1.4 NA objectives). Cortical areas were delineated at lower magnification (4X, 0.16 NA objectives) using bisbenzimide as a fluorescent counterstain. Contours of each cortical area in which anterogradely labeled axons were located were traced with Neurolucida and the limits of each cortical layer were defined. Axons were reconstructed from their entrance in the grey matter. The axonal branches were completely reconstructed and followed throughout the serial sections until they ended and could not be followed further to adjacent sections. Throughout the full extent of the axonal arborisation, all the axonal swellings were charted, assigned to specific cortical layers and their largest diameter was measured. The size frequency distribution of axonal swellings was determined for each cortical layer of each individual axon.

Stereological sampling of laminar distribution of axonal swellings

In order to provide an unbiased size frequency distribution of swellings in each cortical layer for the projection from V1 to the S1 barrel field and the reciprocal projection from the S1 barrel field to V1, a stereological systematic random sampling of these projection fields was performed using the Stereo Investigator software (MBF Bioscience) in cases that received a columnar injection in the visual or somatosensory cortices. These size distributions for a whole population of neurons projecting from the injection sites were compared with the same distributions obtained for individual axons and with the sum of all the single axon reconstructions. This comparison is done to assess if the data obtained from the swellings of single axons is representative of the whole population of swellings sampled.

Projections fields in which anterograde labeling was observed were sampled using the optical fractionator workflow (in Stereo investigator) on approximately 10 equidistant sections covering the full anteroposterior range of the projection, except for the fourth case injected with BDA in V1 in which the projection extended to only 5 sections. On each section, polygonal contours were traced around the projection field in each cortical layer. Axonal swellings were then counted in no less than 100 disectors that were 20x20 μm square and 15 μm height, and evenly distributed at the intersections of an 80x80 μm grid. The maximum diameter was measured for each sampled swelling.

This optical fractionator sampling strategy allowed for the estimation of the total number of swellings in each cortical layer. The total numbers of swellings (N) were calculated by the following equation (West et al. 1991) where ΣQ is the total number of swellings counted within the disectors, ssf is the section sampling fraction (number of sampled sections over the total number of sections on which the terminal projection field appears), asf is the area sampling fraction (ratio of the frame area/the total area of the reference space on the section) and tsf is the thickness sampling fraction (disector height/section thickness):

$$N = \Sigma Q \; x \; ssf^{-1} \; x \; asf^{-1} \; x \; tsf^{-1}$$

Product of ssf, asf and tsf is the overall sampling faction (see Table 8). Coefficients of error (CEs) were calculated according to the procedure described by West and Gundersen (1990), in order to determine whether the sampling effort was sufficient. It is widely accepted as a rule of thumb that CEs below 0.1 are indicative of a sufficient sampling. The objective of this stereological sampling was not to determine the total number of swellings that are labeled for each injection. This number is a function of the injection size. The objective was to obtain unbiased estimates of laminar and size distributions.

Table 8

Stereological sampling parameters for the estimation of the number of anterogradely labeled axonal swellings in each layers in S1BF after injections of BDA into V1 of C57Bl/6 mice

Case	Layer	Number of sections	Total area (mm^2)	Number of dissectors	Number of objects	Sampling fraction	Total estimation	CE
1	I-III	9	8661	106	313	0.004	84662	0.060
	IV	9	5663	117	164	0.006	26279	0.053
	Va	9	3150	117	178	0.011	15865	0.065
	Vbc	9	5407	115	164	0.006	25527	0.050
	VI	9	3950	116	78	0.009	8793	0.097
	Total (Mean)	45	26831	571	897	(0.007)	161126	(0.065)
2	I-III	9	6593	112	329	0.005	64112	0.074
	IV	9	4580	111	118	0.007	16117	0.075
	Va	9	2257	128	139	0.017	8115	0.074
	Vbc	9	3969	119	129	0.009	14243	0.089
	VI	9	2050	111	80	0.016	4890	0.083
	Total (Mean)	45	19449	581	795	(0.011)	107477	(0.079)
3	I-III	9	17372	110	317	0.002	165717	0.075
	IV	9	11941	112	158	0.003	55764	0.052
	Va	9	6617	127	181	0.006	31218	0.060
	Vbc	9	10180	123	156	0.004	42739	0.051
	VI	9	10885	64	111	0.003	20776	0.063
	Total (Mean)	45	56995	536	923	(0.004)	316214	(0.060)
4	I-III	5	2507	106	174	0.013	13519	0.194
	IV	5	1521	105	72	0.021	3427	0.201
	Va	5	940	114	60	0.037	1626	0.192
	Vbc	5	1408	110	90	0.024	3786	0.147
	VI	5	1515	105	141	0.021	6685	0.167
	Total (Mean)	25	7891	540	537	(0.023)	29043	(0.180)
5	I-III	10	5745	118	97	0.006	17793	0.071
	IV	10	3005	105	38	0.009	4097	0.097
	Va	10	1821	120	63	0.018	3602	0.044
	Vbc	10	2506	115	42	0.012	3449	0.052
	VI	10	1398	112	40	0.021	1881	0.070
	Total (Mean)	50	14475	570	280	(0.013)	30822	(0.067)

Sampling of axonal diameters

In order to compare the caliber of the axonal population entering the cortical areas V1 and the somatosensory barrel field, the initial diameter of the axons as they leave the white matter to enter the cortical grey layers was calculated. Axonal diameter changes over short distances and a single point measurement of the axonal diameter was not deemed adequate. To take this into account and to obtain an unbiased estimate of the axons diameters, a weighted average of diameter for the initial 25 μm of each axon was calculated. These diameters are not the caliber of the axons as they emerge from the neuronal cell bodies but rather the caliber of the axons distally, as they enter their target, which is either S1BF or V1.

The Neurolucida software encodes axons as a succession of small segments. Each segment is attributed coordinates in three-dimensional space, a length and a diameter. These segments correspond to the interval between two mouse clicks as the observer traces the axons. These clicks will be done to record changes in direction and/or diameter of the axons. The data were used to calculate the average diameter over the first 25 μm of the tracing from the point of entry of the axons into the cortical grey matter, weighted by the length of the segments recorded over this distance.

The sampling of the measured axons was performed on the same sections that were used for the stereological sampling of axonal swellings (see Table 8) to insure that axons were systematically and randomly selected. Axons were selected as they crossed the line

between the white and grey matter. The total length of this line for each case and the number of sampled sections are given in Table 9.

Table 9

Sampling parameters for the estimation of the number of anterogradely labeled axons as they enter the gray matter in S1BF and V1 after injections of BDA into V1 and S1BF respectively of C57Bl/6 mice

Injection site	Case	Number of sections	Sampled length (mm)	Number of axons	Sampling fraction	Total estimation	CE
V1	1	9	13.281	259	0.333	777	0.071
	2	9	12.215	116	0.333	348	0.094
	3	9	14.372	104	0.500	208	0.067
	4	5	6.567	195	1.000	195	0.183
	5	10	13.967	132	0.500	264	0.091
Mean						358	
S1BF	1	11	11.532	134	0.250	536	0.130
	2	10	6.016	38	1.000	38	0.072
	3	10	5.373	154	1.000	154	0.051
	4	7	6.215	84	0.500	168	0.102
	5	8	6.143	310	1.000	310	0.045
Mean						241	

Statistical analysis

Statistical analyses were performed using SPSS v 16.0 software (SPSS, Chicago, IL, USA).

Results

Labeling of cortical visuotactile connections with CTb

Representative CTb injection sites in the visual cortex are illustrated in Figure 21A (V1) and in the somatosensory barrel field in Figure 21C (S1BF). None of the injections damaged the underlying white matter. In all cases, CTb injections in S1BF and V1 anterogradely labeled axonal terminals and retrogradely labeled numerous neuronal cell bodies in V1 and S1 respectively. Conversely, CTb injections outside of the barrel field of S1 resulted in very few labeled neurons in V1.

In S1, CTb-labeled neurons were found in supragranular layers and layer 4 but they were more numerous in infragranular layers (see Figure 21B). By contrast, in V1, CTb-labeled neurons were more evenly distributed in layers 2/3 to layer 5 (see Figure 21D). In layer 6, neurons with fusiform cell bodies were found along the border of the white matter.

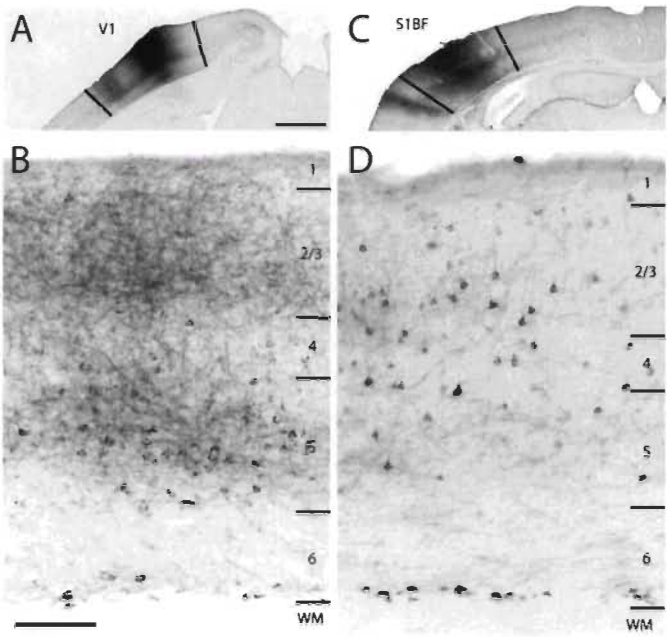

Figure 21. A: An injection of CTb in V1 produced in B: Anterograde and retrograde labeling in S1BF. Note the more abundant retrogradely labeled neurons in layer 5 than in supragranular layers and the intense anterograde labeling in layers 2/3 and 5. C: An injection of CTb in S1BF produced in D: Retrogradely labeled neurons in supragranular and infragranular layers, a typical distribution of lateral connections. Scale: 1000 μm (A/C) and 200 μm (B/D).

In addition, CTb injections in V1 produced intense anterograde axonal labeling in supragranular layers as well as in layer 5. Less intense axonal labeling was observed in layer 4 and only sparse labeling was observed in layer 6 (see Figure 21B). Injections in S1BF produced sparse anterograde labeling in all layers of V1, (see Figure 21D). Anterograde labeling was much lighter in the projection from S1BF to V1 than that of V1 to S1BF. This clearly shows an asymmetry of the reciprocal connections between V1 and S1BF; the projection from V1 to the S1BF being much stronger.

Even though the number of labeled neurons varied between cases, and is dependent upon the injection size, all injections were performed with the same parameters and a comparison of the total number of labeled neurons is instructive here of the strength of the projection. Following CTb injections in V1, the number of retrogradely labeled neurons in S1BF ranged between 10 and 164 (mean = 80.8) and between 15 and 85 (mean = 36.6) in S1 (see Table 10), but this difference was not significant (one-way ANOVA, $p = 0.857$) (see Figure 22A).

Table 10

Numbers and percentage (in parentheses) of retrogradely labeled neurons in supragranular / granular / infragranular layers and layer indices (below) in S1, S1BF and V1 after injections of CTb into V1 and S1BF of C57Bl/6 mice

Injection site	Case	Layer	S1	S1BF	V1
V1	CT9	I-III	14 (16.47)	23 (14.02)	-
		IV	11 (12.94)	25 (15.24)	-
		V	33 (38.82)	55 (33.54)	-
		VI	27 (31.77)	61 (37.20)	-
		Layer Index	-0.62	-0.67	-
	CT20	I-III	4 (25)	0 (0)	-
		IV	0 (0)	0 (0)	-
		V	9 (56.25)	3 (30)	-
		VI	3 (18.75)	7 (70)	-
		Layer Index	-0.5	-1	-
	CT25	I-III	4 (26.67)	13 (23.21)	-
		IV	0 (0)	0 (0)	-
		V	5 (33.33)	27 (48.21)	-
		VI	6 (40)	16 (28.57)	-
		Layer Index	-0.47	-0.54	-
	CT26	I-III	6 (15.39)	19 (16.96)	-
		IV	8 (20.51)	6 (5.36)	-
		V	13 (33.33)	41 (36.61)	-
		VI	12 (30.77)	46 (41.07)	-
		Layer Index	-0.61	-0.64	-
	CT31	I-III	11 (39.29)	8 (12.9)	-
		IV	1 (3.57)	0 (0)	-
		V	8 (28.57)	27 (43.55)	-
		VI	8 (28.57)	27 (43.55)	-
		Layer Index	-0.19	-0.74	-
S1BF	03-02b4	I-III	-	-	89 (31.79)
		IV	-	-	60 (21.43)
		V	-	-	84 (30)
		VI	-	-	47 (16.79)
		Layer Index	-	-	-0.19

Table 10

Numbers and percentage (in parentheses) of retrogradely labeled neurons in supragranular / granular / infragranular layers and layer indices (below) in S1, S1BF and V1 after injections of CTb into V1 and S1BF of C57Bl/6 mice (continued)

Injection site	Case	Layer	S1	S1BF	V1
	04-01b2	I-III	-	-	175 (34.38)
		IV	-	-	104 (20.43)
		V	-	-	86 (16.90)
		VI	-	-	144 (28.29)
		Layer Index	-	-	-0.14
	03-02b5	I-III	-	-	282 (47.08)
		IV	-	-	110 (18.36)
		V	-	-	108 (18.03)
		VI	-	-	99 (16.53)
		Layer Index	-	-	0.15
	03-02b6	I-III	-	-	68 (41.72)
		IV	-	-	38 (23.31)
		V	-	-	37 (22.70)
		VI	-	-	20 (12.27)
		Layer Index	-	-	0.08
	03-02b7	I-III	-	-	227 (33.43)
		IV	-	-	170 (25.04)
		V	-	-	173 (25.48)
		VI	-	-	109 (16.05)
		Layer Index	-	-	-0.11
	Mean ±SEM	I-III	7.8 ± 2.25 (23.93)	12.6 ± 4.54 (15.59)	168.2 ± 45.25 (37.71)
		IV	4 ± 2.57 (10.93)	6.2 ± 5.41 (7.67)	96.4 ± 25.49 (21.61)
		V	13.6 ± 5.61 (37.16)	30.6 ± 9.65 (37.87)	97.6 ± 24.73 (21.88)
		VI	11.2 ± 4.71 (30.60)	31.4 ± 11.02 (38.86)	83.8 ± 24.89 (18.79)
		Layer Index	-0.52 ± 0.09	-0.66 ± 0.09	-0.04 ± 0.08

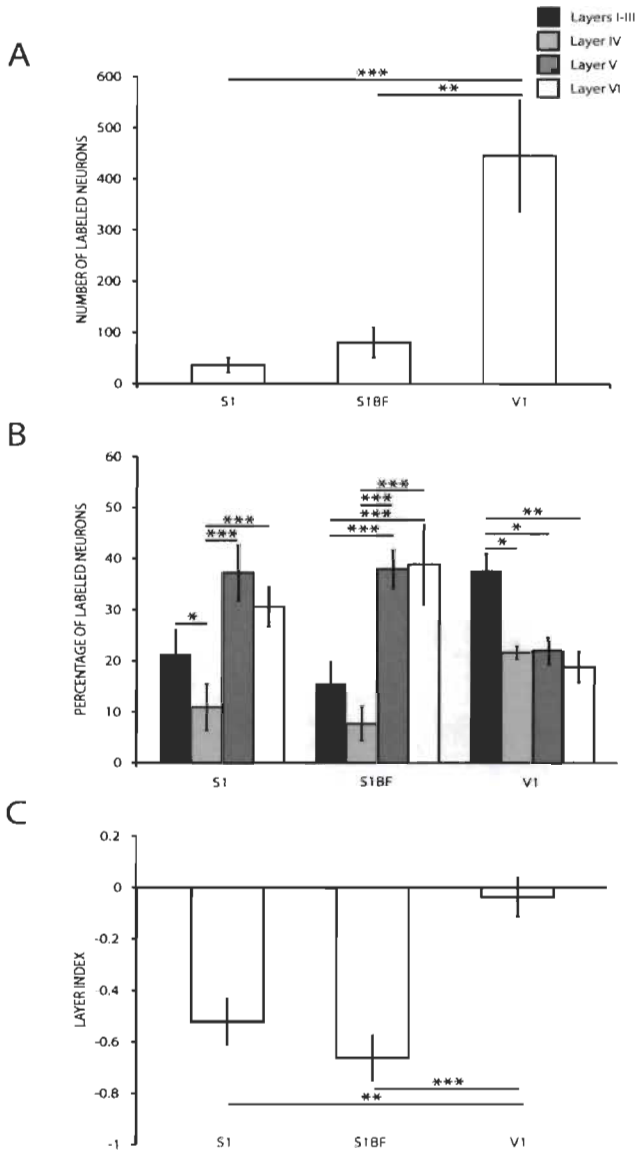

Figure 22. A: Number of retrogradely labeled neurons in cortical areas following an injection of CTb in V1 and S1BF of C57Bl/6 mice. B: Percentage of retrogradely labeled neurons in cortical areas following an injection of CTb in V1 and S1BF of C57Bl/6 mice. C: Layer indices for neocortical areas following an injection of CTb in V1 and S1BF of C57Bl/6 mice.

Similarly, injections of CTb in and outside the somatosensory barrel field retrogradely labeled neurons in V1. Very few neurons were labeled after injections in S1. Of the 5 cases injected with CTb in S1, 3 of them had no retrogradely labeled neurons in V1 and 2 of them had only 2 neurons labeled in layer 5 of V1. Conversely, numerous neurons were labeled in V1 following injections in S1BF. The total number of labeled neurons in V1 following S1BF injections ranged between 163 and 679 (mean 446) (see Table 10). There was a statistically significant difference between the projections (Kruskal-Wallis, $p = 0.009$) Post-hoc tests revealed that the projection from V1 to S1BF was stronger than that from S1 to V1 (Tukey-HSD, $p = 0.001$) and from S1BF to V1 (Tukey-HSD, $p = 0.002$) (see Figure 22A). This is in agreement with the stronger projection of V1 to the S1BF shown by CTb anterograde labeling.

Laminar distribution of Cholera toxin b labeled neurons

In order to classify each projection as a feedforward, feedback or lateral connection, retrogradely labeled neurons in V1 and in the somatosensory cortex within and outside of the barrel field were counted in supragranular layers 1 to 3, layer 4 and infragranular layers 5 and 6 in each case (see Table 10). Injections in V1 retrogradely labeled a greater percentage of neurons in infragranular layers 5 and 6 in S1 and S1BF (67.76% in S1 and 76.73% in S1BF), whereas injections in S1BF retrogradely labeled a greater percentage of neurons in the supragranular layers 1 to 3 (37.71%), (see Figure 22B). More specifically, following injections in V1, the percentage of labeled neurons in S1 was significantly lower in layer 4 (10.93%) than in layers 1 to 3 (23.93%) ($p = 0.016$),

5 (37.16%) ($p < 0.001$) and 6 (30.60%) ($p = 0.001$). There was no significant difference between the percentage of labeled neurons in layer 5 (37.16%) and 6 (30.60%) ($p = 0.848$). The percentage of labeled neurons in S1BF was significantly lower in layers 1 to 3 (15.59%) and layer 4 (7.67%) than in layer 5 (37.87%) ($p < 0.001$) and 6 (38.86%) ($p < 0.001$). There was no significant difference between the percentage of labeled neurons in layer 5 (37.87%) and in layer 6 (38.86%) ($p > 0.999$). Injections in S1BF resulted in a significantly greater percentage of labeled neurons in layers 1 to 3 (37.71%) in V1 than in layer 4 (21.61%) ($p = 0.029$), 5 (21.88%) ($p = 0.046$) and 6 (18.79%) ($p = 0.004$). There was no significant difference between the percentage of labeled neurons in layer 5 (21.88%) and in layer 6 (18.79%) ($p > 0.999$). Note that the proportion of neurons labeled in layers 5 and 6 were always similar showing that these layers do not vary independently.

Significant differences in the percentage of labeled neurons in cortical layers were observed between the projection from V1 to S1BF and S1BF to V1 (see Figure 22B). A greater proportion of labeled neurons was found in layers 1 to 3 of V1 following injections in S1BF compared with S1BF ($p < 0.001$) following injections in V1. A greater proportion of labeled neurons was found in layers 4 of V1 following injections in S1BF compared with S1 ($p = 0.033$) and S1BF ($p = 0.006$) following injections in V1. A lesser proportion of labeled neurons was found in layers 5 of V1 following injections in S1BF compared with S1 ($p = 0.019$) and S1BF ($p = 0.016$) following injections in V1. Also, a greater proportion of labeled neurons were found in layer 6 of S1BF following

injections in V1 compared with S1 ($p = 0.036$) following injections in V1 and V1 ($p < 0.001$) following injections in S1BF.

Following CTb injections in V1, there were more labeled neurons in infragranular than in supragranular layers of S1 and S1BF. Hence, layer indices were negative in all cases ranging between -0.62 and -0.19 in S1 and between -1.0 and -0.54 in S1BF (see Table 10), clearly suggestive of a feedback projection. CTb injections in S1BF produced retrograde labeling of neurons in similar proportion in supra- and infragranular layers in V1 and, in all cases, layer indices were near zero, ranging from -0.19 to 0.15 (see Table 10) indicating a lateral type of connection between two areas of similar hierarchical levels within the cortical network. There was a statistically significant difference between the layer indices (Kruskal-Wallis, $p = 0.003$). Post-hoc tests reveal that the layer indices of V1 and both S1 and S1BF (Tukey-HSD, $p = 0.003$ and $p < 0.001$ resp) (see Figure 22C) were significantly different.

Anterograde BDA labeling of visuotactile connections

The injections of high-molecular weight BDA in both V1 and S1BF resulted in significant anterograde axonal labeling in S1BF and V1 respectively, without significant signs of retrograde transport. None of the injections damaged the underlying white matter. The BDA injections in the barrel field of S1 (see Figure 23A) resulted in anterogradely labeled axons in V1 in each of the 5 cases, confirming the projection observed following the injection of CTb in V1. These injections labeled axons in infra-

and supragranular layers of V1 (see Figure 23B). Upon entering the grey matter, axons travelled up to layer 4 without extensive branching. Some small en-passant axonal swellings were seen as the axons crossed layer 4. In supragranular layers a dense lattice of intercrossing neurites was always present. Labeled terminals were most evident in layers 1 to 3, with a greater density in the superior part of layer 2.

Injections in V1 (see Figure 23C) anterogradely labeled axonal arbors largely restricted to the barrel field in S1, in each of the 5 cases, confirming the projection observed following the injection of CTb in S1BF. Labeled axons were found in infra- and supragranular layers of (see Figure 23D). Axons left the white matter, crossed layer 6 and arborized in layer 5. Axons travelled radially through the granular layer without significant branching. Axonal terminal labeling was most intense in the supragranular layers.

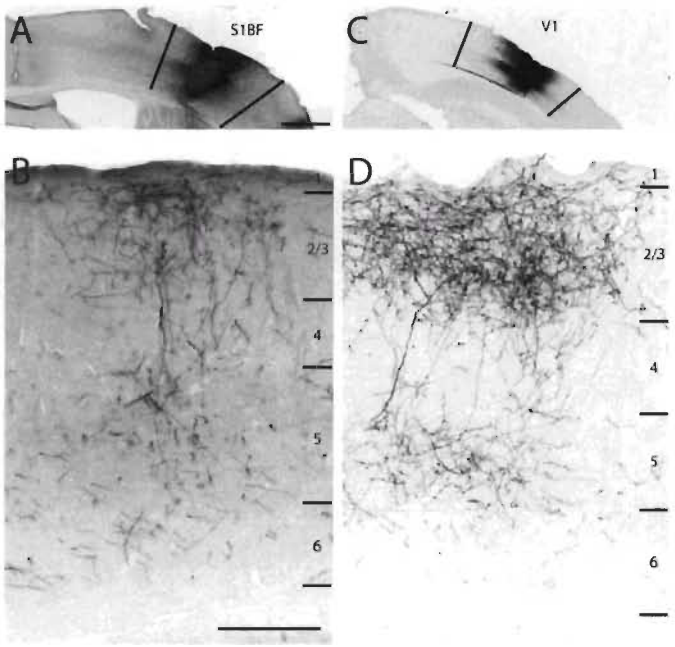

Figure 23. A: An injection of BDA in S1BF produced in B: Anterograde labeling of axons in the supragranular and infragranular layers in V1. C: An injection of BDA in V1 produced in D: Anterograde labeling of axons in the supragranular and infragranular layers in S1BF. Scale: 1000 μm (A/C) and 250 μm (B/D).

Single axon branching morphology

In order to characterize the branching structure and the laminar and size distribution of axonal swellings, a sample of single axons were completely reconstructed from their entrance in the grey matter for the projections from V1 to S1BF and from S1BF to V1. More specifically, branching structure was described in terms of the general appearance of the axons and axonal swellings were described with respect to their laminar position and size distribution.

Axons of the projection from V1 to S1BF (see Figure 24) displayed a wide range of branching structures. Relatively simple branching patterns were observed in three axons

(see Figure 24A, C and F). Upon entering the grey matter, these axons ascended through the infragranular layers without any significant branching, and underwent a few bifurcations within the supragranular layers, forming relatively restricted columnar trees. One axon branched mostly in the supragranular layers but sparsely in infragranular layers and exhibited a somewhat more complex richly arborized tree (see Figure 24D). The medio-lateral extent of the portion of the arbor located in the supragranular layers was wider in this axon than in the more simple ones which had a more restricted projection column. In these three axons, axonal swellings were mostly located in supragranular layers, reflecting their branching structure.

Two axons had more extensive trajectories in the infragranular layers than the other axons of the sample (see Figure 24B and E). One axon (see Figure 24B) bifurcated early after entering the grey matter, sending a long poorly branched extension that coursed tangentially over more than 500 μm in layers 5 and 6, and another branch that ascended through layers 5 and 4 that subsequently arborized sparsely in supragranular layers forming very restricted radial projections in layers 1 to 3. Finally, one axon exhibited extensive tangential travel in the infragranular layers (see Figure 24E). As in the previously described axon, it bifurcated only once to produce two main branches. One ascended to the supragranular layers and formed a tangentially restricted projection column, whereas the other bifurcated in layer 5 in one location (see terminal branches 1 and 3) and another branch travelled extensively over more than 500 μm to ascend in the supragranular layer without any significant branching in another location in the barrel

field. In these two axons, (see Figure 24B and E) swelling were quite evenly distributed across all cortical layers also reflecting to distribution of axonal segments in these cases.

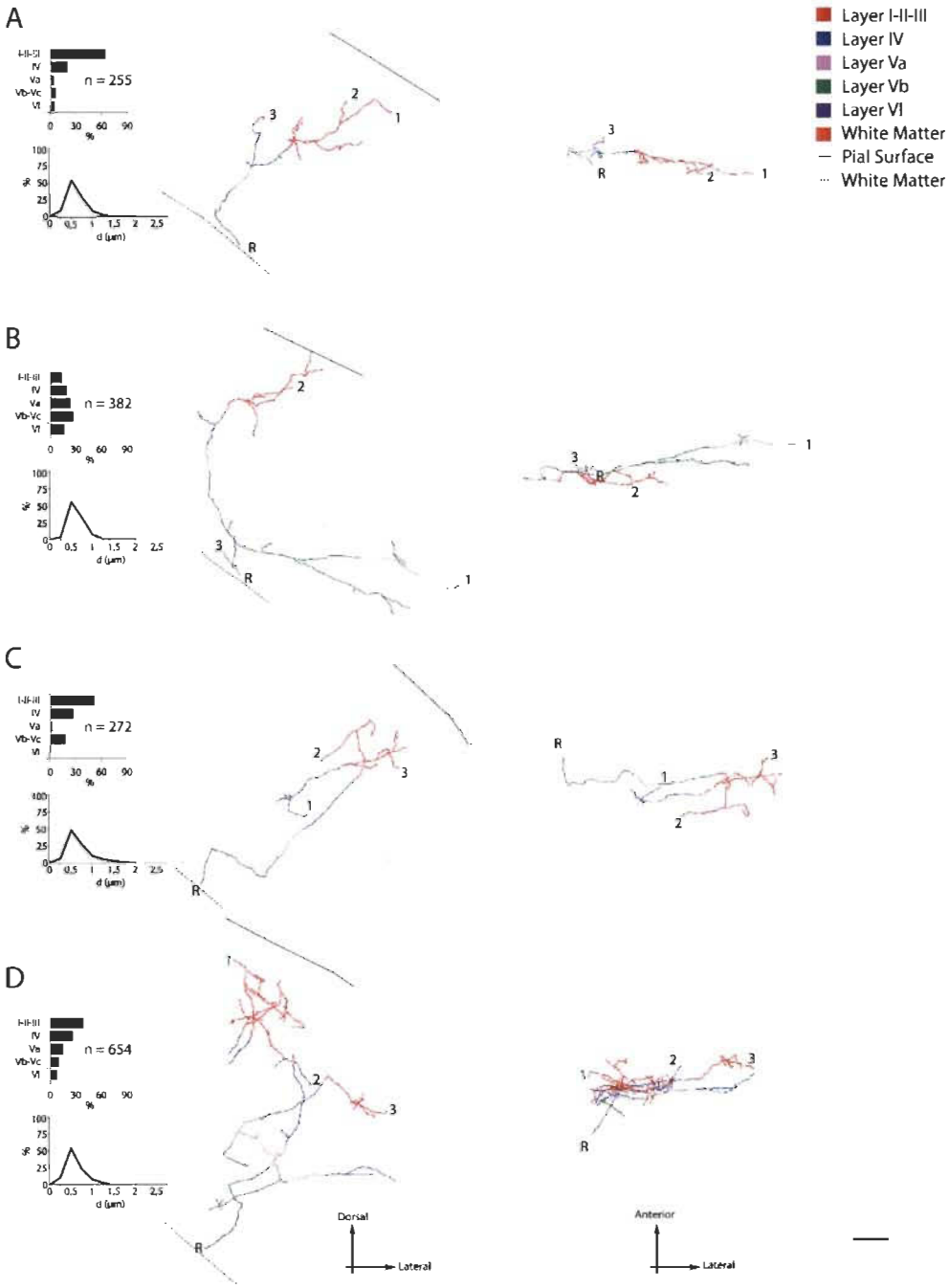

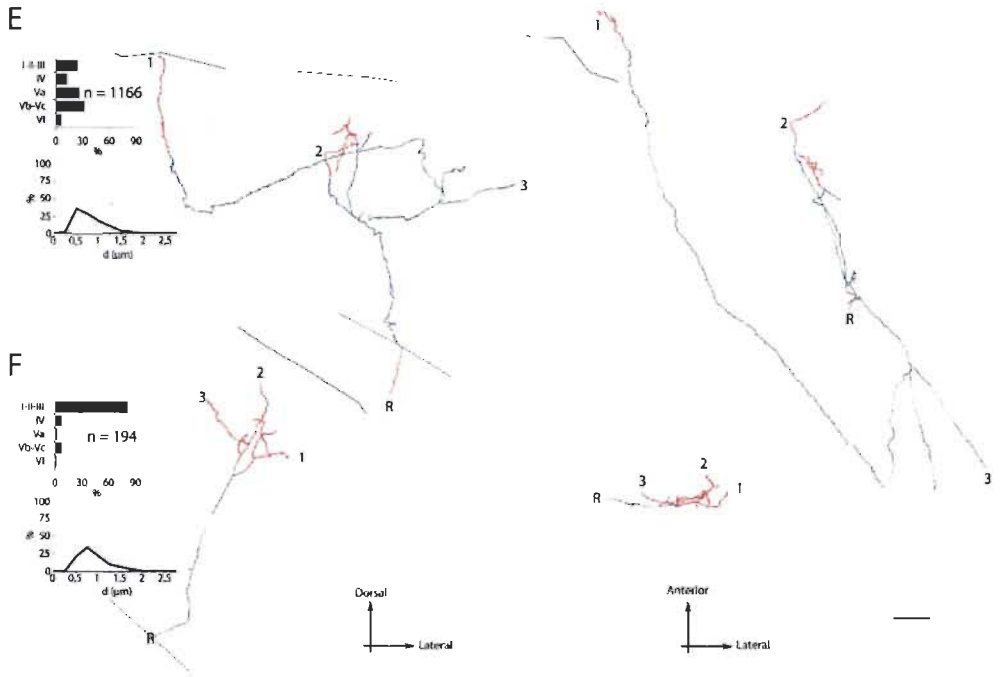

Figure 24. Single axons in S1BF following an injection of BDA in V1 of C57Bl/6J mice. The reconstructed axons are viewed as coronal plane projections on the left panel and as top projections on the right. Each colored segment on the axons corresponds to the layer in which this segment is situated. The full line represents the pial surface and the dotted line the border between layer 6 and the white matter. The R is the root of the axons as they enter they grey matter. The numbers (1/2/3) on the axons are landmarks to facilitate the visualisation of their structure in the two different projections. On the left of axonal structures are histograms of the laminar distribution of terminals (% of axonal swellings for each layer) n is the total number of axonal swellings for each axon; and just below is the size distribution of axonal swellings as a function of their largest diameter (d). Scale: 100 μm.

The size distribution of swellings on individual axons in the projections from V1 to S1BF shows a great predominance of very small swellings (see Figure 24) with a small contingent of much larger swellings. In four of the six reconstructed axons, the largest swellings were no larger than 1.9 μm in diameter (see Figure 24 A-D). On two axons, there were some swellings with diameters greater than 2.5μm (see Figure 24E and F, 2.8 and 2.7 μm resp.).

Axons in the projection from S1BF to V1 (see Figure 25) also displayed diverse morphologies. Three axons showed an extensive tangential coverage (see Figure 25A, B and F). In the axon depicted in Figure 25A, the main trunk ascended through the infragranular layers without any branching. It gave off collateral that circled in a small zone of the mid-supragranular layers before sending a descending unbranched extension back into the deep infragranular layers. The other branch ascended to layer 1 where it bifurcated in two branches (see 1 and 3 in Figure 25A), one of which travelled without branching in layer 1 for a distance exceeding 400 µm.

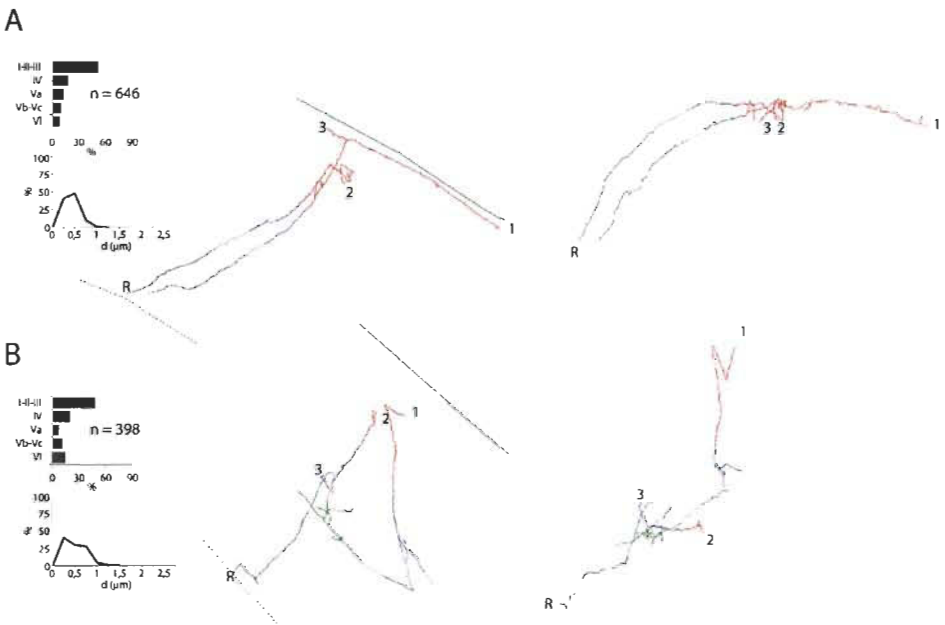

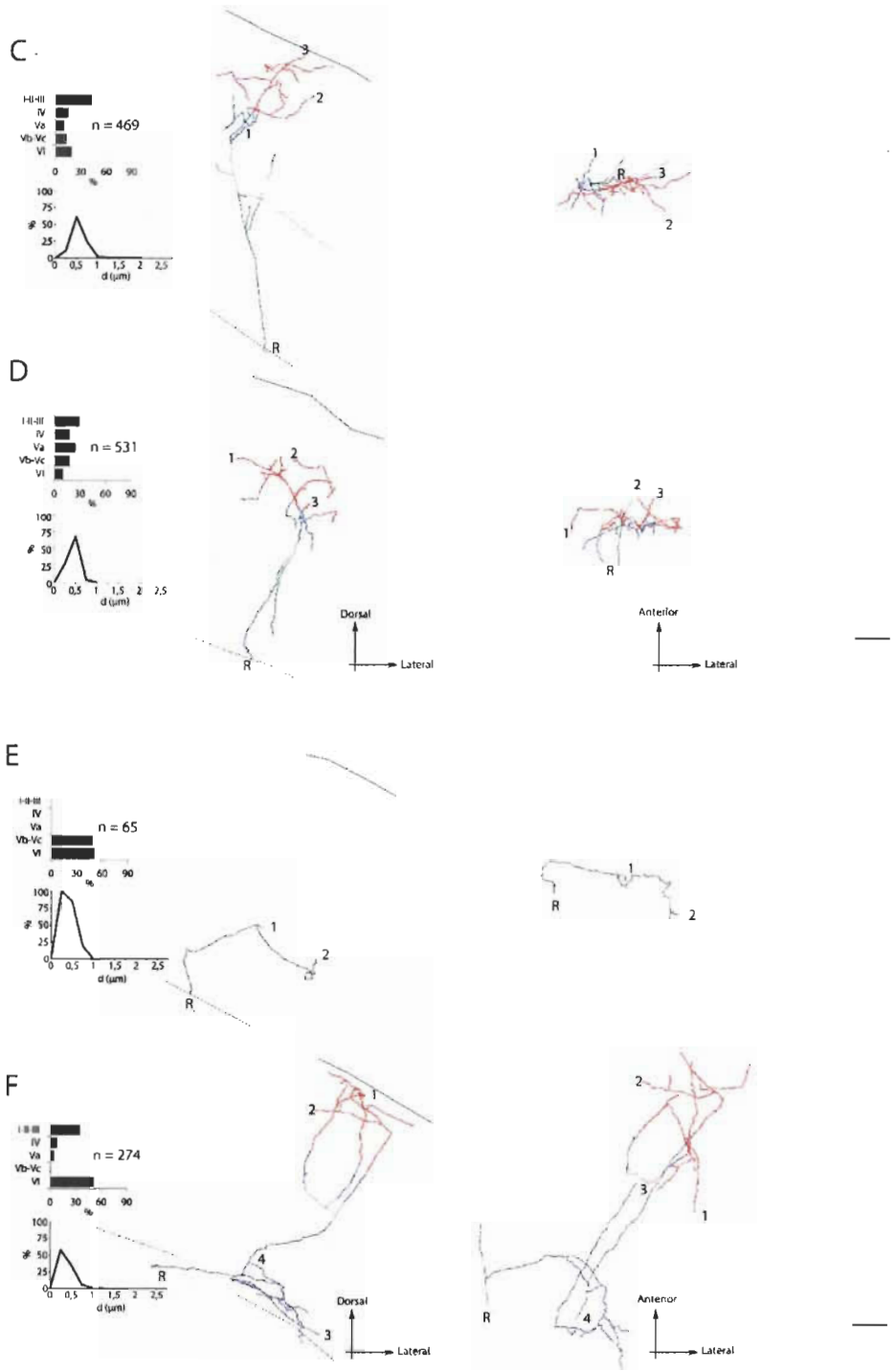

Figure 25. Single axons in V1 following an injection of BDA in S1BF of C57Bl/6J mice. Legends as in Figure 24.

Another axon showed an extensive tangential trajectory (see Figure 25B). Upon entering the grey matter, this axon made two successive right angle turns before ascending through the infragranular layers without branching. While in layer 5, it gave out one branch that ascended through infragranular layers without any significant branching, except for a small terminal tuft. The other branch emerged from layer 5 and travelled vertically in the deeper part of layer 5 and emitted therein several short collaterals and then engaged in a linear tangential course without branching for more than 300 μm. It subsequently made a sharp turn and ascended obliquely towards the pial surface in an anteriorly directed trajectory for approximately 400 μm but did not reach layer 1. The laminar distribution of swellings was similar in axons shown in Figure 25A and B in that the majority were found in supragranular layers.

The axon depicted in Figure 25F is peculiar in that it had a collateral branch that arborized quite significantly in layer 6 and another that ascended to the upper–half of the supragranular layers before arborizing. Also, the top-view of this axon showed that the infragranular focus of arborisation was out of radial register with the supragranular terminal arbors which were located about 300 μm more anteriorly. This is not apparent in the coronal projection that would rather suggest a more restricted columnar organisation for this axon (see Figure 25F). The laminar distribution of swellings for this axon was clearly bimodal with an important population of swellings in supragranular layers and an also very important contingent of swellings in layer 6.

Two axons displayed a restricted tangential extent of their arborisation (see Figure 25C and D). They arborized more importantly in the supragranular layers even though they did emit a few unbranched collaterals in infragranular layers. Top projections of these axons demonstrated the restricted tangential distribution of their arbors that remained within a radius of approximately 300 μm. The tangential extent of the axons projecting from V1 to S1BF was in general greater than that of these two axons. The laminar distribution of swellings of the axon shown in Figure 25C was similar to that of the axon of Figure 25B, in that there was a large contingent of swellings in supragranular layers, but also a significant number of swellings distributed throughout cortical layers. The axon depicted in Figure 25E was peculiar in that it did not reach supragranular layers. Oblique segments ascended through the infragranular layers without any significant branching. Consequently, swellings were found in similar proportions only in layers 5 and 6.

The size distribution of swellings on individual axons in the projection from S1BF to V1 shows a strong dominance of very small swellings with diameters no greater than 1.2 μm (see Figure 25 A, B, D-F). In all the six reconstructed axons, only one axon has a few swellings no larger than 1.8 μm in diameter (see Figure 25C).

Axonal thickness

In order to compare the reciprocal projections between V1 to S1BF at the single axon level, the frequency distributions of the diameters of randomly sampled axons (see

Table 9) as they enter the grey matter were compared (see Figure 26). Within the sampled axons, the size of the mean diameters ranged between 0.1 and 1.9μm for the projection from V1 to S1BF and between 0.1 and 0.5μm for the projection from S1BF to V1. There was a very highly significant difference between the projection from V1 to S1BF and from S1BF to V1 (Kolmogorov-Smirnov tests, $p < 0.001$). In both projections, thin axons are predominant and account for the majority of the axons. In the projection from V1 to the somatosensory barrel field, quite thick axons were found that were never seen in the reciprocal projection from the barrel field to the visual cortex.

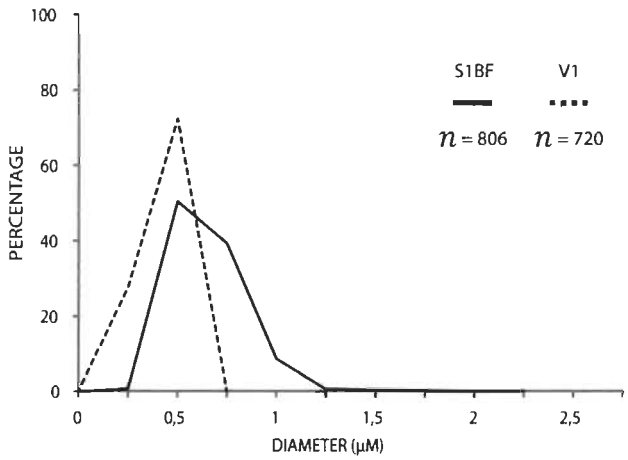

Figure 26. Size distribution of axonal diameters in S1BF (solid line) following BDA injections in V1 and in V1 following injections in S1BF (dotted line). n = the number of counted axons for each projection.

Number of anterogradely labeled axonal swellings

The total number of anterogradely labeled axonal swellings for each injection was estimated through stereological sampling in order to compare the strength of the reciprocal projections between the visual cortex and the somatosensory barrel field. The

estimated numbers of anterogradely labeled axonal swellings in each layers of S1BF are shown in Table 8 and the numbers of anterogradely labeled axonal swellings in each layers of V1 are shown in Table 11.

Even though the total number of labeled swellings and axons is dependent upon the injection size, all our injections were performed with the same parameters and could, within certain limits, be compared. The estimated total number of swellings in S1BF following a BDA injection in V1 ranged between 29 043 and 316 214 (see Table 8) with a mean of 128 936 and the estimated number of swellings in V1 after a BDA injection in S1BF ranged from 9 763 to 134 413 (see Table 11) with a mean of 47 961. This difference did not reach statistical significance (Mann-Whitney, $p = 0.251$).

Table 11

Stereological sampling parameters for the estimation of the number of anterogradely labeled axonal swellings in each layers in V1 after injections of BDA into S1BF of C57Bl/6 mice

Case	Layer	Number of sections	Total area (mm^2)	Number of dissectors	Number of objects	Sampling fraction	Total estimation	CE
1	I-III	11	9174	124	201	0.004	53794	0.089
	IV	11	6717	122	80	0.005	15935	0.078
	Va	11	3229	141	85	0.012	7043	0.098
	Vbc	11	5130	137	137	0.007	18558	0.085
	VI	11	6571	118	194	0.005	39083	0.090
	Total (Mean)	55	30821	642	697	(0.007)	134413	(0.088)
2	I-III	10	1604	105	488	0.018	27043	0.043
	IV	10	779	122	291	0.043	6747	0.056
	Va	10	461	129	241	0.077	3129	0.059
	Vbc	10	600	120	169	0.055	3070	0.072
	VI	10	566	118	89	0.058	1549	0.082
	Total (Mean)	50	4010	594	1278	(0.050)	41538	(0.062)
3	I-III	10	1380	108	209	0.022	9692	0.061
	IV	10	578	119	153	0.057	2696	0.050
	Va	10	461	124	146	0.074	1971	0.061
	Vbc	10	649	128	128	0.054	2355	0.057
	VI	10	607	153	91	0.070	1310	0.059
	Total (Mean)	50	3675	632	727	(0.055)	18024	(0.058)
4	I-III	7	3414	111	254	0.010	25597	0.080
	IV	7	1343	133	106	0.030	3508	0.092
	Va	7	819	115	90	0.043	2102	0.099
	Vbc	7	1317	105	65	0.024	2671	0.094
	VI	7	1295	124	64	0.029	2190	0.093
	Total (Mean)	35	8188	588	579	(0.027)	36068	(0.092)

Table 11

Stereological sampling parameters for the estimation of the number of anterogradely labeled axonal swellings in each layers in V1 after injections of BDA into S1BF of C57Bl/6 mice (continued)

Case	Layer	Number of sections	Total area (mm^2)	Number of dissectors	Number of objects	Sampling fraction	Total estimation	CE
5	I-III	8	1493	121	152	0.025	6192	0.052
	IV	8	709	139	82	0.059	1381	0.040
	Va	8	403	158	56	0.119	472	0.068
	Vbc	8	710	138	52	0.059	883	0.069
	VI	8	678	134	50	0.060	835	0.026
	Total (Mean)	40	3993	690	392	(0.064)	9763	(0.051)

Laminar distribution of axonal swellings

The laminar and size distributions of axonal swellings in the sample of reconstructed single axons in V1 and S1BF (see Figure 27A and C) were compared to the stereological estimates of the laminar and size distributions of swellings labeled following large columnar injections of BDA in these cortices (see Figure 27B and D). The stereologically estimated numbers of anterogradely labeled axonal swellings in each layers of S1BF are shown in Table 8 and the numbers of anterogradely labeled axonal swellings in each layers of V1 are shown in Table 11.

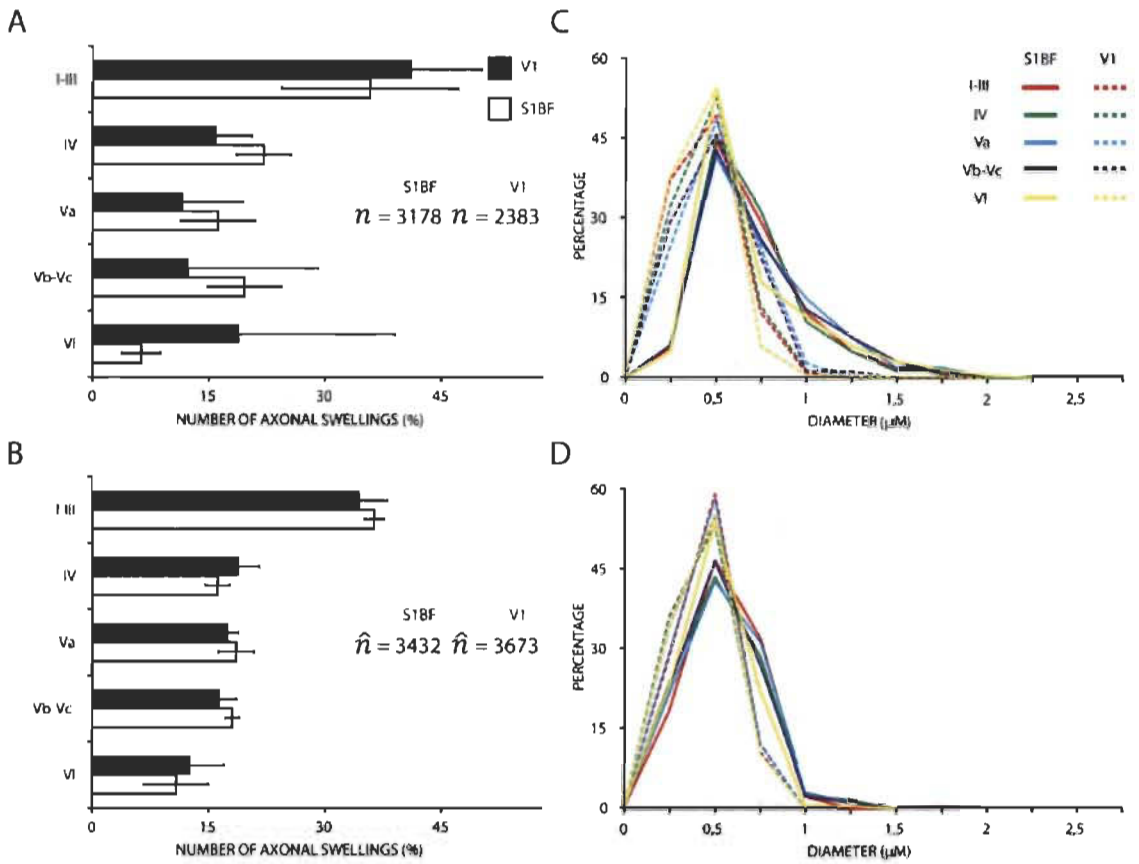

Figure 27. Laminar and size distribution of axonal swellings in S1BF and V1 following an injection of BDA in V1 cortex and S1BF respectively of C57Bl/6J mice from the sample of reconstructed single axons (A and C resp) and from the stereological sampling of these cortical areas following columnar BDA cortical injections (B and D resp). Solid lines correspond to layers in S1BF and dotted lines correspond to layers in V1 (C/D). = the number of swellings estimated by the stereological sampling. n = the total number of swellings measured in the stereological sampling scheme.

Although the laminar distribution of swellings in individual axons exhibits a wide range of patterns (see Figures 24 and 25), the sum of the reconstructed axons in S1BF and V1 produced similar laminar distributions of axonal swellings (see Figure 27A). Furthermore, these distributions were very similar to those obtained with the stereological sampling of cortical layers (see Figure 27B). The stereological sampling

produced smaller variances of the estimates of the number of axonal swellings (see Figure 27B). There were no significant differences in the estimated percentage of axonal swellings in each layer between V1 and S1BF (Kruskal-Wallis, $p = 0.946$).

In both the stereological sampling and the reconstructed axons, both injections in V1 and S1BF resulted in labeling of axons with swellings in layers 1 to 3 and 5. The proportion of swellings found in layer 4 was commensurate with those in infragranular sublayers 5a and 5c and also layer 6.

Size distribution of axonal swellings in cortical layers

Within the stereological sample of axonal swellings, the size of the axonal swellings ranged between 0.3 μm and 2 μm for the projection from V1 to S1BF and between 0.3 μm and 0.9 μm for the projection from S1BF to V1. Within the sample of reconstructed axons, the size of the axonal swellings ranged between 0.3 μm and 2.8 μm for the projection from V1 to S1BF and between 0.2 μm and 1.8 μm for the projection from S1BF to V1.

The systematic random stereological sampling yielded size distributions of the swellings that should be representative of the population of swellings in these projections. The sample of reconstructed axons is quite small and is not statistically representative of the whole population. However, the stereological sampling scheme did not pick up the larger swellings that were observed in the reconstructed axons. These are

quite rare in the overall population and could have been missed. Nevertheless the predominance of smaller swelling in all layers of the projection from S1BF to V1 was observed in both samples (see Figure 27C and 27D).

The laminar size distribution of axonal swellings was compared between the projection from V1 to S1BF and from S1BF to V1 in the samples of reconstructed axons (see Figure 27C) and the stereological samples described above (see Figure 27D). The small sample of reconstructed axons is likely not sufficient to detect with any statistical power the swelling size differences between layers; only the statistical conclusions drawn from the stereological sampling will be considered here.

Within the projection from V1 to S1BF, there was a significant difference of the mean size of axonal swellings between layers (one-way ANOVA, $p = 0.001$), layer 6 swellings being smaller than those of layers 1 to 3 ($p = 0.001$) and layer 5a ($p = 0.001$) (see Figure 27D). Within the projection from S1BF to V1, the mean size of the axonal swellings was significantly different between layers (one-way ANOVA, $p = 0.004$), layer 4 swellings being smaller than those of layers 1 to 3 ($p = 0.021$) and layer 5a ($p = 0.044$). The layer by layer comparisons of these size distributions show that there is a very highly significant difference for all layers pairwise comparisons between S1BF and V1 (Kolmogorov- Smirnov tests, $p < 0.001$). The size distributions for each layers for the stereological sampling (see Figure 27D), clearly show that axonal swellings in V1 are smaller than those in S1BF. The size distributions of swellings for each layers in

the reconstructed axons (see Figure 27C) and in the stereological sampling (see Figure 27D), clearly show a greater asymmetry towards the right in S1BF that in V1.

Discussion

The aim of this study was to describe the structure of the reciprocal connections between visual and somatosensory cortices in the mouse. We show that the primary visual cortex and the barrel field of the primary somatosensory cortex of C57Bl/6J mice are linked by direct reciprocal connections. This supports visuo-tactile interactions at the initial stage of sensory processing in primary sensory cortices. We extend these findings by showing a significant asymmetry of the strength and of the axonal morphology of these reciprocal connections. The projection from V1 to S1 is predominantly to the barrel field and stronger than the reciprocal projection to V1. We also demonstrate that these connections between primary sensory cortices do not fit in the classification scheme of feedforward and feedback cortical projections. Finally, axons in the projection from V1 to S1BF were thicker and had some large anterogradely labeled axonal swellings not found in the projection from S1BF to V1, suggesting a greater importance of Class 1B glutamatergic inputs from the visual cortex to the somatosensory cortex. This asymmetry suggests that, in the mouse, the visual projection to the primary somatosensory cortex has a greater driving influence on the somatosensory cortex than the reciprocal projection from the somatosensory cortex to the visual cortex.

Direct reciprocal projection between visual and somatosensory cortices

Numerous retrogradely labeled neuronal cell bodies were found in V1 and S1 following injections in S1BF and V1 respectively. The projection from V1 to S1BF was more robust than previously shown (Campi et al. 2010; Wang et al. 2012). The projection from the somatosensory to the visual cortex was significant as previously shown in the mouse (Charbonneau et al. 2012; Stehberg et al. 2014; Wang et al. 2012; Zingg et al. 2014), rat (Sieben et al. 2013; Stehberg et al. 2014; Zakiewicz et al. 2014), and gerbil (Henschke et al. 2014).

Direct projections between primary sensory areas are sparse in primates (Cappe et al. 2009; Cappe and Barone 2005; Clavagnier et al. 2004; Falchier et al. 2002; Rockland and Ojima 2003). The greater importance of direct interactions between primary sensory cortices in rodents than in primates could indicate a greater reliance of multisensory processing on low level cortices than on top down feedback projections from higher level multisensory cortices as in primates. The involvement of the direct connections between primary sensory cortices in cross-modal interactions has been demonstrated in rodents (Iurilli et al. 2012; Sieben et al. 2013, 2015). Top down projections to primary sensory cortices from other sensory modalities and non–sensory cortices are nonetheless present and diverse in rodents (Budinger et al. 2006; Budinger and Scheich 2009; Charbonneau et al. 2012; Miller and Vogt 1984; Paperna and Malach 1991; Zingg et al. 2014) and there is direct evidence for a contribution of top down feedback to the primary visual cortex form association cortices in the mouse (Hirokawa et al. 2008; Yoshitake et

al. 2013) and transthalamic pathways (Sieben et al. 2013) in multisensory processing. The relative contribution of direct connections between primary sensory areas and of feedback projections from association cortical areas in multisensory processing is still an open question.

Hierarchical order of primary sensory cortices

The layer indices obtained from the number of retrogradely labeled neurons in supra- and infragranular layers show that the connection of the somatosensory cortex to the visual cortex has features of a feedback projection that is reciprocated by a lateral projection from the visual cortex. This asymmetry suggests that these two primary sensory cortices might not be at the same hierarchical level in the cortical network. Indeed, the asymmetry of reciprocal connections between cortical areas is the basis for establishing hierarchical levels in the cortex (Coogan and Burkhalter 1993; Felleman and Van Essen 1991; Hilgetag et al. 2000; Markov et al. 2014; Rockland and Pandya 1979). Negative layer indices, typical of feedback cortical projections, have also been demonstrated in the mouse projection of somatosensory cortex to V1 (Charbonneau et al. 2012). In the gerbil, the connection from somatosensory to primary visual cortex also has features of a feedback projection, whereas the reciprocal connection has those of a lateral projection (Henschke et al. 2014). One study in the rat however, shows more numerous retrogradely labeled neurons in the supragranular layers of V1 following tracer injections in somatosensory cortex suggesting a feedforward projection (Sieben et al. 2013). In the gerbil, as we have also shown in the mouse (Charbonneau et al. 2012),

V1 receives feedback projections from both the primary auditory and somatosensory cortices. In the gerbil, these projections are reciprocated by a feedforward projection to the auditory cortex and a lateral projection to the somatosensory cortex, and the auditory and somatosensory cortices are reciprocally linked by lateral projections (Henschke et al. 2014). This suggests that primary somatosensory and auditory cortices would be higher in the cortical hierarchy than V1, and possibly at similar levels.

Primary sensory cortices, are the initial portals to cortical networks for specific sensory modalities, and could have been expected to stand at the same hierarchical level and linked by symmetric lateral connections. This is clearly not the case. It is generally believed that in hierarchical cortical networks, a descending pathway is, reciprocated by an ascending projection, and if one is lateral, its counterpart should also be lateral (Felleman and Van Essen 1991). It has been suggested that the hierarchical organization of cortical areas in the rat could be based on half steps in that a feedback projection could be reciprocated by a lateral type projection (Coogan and Burkhalter 1993). Such half steps were not reported in primates, in which feedback projections are strictly paired with feedforward projections (Coogan and Burkhalter 1993). The use of continuous indices such as the layer indices used here, have shown that the cortical areas are not ranked in the cortical hierarchical structure in discrete steps but in a continuum of levels (Markov et al. 2014; Vezoli et al. 2004).

The laminar distribution of anterogradely labeled terminals demonstrates that both projections between V1 and S1BF have features of feedback projections as shown by the dense terminal labeling in both supra- and infragranular layers and by the much lighter labeling in layer 4 (Coogan and Burkhalter 1990, 1993). Indeed, in rodents, feedback projections target both supra- and infragranular layer generally avoiding layers 4 whereas feedforward projections target all cortical layers (Coogan and Burkhalter 1990, 1993). Whether this terminal labeling in layer 4 is a specific attribute of projections between primary sensory cortices is not known. There are no quantitative assessments of the laminar distribution of axonal swellings in cortical projections in rodents showing the absence of layer 4 labeling in feedback projections. We provide here a first quantitative evaluation of the laminar distribution of axonal swellings in corticocortical projections between primary sensory cortices, and show significant terminal labeling in layer 4. Moreover, single axon reconstructions also show axonal branching in layer 4 in both projections. This terminal labeling is quite different to what is seen in feedback projections in primates that target mainly superficial cortical layers. There are no accounts of terminal structure of projections between primary sensory cortices in primates.

In the projection from the somatosensory barrel field to V1, the laminar distribution of retrogradely labeled neurons in the barrel field and the terminal labeling in V1 both indicate that this projection has features of a feedback projection type. However, in the projection from the visual cortex to the barrel field, the retrograde labeling and the

terminal labeling are not strictly consistent with a feedback or feedforward types of projections. The laminar distribution of terminals in the barrel field is the same as the one in V1 and suggests a feedback projection whereas the laminar distribution of retrogradely labeled neurons yields layer indices close to 0 suggesting a lateral type projection. This could be particular to projections between primary sensory cortices and could also indicate that a dichotomous classification of cortical projections in feedforward and feedback types is not appropriate to describe all possibilities.

Asymmetry of the strength of the reciprocal projections between V1 and S1BF

Retrograde transport of cholera toxin showed a stronger projection from V1 to S1BF than from S1 and S1BF to V1. Similarly, a strong projection of the visual cortex to the somatosensory cortex and a moderate reciprocal projection have been shown in the gerbil (Henschke et al. 2014). In the gerbil, the primary visual cortex has the strongest multisensory inputs receiving similar moderate inputs from the primary auditory and somatosensory cortices. On the other hand, the somatosensory cortex receives a strong input from the visual cortex but only a faint input from the auditory cortex. The primary auditory cortex receives only faint inputs from the other primary sensory cortices (Henschke et al. 2014). These observations suggest that the mutual influences between the senses are not equivalent in strength. In the mouse, as in the gerbil, the influence of the visual cortex on the somatosensory cortex would be the stronger one.

A functional asymmetric reciprocity has also been shown between primary visual and somatosensory cortices in the mouse. Visual stimulation produces a small subthreshold depolarisation of layer 2/3 neurons of the somatosensory cortex whereas whisker deflection hyperpolarizes neurons in these layers by direct corticocortical recruiting of local translaminar inhibitory circuits (Iurilli et al. 2012).

Size of axonal swellings

The asymmetry of the reciprocal projections between V1 and S1BF is also seen in the size distribution of axonal swellings. All cortical layers in S1BF had some larger swellings not seen in V1. The size distributions we obtained here are commensurate with those reported in the reciprocal connections between primary and secondary auditory cortices in mice (Covic and Sherman 2011). Class 1B synapses are anatomically correlated with larger synaptic terminals and Class 2 synapses with smaller synaptic terminals (Covic and Sherman 2011; see Sherman and Guillery 2013a). We surmise that the larger swellings in the projection from V1 to S1BF in our results, reflects a greater proportion of Class 1 terminals therein and that the large population of smaller swellings, which appears to be predominant in both projections, could be Class 2 terminals.

In thalamocortical and corticothalamic pathways, Class 1B and 2 are respectively considered drivers and modulators (Lee and Sherman 2008, 2009a, 2009b; Petrof and Sherman 2013; Reichova and Sherman 2004; Sherman and Guillery 1996, 1998, 2013a;

Viaene et al. 2011). This model of glutamatergic transmission predicts that information flow depends on Class 1 pathways (Covic and Sherman 2011; Sherman and Guillery 2013a). If this is the case, our results would indicate that visual information is transmitted to the somatosensory cortex while tactile information can mostly modulate activity in the visual cortex.

The presence of larger terminals in S1BF not found in V1 would indicate that V1 might exert a driving influence on the somatosensory cortex that is not reciprocated in its projection back to the visual cortex. This asymmetry could reflect the greater influence of vision on whisker mediated tactile sensing and navigation in mice, and the relative importance of the different senses in rodents, which rely less on visual stimuli compared to the more visual carnivores and primates (Whishaw and Kolb 2004). Moreover, the benefit of multisensory interactions is larger for some modalities (Hollensteiner et al. 2015). The modality precision hypothesis states that the resolution of intersensory discrepancies will be in favor of the more precise of the two modalities (see Welch and Warren 1986 for review and references). This theory is based on an order of dominance between sensory modalities derived from their respective spatial precision. Whisker mediated tactile sensing is spatially more precise than vision in rats and mice, tactile acuity greatly surpassing their visual discrimination capabilities (Carvell and Simons 1990; Prusky et al. 2000; Wu et al. 2013). The presence of the larger presumed Class 1 terminals in the projection from the visual cortex to the barrel field would suggest that the visual cortex provides the somatosensory cortex with more

specific visual information than the reciprocal projection of S1BF to V1. Indeed, Class 1 responses are mediated by ionotropic receptors which exhibit fast postsynaptic response dynamics compared to the much slower Class 2 metabotropic mediated responses. Class 1B inputs will therefore maintain the highly specific temporal attributes of the conveyed information (see Sherman and Guillery 2013a). In visuo-tactile integration, the less precise visual information will contribute in providing additional information to the somatosensory cortex through a stronger driving projection. The absence of larger terminals in the projection from the barrel field to the visual cortex suggests that it has more modulatory influence on visual cortex activity. This could indicate that in the mouse, vision is more important to enhance the context of whisking and that tactile information is not as important for the enhancement of visual information.

It is noteworthy that there are very few larger swellings in the visual cortex projection to the barrel field. This is also observed in many other cortical and subcortical pathways. Even though Class 1 inputs are considered as the main information carriers in thalamic circuits, it is common that they are vastly outnumbered by Class 2 inputs, accounting for less than 10% of the total number of synapses in thalamus, with some estimates putting them as low as 2% (Huppé-Gourgues et al. 2006; Van Horn et al. 2000; Wang et al. 2002). Retinogeniculate projections are considered as Class 1 inputs and are functionally the dominant input to geniculate neurons however they account for only 5% of geniculate synapses whereas cortical inputs account for 30 to 40% of synapses therein (Erisir et al. 1998; Van Horn et al. 2000). We cannot evaluate the

proportions of terminals that could be assigned to these functional classes having no basis for determining a cut-off size as a reliable criterion for such a classification. However, we do provide the first quantitative unbiased stereological sampling of axonal swellings laminar and size distributions in a cortical connection. This sampling clearly shows that small terminals, that would most likely have Class 2 properties, largely outnumber the larger terminals.

In the projection from V1 to S1BF, there were no significant differences of the size distributions of axonal swellings between layers. This pattern is different than what was reported in the corticocortical connection between auditory (Covic and Sherman 2011) and visual cortices (De Pasquale and Sherman 2011). In the reciprocal connection between primary and secondary auditory cortices, layers 5a and 6 received almost only Class 2 inputs whereas layer 5b received almost only Class 1B inputs. This was correlated with anatomical observations showing significantly smaller terminals in layers 4 and 5b than in layers 5a and 6 (Covic and Sherman 2011). We show here that there is a wide range of terminal sizes in the supragranular layers in the somatosensory cortex that would support the presence of the two types of postsynaptic responses. Conversely, in the projection from S1BF to V1, the swellings in layer 4 were smaller than those in the bottom tiers of layer 5. Whether this indicates a greater contribution of Class 1 inputs therein is possible, but very large terminals were not observed in this projection to the somatosensory cortex.

Single axon morphology

This is the only account of single axon morphology of interareal connections between primary sensory cortices. Although we have here only small samples of axons, significant observations can be drawn from these. There is a diversity of morphologies in both projections; supporting previous studies in showing that a single cortical projection likely comprises several morphofunctional conduction channels (see Rockland 2015 for further references and discussion). This is further supported by the diversity in the laminar distribution of terminals for each of these axons. The overall laminar distribution of terminals results from the sum of individual axons that have very different terminal arbor structures. Axonal morphologies exhibit a mosaic of features. Some axons had terminal arbors that form a more or less defined columnar projection with a limited tangential spread, whereas others were widely divergent over large distances. Some axons show both features. These are not typical of axons in cortical feedforward and feedback projections in monkeys. In general, feedforward axons have a more focused structure whereas feedback axons appear to travel greater distances and cross functional domains such as ocular dominance columns (see Rockland 2002 for review). Such a mixture of columnar and divergent features could be particular to connections between primary sensory cortices or can also be related to the less-modular, salt-and-pepper organisation of the mouse cortex. The more divergent axons seen here were in the projection from V1 to the barrel field and would likely target more than one barrel.

In corticothalamic projections there are two very distinct types of axons (see Sherman and Guillery 2013b for extended discussion). Thick axons originate from layer 5 pyramidal neurons and bear type II axon terminals that convey Class 1 inputs. Thin axons are issued by neurons of layer 6 and bear type I axon terminals that convey Class 2 inputs (Bourassa and Deschenes 1995; Bourassa et al. 1995; Sherman and Guillery 2013a). There is no evidence here for corticocortical axons with exclusively large terminals similar to the thick corticothalamic axons issued by layer 5 neurons. There are several reconstructed axons in our sample that bear only very small terminals and axon on which a wider range of terminal sizes occur. On these particular axons, again very small terminals largely outnumber the larger ones. This might indicate two distinct types of axons on the basis of the presence of some larger terminals.

Axons entering the somatosensory barrel field were significantly thicker than the axons entering the primary visual cortex. Moreover in S1BF there were a few quite thick axons that were never observed in the projection to the visual cortex, further supporting the asymmetric projections between the two primary sensory cortices. Previous studies in primates have shown that corticofugal axons originating from different cortical areas have different diameters whereas the thickness of axons of inter-area connections was not different (Tomasi et al. 2012). Another study showed that corticocortical projections to different targets may have axons of different diameters (Innocenti et al. 2014). Our results show here that both projections comprise mainly a population of quite thin axons with the projection to the visual cortex having the thinner axons and that the projection

of S1BF to the visual cortex contains a few larger caliber axons. Axonal diameter is related to conduction speeds. Therefore, we might expect that the projection from the somatosensory barrel field is more homogeneous in this respect than the projection from the visual cortex to the barrel field. The greater range in axon diameters in the projection to the barrel field supports the idea that a single connection can be a complex channel comprising a range of parallel axonal pathways that might generate different conduction delays (Innocenti et al. 2014).

Conclusions

This study shows a direct and reciprocal connection of lateral type from V1 to S1BF and of feedback type from S1BF to V1. This direct link between the visual cortex and the barrel field further supports the notion that primary sensory cortices integrate multisensory inputs. This study indicates that these heteromodal connections between low-level primary sensory cortices although reciprocal, are certainly not symmetrical. This reciprocal connection between the visual cortex and the barrel field could be the anatomical substrate of the influence of vision on tactile sensing and navigation by the whiskers in mice. We show here that the reciprocal connection between the visual and somatosensory cortex of the mouse would be a good experimental model for the study of functional and behavioral asymmetries between sensory modalities.

Acknowledgements

We are grateful to Nadia Desnoyers for animal care and maintenance. This work was supported by discovery grants of the Natural Sciences and Engineering Research Council of Canada (NSERC) to DB and GB, and the Canadian Foundation for Innovation to DB. SR was supported by an NSERC undergraduate student award. Contributions from UQTR are also acknowledged.

References

Berezovskii VK, Nassi JJ and Born RT. 2011. Segregation of feedforward and feedback projections in mouse visual cortex. J Comp Neurol. 2011/05/28:3672-3683.

Bizley JK and King AJ. 2009. Visual influences on ferret auditory cortex. Hear Res. 258:55-63.

Bizley JK, Nodal FR, Bajo VM, Nelken I and King AJ. 2007. Physiological and anatomical evidence for multisensory interactions in auditory cortex. Cereb Cortex. 17:2172-2189.

Bourassa J and Deschenes M. 1995. Corticothalamic projections from the primary visual cortex in rats: A single fiber study using biocytin as an anterograde tracer. Neuroscience. 66:253-263.

Bourassa J, Pinault D and Deschenes M. 1995. Corticothalamic projections from the cortical barrel field to the somatosensory thalamus in rats: A single-fibre study using biocytin as an anterograde tracer. Eur J Neurosci. 7:19-30.

Brosch M, Selezneva E and Scheich H. 2005. Nonauditory events of a behavioral procedure activate auditory cortex of highly trained monkeys. J Neurosci. 2005/07/22:6797-6806.

Budinger E, Heil P, Hess A and Scheich H. 2006. Multisensory processing via early cortical stages: Connections of the primary auditory cortical field with other sensory systems. Neuroscience. 143:1065-1083.

Budinger E, Laszcz A, Lison H, Scheich H and Ohl FW. 2008. Non-sensory cortical and subcortical connections of the primary auditory cortex in Mongolian gerbils: Bottom-up and top-down processing of neuronal information via field AI. Brain Res. 1220:2-32.

Budinger E and Scheich H. 2009. Anatomical connections suitable for the direct processing of neuronal information of different modalities via the rodent primary auditory cortex. Hear Res. 258:16-27.

Campi KL, Bales KL, Grunewald R and Krubitzer L. 2010. Connections of auditory and visual cortex in the prairie vole (Microtus ochrogaster): Evidence for multisensory processing in primary sensory areas. Cereb Cortex. 2009/04/28:89-108.

Cappe C and Barone P. 2005. Heteromodal connections supporting multisensory integration at low levels of cortical processing in the monkey. Eur J Neurosci. 22:2886- 2902.

Cappe C, Rouiller EM and Barone P. 2009. Multisensory anatomical pathways. Hear Res. 2009/05/05:28-36.

Carvell GE and Simons DJ. 1990. Biometric analyses of vibrissal tactile discrimination in the rat. J Neurosci. 10:2638-2648.

Caviness VS. 1975. Architectonic map of neocortex of the normal mouse. J Comp Neurol. 164:247-263.

Charbonneau V, Laramée ME, Boucher V, Bronchti G and Boire D. 2012. Cortical and subcortical projections to primary visual cortex in anophthalmic enucleated and sighted mice. Eur J Neurosci. 2012/07/12:2949-2963.

Clavagnier S, Falchier A and Kennedy H. 2004. Long-distance feedback projections to area V1: Implications for multisensory integration, spatial awareness, and visual consciousness. Cogn Affect Behav Neurosci. 2004/10/06:117-126.

Coogan TA and Burkhalter A. 1990. Conserved patterns of cortico-cortical connections define areal hierarchy in rat visual cortex. Exp Brain Res. 80:49-53.

Coogan TA and Burkhalter A. 1993. Hierarchical organization of areas in rat visual cortex. J Neurosci. 13:3749-3772.

Covic EN and Sherman SM. 2011. Synaptic properties of connections between the primary and secondary auditory cortices in mice. Cereb Cortex. 21:2425-2441.

De Pasquale R and Sherman SM. 2011. Synaptic properties of corticocortical connections between the primary and secondary visual cortical areas in the mouse. J Neurosci. 31:16494-16506.

Driver J and Noesselt T. 2008. Multisensory interplay reveals crossmodal influences on 'sensory-specific' brain regions, neural responses, and judgments. Neuron. 2008/01/11:11-23.

Erisir A, Van Horn SC and Sherman SM. 1998. Distribution of synapses in the lateral geniculate nucleus of the cat: Differences between laminae A and A1 and between relay cells and interneurons. J Comp Neurol. 390:247-255.

Ernst MO and Bulthoff HH. 2004. Merging the senses into a robust percept. Trends Cogn Sci. 8:162-169.

Falchier A, Cappe C, Barone P and Schroeder CE. 2013. Sensory convergence in low-level cortices. In Stein BE. The new handbook of multisensory processing. The MIT Press, Cambridge MA, London England, pp. 67-79.

Falchier A, Clavagnier S, Barone P and Kennedy H. 2002. Anatomical evidence of multimodal integration in primate striate cortex. J Neurosci. 2002/07/05:5749-5759.

Felleman DJ and Van Essen DC. 1991. Distributed hierarchical processing in the primate cerebral cortex. Cereb Cortex. 1:1-47.

Foxe JJ, Morocz IA, Murray MM, Higgins BA, Javitt DC and Schroeder CE. 2000. Multisensory auditory-somatosensory interactions in early cortical processing revealed by high-density electrical mapping. Brain Res Cogn Brain Res. 2000/09/09:77-83.

Franklin, BJ and Paxinos, G. 2008. The Mouse Brain in Stereotaxic Coordinates.

Ghazanfar AA and Schroeder CE. 2006. Is neocortex essentially multisensory? Trends Cogn Sci. 10:278-285.

Giard MH and Peronnet F. 1999. Auditory-visual integration during multimodal object recognition in humans: A behavioral and electrophysiological study. J Cogn Neurosci. 1999/10/08:473-490.

Godement P, Saillour P and Imbert M. 1979. Thalamic afferents to the visual cortex in congenitally anophthalmic mice. Neurosci Lett. 13:271-278.

Gonchar Y and Burkhalter A. 1999. Differential subcellular localization of forward and feedback interareal inputs to parvalbumin expressing GABAergic neurons in rat visual cortex. J Comp Neurol. 406:346-360.

Gonchar Y and Burkhalter A. 2003. Distinct GABAergic targets of feedforward and feedback connections between lower and higher areas of rat visual cortex. J Neurosci. 23:10904-10912.

Henschke JU, Noesselt T, Scheich H and Budinger E. 2014. Possible anatomical pathways for short-latency multisensory integration processes in primary sensory cortices. Brain Struct Funct. 220:955-977.

Hilgetag CC, O'Neill MA and Young MP. 2000. Hierarchical organization of macaque and cat cortical sensory systems explored with a novel network processor. Philos Trans R Soc Lond B Biol Sci. 355:71-89.

Hirokawa J, Bosch M, Sakata S, Sakurai Y and Yamamori T. 2008. Functional role of the secondary visual cortex in multisensory facilitation in rats. Neuroscience. 153:1402-1417.

Hishida R, Kudoh M and Shibuki K. 2014. Multimodal cortical sensory pathways revealed by sequential transcranial electrical stimulation in mice. Neurosci Res. 87:49-55.

Hollensteiner KJ, Pieper F, Engler G, Konig P and Engel AK. 2015. Crossmodal integration improves sensory detection thresholds in the ferret. PLoS One. 10:e0124952.

Huppé-Gourgues F, Bickford ME, Boire D, Ptito M and Casanova C. 2006. Distribution, morphology, and synaptic targets of corticothalamic terminals in the cat lateral posterior pulvinar complex that originate from the posteromedial lateral suprasylvian cortex. J Comp Neurol. 497:847-863.

Innocenti GM, Vercelli A and Caminiti R. 2014. The diameter of cortical axons depends both on the area of origin and target. Cereb Cortex. 24:2178-2188.

Iurilli G, Ghezzi D, Olcese U, Lassi G, Nazzaro C, Tonini R, Tucci V, Benfenati F and Medini P. 2012. Sound-driven synaptic inhibition in primary visual cortex. Neuron. 73:814-828.

Kaas JH and Collins CE. 2013. The resurrection of multisensory cortex in primates: Connection patterns that integrate modalities. In Calvert GA., Spence C. & Stein B. The handbook of multisensory processes. The MIT Press, Cambridge, pp. 285-293.

Laurienti PJ, Burdette JH, Wallace MT, Yen YF, Field AS and Stein BE. 2002. Deactivation of sensory-specific cortex by cross-modal stimuli. J Cogn Neurosci. 14:420-429.

Lee CC and Sherman SM. 2008. Synaptic properties of thalamic and intracortical inputs to layer 4 of the first- and higher-order cortical areas in the auditory and somatosensory systems. J Neurophysiology. 100:317-326.

Lee CC and Sherman SM. 2009a. Glutamatergic inhibition in sensory neocortex. Cereb Cortex. 19:2281-2289.

Lee CC and Sherman SM. 2009b. Modulator property of the intrinsic cortical projection from layer 6 to layer 4. Front Syst Neurosci. 3:3.

Macaluso E. 2006. Multisensory processing in sensory-specific cortical areas. Neuroscientist. 2006/07/15:327-338.

Markov NT, Vezoli J, Chameau P, Falchier A, Quilodran R, Huissoud C, Lamy C, Misery P, Giroud P, Ullman S, Barone P, Dehay C, Knoblauch K and Kennedy H. 2014. Anatomy of hierarchy: Feedforward and feedback pathways in macaque visual cortex. J Comp Neurol. 522:225-259.

Miller MW and Vogt BA. 1984. Direct connections of rat visual cortex with sensory, motor, and association cortices. J Comp Neurol. 226:184-202.

Paperna T and Malach R. 1991. Patterns of sensory intermodality relationships in the cerebral cortex of the rat. J Comp Neurol. 308:432-456.

Petrof I and Sherman SM. 2013. Functional significance of synaptic terminal size in glutamatergic sensory pathways in thalamus and cortex. J Physiol. 591:3125-3131.

Prusky GT, West PW and Douglas RM. 2000. Behavioral assessment of visual acuity in mice and rats. Vision Res. 40:2201-2209.

Reichova I and Sherman SM. 2004. Somatosensory corticothalamic projections: Distinguishing drivers from modulators. J Neurophysiology. 92:2185-2197.

Rockland KS. 2002. Visual cortical organization at the single axon level: A beginning. Neurosci Res. 42:155-166.

Rockland KS. 2015. Article about connections. Front Neuroanat. 9:61.

Rockland KS and Ojima H. 2003. Multisensory convergence in calcarine visual areas in macaque monkey. Int J Psychophysiol. 2003/09/27:19-26.

Rockland KS and Pandya DN. 1979. Laminar origins and terminations of cortical connections of the occipital lobe in the rhesus monkey. Brain Res. 179:3-20.

Schroeder CE, Smiley J, Fu KG, McGinnis T, O'Connell MN and Hackett TA. 2003. Anatomical mechanisms and functional implications of multisensory convergence in early cortical processing. Int J Psychophysiol. 2003/09/27:5-17.

Sherman SM and Guillery RW. 1996. Functional organization of thalamocortical relays. J Neurophysiol. 76:1367-1395.

Sherman SM and Guillery RW. 1998. On the actions that one nerve cell can have on another: Distinguishing "drivers" from "modulators". Proc Natl Acad Sci U S A. 95:7121-7126.

Sherman, SM and Guillery, RW. 2013a. Functional connections of cortical areas. Cambridge MA, London England: MIT Press.

Sherman, SM and Guillery, RW. 2013b. Functional connections of cortical areas. A new view from the thalamus. Cambridge, Massachusetts; London, England: MIT Press.

Sieben K, Bieler M, Roder B and Hanganu-Opatz IL. 2015. Neonatal Restriction of Tactile Inputs Leads to Long-Lasting Impairments of Cross-Modal Processing. PLoS Biol. 13:e1002304.

Sieben K, Roder B and Hanganu-Opatz IL. 2013. Oscillatory entrainment of primary somatosensory cortex encodes visual control of tactile processing. J Neurosci. 33:5736-5749.

Stehberg J, Dang PT and Frostig RD. 2014. Unimodal primary sensory cortices are directly connected by long-range horizontal projections in the rat sensory cortex. Front Neuroanat. 8:93.

Stein BE and Meredith MA. 1993. The Merging of the Senses.

Stein BE and Stanford TR. 2008. Multisensory integration: Current issues from the perspective of the single neuron. Nat Rev Neurosci. 2008/03/21:255-266.

Tomasi S, Caminiti R and Innocenti GM. 2012. Areal differences in diameter and length of corticofugal projections. Cereb Cortex. 22:1463-1472.

Van Horn SC, Erisir A and Sherman SM. 2000. Relative distribution of synapses in the A-laminae of the lateral geniculate nucleus of the cat. J Comp Neurol. 416:509-520.

Vezoli J, Falchier A, Jouve B, Knoblauch K, Young M and Kennedy H. 2004. Quantitative analysis of connectivity in the visual cortex: Extracting function from structure. Neuroscientist. 10:476-482.

Viaene AN, Petrof I and Sherman SM. 2011. Synaptic properties of thalamic input to layers 2/3 and 4 of primary somatosensory and auditory cortices. J Neurophysiol. 105:279-292.

Wang Q and Burkhalter A. 2007. Area map of mouse visual cortex. J Comp Neurol. 502:339-357.

Wang Q, Sporns O and Burkhalter A. 2012. Network analysis of corticocortical connections reveals ventral and dorsal processing streams in mouse visual cortex. J Neurosci. 2012/03/30:4386-4399.

Wang S, Eisenback MA and Bickford ME. 2002. Relative distribution of synapses in the pulvinar nucleus of the cat: Implications regarding the "driver/modulator" theory of thalamic function. J Comp Neurol. 454:482-494.

Welch RB and Warren DH. 1986. Intersensory interactions. In Boff KR., Kaufman L. & Thomas JP. Handbook of perception and human performance. J. Wiley, New York, pp. 25-1-25-36.

West MJ. and Gundersen H.J. 1990. Unbiased stereological estimation of the number of neurons in the human hippocampus. J.Comp Neurol. 296: 1-22.

West MJ, Slomianka L and Gundersen HJ. 1991. Unbiased stereological estimation of the total number of neurons in the subdivisions of the rat hippocampus using the optical fractionator. Anat Rec. 231:482-497.

Whishaw IQ and Kolb B. 2004. The Behavior of the Laboratory Rat: A Handbook with Tests: Oxford University Press, USA.

Wu HP, Ioffe JC, Iverson MM, Boon JM and Dyck RH. 2013. Novel, whisker-dependent texture discrimination task for mice. Behav Brain Res. 237:238-242.

Yamashita A, Valkova K, Gonchar Y and Burkhalter A. 2003. Rearrangement of synaptic connections with inhibitory neurons in developing mouse visual cortex. J Comp Neurol. 2003/08/06:426-437.

Yoshitake K, Tsukano H, Tohmi M, Komagata S, Hishida R, Yagi T and Shibuki K. 2013. Visual map shifts based on whisker-guided cues in the young mouse visual cortex. Cell Rep. 5:1365-1374.

Zakiewicz IM, Bjaalie JG and Leergaard TB. 2014. Brain-wide map of efferent projections from rat barrel cortex. Front Neuroinform. 8:5.

Zingg B, Hintiryan H, Gou L, Song MY, Bay M, Bienkowski MS, Foster NN, Yamashita S, Bowman I, Toga AW and Dong HW. 2014. Neural networks of the mouse neocortex. Cell. 156:1096-1111.

Chapitre III

Effects of enucleation on the direct reciprocal corticocortical connections between primary visual and somatosensory cortices of the mouse[1]

[1] Le contenu de ce chapitre est présenté sous forme de manuscrit qui a été soumis durant l'automne 2016 dans la revue European Journal of Neuroscience: Massé, I.O., Bronchti, G. et Boire, D.

Title: Effects of enucleation on the direct reciprocal corticocortical connections between primary visual and somatosensory cortices of the mouse.

Authors: Ian O. Massé, Gilles Bronchti, Denis Boire

Affiliations:

Département d'anatomie
Université du Québec à Trois-Rivières
Canada, G9A 2W7

Running title: Enucleation effects on visuo-tactile connections.

Abstract: In the sensory deprived brain, the intermodal cortical connections appear to play a more significant role in sensory processing. Although some studies report enhanced functional intermodal cortical connectivity in the blind, others report a contradictory finding of decreased functional connectivity of the visual cortex in blind subjects. The purpose of this study is to compare the direct reciprocal intermodal corticocortical connections between the primary visual (V1) and somatosensory (S1) cortices in intact and C57Bl/6 mice enucleated at birth, and to determine quantitative differences in the strength and laminar distribution of neurons and terminals in these projections through iontophoretic injections of high molecular weight biotinylated dextrans (BDA) and of the B fragment of cholera toxin (CTB). The size of axonal swellings was measured and frequency distribution determined for each cortical layer. Axon diameters were also sampled in these connections. CTB labeled neurons were used to estimate the relative weight of projections between V1 and S1, and their laminar distribution used to classify them as feedback, feedforward or lateral projections. CTB injections in V1 resulted in a greater proportion of labeled cells in S1 of intact mice than of enucleated mice. Following injections of BDA in V1, a greater range of swelling size was observed in S1 of intact mice compared to enucleated mice, suggesting that normal sensory activity is required for the normal development of Class 1 driver projections from V1 or that a homeostatic adjustment of these terminals size is produced by high levels of activity in these projection neurons. This study provides evidence for

alterations in intermodal connections through anatomical changes following visual deprivation.

Keywords: Blind, intermodal, cross-modal, corticocortical connections, visuo-haptic interaction.

Introduction

Visually deprived humans have greater abilities in processing somatosensory stimuli than sighted individuals (Van Boven et al., 2000; Wan et al., 2010). These capabilities appear to be correlated with the activation of their visual cortex by somatosensory stimuli (Gougoux et al., 2005; Röder et al., 2001). This somatosensory activation of the visual cortex has also been observed in visually deprived rodents (Nys et al., 2014; Toldi et al., 1988, 1994; Van Brussel et al., 2011). These results suggest underlying intermodal plasticity following the loss of visual inputs.

Several mechanisms have been put forth to explain how intermodal interactions are established in visually deprived individuals (Bavelier & Neville, 2002). The first mechanism involves subcortical pathways directly conveying non-visual activity to the primary visual cortex (V1). The second mechanism involves a reorganization of intermodal cortical circuits which includes two hypotheses. The first hypothesis suggested that the existing connections between the visual areas and the areas of other modalities are amplified in the blind, as to increase the amount of non-visual sensory information that can be sent to the occipital cortex (Kahn & Krubitzer, 2002; Karlen et al., 2006; Klinge et al., 2010; Wittenberg et al., 2004). The second hypothesis proposed that these existing connections are reduced in the blind, because of the lack of coordination between the sensory systems (Pascual-Leone et al., 2005). The third and last mechanism proposed instead that intermodal corticocortical connections in the blind are unmasked by synaptic changes (Pascual-Leone et al., 2005; Pascual-Leone &

Hamilton, 2001). In the present study, we set out to investigate the influence of the visual experience during the postnatal life on the development of the corticocortical connections between V1 and the primary somatosensory cortex (S1) in mice.

It is known that activity from sensory receptors can significantly influence the development of cortical connectivity. Although some studies report amplified functional intermodal cortical connectivity (Fujii et al., 2009; Klinge et al., 2010), others report a reduced connectivity of the visual cortex with other primary sensory cortices in blind subjects (Liu et al., 2007; Yu et al., 2008). Few studies have been devoted to the effects of blindness on the efferents of V1. The topography and size of striate extrastriate projections were altered in rodents enucleated at birth (Bravo & Inzunza, 1994; Laing et al., 2012; Laramée et al., 2013).

In contrast to primates (Cappe & Barone, 2005; Clavagnier et al., 2004), there are significant direct connections between primary sensory cortices in rodents (Budinger et al., 2006; Budinger & Scheich, 2009; Campi et al., 2010; Charbonneau et al., 2012; Henschke et al., 2014; Iurilli et al., 2012; Massé et al., 2016; Paperna & Malach, 1991; Sieben et al., 2013; Stehberg et al., 2014; Wang & Burkhalter, 2007; Zingg et al., 2014). The mouse is therefore an interesting model for the study of alterations in intermodal connections between primary sensory cortices following visual deprivation.

The projections between V1 and S1BF in intact and C57Bl/6 mice enucleated at birth will be studied in order to quantify the relative strengths of the connections with both retrograde and anterograde tracers. The size of axonal swellings and axons will be compared between intact and enucleated cases to study the effects of blindness on the driving influence of V1 on S1BF and the conduction velocity of its axons.

Methods

Animals were treated in accordance with the regulations of the Canadian Council for the Protection of Animals and the study was approved by the Animal Care committee of the Université du Québec à Trois-Rivières. C57Bl/6J mice ($n = 40$) (Charles River, Montreal, QC, Canada) from our colonies were used. Intact C57Bl/6J mice ($n = 20$) served as controls and neonatally enucleated C57Bl/6J mice ($n = 20$) were studied as a model of visual deprivation. All animals were kept under a light/dark cycle of 14/10 hours and were adults (60 days) when sacrificed.

Neonatal enucleation

Bilateral enucleations of C57Bl/6J mouse pups were performed within 24h following birth under deep anesthesia by hypothermia. The palpebral fissure was opened with a scalpel, the eyeball was gently pulled out and the optic nerve was sectioned. Ocular orbits were filled with Gelfoam (Upjohn, Kalamazoo, MI, USA) and newborns were warmed until complete awakening before being returned to their home cage.

Tracing procedures

All animals were adults (60 days) when the cortical tracer injections were performed. Surgical anesthesia was achieved and maintained with inhalation of 1.5-2.5% isoflurane and vital signs were monitored throughout the procedures. The animals were mounted on a stereotaxic apparatus. Mice were protected from ocular dryness by applying ophthalmic ointment (Polysporin; Pfizer, Toronto, ON, Canada). A scalp incision was made along the midline to expose the skull. For injections in the primary visual cortex (V1), a small craniotomy was performed 3.7 mm caudal and 2.5 mm lateral to Bregma or, for injections in the barrel field of the primary somatosensory cortex (S1BF), 1.5 mm caudal to Bregma and 2.9 mm from the midline. The dura was incised and a glass micropipette filled with a solution of the b-fragment of cholera toxin (CTb) or biotinylated dextran amine (BDA) was inserted into the cortex. Retrograde and anterograde neuronal tracing was achieved with iontophoretic injections of 1% solution of CTb and of a 10% solution of high molecular weight BDA (10 kDa) (Molecular Probes, Cedarlane Laboratories, Ontario, Canada) respectively in phosphate-buffered saline (PBS) through glass micropipettes (20 μm tip diameter) into V1 for 20 animals and S1BF for 20 animals for each tracer. A 1.5 μA positive current with a 7-s duty cycle was applied for 10 min, starting at a depth of 500 μm and ending at 100 μm from the pial surface, 2 min at each 100 μm. The mice were kept warm until they recovered from anesthesia and postoperative pain was managed with buprenorphine (Temgesic, Schering-Plough, Hertfordshire, UK; i.p.; 0.009 mg/kg) injected before anesthesia was induced.

After a 2-day survival period for CTb injections and 7-day survival period for BDA injections, mice received an intraperitoneal injection of 120 mg/kg sodium pentobarbital (Euthanyl; Bimeda-MTC, Cambridge, ON, Canada) and were perfused through the heart with PBS (pH 7.4) followed by phosphate-buffered 4% paraformaldehyde. Brains were harvested, postfixed for 1-2 hours, cryoprotected with 30% sucrose and frozen prior to sectioning and CTb or BDA processing.

Serial 50-μm-thick coronal sections were taken using a freezing microtome. One series was processed for CTb immunohistochemistry and the other was mounted on slides and stained with cresyl violet to identify the cortical areas and layers. Sections processed for BDA histochemisty were counterstained with bisbenzimide to identify the cortical areas and layers.

To visualize CTb labeled neurons, free-floating sections were treated for 45 min with 0.15% H2O2 and 70% methanol to quench endogenous peroxidase and thoroughly rinsed in 0.05 M Tris-HCl-buffered 0.9% saline solution (TBS, pH 8.0) containing 0.5% Triton X-100 (TBSTx). Sections were then incubated in 2% normal donkey serum (NDS) for 2 hours and transferred to a solution of primary antibody (goat polyclonal anti-CTb 1:4 000; Molecular Probes) with 1% NDS in PBS-Tx for 2 days at 4°C. Subsequently, sections were rinsed in PBS-Tx and incubated in a secondary antibody (biotinylated donkey anti-goat; 1:500; Molecular Probes) solution with 1% NDS in PBS-Tx for 2 hours at room temperature. Following further rinsing, the sections were

then incubated for 90 min in an avidin-biotin complex solution (Elite Vectastain, Vector Laboratories, PK4000 Standard kit) in TBS-Tx, pH 8.0, rinsed in TBS, and then incubated in a 0.015% '3-diaminobenzidine (DBA) solution. Labeled neurons were revealed by the addition of 0.005% H2O2. Sections were washed and mounted on gelatin-subbed slides, air-dried, dehydrated and cover-slipped with Permount mounting media (Fisher Scientific, Ottawa, ON, Canada).

For BDA staining, after quenching endogenous peroxidase, sections were incubated for 90 min in an avidin-biotin complex solution (ABC Vectastain elite), washed and BDA was revealed using nickel-intensified DAB (Sigma-Aldrich, St-Louis, MO, USA) as a chromogen. Sections were pre-incubated for 30 min in Tris-buffered (TB) (0.05 m)-nickel ammonium sulfate 0.4%, pH 8.0, followed by 10 min in TB-nickel ammonium containing 0.015% DAB and 0.005% H2O2. Sections were dehydrated in ethanol, cleared in xylenes and cover-slipped with Eukitt mounting media.

Charting of retrogradely labeled neurons

All CTb retrogradely labeled neurons on one of every two sections of S1, S1BF, V2M, V2L, M1, M2, S2 and of V1 were plotted using an Olympus BX51WI microscope (20 x 0.75 NA objective) equipped with a three-axis computer-controlled stepping motor system coupled to a personal computer and to a color Optronix CCD camera and driven by the Neurolucida software (MBF Biosciences, Williston, VT, USA).

The whole primary and secondary somatosensory, motor and visual cortices were systematically and randomly sampled on sections spaced 200 μm apart. Cortical areas were delineated at lower magnification (4 X, 0.16 NA objective) on adjacent Nissl-stained sections. Borders between cortical areas were delineated according to the cytoarchitectonic descriptions provided by Caviness (1975) and the mouse brain atlas of Franklin and Paxinos (2008). Contours of each cortical area in which retrogradely labeled cells were located were traced with Neurolucida and the limits of each cortical layer were traced. These contours were superimposed on the images of CTb-reacted sections and resized for shrinkage differences between the Nissl and CTb sections. This allowed plotted neurons in each cortical area to be assigned to supragranular, granular or infragranular layers for the calculation of layer indices. These indices provide a quantitative assessment of the laminar distribution of retrogradely labeled neurons and are instrumental in the classification of corticocortical feedback, feedforward and lateral connections (Felleman & Van Essen, 1991). Layer indices (L) were calculated using the contrast formula where S and I are the numbers of labeled neurons in supragranular and infragranular layers respectively (Budinger et al., 2006, 2008; Budinger & Scheich, 2009; Cappe & Barone, 2005):

$$L = ((S-I)) / ((S+I))$$

The indices range between -1 and 1. Negative values indicate feedback connections mostly originating in infragranular layers and positive values indicate feedforward connections mostly originating in supragranular layers. Values near zero indicate lateral

connections. All photomicrographs were cropped and luminosity and contrast were adjusted with Adobe Photoshop software.

Stereological sampling of laminar distribution of axonal swellings

In order to provide an unbiased size frequency distribution of axonal swellings in each cortical layer for the projection from V1 to the S1 barrel field and the reciprocal projection from the S1 barrel field to V1, a stereological systematic random sampling of these projection fields was performed using the Stereo Investigator software (MBF Bioscience).

Projection fields in which anterograde labeling was observed were sampled using the optical fractionator workflow (in Stereo Investigator) on approximately 10 equidistant sections covering the full anteroposterior range of the projection, except for the fourth intact case injected with BDA in V1 in which the projection extended to only 5 sections. On each section, polygonal contours were traced around the projection field in each cortical layer. Axonal swellings were then counted in no less than 100 square disectors of 20 μm side length and 15 μm height, evenly distributed at the intersections of an 80x80 μm sampling spacing grid. The maximum diameter was measured for each sampled swelling at higher magnification (100X, 1.4 NA objective).

This optical fractionator sampling strategy allowed for the estimation of the total number of swellings in each cortical layer. The total numbers of swellings (N) were

calculated by the following equation (West et al., 1991) where ΣQ is the total number of swellings counted within the disectors, ssf is the section sampling fraction (number of sampled sections over the total number of sections on which the terminal projection field appears), asf is the area sampling fraction (ratio of the frame area/the total area of the reference space on the section) and tsf is the thickness-sampling fraction (disector height/section thickness):

$$N = \Sigma Q \times ssf^{\wedge}(-1) \times asf^{\wedge}(-1) \times tsf^{\wedge}(-1)$$

Product of ssf, asf and tsf is the overall sampling faction (see Tables 12, 13, 14 and 15). Coefficients of error (CEs) were calculated according to the procedure described by West and Gundersen (1990), in order to determine whether the sampling effort was sufficient. It is widely accepted as a rule of thumb that CEs below 0.1 are indicative of a sufficient sampling. The main objective of this stereological sampling was not to determine the total number of swellings that are labeled for each injection, as this number is a function of the injection size, but to obtain unbiased estimates of laminar and size distributions.

Table 12

Stereological sampling parameters for the estimation of the number of anterogradely labeled axonal swellings in each layers in S1BF after injections of BDA into V1 of intact C57Bl/6 mice

Case	Layer	Number of sections	Total area (mm^2)	Number of dissectors	Number of objects	Sampling fraction	Total estimation	CE
1	I-III	9	8661	106	313	0.004	84662	0.060
	IV	9	5663	117	164	0.006	26279	0.053
	Va	9	3150	117	178	0.011	15865	0.065
	Vbc	9	5407	115	164	0.006	25527	0.050
	VI	9	3950	116	78	0.009	8793	0.097
	Total (Mean)	45	26831	571	897	(0.007)	161126	(0.065)
2	I-III	9	6593	112	329	0.005	64112	0.074
	IV	9	4580	111	118	0.007	16117	0.075
	Va	9	2257	128	139	0.017	8115	0.074
	Vbc	9	3969	119	129	0.009	14243	0.089
	VI	9	2050	111	80	0.016	4890	0.083
	Total (Mean)	45	19449	581	795	(0.011)	107477	(0.079)
3	I-III	9	17372	110	317	0.002	165717	0.075
	IV	9	11941	112	158	0.003	55764	0.052
	Va	9	6617	127	181	0.006	31218	0.060
	Vbc	9	10180	123	156	0.004	42739	0.051
	VI	9	10885	64	111	0.003	20776	0.063
	Total (Mean)	45	56995	536	923	(0.004)	316214	(0.060)
4	I-III	5	2507	106	174	0.013	13519	0.194
	IV	5	1521	105	72	0.021	3427	0.201
	Va	5	940	114	60	0.037	1626	0.192
	Vbc	5	1408	110	90	0.024	3786	0.147
	VI	5	1515	105	141	0.021	6685	0.167
	Total (Mean)	25	7891	540	537	(0.023)	29043	(0.180)
5	I-III	10	5745	118	97	0.006	17793	0.071
	IV	10	3005	105	38	0.009	4097	0.097
	Va	10	1821	120	63	0.018	3602	0.044
	Vbc	10	2506	115	42	0.012	3449	0.052
	VI	10	1398	112	40	0.021	1881	0.070
	Total (Mean)	50	14475	570	280	(0.013)	30822	(0.067)

Table 13

Stereological sampling parameters for the estimation of the number of anterogradely labeled axonal swellings in each layers in S1BF after injections of BDA into V1 of enucleated C57Bl/6 mice

Case	Layer	Number of sections	Total area (mm^2)	Number of dissectors	Number of objects	Sampling fraction	Total estimation	CE
IC-01	I-III	10	7596	111	106	0.009	23344	0.076
	IV	10	5712	117	100	0.010	15712	0.079
	Va	10	3582	119	99	0.010	9590	0.070
	Vbc	10	6726	114	119	0.008	22596	0.071
	VI	10	5632	113	74	0.014	11869	0.085
	Total (Mean)	50	29248	574	498	(0.010)	83111	(0.076)
IC-02	I-III	11	9185	125	103	0.010	27566	0.087
	IV	11	6728	123	40	0.025	7968	0.078
	Va	11	3230	142	45	0.022	3729	0.093
	Vbc	11	5141	138	70	0.014	9483	0.078
	VI	11	6582	119	99	0.010	19945	0.089
	Total (Mean)	55	30866	647	357	(0.016)	68691	(0.085)
IC-03	I-III	10	1382	144	167	0.006	5161	0.063
	IV	10	1534	139	85	0.012	3020	0.081
	Va	10	1020	133	119	0.008	2937	0.068
	Vbc	10	1922	125	73	0.014	3613	0.102
	VI	10	2375	122	134	0.008	8395	0.106
	Total (Mean)	50	8233	663	578	(0.010)	23126	(0.084)
IC-04	I-III	10	10264	109	232	0.004	70308	0.046
	IV	10	4180	135	233	0.004	23213	0.045
	Va	10	2840	143	233	0.004	14896	0.036
	Vbc	10	5188	127	220	0.005	28920	0.053
	VI	10	6240	114	229	0.004	40346	0.048
	Total (Mean)	50	28712	628	1147	(0.004)	177683	(0.046)
IC-05	I-III	10	1615	106	247	0.004	13688	0.042
	IV	10	780	123	148	0.007	3432	0.055
	Va	10	472	130	123	0.008	1597	0.059
	Vbc	10	611	121	87	0.012	1580	0.071
	VI	10	577	119	46	0.022	801	0.077
	Total (Mean)	50	4055	599	651	(0.011)	21098	(0.061)

Table 14

Stereological sampling parameters for the estimation of the number of anterogradely labeled axonal swellings in each layers in V1 after injections of BDA into S1BF of intact C57Bl/6 mice

Case	Layer	Number of sections	Total area (mm^2)	Number of dissectors	Number of objects	Sampling fraction	Total estimation	CE
1	I-III	11	9174	124	201	0.004	53794	0.089
	IV	11	6717	122	80	0.005	15935	0.078
	Va	11	3229	141	85	0.012	7043	0.098
	Vbc	11	5130	137	137	0.007	18558	0.085
	VI	11	6571	118	194	0.005	39083	0.090
	Total (Mean)	55	30821	642	697	(0.007)	134413	(0.088)
2	I-III	10	1604	105	488	0.018	27043	0.043
	IV	10	779	122	291	0.043	6747	0.056
	Va	10	461	129	241	0.077	3129	0.059
	Vbc	10	600	120	169	0.055	3070	0.072
	VI	10	566	118	89	0.058	1549	0.082
	Total (Mean)	50	4010	594	1278	(0.050)	41538	(0.062)
3	I-III	10	1380	108	209	0.022	9692	0.061
	IV	10	578	119	153	0.057	2696	0.050
	Va	10	461	124	146	0.074	1971	0.061
	Vbc	10	649	128	128	0.054	2355	0.057
	VI	10	607	153	91	0.070	1310	0.059
	Total (Mean)	50	3675	632	727	(0.055)	18024	(0.058)
4	I-III	7	3414	111	254	0.010	25597	0.080
	IV	7	1343	133	106	0.030	3508	0.092
	Va	7	819	115	90	0.043	2102	0.099
	Vbc	7	1317	105	65	0.024	2671	0.094
	VI	7	1295	124	64	0.029	2190	0.093
	Total (Mean)	35	8188	588	579	(0.027)	36068	(0.092)
5	I-III	8	1493	121	152	0.025	6192	0.052
	IV	8	709	139	82	0.059	1381	0.040
	Va	8	403	158	56	0.119	472	0.068
	Vbc	8	710	138	52	0.059	883	0.069
	VI	8	678	134	50	0.060	835	0.026
	Total (Mean)	40	3993	690	392	(0.064)	9763	(0.051)

Table 15

Stereological sampling parameters for the estimation of the number of anterogradely labeled axonal swellings in each layers in V1 after injections of BDA into S1BF of enucleated C57Bl/6 mice

Case	Layer	Number of sections	Total area (mm^2)	Number of dissectors	Number of objects	Sampling fraction	Total estimation	CE
IC-06	I-III	10	3284	116	36	0.028	3697	0.060
	IV	10	1448	130	32	0.031	1293	0.054
	Va	10	982	142	26	0.039	652	0.057
	Vbc	10	1471	125	26	0.039	1110	0.080
	VI	10	1875	116	18	0.056	1056	0.052
	Total (Mean)	50	9060	629	138	(0.039)	7808	(0.061)
IC-07	I-III	10	8722	123	59	0.017	15177	0.069
	IV	10	3326	135	52	0.019	4647	0.073
	Va	10	1919	139	39	0.026	1954	0.083
	Vbc	10	3572	123	46	0.022	4846	0.085
	VI	10	3974	127	49	0.020	5562	0.058
	Total (Mean)	50	21513	647	245	(0.021)	32186	(0.074)
IC-08	I-III	10	1391	109	21	0.048	974	0.067
	IV	10	589	120	14	0.071	247	0.083
	Va	10	472	125	15	0.067	203	0.072
	Vbc	10	650	129	14	0.071	258	0.098
	VI	10	618	154	9	0.111	130	0.094
	Total (Mean)	50	3720	637	73	(0.074)	1812	(0.083)
IC-09	I-III	10	4451	112	66	0.015	9516	0.056
	IV	10	1901	124	54	0.019	3003	0.056
	Va	10	1017	145	65	0.015	1654	0.047
	Vbc	10	2090	111	65	0.015	4440	0.042
	VI	10	1017	118	57	0.018	1782	0.063
	Total (Mean)	50	10476	610	307	(0.016)	20395	(0.053)
IC-10	I-III	8	3102	110	47	0.021	4879	0.087
	IV	8	1242	128	42	0.024	1501	0.067
	Va	8	733	127	33	0.030	701	0.102
	Vbc	8	1249	129	35	0.029	1247	0.082
	VI	8	1429	122	26	0.038	1121	0.123
	Total (Mean)	40	7755	616	183	0.028	9449	0.092

Sampling of axonal diameters

In order to compare the caliber of the axonal population entering the cortical areas V1 and the somatosensory barrel field between the intact and enucleated at birth cases, the initial diameter of the axons as they leave the white matter to enter the cortical grey layers of the target was calculated. Axonal diameter changes over short distances and a single point measurement of the axonal diameter was not deemed adequate. To take this into account and to obtain an unbiased estimate of the axons diameters, a weighted average of diameter for the initial 25 μm of each axon was calculated.

The Neurolucida software encodes reconstructions of traced axons as a succession of small segments. Each segment is attributed coordinates in three-dimensional space, a length and a diameter. These segments correspond to the interval between two mouse clicks as the observer traces the axons. These clicks were done to record changes in direction and/or diameter of the axons. The data were used to calculate the average diameter over the first 25 μm of the tracing from the point of entry of the axons into the cortical grey matter, weighted by the length of the segments recorded over this distance.

The sampling of the measured axons was performed on the same sections that were used for the stereological sampling of axonal swellings (see Table 12) to ensure that axons were systematically and randomly selected. Axons were selected as they crossed the line between the white and grey matter. The total length of this line for each case and the number of sampled sections are given in Table 16.

Table 16

Sampling parameters for the estimation of the diameter of anterogradely labeled axons as they enter the gray matter in S1BF and V1 after injections of BDA into V1 and S1BF respectively of intact and enucleated at birth C57Bl/6 mice

Injection site	Group	Case	Number of sections	Sampled length (mm)	Number of axons
V1	Intact	1	9	13.281	259
		2	9	12.215	116
		3	9	14.372	104
		4	5	6.567	195
		5	10	13.967	132
V1	Enucleated	1	10	18.845	213
		2	11	11.763	117
		3	10	17.524	52
		4	10	14.467	326
		5	10	8.171	48
S1BF	Intact	1	11	11.532	134
		2	10	6.016	38
		3	10	5.373	154
		4	7	6.215	84
		5	8	6.143	310
S1BF	Enucleated	1	10	13.135	25
		2	10	13.314	83
		3	10	10.489	3
		4	10	15.750	42
		5	8	8.312	19

Statistical analysis

Statistical analyses were performed using SPSS v 16.0 software (SPSS, Chicago, IL, USA). To test for significance of the differences in the relative abundance of labeled neurons in each cortical area between intact and enucleated cases, Wilcoxon and Tukey HSD tests were performed with a significance level of $p < 0.05$. To test for significance of the differences in the layer indices in each cortical area between intact and enucleated cases, Kruskal-Wallis and Tukey HSD tests were performed with a significance level of $p < 0.05$. To test for significance of the differences in the size distribution of the diameters, Kolmogorov-Smirnov analyses were performed.

Results

Labeling of cortical visuotactile connections with CTb

Representative CTb injections sites in the visual cortex of intact (see Figure 28A) and enucleated mice (see Figure 28C), and in the somatosensory barrel field in intact (see Figure 29A) and enucleated mice (see Figure 29C) show that in all the intact cases, CTb injections in V1 anterogradely labeled axonal terminals and retrogradely labeled numerous neuronal cell bodies in S1 (see Figure 28B). Conversely, CTb injections in V1 of the enucleated cases resulted in very few labeled neurons in S1 (see Figure 28D). CTb injections in S1BF produced similar anterograde and retrograde labeling in V1 of intact and enucleated cases (see Figures 29B and 29D respectively).

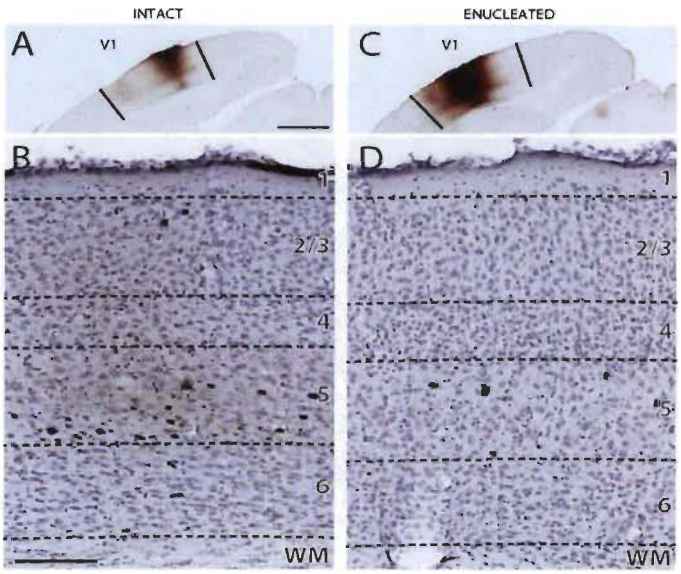

Figure 28. A: An injection of CTb in V1 of intact C57Bl/6 mice produced in B: Anterograde and retrograde labeling in S1BF. C: An injection of CTb in V1 of enucleated C57Bl/6 mice produced in D: Anterograde and retrograde labeling in S1BF. Scales: 1000 μm (A/C) and 200 μm (B/D).

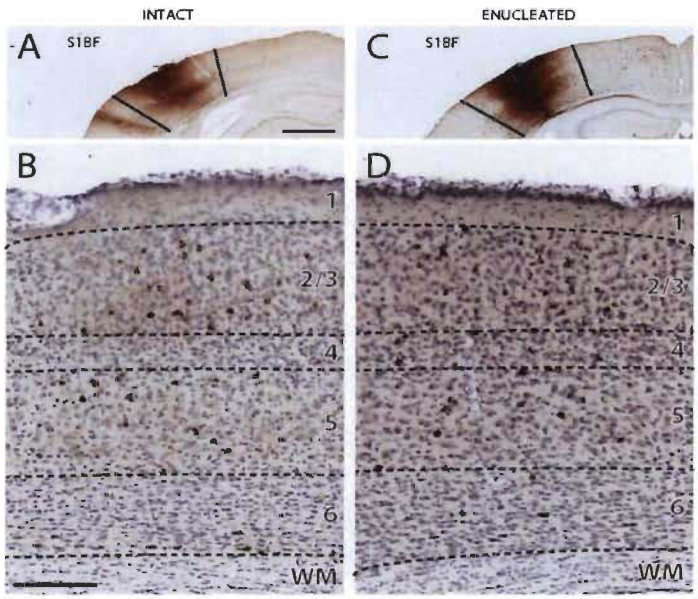

Figure 29. A: An injection of CTb in S1BF of intact C57Bl/6 mice produced in B: Anterograde and retrograde labeling in V1. C: An injection of CTb in S1BF of enucleated C57Bl/6 mice produced in D: Anterograde and retrograde labeling in V1. Scales: 1000 μm (A/C) and 200 μm (B/D).

CTb injections in V1 and S1BF labeled numerous neurons in the primary and secondary somatosensory, motor and visual cortices. None of the injections damaged the underlying white matter. All the observed retrogradely labeled neurons were plotted in S1, S1BF, V2M and V2L following CTb injections in V1 and were plotted in M1, M2, S2 and V1 following CTb injections in S1BF. Quantifications of labeled neurons were performed in V2M, V2L, M1, M2 and S2 in order to compare the projections between V1 and S1 as a ratio of the number of labeled neurons in these areas over the total number of labeled neurons rather than absolute numbers of neurons which are directly related to the differences in injection size.

Even though the number of labeled neurons varied between cases, and is dependent upon the injection size, all injections were performed with the same parameters and a comparison of the percentage of labeled neurons is instructive of the strength of the projections. Quantifications for all cases are detailed for the intact and enucleated cases in Table 17 and a comparison of the percentage of retrogradely labeled neurons in cortical areas is illustrated in Figure 30A. There were statistically significant differences in the percentage of labeled neurons observed in S1 (Wilcoxon, $p = 0.032$) and V2M (Wilcoxon, $p = 0.016$) between the intact and enucleated cases following injections in V1. Conversely, CTb injections in S1BF resulted in no statistically significant differences in the percentage of labeled neurons in V1.

Significant differences in the percentage of labeled neurons in cortical layers were observed between the intact and enucleated cases following injections in V1 (see Figure 30B). A greater proportion of labeled neurons was found in layers 1 to 3 of S1 in the intact cases compared to the enucleated cases (Wilcoxon, $p = 0.032$). Significant differences in the percentage of labeled neurons in cortical layers were also observed between the intact and enucleated cases following injections in S1BF (see Figure 30C). A lesser proportion of labeled neurons was found in layer V of S2 in the intact cases compared to the enucleated cases (Wilcoxon, $p = 0.008$).

Table 17

Number and percentage (in parentheses) of retrogradely labeled neurons in neocortical areas after injections of CTb into the primary visual cortex (V1) and the primary somatosensory cortex (S1) of intact and enucleated C57Bl/6 mice

Injection site	Case	Cortical area			
		S1	S1BF	V2M	V2L
V1 Intact	CT9	85 (4.43)	164 (8.55)	448 (23.35)	1222 (63.68)
	CT20	16 (1.59)	10 (1.00)	183 (18.23)	795 (79.18)
	CT25	15 (1.87)	56 (6.97)	93 (11.58)	639 (79.58)
	CT26	39 (10.74)	112 (30.85)	45 (12.40)	167 (46.01)
	CT31	28 (3.14)	62 (6.94)	181 (20.67)	622 (69.65)
	Mean ± SEM	36.60 ± 14.39	80.80 ± 29.45	190.00 ± 77.91	689.00 ± 189.54
		(4.35 ± 1.87)	(10.86 ± 5.77)	(17.16 ± 2.54)	(67.62 ± 6.91)
V1 Enu	CT52	5 (0.52)	9 (0.94)	272 (28.42)	671 (70.12)
	CT53	5 (0.79)	2 (0.32)	143 (22.59)	483 (76.30)
	CT54	21 (1.14)	18 (0.98)	507 (27.63)	1289 (70.25)
	CT55	6 (0.76)	14 (1.77)	227 (28.63)	546 (68.85)
	CT57	28 (2.60)	12 (1.11)	333 (30.92)	704 (65.37)
	Mean ± SEM	13.00 ± 5.40	11.00 ± 3.00	296.40 ± 68.30	738.60 ± 160.30
		(1.16 ± 0.42)	(1.02 ± 0.26)	(27.64 ± 1.54)	(70.18 ± 1.98)

Table 17

Number and percentage (in parentheses) of retrogradely labeled neurons in neocortical areas after injections of CTb into the primary visual cortex (V1) and the primary somatosensory cortex (S1) of intact and enucleated C57Bl/6 mice (continued)

Injection site	Case	Cortical area			
		M1	M2	S2	V1
S1 Intact	03-02b7	148 (11.23)	209 (15.86)	415 (31.49)	546 (41.43)
	04-01b2	726 (37.10)	573 (29.28)	582 (29.74)	76 (3.88)
	03-02b4	800 (24.17)	1510 (45.62)	600 (18.13)	400 (12.09)
	03-02b5	929 (26.84)	1197 (34.59)	1181 (34.12)	154 (4.45)
	03-02b6	450 (23.40)	323 (16.80)	1117 (58.09)	33 (1.72)
	Mean ± SEM	610.60 ± 156.20 (24.55 ± 4.62)	762.40 ± 283.17 (28.43 ± 6.26)	779.00 ± 173.06 (34.31 ± 7.32)	241.80 ± 110.78 (12.71 ± 8.26)
S1 Enu	1	313 (25.93)	574 (47.56)	243 (20.13)	77 (6.38)
	2	124 (11.05)	339 (30.21)	381 (33.96)	278 (24.78)
	3	328 (26.95)	617 (50.70)	220 (18.08)	52 (4.27)
	4	158 (11.41)	600 (43.32)	387 (27.94)	240 (17.33)
	5	115 (9.02)	535 (41.96)	409 (32.08)	216 (16.94)
	Mean ± SEM	207.60 ± 52.22 (16.87 ± 4.40)	533.00 ± 56.38 (42.75 ± 3.91)	328.00 ± 44.54 (26.44 ± 3.54)	172.60 ± 50.76 (13.94 ± 4.25)

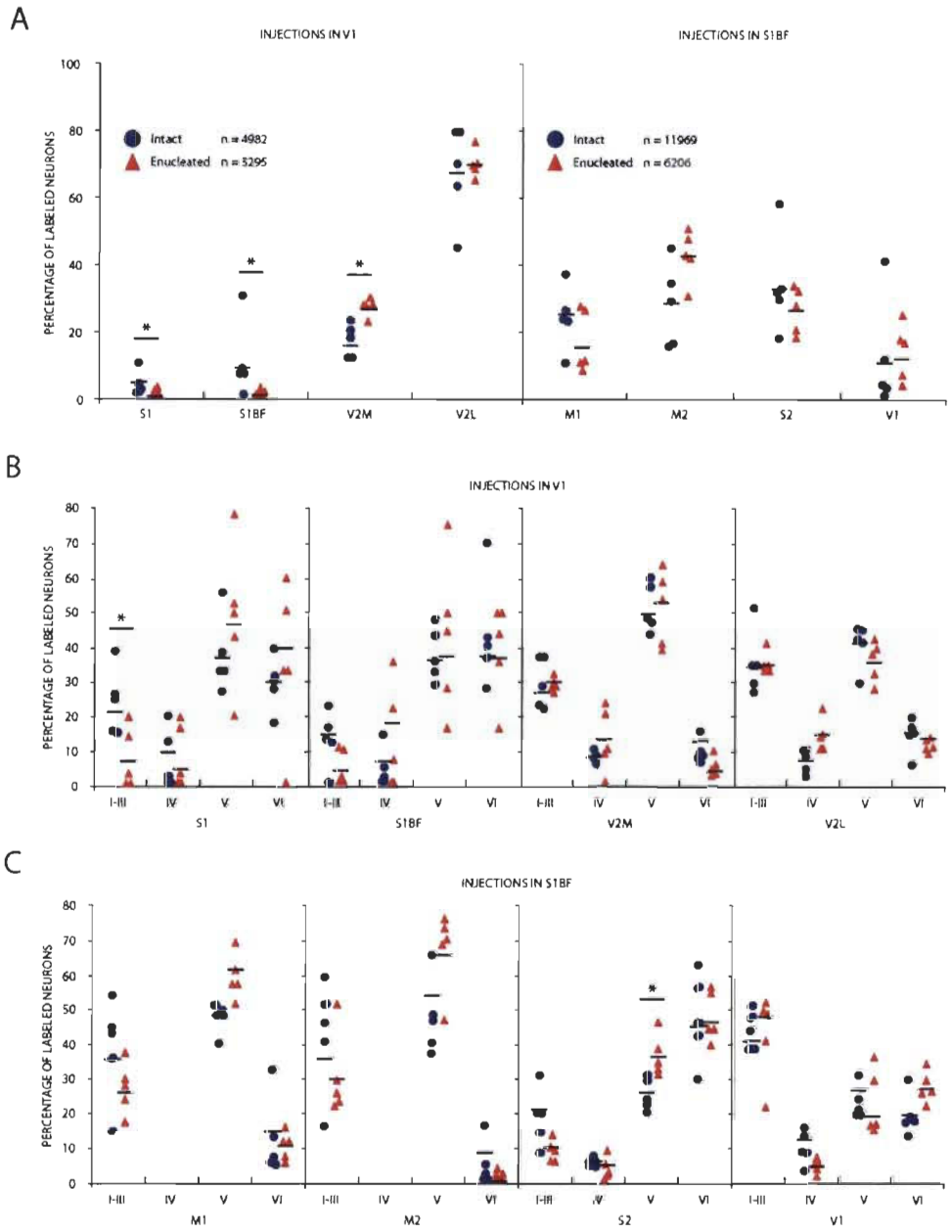

Figure 30. A: Percentage of retrogradely labeled neurons in cortical areas following an injection of CTb in V1 and S1BF. Percentage of retrogradely labeled neurons in each cortical layer following an injection of CTb in V1 (B) and in S1BF (C).

Laminar distribution of Cholera toxin b labeled neurons

Layer indices are summarized for the intact and enucleated cases in Table 18, and illustrated in Figure 31. Following CTb injections in V1 of the intact and the enucleated cases, there were more labeled neurons in infragranular than in supragranular layers of S1, S1BF, V2M and V2L. Hence, layer indices were negative in the majority of the cases, indicating the structure of a feedback projection to V1 from S1, S1BF, V2M and V2L. There was a statistically significant difference in the layer indices of S1 between intact and enucleated cases (Kruskal-Wallis, $p = 0.032$).

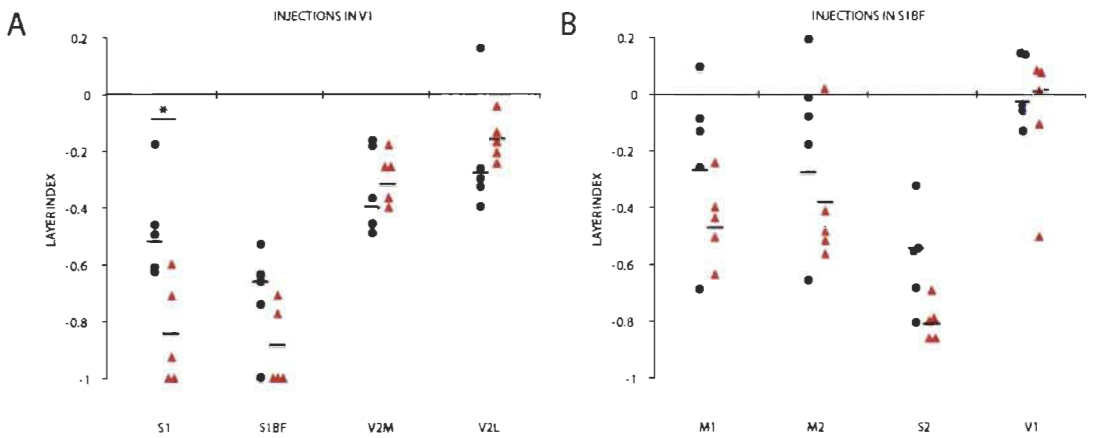

Figure 31. Layer indices for neocortical areas following an injection of CTb in V1 and S1BF.

CTb injections in S1BF of the intact and the enucleated cases labeled more neurons in infragranular than in supragranular layers of M1, M2 and S2. Hence, layer indices were negative in the majority of the cases, suggestive of feedback projections to S1BF from M1, M2 and S2. There were labeled neurons in similar proportion in supra- and

infragranular layers in V1 and, in all cases except one, layer indices were near zero, indicating a lateral type of connection between two areas of similar hierarchical levels within the cortical network.

Table 18

Numbers of retrogradely labeled neurons in layers I-III/IV/V/VI and layer indices (below) in neocortical areas after injections of CTb into the primary visual cortex (V1) and the primary somatosensory cortex (S1) of intact and enucleated C57Bl/6 mice

Injection site	Case	Cortical area			
		S1	S1BF	V2M	V2L
V1	CT9	14 / 11 / 33 / 27 -0.62	23 / 25 / 55 / 61 -0.67	106 / 50 / 219 / 73 -0.47	338 / 113 / 555 / 216 -0.39
Intact	CT20	4 / 0 / 9 / 3 -0.5	0 / 0 / 3 / 7 -1.00	42 / 14 / 111 / 16 -0.50	239 / 90 / 339 / 127 -0.32
	CT25	4 / 0 / 5 / 6 -0.47	13 / 0 / 27 / 16 -0.54	35 / 8 / 41 / 9 -0.18	333 / 67 / 195 / 44 0.16
	CT26	6 / 8 / 13 / 12 -0.61	19 / 6 / 41 / 46 -0.64	13 / 3 / 26 / 3 -0.38	57 / 5 / 70 / 35 -0.30
	CT31	11 / 1 / 8 / 8 -0.19	8 / 0 / 27 / 27 -0.74	67 / 14 / 86 / 14 -0.20	218 / 32 / 278 / 94 -0.26
	Mean Sup/Inf ± SEM	8 ± 2/25 ± 10 -0.52 ± 0.09	13 ± 5/62 ± 21 -0.66 ± 0.09	53 ± 18/120 ± 52 -0.39 ± 0.08	237 ± 57/391 ± 127 -0.25 ± 0.11
V1	CT52	1 / 0 / 1 / 3 -0.60	1 / 0 / 4 / 4 -0.78	83 / 66 / 110 / 13 -0.19	223 / 156 / 193 / 99 -0.13
Enu	CT53	0 / 1 / 4 / 0 -1.00	0 / 0 / 1 / 1 -1.00	41 / 31 / 57 / 14 -0.27	200 / 67 / 158 / 58 -0.04
	CT54	3 / 0 / 11 / 7 -0.71	2 / 4 / 3 / 9 -0.71	165 / 57 / 271 / 14 -0.27	461 / 191 / 495 / 142 -0.16
	CT55	0 / 1 / 3 / 2 -1.00	0 / 5 / 4 / 5 -1.00	67 / 2 / 145 / 13 -0.40	195 / 58 / 219 / 74 -0.20
	CT57	1 / 1 / 12 / 14 -0.93	0 / 1 / 9 / 2 -1.00	93 / 32 / 196 / 12 -0.38	238 / 80 / 296 /90 -0.24
	Mean Sup/Inf ± SEM	1 ± 1/11 ± 5 -0.84 ± 0.09	1 ± 0/8 ± 3 -0.87 ± 0.07	90 ± 23/169 ± 41 -0.31 ± 0.04	263 ± 56/365 ± 83 -0.16 ± 0.04

Table 18

Numbers of retrogradely labeled neurons in layers I-III/IV/V/VI and layer indices (below) in neocortical areas after injections of CTb into the primary visual cortex (V1) and the primary somatosensory cortex (S1) of intact and enucleated C57Bl/6 mice (continued)

Injection site	Case	Cortical area			
		M1	M2	S2	V1
S1	03-02b7	81 / 0 / 58 / 9 0.10	103 / 0 / 104 / 2 -0.01	38 / 26 / 87 / 264 -0.81	216 / 94 / 137 / 99 -0.04
Intact	04-01b2	332 / 0 / 348 / 46 -0.09	340 / 0 / 221 / 12 0.19	122 / 47 / 142 / 271 -0.54	34 / 3 / 16 / 23 -0.07
	03-02b4	127 / 0 / 404 / 269 -0.68	259 / 0 / 990 / 261 -0.66	124 / 40 / 179 / 257 -0.56	157 / 40 / 127 / 76 -0.13
	03-02b5	405 / 0 / 451 / 73 -0.13	551 / 0 / 573 / 73 -0.08	373 / 75 / 368 / 365 -0.33	79 / 15 / 32 / 28 0.14
	03-02b6	167 / 0 / 221 / 62 -0.26	133 / 0 / 178 / 12 -0.18	169 / 60 / 257 / 631 -0.68	16 / 5 / 7 / 5 0.14
	Mean Sup/Inf ± SEM	222 ± 70/388 ± 120 -0.27 ± 0.15	277 ± 90/485 ± 239 -0.27 ± 0.16	165 ± 63/564 ± 134 -0.55 ± 0.09	100 ± 42/110 ± 51 -0.05 ± 0.06
S1	1	58 / 0 / 217 / 38 -0.63	128 / 0 / 440 / 6 -0.55	17 / 5 / 84 / 137 -0.86	32 / 5 / 23 / 17 -0.11
Enu	2	31 / 0 / 73 / 20 -0.50	88 / 0 / 240 / 11 -0.48	40 / 8 / 180 / 153 -0.79	144 / 13 / 48 / 73 0.09
	3	94 / 0 / 194 / 40 -0.43	151 / 0 / 452 / 14 -0.51	15 / 8 / 75 / 122 -0.86	12 / 3 / 19 / 18 -0.51
	4	47 / 0 / 101 / 10 -0.41	178 / 0 / 415 / 7 -0.41	53 / 38 / 123 / 173 -0.70	119 / 6 / 42 / 73 0.02
	5	44 / 0 / 62 / 9 -0.24	275 / 0 / 256 / 4 0.28	39 / 25 / 161 / 184 -0.80	108 / 16 / 34 / 58 0.08
	Mean Sup/Inf ± SEM	55 ± 12/153 ± 43 -0.47 ± 0.07	164 ± 35/369 ± 54 -0.39 ± 0.12	33 ± 8/278 ± 36 -0.79 ± 0.03	83 ± 29/81 ± 20 0.01 ± 0.13

Laminar distribution of axonal swellings

An injection of BDA in V1 of intact and enucleated mice produced anterograde labeling of axons in S1, largely restricted to the barrelfield in each of the 10 cases. Labeled axons were found in infra- and supragranular layers of S1BF. Axonal terminal labeling was most intense in the supragranular layers. Labeling was similar in both the intact and enucleated cases, except that labeling in layer 1 was much more pronounced in the enucleated group. Quite large swellings were observed in S1BF of intact (see Figure 32A) but not in the enucleated mice (see Figure 32B).

An injection of BDA in S1BF of intact and enucleated mice produced anterograde labeling of axons in infra- and supragranular layers of V1 in the intact group and to a lesser extent in the enucleated group. Labeled terminals were most evident in layers 1 to 3, with a greater density in the lower part of layer 2 in the intact group and in the superior part of layer 2 in the enucleated group. In both intact (see Figure 32C) and in enucleated mice (see Figure 32D) only quite small swellings were observed. None of the injections damaged the underlying white matter.

The injections of BDA in both V1 and S1BF of intact and enucleated mice resulted in anterograde axonal labeling in S1BF and V1 respectively, without signs of retrograde transport. In order to compare the labeling of axonal terminals in intact and enucleated cases, stereological estimates were performed of the laminar distribution of axonal

swellings in S1BF and V1 (see Figures 33A and 33B respectively) following an injection of BDA in V1 and S1BF respectively.

There were no significant differences in the laminar distribution of axonal swellings in S1BF and V1 between the intact and enucleated cases. The stereologically estimated numbers of anterogradely labeled axonal swellings in each layers of S1 are given in Table 12 and 13 for the intact and enucleated C57Bl/6 mice respectively and the numbers of anterogradely labeled axonal swellings in each layers of V1 are shown in Table 14 and 15 for the intact and enucleated C57Bl/6 mice respectively.

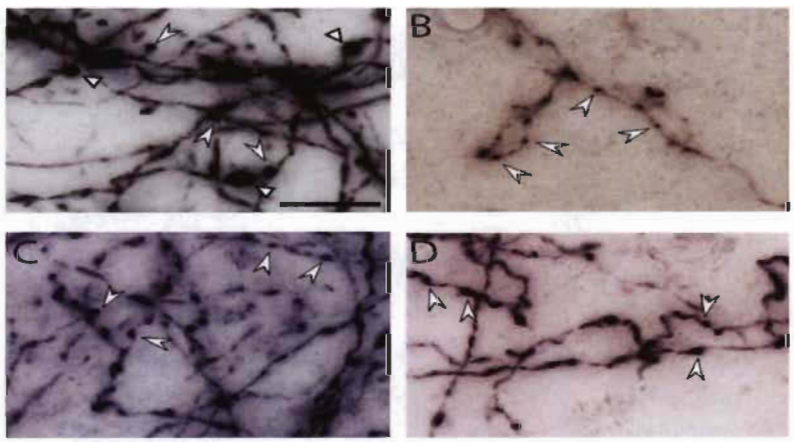

Figure 32. High power photomicrographs of swellings in S1BF of intact and enucleated mice (A and B resp). High power photomicrographs of swellings in V1 of intact and enucleated mice (C and D resp). Black arrows point larger axonal swellings and white arrows point smaller swellings. Scales: 25 μm.

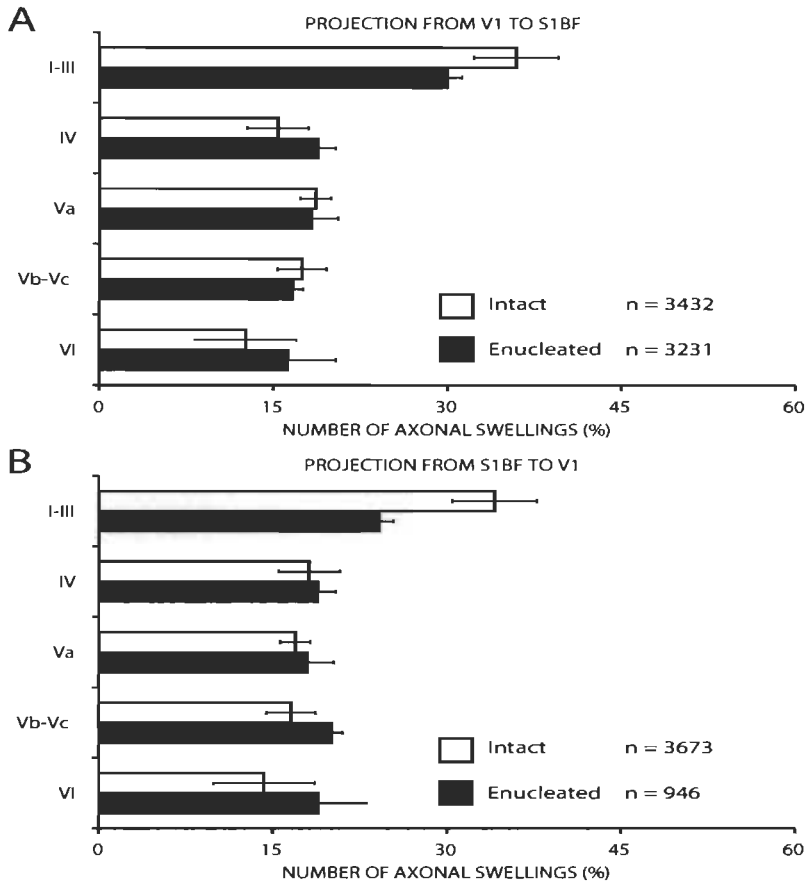

Figure 33. Laminar distribution of the number of axonal swellings in S1BF (A) and V1 (B) following and injection of BDA in V1 and S1BF respectively of intact and enucleated mice. *n* = number of counted swellings.

Size distribution of axonal swellings in cortical layers

The size distribution of axonal swellings counted with the systematic stereological sampling was compared between the intact and enucleated groups for each cortical layers for the projection from V1 to S1BF (see Figure 34 A-B) and from S1BF to V1 (see Figure 34C-D). The size of the axonal swellings ranged between 0.3 μm and 2 μm for the intact cases in the projection from V1 to S1BF and between 0.2 μm and 1.3 μm for the enucleated cases. The axonal swellings in S1BF of the intact group were larger

than in the enucleated group in layers 1 to 3 (Kolmogorov-Smirnov tests, $p < 0.001$), layer 4 (Kolmogorov-Smirnov tests, $p < 0.001$), layer 5a (Kolmogorov-Smirnov tests, $p < 0.001$), layers 5b and 5c (Kolmogorov-Smirnov tests, $p < 0.001$) and layer 6 (Kolmogorov-Smirnov tests, $p = 0.001$) (see Figure 34B). The size of the axonal swellings ranged between 0.3 µm and 0.9 µm for the intact cases in the projection from S1BF to V1 and between 0.1 µm and 1.4 µm for the enucleated cases. The axonal swellings in V1 of the intact group were smaller than in the enucleated group in layers 1 to 3 (Kolmogorov-Smirnov tests, $p = 0.014$) and layer 4 (Kolmogorov-Smirnov tests, $p = 0.036$) (see Figure 34D).

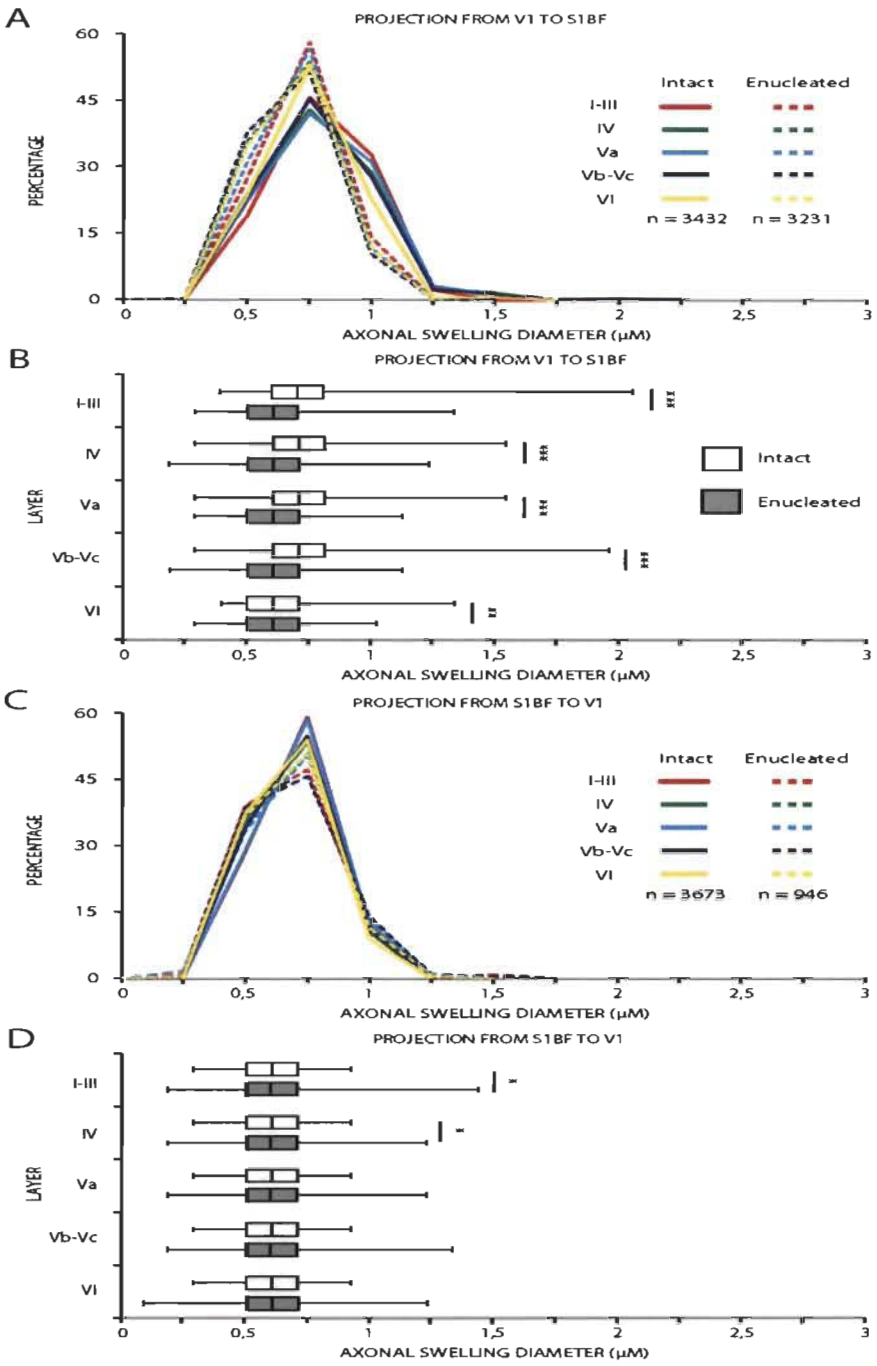

Figure 34. Size distribution (A and C) and box plot representation (B and D) of axonal swelling size in S1BF (A and B) and V1 (C and D) following injections of BDA in V1 and S1BF respectively of intact and enucleated mice. The box plots depict the minimum and maximum values, the upper (Q3) and lower (Q1) quartiles and the median.

Axonal thickness

The size distribution of the diameters of randomly sampled axons (see Table 16) as they enter the grey matter was compared between the intact and enucleated cases for the projection from V1 to S1BF (see Figure 35 A-C) and from S1BF to V1 (see Figure 34 B-C). Axon thickness ranged between 0.1 and 1.9 for the intact cases in the projection from V1 to S1BF and between 0.1 and 1.2 for the enucleated cases. The axons in S1BF of the intact group were larger than in the enucleated group (Kolmogorov-Smirnov tests, $p < 0.001$) (see Figure 35C). Axon thickness ranged between 0.1 and 0.5 for the intact cases in the projection from S1BF to V1 and between 0.1 and 0.7 for the enucleated cases. The axons in V1 of the intact group were not significantly different than in the enucleated group (see Figure 35C).

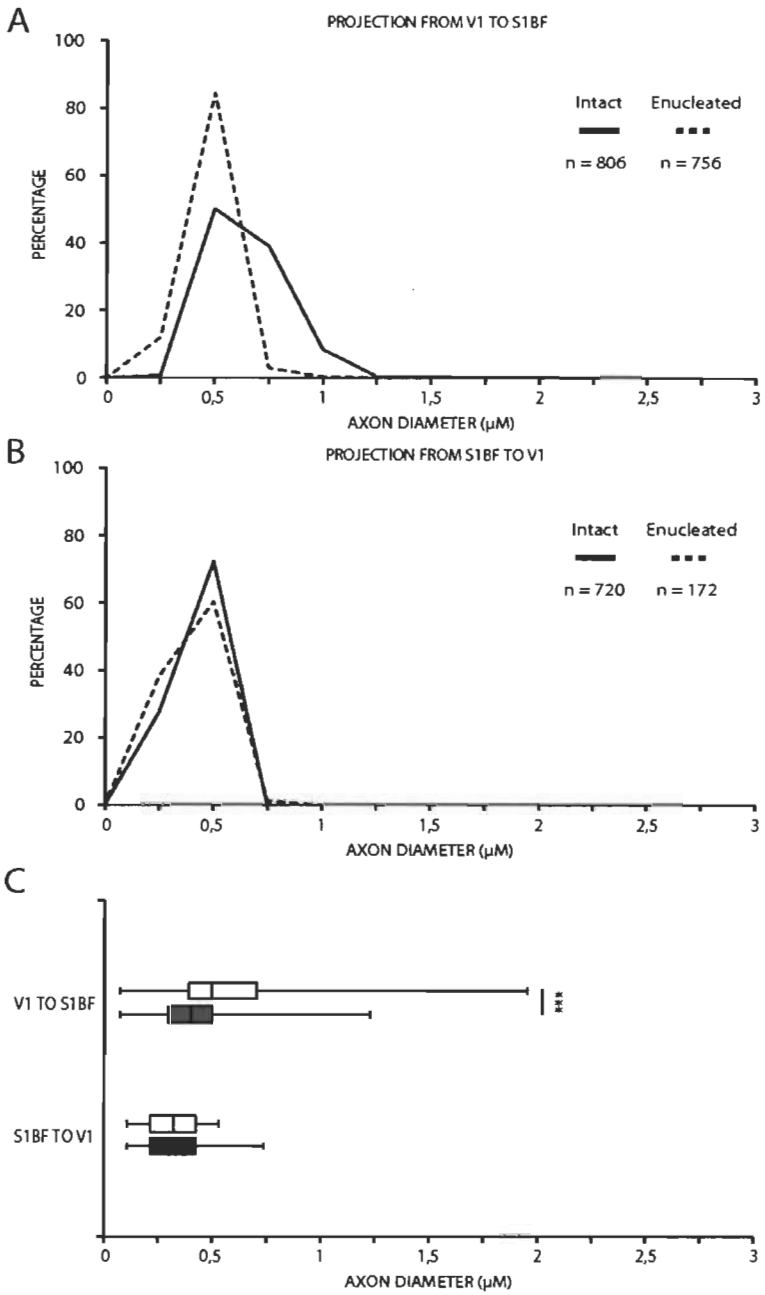

Figure 35. Size distribution (A and B) and box plot representation (C) of the diameters of randomly sampled axons as they enter the gray matter in S1BF (A and C) and V1 (B and C) following an injection of BDA in V1 and S1BF respectively of intact and enucleated mice.

Discussion

The effects of enucleation on V1 afferent projections

Visual pathways are generally affected by loss of sight. Bilateral enucleation results in a significant reduction of the size of DLG and/or V1 in the opossum (Karlen & Krubitzer, 2009), mouse (Heumann & Rabinowicz, 1980; Massé et al., 2014), rat (Heumann & Rabinowicz, 1980), cat (Berman, 1991), and monkey (Dehay et al., 1989, 1996; Rakic, 1988; Rakic et al., 1991). Moreover, visual input and spontaneous retinal activity play important roles in the determination of cortical areas and their connectivity (see Pallas, 2001 for review). Our results show that enucleation reduces the strength of somatosensory projections to the visual cortex, but has no effect on the strength of visual projections to the somatosensory cortex. This reduction in the number of projecting neurons was previously demonstrated in the enucleated mice (Charbonneau et al., 2012), but our study provides a comparison between the number of projecting neurons found inside the barrel field, inside the rest of S1 and inside the secondary somatosensory cortex instead of considering the whole somatosensory cortex as a single group. Long term visual deprivation would decrease the somatosensory afferents to the deprived visual cortex. Similarly, short transient reduction of somatosensory activity by the trimming of whiskers in the first five days after birth also significantly reduced the direct projection of the visual cortex to the somatosensory cortex cross-modal synchrony in S1 in adult rats (Sieben et al., 2015). Previous studies have also demonstrated a decreased functional connectivity between the visual cortex and the somatosensory cortex as well as between the motor cortex and the temporal multisensory areas in blind humans (Liu et

al., 2007; Yu et al., 2008). This reduction in connectivity following visual deprivation could be specific to the somatosensory modality, since the number of neurons projecting from the primary auditory cortex to V1 was not altered by early enucleation in mice (Charbonneau et al., 2012). Moreover there are no major changes in cross-modal connectivity patterns in deaf cats and ferrets (see Meredith & Lomber, 2016 for review). Conversely, a transient visual deprivation in early life in humans, results in auditory activation of the visual cortex, and this activation was interpreted as resulting from maintained exuberant cross-modal corticocortical projections that would otherwise be pruned out by normal visual activity during development (Collignon et al., 2015).

However, even though there is a reduction in the projection from S1 to V1 in the visually deprived mice, there is evidence for cross-modal activation of the visual cortex by tactile inputs in mice following binocular enucleation at birth (Nys et al. in prep) and following monocular enucleation in adult mice (Nys et al., 2014, 2015; Van Brussel et al., 2011) and many examples of cross-modal activation of the visual cortex in blind humans (see Bavelier & Neville, 2002; Merabet & Pascual-Leone, 2010 for review). These activations in mice would therefore be produced by a diminished projection from the somatosensory cortex in the chronically blind mice. The absence of tactile activity in the visual cortex in intact mice would be explained by the overwhelming predominance of visual input from the intact visual pathways. There are many examples of cross-modal activity in intact visual cortex. This activity can be conveyed to the visual cortex by the already present projections between primary sensory cortices that are quite strong in

rodents, or by descending projections for multisensory association cortices (see Meredith & Lomber, 2016 for review). Similarly, blind individuals are more efficient than sighted individuals in tactile discrimination tasks by having a better spatial resolution for detecting tactile stimuli (Van Boven et al., 2000) and by detecting more easily vibrotactile stimuli (Wan et al., 2010) and these abilities could be related to amplified feedback projections from the multisensory associative areas to V1 (Fujii et al., 2009). Our result could suggest that amplification of these pathways might not be the substrate for these enhanced functional capabilities.

Our results show that visual deprivation could affect the development of the feedback projections from different extrastriate cortical areas in mice. Indeed, there was a reduced number of labeled neurons in V2M, whereas the number of labeled neurons was not changed in V2L in the enucleated mice. Similar observations were obtained in humans showing that the development of visual areas depend differently on visual experience. More specifically, early visual areas are more dependent on normal visual experience than higher level cortical areas and that ventral stream visual areas depend more on normal visual input than the dorsal stream areas, these differences arising from differences in connectivity patterns (Qin et al., 2013). The mouse visual cortex also comprises several functionally distinct extrastriate visual areas (Olavarria et al., 1982; Olavarria & Montero, 1989; Wang & Burkhalter, 2007). Moreover these areas have distinct connectivity patterns (Wang et al., 2011, 2012) and functional properties suggesting similar dorsal and ventral streams of processing (Andermann et al., 2011;

Glickfeld et al., 2013, 2014; Marshel et al., 2011; Matsui & Ohki, 2013). In the mouse, the medial/anterior extrastriate areas have similar connectivity patterns to dorsal stream areas in primates and lateral areas to ventral stream areas (Wang et al., 2012). Our present results suggest that in mice, the medial/dorsal stream areas might be more dependent on normal visual input for their development than in humans, and might reveal network structure differences between rodents and primates.

Our results also show that the strength of the projection of the visual cortex to the somatosensory cortex is not altered by early enucleation. There are only a few studies showing the effects of altered activity on the efferent projections of a brain structure and these have mainly concentrated on terminal structure rather than on the neurons of origin of these efferent projections (Garraghty et al., 1986, 1987; Hsiao & Sherman, 1986; Lachica et al., 1990; Pallas, 2001; Raczkowski et al., 1988; Ruthazer & Stryker, 1996; Sur et al., 1982). We had expected to find that blindness could induce a reduction in the size of visual cortex efferent projections. Perhaps remaining spontaneous activity and cross-modal activations are sufficient to maintain a normal complement of efferent visual cortical projections at least to another non-deprived specific sensory cortex. The lesser postnatal size increase of the visual cortex seen in enucleated mice compared to the intact cases (Massé et al., 2014) could be explained by the reduction we observed in the number of neurons projecting from primary sensory cortices of other modalities such as S1. This size reduction of V1 however, would not affect the efferent projections to the barrel field.

The effects of enucleation on the structure of the projections between V1 and S1

In addition to the reduction of the number of neurons of S1 projecting to V1 in the enucleated mice (Charbonneau et al., 2012), we further show that this is mainly explained by a loss of projection of supragranular layer neurons of S1. In primates and rodents, feedforward projections originate mainly from supragranular layer neurons and feedback projections, from infragranular layer neurons (Coogan & Burkhalter, 1990, 1993; Felleman & Van Essen, 1991; Rockland & Pandya, 1979). This pathway specific laminar distribution of projection neurons emerges from an initial uniform laminar distribution of neurons mainly through selective elimination of supragranular layer projections in corticocortical feedback (Batardiere et al., 1998; Batardiere et al., 2002; Kennedy et al., 1989) as well as in interhemispheric callosal projections (Innocenti & Caminiti, 1980). Several studies have shown that normal visual experience is necessary for the development of a normal complement of callosal projections and that altered visual experience results in the supranormal elimination of callosal projections of supragranular layer neurons (Boire et al., 1995; Frost & Moy, 1989; Frost et al., 1990; Innocenti & Frost, 1980; Innocenti et al., 1985). Therefore, as in cats, normal visual experience is required for the normal establishment of supragranular layer projections in the cortex.

The effects of enucleation on the thickness of axons and size axonal swellings

Visual deprivation also affected the size of axonal swellings in the projection from the visual cortex to the barrel field of the primary somatosensory cortex. Indeed, the

larger axonal swelling observed in this projection in the intact mice were no longer present in the enucleated mice. There is evidence for two types of glutamatergic synaptic contacts in corticocortical connections (Covic & Sherman, 2011; De Pasquale & Sherman, 2011; Petrof & Sherman, 2013). Class 1 synapses have larger initial excitatory postsynaptic potentials, exhibit paired-pulse depression, are limited to ionotropic glutamate receptor activation and are anatomically correlated with larger synaptic terminals and Class 2 synapses have smaller initial excitatory postsynaptic potentials, exhibit paired-pulse facilitation, are limited to metabotropic glutamate receptor activation and are anatomically correlated with smaller synaptic terminals (Sherman & Guillery, 2013). Class 1 and 2 are respectively considered drivers and modulators (Lee & Sherman, 2008, 2009a, 2009b; Petrof & Sherman, 2013; Reichova & Sherman, 2004; Sherman & Guillery, 1996, 1998, 2013; Viaene et al., 2011). We surmise that the larger swellings in the projection from V1 to S1BF in our results reflect a greater proportion of Class 1 terminals therein and that the large population of smaller swellings, which appears to be predominant in both projections, to be Class 2 terminals. Axonal bouton size is positively correlated with the number of synaptic vesicles, active zone area and the number of active zones (Pierce & Lewin, 1994; Pierce & Mendell, 1993; Schikorski & Stevens, 1997; Streichert & Sargent, 1989; Yeow & Peterson, 1991). Both pre- and postsynaptic activity blockade result in an increase in post-synaptic density and size of the synaptic active zone, bouton volume and increases neurotransmitter release (Murthy et al., 2001). This could be related to "disuse hypersensitivity" (Cannon, 1939; Duclert & Changeux, 1995; Murthy et al., 2001; Sharpless, 1964, 1975a, 1975b) and regulated

by homeostatic regulation of synaptic strength (Turrigiano & Nelson, 2000). Our results suggest that either Class 1 terminals might not form in the absence of normal sensory activity or that these visual cortex projection neurons are highly active in the enucleated mice reducing the size of these terminals. Our result also show that even the size distribution of the smaller terminals is shifted towards lower diameter values, suggesting that the size of all terminals is equally affected by the altered activity in the visual cortex of the enucleated mice. There is yet no direct experimental demonstration that increased activity results in decreased synaptic size (see Murthy et al., 2001 for review). The activity levels in the visual cortex of binocularly enucleated mice are not known. Increase metabolic activity was reported in blind humans (De Volder et al., 1997; Wanet-Defalque et al., 1988). The visual cortex in these mice is not likely silent, it is activated by auditory stimulation in enucleated rats (Piché et al., 2007) and mice (Nys et al., in prep) and by tactile stimulation in monocularly enucleated mice (Nys et al., 2014, 2015; Van Brussel et al., 2011).

Different corticocortical projections include axons of different diameters depending on their source and the cortical areas they target (Anderson & Martin, 2002; Caminiti et al., 2009, 2013; Innocenti et al., 2014; Tomasi et al., 2012). The range of axonal diameters was greater in V1 projections to S1BF than in the reciprocal projection back to V1. We would therefore expect faster conduction velocities in some axons in the projection of V1 to S1BF. Axonal diameter is not the only variable that determines conduction delays however, pathway length, axonal geometry and branching structure

will also influence conduction speed in axons (see Debanne, 2004 for review). This asymmetry in this reciprocal projection between these primary sensory cortices is not known.

Axonal thickness in the projection from V1 to S1BF was also reduced in the enucleated mice. This reduction is commensurate with the axonal swelling size reduction in these mice. Indeed, the bouton size and axonal thickness are positively correlated in corticocortical projections (Innocenti & Caminiti, 2016). Few studies have examined the effects of sensory activity on the diameter of axons in corticocortical connections. Some studies show that afferent sensory activity is important for the development of very local cortical intra-areal projections (Bruno et al., 2009; Cheetham et al., 2007). We know of no reports on the role of sensory afferent activity on the structure of single axons in corticocortical interareal projections activity. There are some indications that axonal structure would be altered by sensory deprivation. For example, the topography of striate extrastriate projections is abnormal in anophthalmic and in enucleated mice (Laramée et al., 2014) and in enucleated rats, (Laing et al., 2012, 2013). Moreover, cross-modal rewiring of visual inputs to the auditory thalamus in ferret demonstrated that the nature of sensory activity is important in shaping the local horizontal connectivity within the auditory cortex (Gao & Pallas, 1999). The changes observed here in the size distribution of axonal swellings and diameter might reflect further changes in branching structure and terminal field size of the axons.

Conclusions

In the current study, we asked how visual experience shapes cortical circuitry by comparing the direct reciprocal intermodal corticocortical connections between V1 and S1 in intact and C57BL/6 mice enucleated at birth, and determining quantitative differences in the strength and laminar distribution of neurons and terminals in these projections. We show that enucleation significantly reduced the strength of the somatosensory projections to the visual cortex without affecting the strength of the visual, motor and somatosensory afferents to the somatosensory cortex. Moreover enucleation reduced the larger axonal swellings which were no longer observed and axonal thickness was reduced in the visual cortex projection to the primary somatosensory cortex. The absence of larger axonal swellings in the projection from V1 to S1 of enucleated mice could indicate that normal sensory activity is required for the normal development of Class 1 driver projections from V1 or a homeostatic adjustment of these terminals size is produced by high levels of activity in these projection neurons.

Acknowledgements

We are grateful to Nadia Desnoyers for animal care and maintenance. This work was supported by discovery grants of the Natural Sciences and Engineering Research Council of Canada (NSERC) to DB and GB, and the Canadian Foundation for Innovation to DB.

References

Andermann, M. L., Kerlin, A. M., Roumis, D. K., Glickfeld, L. L. & Reid, R. C. (2011) Functional specialization of mouse higher visual cortical areas. Neuron, 72, 1025-1039.

Anderson, J. C. & Martin, K. A. (2002) Connection from cortical area V2 to MT in macaque monkey. J. Comp. Neurol., 443, 56-70.

Batardiere, A., Barone, P., Dehay, C. & Kennedy, H. (1998) Area-specific laminar distribution of cortical feedback neurons projecting to cat area 17: Quantitative analysis in the adult and during ontogeny. J. Comp. Neurol., 396, 493-510.

Batardiere, A., Barone, P., Knoblauch, K., Giroud, P., Berland, M., Dumas, A. M. & Kennedy, H. (2002) Early specification of the hierarchical organization of visual cortical areas in the macaque monkey. Cereb. Cortex, 12, 453-465.

Bavelier, D. & Neville, H. J. (2002) Cross-modal plasticity: Where and how? Nat. Rev. Neurosci., 3, 443-452.

Berman, N. E. (1991) Alterations of visual cortical connections in cats following early removal of retinal input. Brain Res. Dev. Brain Res., 63, 163-180.

Boire, D., Morris, R., Ptito, M., Lepore, F. & Frost, D. O. (1995) Effects of neonatal splitting of the optic chiasm on the development of feline visual callosal connections. Exp. Brain Res., 104, 275-286.

Bravo, H. & Inzunza, O. (1994) Effect of pre- and postnatal retinal deprivation on the striate-peristriate cortical connections in the rat. Biol. Res., 27, 73-77.

Bruno, R. M., Hahn, T. T., Wallace, D. J., de Kock, C. P. & Sakmann, B. (2009) Sensory experience alters specific branches of individual corticocortical axons during development. J. Neurosci., 29, 3172-3181.

Budinger, E., Heil, P., Hess, A. & Scheich, H. (2006) Multisensory processing via early cortical stages: Connections of the primary auditory cortical field with other sensory systems. Neuroscience, 143, 1065-1083.

Budinger, E., Laszcz, A., Lison, H., Scheich, H. & Ohl, F. W. (2008) Non-sensory cortical and subcortical connections of the primary auditory cortex in Mongolian gerbils: Bottom-up and top-down processing of neuronal information via field AI. Brain Res., 1220, 2-32.

Budinger, E. & Scheich, H. (2009) Anatomical connections suitable for the direct processing of neuronal information of different modalities via the rodent primary auditory cortex. Hear. Res., 258, 16-27.

Caminiti, R., Carducci, F., Piervincenzi, C., Battaglia-Mayer, A., Confalone, G., Visco-Comandini, F., Pantano, P. & Innocenti, G. M. (2013) Diameter, length, speed, and conduction delay of callosal axons in macaque monkeys and humans: Comparing data from histology and magnetic resonance imaging diffusion tractography. J. Neurosci., 33, 14501-14511.

Caminiti, R., Ghaziri, H., Galuske, R., Hof, P. R. & Innocenti, G. M. (2009) Evolution amplified processing with temporally dispersed slow neuronal connectivity in primates. Proc. Natl. Acad. Sci. U. S. A., 106, 19551-19556.

Campi, K. L., Bales, K. L., Grunewald, R. & Krubitzer, L. (2010) Connections of auditory and visual cortex in the prairie vole (Microtus ochrogaster): Evidence for multisensory processing in primary sensory areas. Cereb. Cortex, 20, 89-108.

Cannon, W. B. (1939) A law of denervation. Am. J. Med. Sci., 198, 737-750.

Cappe, C. & Barone, P. (2005) Heteromodal connections supporting multisensory integration at low levels of cortical processing in the monkey. Eur. J. Neurosci., 22, 2886-2902.

Caviness, V. S. (1975) Architectonic map of neocortex of the normal mouse. J. Comp. Neurol., 164, 247-263.

Charbonneau, V., Laramée, M. E., Boucher, V., Bronchti, G. & Boire, D. (2012) Cortical and subcortical projections to primary visual cortex in anophthalmic, enucleated and sighted mice. Eur. J. Neurosci., 36, 2949-2963.

Cheetham, C. E., Hammond, M. S., Edwards, C. E. & Finnerty, G. T. (2007) Sensory experience alters cortical connectivity and synaptic function site specifically. J. Neurosci., 27, 3456-3465.

Clavagnier, S., Falchier, A. & Kennedy, H. (2004) Long-distance feedback projections to area V1: Implications for multisensory integration, spatial awareness, and visual consciousness. Cogn. Affect. Behav. Neurosci., 4, 117-126.

Collignon, O., Dormal, G., de, H. A., Lepore, F., Lewis, T. L. & Maurer, D. (2015) Long-Lasting Crossmodal Cortical Reorganization Triggered by Brief Postnatal Visual Deprivation. Curr. Biol., 25, 2379-2383.

Coogan, T. A. & Burkhalter, A. (1990) Conserved patterns of cortico-cortical connections define areal hierarchy in rat visual cortex. Exp. Brain Res., 80, 49-53.

Coogan, T. A. & Burkhalter, A. (1993) Hierarchical organization of areas in rat visual cortex. J. Neurosci., 13, 3749-3772.

Covic, E. N. & Sherman, S. M. (2011) Synaptic properties of connections between the primary and secondary auditory cortices in mice. Cereb. Cortex, 21, 2425-2441.

De Pasquale R. & Sherman, S. M. (2011) Synaptic properties of corticocortical connections between the primary and secondary visual cortical areas in the mouse. J. Neurosci., 31, 16494-16506.

De Volder, A. G., Bol, A., Blin, J., Robert, A., Arno, P., Grandin, C., Michel, C. & Veraart, C. (1997) Brain energy metabolism in early blind subjects: Neural activity in the visual cortex. Brain Res., 750, 235-244.

Debanne, D. (2004) Information processing in the axon. Nat. Rev. Neurosci., 5, 304-316.

Dehay, C., Giroud, P., Berland, M., Killackey, H. & Kennedy, H. (1996) Contribution of thalamic input to the specification of cytoarchitectonic cortical fields in the primate: Effects of bilateral enucleation in the fetal monkey on the boundaries, dimensions, and gyrification of striate and extrastriate cortex. J. Comp. Neurol., 367, 70-89.

Dehay, C., Horsburgh, G., Berland, M., Killackey, H. & Kennedy, H. (1989) Maturation and connectivity of the visual cortex in monkey is altered by prenatal removal of retinal input. Nature, 337, 265-267.

Duclert, A. & Changeux, J. P. (1995) Acetylcholine receptor gene expression at the developing neuromuscular junction. Physiol. Rev., 75, 339-368.

Felleman, D. J. & Van Essen, D. C. (1991) Distributed hierarchical processing in the primate cerebral cortex. Cereb. Cortex, 1, 1-47.

Franklin, B. J. & Paxinos, G. (2008) The Mouse Brain in Stereotaxic Coordinates. Academic Press, San Diego.

Frost, D. O. & Moy, Y. P. (1989) Effects of dark rearing on the development of visual callosal connections. Exp. Brain Res., 78, 203-213.

Frost, D. O., Moy, Y. P. & Smith, D. C. (1990) Effects of alternating monocular occlusion on the development of visual callosal connections. Exp. Brain Res., 83, 200-209.

Fujii, T., Tanabe, H. C., Kochiyama, T. & Sadato, N. (2009) An investigation of cross-modal plasticity of effective connectivity in the blind by dynamic causal modeling of functional MRI data. Neurosci. Res., 65, 175-186.

Gao, W. J. & Pallas, S. L. (1999) Cross-modal reorganization of horizontal connectivity in auditory cortex without altering thalamocortical projections. J. Neurosci., 19, 7940-7950.

Garraghty, P. E., Frost, D. O. & Sur, M. (1987) The morphology of retinogeniculate X- and Y-cell axonal arbors in dark-reared cats. Exp. Brain Res., 66, 115-127.

Garraghty, P. E., Sur, M., Weller, R. E. & Sherman, S. M. (1986) Morphology of retinogeniculate X and Y axon arbors in monocularly enucleated cats. J. Comp. Neurol., 251, 198-215.

Glickfeld, L. L., Andermann, M. L., Bonin, V. & Reid, R. C. (2013) Cortico-cortical projections in mouse visual cortex are functionally target specific. Nat. Neurosci., 16, 219-226.

Glickfeld, L. L., Reid, R. C. & Andermann, M. L. (2014) A mouse model of higher visual cortical function. Curr. Opin. Neurobiol., 24, 28-33.

Gougoux, F., Zatorre, R. J., Lassonde, M., Voss, P., & Lepore, F. (2005) A functional neuroimaging study of sound localization: visual cortex activity predicts performance in early-blind individuals. PLoS Biol, 3, e27.

Henschke, J. U., Noesselt, T., Scheich, H. & Budinger, E. (2014) Possible anatomical pathways for short-latency multisensory integration processes in primary sensory cortices. Brain Struct. Funct., 10, 1007-1030.

Heumann, D. & Rabinowicz, T. (1980) Postnatal development of the dorsal lateral geniculate nucleus in the normal and enucleated albino mouse. Exp. Brain Res., 38, 75-85.

Hsiao, C. F. & Sherman, S. M. (1986) Alpha and beta cells projecting from retina to lamina A of the lateral geniculate nucleus in normal cats, monocularly deprived cats, and young kittens. Exp. Brain Res., 61, 413-431.

Innocenti, G. M., & Caminiti, R. (1980) Postnatal shaping of callosal connections from sensory areas. Exp. Brain Res., 38, 381-394.

Innocenti, G. M., & Caminiti, R. (2016) Axon diameter relates to synaptic bouton size: Structural properties define computationally different types of cortical connections in primates. Brain Struct. Funct.

Innocenti, G. M., & Frost, D. O. (1980) The postnatal development of visual callosal connections in the absence of visual experience or of the eyes. Exp. Brain Res., 39, 365-375.

Innocenti, G. M., Frost, D. O. & Illes, J. (1985) Maturation of visual callosal connections in visually deprived kittens: A challenging critical period. J. Neurosci., 5, 255-267.

Innocenti, G. M., Vercelli, A. & Caminiti, R. (2014) The diameter of cortical axons depends both on the area of origin and target. Cereb. Cortex, 24, 2178-2188.

Iurilli, G., Ghezzi, D., Olcese, U., Lassi, G., Nazzaro, C., Tonini, R., Tucci, V., Benfenati, F. & Medini, P. (2012) Sound-driven synaptic inhibition in primary visual cortex. Neuron, 73, 814-828.

Kahn, D. M. & Krubitzer, L. (2002) Massive cross-modal cortical plasticity and the emergence of a new cortical area in developmentally blind mammals. Proc. Natl. Acad. Sci. U. S. A., 99, 11429-11434.

Karlen, S. J., Kahn, D. M. & Krubitzer, L. (2006) Early blindness results in abnormal corticocortical and thalamocortical connections. Neuroscience, 142, 843-858.

Karlen, S. J. & Krubitzer, L. (2009) Effects of bilateral enucleation on the size of visual and nonvisual areas of the brain. Cereb. Cortex, 19, 1360-1371.

Kennedy, H., Bullier, J. & Dehay, C. (1989) Transient projection from the superior temporal sulcus to area 17 in the newborn macaque monkey. Proc. Natl. Acad. Sci. U. S. A., 86, 8093-8097.

Klinge, C., Eippert, F., Roder, B. & Buchel, C. (2010) Corticocortical connections mediate primary visual cortex responses to auditory stimulation in the blind. J. Neurosci., 30, 12798-12805.

Lachica, E. A., Crooks, M. W. & Casagrande, V. A. (1990) Effects of monocular deprivation on the morphology of retinogeniculate axon arbors in a primate. J. Comp. Neurol., 296, 303-323.

Laing, R. J., Bock, A. S., Lasiene, J. & Olavarria, J. F. (2012) Role of retinal input on the development of striate-extrastriate patterns of connections in the rat. J. Comp. Neurol., 520, 3256-3276.

Laing, R. J., Lasiene, J. & Olavarria, J. F. (2013) Topography of striate-extrastriate connections in neonatally enucleated rats. Biomed. Res. Int., 2013, 1-9.

Laramée, M. E., Bronchti, G. & Boire, D. (2014) Primary visual cortex projections to extrastriate cortices in enucleated and anophthalmic mice. Brain Struct. Funct., 219, 2051-2070.

Laramée, M. E., Rockland, K. S., Prince, S., Bronchti, G. & Boire, D. (2013) Principal component and cluster analysis of layer V pyramidal cells in visual and non-visual cortical areas projecting to the primary visual cortex of the mouse. Cereb. Cortex, 23, 714-728.

Lee, C. C. & Sherman, S. M. (2008) Synaptic properties of thalamic and intracortical inputs to layer 4 of the first- and higher-order cortical areas in the auditory and somatosensory systems. J. Neurophysiol., 100, 317-326.

Lee, C. C. & Sherman, S. M. (2009a) Glutamatergic inhibition in sensory neocortex. Cereb. Cortex, 19, 2281-2289.

Lee, C. C. & Sherman, S. M. (2009b) Modulator property of the intrinsic cortical projection from layer 6 to layer 4. Front Syst. Neurosci., 3, 3-8.

Liu, Y., Yu, C., Liang, M., Li, J., Tian, L., Zhou, Y., Qin, W., Li, K. & Jiang, T. (2007) Whole brain functional connectivity in the early blind. Brain, 130, 2085-2096.

Marshel, J. H., Garrett, M. E., Nauhaus, I. & Callaway, E. M. (2011) Functional specialization of seven mouse visual cortical areas. Neuron, 72, 1040-1054.

Massé, I. O., Guillemette, S., Laramée, M. E., Bronchti, G. & Boire, D. (2014) Strain differences of the effect of enucleation and anophthalmia on the size and growth of sensory cortices in mice. Brain Res., 1588, 113-126.

Massé, I. O., Ross, S., Bronchti, G. & Boire, D. (2016) Asymmetric Direct Reciprocal Connections Between Primary Visual and Somatosensory Cortices of the Mouse. Cereb. Cortex.

Matsui, T. & Ohki, K. (2013) Target dependence of orientation and direction selectivity of corticocortical projection neurons in the mouse V1. Front Neural Circuits, 7, 143-152.

Merabet, L. B. & Pascual-Leone, A. (2010) Neural reorganization following sensory loss: The opportunity of change. Nat. Rev. Neurosci., 11, 44-52.

Meredith, M. A. & Lomber, S. G. (2016) Species-dependent role of crossmodal connectivity among the primary sensory cortices. Hear. Res., 10, 1016-1023.

Murthy, V. N., Schikorski, T., Stevens, C. F. & Zhu, Y. (2001) Inactivity produces increases in neurotransmitter release and synapse size. Neuron, 32, 673-682.

Nys, J., Aerts, J., Ytebrouck, E., Vreysen, S., Laeremans, A. & Arckens, L. (2014) The cross-modal aspect of mouse visual cortex plasticity induced by monocular enucleation is age dependent. J. Comp. Neurol., 522, 950-970.

Nys, J., Scheyltjens, I. & Arckens, L. (2015) Visual system plasticity in mammals: The story of monocular enucleation-induced vision loss. Front Syst. Neurosci., 9, 60-80.

Olavarria, J., Mignano, L. R. & Van Sluyters, R. C. (1982) Pattern of extrastriate visual areas connecting reciprocally with striate cortex in the mouse. Exp. Neurol., 78, 775-779.

Olavarria, J. & Montero, V. M. (1989) Organization of visual cortex in the mouse revealed by correlating callosal and striate-extrastriate connections. Vis. Neurosci., 3, 59-69.

Pallas, S. L. (2001) Intrinsic and extrinsic factors that shape neocortical specification. Trends Neurosci., 24, 417-423.

Paperna, T. & Malach, R. (1991) Patterns of sensory intermodality relationships in the cerebral cortex of the rat. J. Comp. Neurol., 308, 432-456.

Pascual-Leone, A., Amedi, A., Fregni, F. & Merabet, L. B. (2005) The plastic human brain cortex. Annu. Rev. Neurosci., 28, 377-401.

Pascual-Leone, A. & Hamilton, R. (2001) The metamodal organization of the brain. Prog. Brain Res., 134, 427-445.

Petrof, I. & Sherman, S. M. (2013) Functional significance of synaptic terminal size in glutamatergic sensory pathways in thalamus and cortex. J. Physiol., 591, 3125-3131.

Piché, M., Chabot, N., Bronchti, G., Miceli, D., Lepore, F. & Guillemot, J. P. (2007) Auditory responses in the visual cortex of neonatally enucleated rats. Neuroscience, 145, 1144-1156.

Pierce, J. P. & Lewin, G. R. (1994) An ultrastructural size principle. Neuroscience, 58, 441-446.

Pierce, J. P. & Mendell, L. M. (1993) Quantitative ultrastructure of Ia boutons in the ventral horn: Scaling and positional relationships. J. Neurosci., 13, 4748-4763.

Qin, W., Liu, Y., Jiang, T. & Yu, C. (2013) The development of visual areas depends differently on visual experience. PLoS One., 8, 1-10.

Raczkowski, D., Uhlrich, D. J. & Sherman, S. M. (1988) Morphology of retinogeniculate X and Y axon arbors in cats raised with binocular lid suture. J. Neurophysiol., 60, 2152-2167.

Rakic, P. (1988) Specification of cerebral cortical areas. Science, 241, 170-176.

Rakic, P., Suner, I. & Williams, R. W. (1991) A novel cytoarchitectonic area induced experimentally within the primate visual cortex. Proc. Natl. Acad. Sci. U. S. A., 88, 2083-2087.

Reichova, I. & Sherman, S. M. (2004) Somatosensory corticothalamic projections: Distinguishing drivers from modulators. J. Neurophysiol., 92, 2185-2197.

Rockland, K. S. & Pandya, D. N. (1979) Laminar origins and terminations of cortical connections of the occipital lobe in the rhesus monkey. Brain Res., 179, 3-20.

Röder, B., Rosler, F. & Neville, H. J. (2001) Auditory memory in congenitally blind adults: a behavioral-electrophysiological investigation. Brain Res Cogn Brain Res, 11, 289-303.

Ruthazer, E. S. & Stryker, M. P. (1996) The role of activity in the development of long-range horizontal connections in area 17 of the ferret. J. Neurosci., 16, 7253-7269.

Schikorski, T. & Stevens, C. F. (1997) Quantitative ultrastructural analysis of hippocampal excitatory synapses. J. Neurosci., 17, 5858-5867.

Sharpless, S. K. (1964) Reorganization of function in the nervous system-use and disuse. Annu. Rev. Physiol., 26, 357-388.

Sharpless, S.K. (1975a) Disuse sensitivity. In A.H Riessen (ed), The developmental neuropsychology of sensory deprivation. Academic Press, New York, pp. 125-152.

Sharpless, S. K. (1975b) Supersensitivity-like phenomena in the central nervous system. Fed. Proc., 34, 1990-1997.

Sherman, S. M. & Guillery, R. W. (1996) Functional organization of thalamocortical relays. J. Neurophysiol., 76, 1367-1395.

Sherman, S. M. & Guillery, R. W. (1998) On the actions that one nerve cell can have on another: Distinguishing "drivers" from "modulators". Proc. Natl. Acad. Sci. U. S. A., 95, 7121-7126.

Sherman, S.M. & Guillery, R.W. (2013) Functional connections of cortical areas. MIT Press, Cambridge MA , London England.

Sieben, K., Bieler, M., Roder, B. & Hanganu-Opatz, I. L. (2015) Neonatal Restriction of Tactile Inputs Leads to Long-Lasting Impairments of Cross-Modal Processing. PLoS Biol., 13, 1-26.

Sieben, K., Roder, B. & Hanganu-Opatz, I. L. (2013) Oscillatory entrainment of primary somatosensory cortex encodes visual control of tactile processing. J. Neurosci., 33, 5736-5749.

Stehberg, J., Dang, P. T. & Frostig, R. D. (2014) Unimodal primary sensory cortices are directly connected by long-range horizontal projections in the rat sensory cortex. Front. Neuroanat., 8, 93-112.

Streichert, L. C. & Sargent, P. B. (1989) Bouton ultrastructure and synaptic growth in a frog autonomic ganglion. J. Comp. Neurol., 281, 159-168.

Sur, M., Humphrey, A. L. & Sherman, S. M. (1982) Monocular deprivation affects X- and Y-cell retinogeniculate terminations in cats. Nature, 300, 183-185.

Toldi, J., Farkas, T. & Volgyi, B. (1994) Neonatal enucleation induces cross-modal changes in the barrel cortex of rat. A behavioural and electrophysiological study. Neurosci. Lett., 167, 1-4.

Toldi, J., Joo, F., Feher, O. & Wolff, J. R. (1988) Modified distribution patterns of responses in rat visual cortex induced by monocular enucleation. Neuroscience, 24, 59-66.

Tomasi, S., Caminiti, R. & Innocenti, G. M. (2012) Areal differences in diameter and length of corticofugal projections. Cereb. Cortex, 22, 1463-1472.

Turrigiano, G. G. & Nelson, S. B. (2000) Hebb and homeostasis in neuronal plasticity. Curr. Opin. Neurobiol., 10, 358-364.

Van Boven, R. W., Hamilton, R. H., Kauffman, T., Keenan, J. P. & Pascual-Leone, A. (2000) Tactile spatial resolution in blind braille readers. Neurology, 54, 2230-2236.

Van Brussel, L., Gerits, A. & Arckens, L. (2011) Evidence for cross-modal plasticity in adult mouse visual cortex following monocular enucleation. Cereb. Cortex, 21, 2133-2146.

Viaene, A. N., Petrof, I. & Sherman, S. M. (2011) Synaptic properties of thalamic input to layers 2/3 and 4 of primary somatosensory and auditory cortices. J. Neurophysiol., 105, 279-292.

Wan, C. Y., Wood, A. G., Reutens, D. C. & Wilson, S. J. (2010) Congenital blindness leads to enhanced vibrotactile perception. Neuropsychologia, 48, 631-635.

Wanet-Defalque, M. C., Veraart, C., De, V. A., Metz, R., Michel, C., Dooms, G. & Goffinet, A. (1988) High metabolic activity in the visual cortex of early blind human subjects. Brain Res., 446, 369-373.

Wang, Q. & Burkhalter, A. (2007) Area map of mouse visual cortex. J. Comp. Neurol., 502, 339-357.

Wang, Q., Gao, E. & Burkhalter, A. (2011) Gateways of ventral and dorsal streams in mouse visual cortex. J. Neurosci., 31, 1905-1918.

Wang, Q., Sporns, O. & Burkhalter, A. (2012) Network analysis of corticocortical connections reveals ventral and dorsal processing streams in mouse visual cortex. J. Neurosci., 32, 4386-4399.

West, M. J. & Gundersen, H. J. (1990) Unbiased stereological estimation of the number of neurons in the human hippocampus. J.Comp Neurol., 296, 1-22.

West, M. J., Slomianka, L. & Gundersen, H. J. (1991) Unbiased stereological estimation of the total number of neurons in the subdivisions of the rat hippocampus using the optical fractionator. Anat. Rec., 231, 482-497.

Wittenberg, G. F., Werhahn, K. J., Wassermann, E. M., Herscovitch, P. & Cohen, L. G. (2004) Functional connectivity between somatosensory and visual cortex in early blind humans. Eur. J. Neurosci., 20, 1923-1927.

Yeow, M. B. & Peterson, E. H. (1991) Active zone organization and vesicle content scale with bouton size at a vertebrate central synapse. J. Comp. Neurol., 307, 475-486.

Yu, C., Liu, Y., Li, J., Zhou, Y., Wang, K., Tian, L., Qin, W., Jiang, T. & Li, K. (2008) Altered functional connectivity of primary visual cortex in early blindness. Hum. Brain Mapp., 29, 533-543.

Zingg, B., Hintiryan, H., Gou, L., Song, M. Y., Bay, M., Bienkowski, M. S., Foster, N. N., Yamashita, S., Bowman, I., Toga, A. W. & Dong, H. W. (2014) Neural networks of the mouse neocortex. Cell, 156, 1096-1111.

Discussion

L'objectif général de cette thèse était de mieux comprendre comment les cortex sensoriels primaires contribuent au traitement de l'information sensorielle et non sensorielle. Les travaux de cette thèse ont été présentés en trois objectifs spécifiques. Pour mieux comprendre comment les cortex sensoriels primaires contribuent à ce traitement, nous avons déterminé la provenance et la nature des projections afférentes aux cortex sensoriels primaires, dont S1, pour lesquelles un inventaire complet et quantitatif n'avait pas été réalisé chez la souris. Suite à la démonstration que le champ de tonneaux de S1 possède plus de connexions qui ciblent des aires corticales sensorielles telles que V1, nous avons poussé l'étude de la structure de cette connexion entre deux cortex sensoriels primaires pour mieux comprendre comment ces modalités s'influencent mutuellement. Le deuxième objectif était donc d'étudier la microcircuiterie des connexions corticocorticales directes et réciproques entre le cortex visuel et somatosensoriel primaire de la souris. Suite à la démonstration que la projection de V1 vers S1 à une influence inductrice, nous nous sommes interrogés sur l'influence de l'expérience visuelle pendant la période de vie postnatale sur le développement des connexions corticocorticales entre V1 et S1. Le troisième et dernier objectif était donc d'étudier l'impact de la perte de la vision sur la microcircuiterie des connexions entre V1 et S1 à l'aide d'un échantillon de souris énucléées à la naissance. Les sections de la discussion sont dédiées à la signification de nos résultats dans le contexte des connaissances actuelles sur les interactions multisensorielles et la hiérarchie des sens.

Objectif 1 : Projections afférentes corticales et sous-corticales du cortex somatosensoriel primaire de la souris

Notre première étude a confirmé que S1 chez la souris reçoit des projections des cortex moteurs, des aires corticales associatives multisensorielles, des noyaux thalamiques et des cortex sensoriels primaires des autres modalités sensorielles, ce qui soutient ce qui avait été démontré précédemment dans la littérature (Zakiewicz, Bjaalie, & Leergaard, 2014; Zingg et al., 2014), et l'hypothèse selon laquelle les aires primaires ne sont pas limités au traitement unisensoriel (Ghazanfar & Schroeder, 2006; Kayser, Petkov, Augath, & Logothetis, 2007; Wallace et al., 2004). Par rapport aux études neuroanatomiques antérieures (Budinger, Heil, Hess, & Scheich, 2006; Budinger, Laszcz, Lison, Scheich, & Ohl, 2008; Budinger & Scheich, 2009; Charbonneau et al., 2012; Henschke, Noesselt, Scheich, & Budinger, 2014; Zakiewicz et al., 2014; Zingg et al., 2014), notre analyse contribue des informations plus complètes et détaillées sur les afférences de S1 telles que leur distribution laminaire et leur poids relatif, et prend en compte les différentes parties de ce cortex sensoriel primaire ainsi que l'ensemble des afférences sous-corticales. Nos résultats apportent une contribution aux efforts à grande échelle qui consistent à cartographier l'ensemble des connexions du cerveau des rongeurs, tels que le *Mouse Brain Connectome Project* et l'*Allen Mouse Brain Connectivity Atlas*. Les images fournit par ces bases de données permettent de facilement répertorier certaines projections bien connues de S1 telles que les projections vers le cortex moteur et le striatum, mais l'existence de projections plus petites vers d'autres cibles tel que V1 et les régions sous-corticales ne peut être confirmé que par une analyse plus détaillée comme celle présentée dans notre étude.

Notre première étude contribue de manière originale à la recherche sur les projections de S1 en démontrant que ces trois parties ont des projections différentes. En effet, la partie caudale de S1BF possède plus de connexions qui ciblent des aires corticales et sous-corticales sensorielles des autres modalités telles que des aires visuelles, auditives, olfactives et associatives, dont le cortex auditif et visuel, en plus du cortex perirhinal et ectorhinal qui sont impliqué dans le traitement sensoriel (Naber, Witter, & Lopes da Silva, 2000; Rodgers, Benison, Klein, & Barth, 2008), ainsi que certaines régions sous-corticales, telles que le noyau thalamique ventral latéral qui module les processus nociceptifs (Blomqvist, Ericson, Broman, & Craig, 1992; Craig, Jr. & Burton, 1981; Miletic & Coffield, 1989), comparativement à la partie rostrale du champ de tonneaux et à la partie de S1 à l'extérieur du champ de tonneaux dont les connexions ciblent davantage des aires somatosensorielles et motrices. De plus, la partie caudale du champ de tonneaux est la seule partie de S1 à recevoir des projections de V1. Les projections vers S1 seraient surtout de nature *feedback*, mais les projections auditives seraient de nature *feedback* alors que les projections visuelles seraient de nature latérale, ce qui démontre que les différentes modalités sensorielles n'ont pas la même influence envers S1. S1 reçoit des projections de nature *feedback* des cortex pariétal et temporal associatifs, ce qui soutient l'importance de S1 dans le codage prédictif et le modèle de la hiérarchie inversé. Les indices laminaires démontrent que malgré la nature *feedback* des projections dans l'ensemble, les informations contextuelles des aires associatives vers S1 n'ont pas toute la même structure et auraient possiblement des contributions fonctionnelles différentes.

La multimodalité du cortex somatosensoriel primaire

Dans les modèles traditionnels de l'organisation des cortex sensoriels, l'information de chaque modalité est d'abord traitée séparément dans les cortex spécifiques avant son intégration ultérieure dans les aires associatives d'ordre supérieur. Ce modèle d'organisation a été contesté par la démonstration d'interactions multisensorielles dans les cortex sensoriels primaires (Driver & Noesselt, 2008; Ghazanfar & Schroeder, 2006). La modalité qui est associée à un cortex sensoriel spécifique pourrait être définie comme dominante (Pascual-Leone & Hamilton, 2001). Par exemple, l'information somatosensorielle serait dominante dans le cortex somatosensoriel primaire. Par conséquent, les autres modalités peuvent être définies comme non dominante par rapport au même cortex. Par exemple, l'information visuelle et auditive serait non dominante dans le cortex somatosensoriel primaire. En effet, les résultats de notre première étude démontrent que malgré la dominance des afférences somatosensorielles, la partie caudale du champ de tonneaux reçoit des afférences des aires corticales dédiées à d'autres modalités.

Bien qu'on puisse s'attendre à ce que l'influence entre les différentes modalités sensorielles soit similaire, des études récentes ont démontré que ce ne serait pas le cas. Par exemple, pour mieux comprendre le caractère synaptique des connexions entre les cortex sensoriels primaires, ainsi que leur impact sur la réactivité aux stimuli des autres modalités, Iurilli et ses collaborateurs (2012) ont mesuré les réponses synaptiques des neurones pyramidaux dans V1, S1 et A1 lors de la stimulation des modalités sensorielles

non dominante, en utilisant des enregistrements in vivo de cellules entières guidées par imagerie de signal intrinsèque. Les auteurs ont démontré qu'une stimulation des vibrisses et une stimulation acoustique ont évoqué une hyperpolarisation des cortex sensoriels primaires non somatosensoriels et non auditifs respectivement tandis qu'une stimulation visuelle a évoqué une légère dépolarisation sous le seuil dans S1 et aucune réponse détectable dans A1 (voir Figure 36). Cela pourrait suggérer des différences fonctionnelles dans les influences relatives des projections entre V1, S1 et A1.

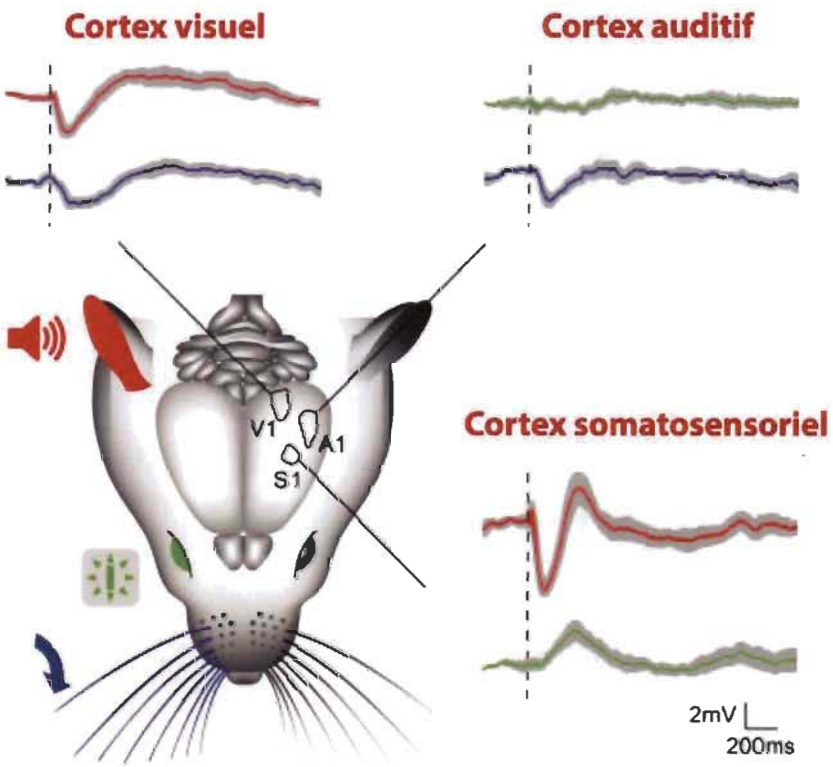

Figure 36. Asymétrie fonctionnelle entre les cortex sensoriels primaires de la souris (Iurilli et al., 2012).

En ce qui concerne les autres études sur la connectivité corticocorticale, des connexions directes et réciproques entre les aires primaires ont été démontrées chez les rongeurs (Budinger et al., 2006; Campi, Bales, Grunewald, & Krubitzer, 2010; Charbonneau et al., 2012; Laramée, Kurotani, Rockland, Bronchti, & Boire, 2011; Larsen, Luu, Burns, & Krubitzer, 2009; Sieben, Roder, & Hanganu-Opatz, 2013; Wang & Burkhalter, 2007). De manière similaire à notre première étude, des neurones rétrogradement marqués ont été quantifiées après des injections de traceur rétrograde dans V1 chez la souris (Charbonneau et al., 2012) et dans le cortex auditif primaire de la gerbille (Budinger & Scheich, 2009). Les résultats de ces deux études et de notre première étude démontrent que chez les rongeurs, V1 reçoit plus de projections des cortex dédiées aux autres modalités sensorielles. Ainsi, V1 serait le cortex sensoriel primaire le plus multisensoriel comparativement au cortex auditif primaire qui ne reçoit que peu de projections des autres cortex sensoriels primaires (Budinger & Scheich, 2009; Henschke et al., 2014). Ces observations suggèrent que les influences mutuelles entre les sens ne sont pas équivalentes en force. L'influence du cortex auditif primaire sur V1 serait plus forte que les autres influences observées entre les cortex sensoriels primaires.

Les voies les plus rapides vers S1

La combinaison de l'information des différentes modalités sensorielles réduit les temps de réaction (Hoefer et al., 2013; Molholm et al., 2002; Noesselt et al., 2010; Teder-Salejarvi, McDonald, Di, & Hillyard, 2002), ce qui peut être crucial pour la survie

de l'individu. En effet, les interactions audiosomatosensorielle (Hoefer et al., 2013) et visuosomatosensorielles (Macaluso, 2006) doivent être traitées rapidement dans leur réseau intermodal respectif. Afin d'éliciter des réponses avec un très court temps de latence, les voies neuroanatomiques qui transportent l'information sensorielle intermodale vers les cortex sensoriels primaires doivent être très courtes et doivent couvrir le moins de synapses possible. Parmi les trois sources, les deux voies les plus rapides vers les cortex sensoriels primaires seraient les afférences acheminés par les connexions thalamocorticales provenant du thalamus et les connexions corticocorticales directes entre les cortex sensoriels primaires (Budinger et al., 2006; Cappe, Rouiller, & Barone, 2009; Kayser, Petkov, Augath, & Logothetis, 2005; Schroeder et al., 2003; Sieben et al., 2013). Les résultats de notre première étude suggèrent qu'il existe effectivement des connexions entre le champ de tonneaux, des noyaux thalamiques et des cortex sensoriels primaires des autres modalités, et que ce serait le moyen le plus rapide, et donc le plus efficace de transmettre des informations sensorielles des autres modalités vers S1BF.

Les voies descendantes des aires associatives vers S1

Les trois parties de S1 reçoivent des afférences de plusieurs aires associatives et multisensorielles d'ordre supérieur, telles que les cortex pariétal et temporal associatifs, les cortex rétrospléniaux agranulaire et granulaire, et les cortex ectorhinal, périrhinal, orbital et insulaire. S1 reçoit donc des afférences de plusieurs sources différentes par le biais des voies descendantes. De plus, la distribution laminaire des neurones

rétrogradement marqués suggère que S1 chez la souris, reçoit des projections de type *feedback* de ces aires. Ces différentes aires pourraient avoir un rôle de modulation, mais à différent degré étant donné que les indices laminaires, même si dans l'ensemble négatif, l'étaient à différents degrés. Ces projections de type *feedback* pourraient moduler l'information dans le cortex somatosensoriel primaire (Bullier, 2001), de sorte que les signaux ascendants deviennent consciemment accessibles (Tononi & Koch, 2008). En effet, S1 aurait un rôle clé dans le codage prédictif qui est le processus d'appariement du système nerveux entre l'information sensorielle des stimuli tactiles acheminée par les signaux ascendants et les attentes envers l'environnement généré à l'interne par les signaux descendants (Grossberg, 1980; Lee & Mumford, 2003; Llinas & Pare, 1991).

Spécificité des espèces aux niveaux des connexions entre aires primaires : rongeurs vs non-rongeurs

Bien que la connectivité d'un cortex sensoriel primaire à un autre cortex sensoriel primaire ait récemment reçu beaucoup d'attention (pour revue, voir Meredith & Lomber, 2016), la littérature démontre clairement l'existence de la connectivité corticocorticale entre aires primaires de différentes modalités chez les rongeurs (pour revue, voir Henschke et al., 2014), mais il existe peu de preuves cohérentes chez les non-rongeurs tels que les carnivores et les primates non-humains. L'une des principales sources d'erreur dans l'interprétation de la littérature originale est l'ambiguïté dans la définition de ce qu'est un cortex sensoriel primaire. Le terme A1 par exemple, n'est pas interchangeable avec le terme cortex auditif ou cortex auditif de bas niveau. Il semble

intuitif que, pour les animaux avec un cortex de plus grande taille, il y ait simplement plus de tissus et plus de régions à partir desquelles les projections vers les aires primaires pourraient survenir. Effectivement, il est possible que l'évolution de nouvelles aires corticales chez les non-rongeurs offre des représentations élargies des capacités de traitement contenues dans les cortex sensoriels primaires chez les rongeurs. Il est également possible que la dépendance comportementale des carnivores et des primates sur certains sens la vision et l'ouïe, comparativement aux rongeurs qui dépendent plus du toucher peut également contribuer à la distinction entre leurs cortex primaires. Néanmoins, toutes les espèces doivent faire face à un environnement sensoriel complexe et il existe une littérature considérable qui documente des projections corticales d'aire de niveau supérieur (non primaire) vers les cortex sensoriels primaires d'une autre modalité qui pourraient remplir la même fonction que les connexions entre cortex sensoriels primaires de différentes modalités vues chez les rongeurs.

Objectif 2 : Les connexions corticocorticales directes et réciproques entre le cortex visuel et somatosensoriel primaire de la souris

Le deuxième objectif de cette thèse était d'étudier la microcircuiterie des connexions corticocorticales directes et réciproques entre les cortex visuel et somatosensoriel primaires de la souris afin de mieux comprendre comment deux modalités s'influencent mutuellement. L'étude de la morphologie des axones et de leurs boutons terminaux a aussi permis d'en apprendre davantage sur la fonction de ces connexions.

La position hiérarchique des cortex sensoriels primaires

L'asymétrie des connexions réciproques entre les aires corticales est à la base de l'établissement des niveaux hiérarchiques dans le cortex (Coogan & Burkhalter, 1993; Felleman & Van Essen, 1991; Hilgetag, O'Neill, & Young, 2000; Markov et al., 2014; Rockland & Pandya, 1979). Il est aussi généralement cru que si une voie est descendante, la voie réciproque sera ascendante, et si une projection est latérale, son homologue devrait également être latéral (Felleman & Van Essen, 1991).

Étant donné que les cortex sensoriels primaires sont les portails d'entrée du cortex pour les voies sensorielles ascendantes de chaque modalité provenant du thalamus, on aurait pu s'attendre à ce que V1 et S1 soient positionnés au même niveau dans la hiérarchie et réciproquement connectés par des projections latérales symétriques. Nos résultats démontrent que ce n'est pas le cas. La projection de S1BF vers V1 serait de type *feedback* alors que la projection réciproque de V1 vers S1BF serait de type latéral. Cette asymétrie suggère que ces deux cortex sensoriels primaires ne sont pas au même niveau dans la hiérarchie corticale.

Chez la gerbille et la souris, le cortex visuel primaire reçoit des projections *feedback* à la fois du cortex auditif primaire et du cortex somatosensoriel primaire (Charbonneau et al., 2012; Henschke et al., 2014). Chez la gerbille, ces projections sont en réciprocité avec une projection *feedforward* vers le cortex auditif et une projection latérale vers le cortex somatosensoriel tandis que le cortex auditif primaire et le cortex somatosensoriel

primaire sont réciproquement connectés par des projections latérales (Henschke et al., 2014). Ces résultats et les nôtres suggèrent que le cortex auditif primaire et le cortex somatosensoriel primaire sont positionnés plus haut dans la hiérarchie corticale que le cortex visuel primaire, et possiblement au même niveau.

Notre étude est la première à comparer la réciprocité entre le marquage rétrograde et antérograde. La distribution laminaire des boutons terminaux antérogradement marqués démontre que les projections réciproques entre le cortex visuel primaire et le cortex somatosensoriel primaire ont toute les deux des caractéristiques d'une projection *feedback* (Coogan & Burkhalter, 1990, 1993). Dans la projection du champ de tonneaux vers le cortex visuel primaire, la distribution laminaire des neurones rétrogradement marqués et des boutons terminaux antérogradement marqués suggère que cette projection a des caractéristiques d'une projection *feedback.* Cependant, dans la projection du cortex visuel primaire vers le champ de tonneaux, la distribution laminaire des neurones rétrogradement marqués suggère que cette projection a des caractéristiques d'une projection latérale alors que la distribution laminaire des boutons terminaux antérogradement marqués suggère que cette projection a des caractéristiques d'une projection *feedback.* Cette contradiction pourrait être propre aux connexions corticocorticales entre les cortex sensoriels primaires et pourrait également suggérer que la classification dichotomique des projections corticales en type *feedforward* ou *feedback* n'est pas appropriée.

L'asymétrie du poids des projections

Le transport rétrograde de la sous-unité B de la toxine du choléra a démontré une projection plus forte de V1 vers S1 que de S1 vers V1. De manière similaire, une forte projection du cortex visuel primaire vers le cortex somatosensoriel primaire et une projection réciproque modérée a été démontrée chez la gerbille (Henschke et al., 2014). Chez la gerbille, le cortex visuel primaire a les plus fortes projections multisensorielles et reçoit des projections modérées et similaires du cortex auditif primaire et du cortex somatosensoriel primaire. D'un autre côté, le cortex somatosensoriel reçoit une forte projection du cortex visuel, mais seulement une faible projection du cortex auditif. Le cortex auditif primaire ne reçoit que des faibles projections des autres cortex sensoriels primaires (Henschke et al., 2014). Ces observations suggèrent que les influences mutuelles entre les sens ne sont pas équivalentes en force. Chez la souris, comme chez la gerbille, l'influence du cortex visuel sur le cortex somatosensoriel serait la plus forte.

L'asymétrie de la taille des boutons terminaux

L'asymétrie des projections réciproques entre V1 et S1 a également été observée dans la distribution de taille des boutons terminaux. Il y avait de gros boutons terminaux dans toutes les couches corticales du champ de tonneaux qui n'étaient pas présents dans le cortex visuel primaire.

La distribution de taille que nous avons obtenue dans notre deuxième étude emploie la même mesure que celle des connexions entre le cortex auditif primaire et secondaire

chez la souris (Covic & Sherman, 2011). Nous supposons que les gros boutons terminaux que nous avons observés dans la projection de V1 vers le champ de tonneaux reflètent la présence de réponses postsynaptiques de Classe 1 et que la grande population de petits terminaux, qui semble être prédominante dans les deux projections reflètent la présence de réponses postsynaptiques de Classe 2.

Dans les voies thalamocorticales et corticothalamiques, les réponses postsynaptiques de Classe 1 et de Classe 2 sont respectivement considérées comme inductrices et modulatrices (Lee & Sherman, 2008; Lee & Sherman, 2009a, 2009b; Petrof & Sherman, 2013; Reichova & Sherman, 2004; Sherman & Guillery, 1996, 1998, 2013a; Viaene et al., 2011a). Ce modèle de transmission glutamatergique stipule que la transmission de l'information sensorielle dépend des voies inductrices (Covic & Sherman, 2011; Sherman & Guillery, 2013a). Si tel est le cas, les résultats de notre deuxième étude démontrent que l'information visuelle est induite au cortex somatosensoriel tandis que l'information tactile a une influence modulatrice prédominante sur le cortex visuel.

L'asymétrie du diamètre des axones

Dans les projections corticothalamiques, il existe deux types très distincts d'axones (Sherman & Guillery, 2013a). Des axones de gros diamètre qui proviennent des neurones de la couche 5 et qui transmettent des réponses postsynaptiques de Classe 1 et des axones de petit diamètre qui proviennent des neurones de la couche 6 et qui

transmettent des réponses postsynaptiques de Classe 2 (Bourassa et al., 1995; Bourassa & Deschenes, 1995; Sherman & Guillery, 2013b). Il n'y a aucun cas d'axone dans nos résultats avec seulement de gros boutons comme les axones corticothalamiques de gros diamètre. Plusieurs axones dans notre échantillon n'avaient que de très petits boutons alors que d'autres avaient un large éventail de taille de boutons. Sur ces axones, les très petits boutons étaient plus nombreux que les gros. Ces résultats suggèrent qu'il y aurait deux types distincts d'axones, sur la base de la présence ou de l'absence des gros boutons. De plus, les axones qui entraient dans S1BF étaient significativement plus gros que les axones qui entraient dans V1. Il y avait quelques axones très gros qui n'ont jamais été observés dans la projection vers V1, ce qui démontre encore une fois que ces connexions sont asymétriques. Une étude a démontré que les projections corticocorticales vers différentes cibles peuvent avoir des axones de diamètre différent (Innocenti, Vercelli, & Caminiti, 2014). Nos résultats démontrent que les deux projections sont principalement constituées d'une population d'axones assez mince avec la projection vers V1 ayant les axones plus minces et la projection vers S1BF ayant les axones de plus gros calibre. Le diamètre des axones est directement lié à leur vitesse de conduction, ce qui suggère que certains axones dans la projection vers S1BF ont une vitesse de conduction plus rapide que ceux dans la projection réciproque.

L'hypothèse de la précision des modalités sensorielles

La présence de gros boutons terminaux dans le champ de tonneaux et leur absence dans le cortex visuel primaire suggère que l'influence inductrice de V1 sur S1 n'est pas

réciproque. Cette asymétrie pourrait refléter l'influence inductrice de la vision sur la détection et la navigation tactile médiée par les vibrisses chez la souris, et l'importance relative des différentes modalités sensorielles chez les rongeurs qui dépendent moins des stimuli visuels par rapport aux primates (Whishaw & Kolb, 2004). En effet, le bénéfice des interactions multisensorielles serait plus grand pour certaines modalités sensorielles (Hollensteiner, Pieper, Engler, Konig, & Engel, 2015). L'hypothèse de la précision des modalités sensorielles stipule que la résolution des divergences entre les modalités se fera en faveur de la plus précise des deux (Welch & Warren, 1986). Cette hypothèse est basée sur un ordre de dominance entre les modalités qui s'appuie sur leur précision spatiale respective. Ainsi, les vibrisses sont spatialement plus précises dans la détection et la navigation que la vision pour les rongeurs chez qui leur acuité tactile dépasse largement leurs capacités de discrimination visuelle (Carvell & Simons, 1990; Prusky, West, & Douglas, 2000; Wu, Ioffe, Iverson, Boon, & Dyck, 2013). On s'est donc questionné sur comment cet aspect de la dominance des modalités sensorielles pourrait se refléter chez l'humain qui dépend plus des stimuli visuels comparativement aux rongeurs. Une étude a démontré que lorsque l'on varie le degré de congruence spatiale entre ce que l'on voie et ce que l'on entend, la vision domine l'audition dans ce qui est connu comme l'effet de la ventriloquie (Shams & Beierholm, 2010). De plus, dans une tâche d'identification d'objet, des études ont démontré que la vision domine le toucher (Gori, Del, Sandini, & Burr, 2008; Gori, Sandini, & Burr, 2012). On pourrait donc s'attendre à retrouver des connexions avec une influence inductrice de S1 et A1 vers V1 dont les connexions réciproques auraient une influence modulatrice chez l'humain.

Les prothèses

La connaissance des mécanismes d'interactions visuotactiles et d'influence mutuelle entre la modalité visuelle et somatosensorielle est applicable au sentiment de propriété du corps, à l'illusion de la main en caoutchouc, et à la recherche sur les prothèses. Le sentiment de propriété du corps se réfère à l'état perceptif particulier qui identifie les différentes parties de notre corps comme étant les nôtres. Cette autoattribution est médiée par des interactions multisensorielles (Botvinick & Cohen, 1998; Rochat, 1998; van den Bos & Jeannerod, 2002). L'autoattribution de notre main par exemple, dépend de l'interaction entre la vision de la main et le *feedback* tactile.

L'illusion de la main en caoutchouc est une illusion perceptive qui suscite un sentiment de propriété d'une main étrangère en caoutchouc (Botvinick & Cohen, 1998). Elle peut être induite quand une fausse main d'apparence réaliste est placée à la vue de l'individu, et est touchée tout en touchant synchroniquement la main de cet individu, qui est caché de sa vue (voir Figure 37). Plus précisément, il a été démontré que, après les stimulations visuotactiles synchrones, l'emplacement perçu de la main de l'individu est décalé vers la main en caoutchouc.

Cette illusion ne se produit pas lorsque la main en caoutchouc et la main de l'individu sont touchées de manière asynchrone, à savoir lorsque le décalage temporel est de plus de 300 ms (Shimada, Fukuda, & Hiraki, 2009), selon le principe de contiguïté temporelle des interactions multisensorielles rapportées dans la littérature.

Une étude antérieure a démontré que l'illusion de la main en caoutchouc entraine un recalibrage des représentations proprioceptives dans l'espace péripersonnel (Ehrsson, Spence, & Passingham, 2004), et une autre a démontré l'implication du cortex somatosensoriel primaire dans cette illusion (Schaefer, Flor, Heinze, & Rotte, 2007).

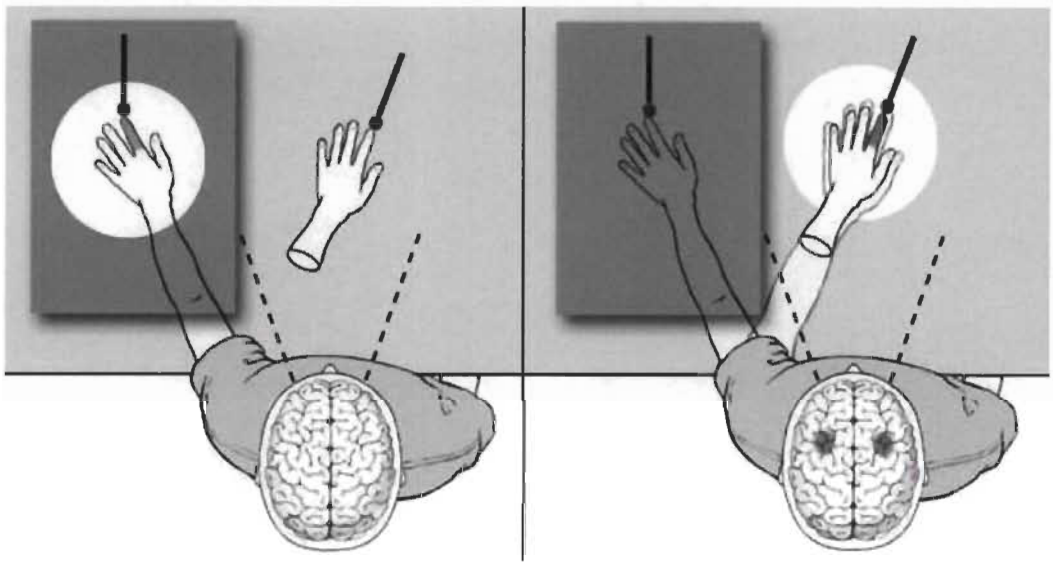

Figure 37. L'illusion de la main en caoutchouc (Botvinick & Cohen, 1998).

Pour que l'illusion se produise, les signaux ascendants, tels que les afférences visuelles et tactiles, doivent prendre le dessus sur les signaux descendants, telles que les attentes que la main étrangère en caoutchouc ne fasse pas partie de notre corps (Slater, Spanlang, Sanchez-Vives, & Blanke, 2010). L'illusion de la main en caoutchouc est une découverte particulièrement intéressante pour la recherche sur les prothèses, soit la restauration des fonctions motrices et sensorielles d'un membre perdu avec un substitut artificiel qui est ressenti et agit comme un membre organique. Une étude antérieure a démontré qu'il est possible d'induire l'illusion chez des amputés en touchant des points

spécifiques sur le membre restant (Ehrsson et al., 2008). L'étude suggère que des effets similaires pourraient être obtenus avec une prothèse et des capteurs artificiels qui fournissent un *feedback* tactile synchrone grâce à une gamme de stimulateurs tactiles sur le moignon. La prothèse envisagée avec un tel *feedback* tactile jumelé au contrôle visuel, pourrait être plus facilement incorporé dans l'espace péripersonnel ce qui pourrait en retour améliorer son contrôle volontaire (Childress, 1973).

Comme nous l'avons vu dans les résultats de notre deuxième étude, l'asymétrie reflétée dans la plus grande influence de la vision sur la détection et la navigation tactile médiée par les vibrisses chez la souris démontre l'importance relative des différentes modalités sensorielles chez les rongeurs qui dépendent moins des stimuli visuels par rapport aux primates (Whishaw & Kolb, 2004). L'humain dépend plus des stimuli visuels par rapport aux rongeurs, ce qui est reflété dans la dominance de la vision sur les autres modalités sensorielles (Gori et al., 2008, 2012; Shams & Beierholm, 2010). Le bénéfice des interactions visuotactiles serait donc plus grand pour la modalité visuelle (Hollensteiner et al., 2015), car chez l'humain, l'acuité visuelle est spatialement plus précise dans la détection et la navigation, et dépasse largement leurs capacités de discrimination tactile (Witten & Knudsen, 2005). Le *feedback* tactile synchrone fourni par une prothèse et des capteurs artificiels serait donc important dans la résolution des divergences entre la modalité visuelle et somatosensorielle basée sur la dominance de la vision (Welch & Warren, 1986). Les divergences lors de l'illusion de la main en caoutchouc seraient entre les signaux ascendants et descendants. Les signaux ascendants

dans l'illusion de la main en caoutchouc seraient en fonction de la synchronisation entre les stimuli visuels et tactiles (Armel & Ramachandran, 2003). Les signaux descendants dans cette illusion seraient plutôt en fonction de la position anatomiquement correcte de la prothèse par rapport à un vrai membre, et de l'apparence réaliste de celle-ci (Ehrsson et al., 2004; Pavani, Spence, & Driver, 2000; Tsakiris & Haggard, 2005). Des stimuli asynchrones dans le premier cas ou une apparence artificielle dans le second pourraient inhiber l'illusion et donc l'utilisation de la prothèse chez l'amputé.

Les interfaces humain-robot

La connaissance des mécanismes d'interactions visuotactiles et de l'influence mutuelle entre la modalité visuelle et somatosensorielle est aussi applicable à l'utilisation d'outils. L'utilisation d'outils permet d'étendre le champ d'interaction avec l'environnement et l'espace péripersonnel (Goldenberg & Spatt, 2009; Peeters et al., 2009). Les progrès récents dans le domaine de la robotique ont attiré l'attention sur une catégorie spécifique d'outils, les interfaces humain-robot. Les outils robotiques, tels que les robots chirurgicaux sont conçus pour fonctionner à des endroits éloignés ou dans des environnements virtuels sous un contrôle humain direct (Rosen, Hannaford, & Satava, 2011; Suematsu & del Nido, 2004). Ces outils sans précédent augmentent considérablement la précision, la force et l'accessibilité de la manipulation humaine sur le corps humain ou dans certains systèmes industriels. Avec de tels dispositifs, l'utilisateur détecte les positions et les mouvements de la cible et envoie ces informations à un robot qui est en contact avec l'environnement à distance

(Stone, 2000). Les chirurgiens interagissent maintenant fréquemment avec ces robots pour effectuer des tâches complexes, telles que les chirurgies laparoscopiques (Kenngott et al., 2012; Rassweiler, Safi, Subotic, Teber, & Frede, 2005; Tavakoli, Aziminejad, Patel, & Moallem, 2007). Le but de ces robots est d'augmenter l'immersion entre le chirurgien et l'environnement à distance, ainsi que la précision et l'intuitivité de l'utilisation du système (Octavia, Raymaekers, & Coninx, 2011). En dépit des avancées dans le domaine de la robotique, l'étude des interfaces humain-robot en est encore à ses débuts et peu d'attention a été accordée à l'influence des différentes modalités qui contribuent à l'extension d'un corps et de son espace péripersonnel lors de l'utilisation d'outils (Moizumi, Yamamoto, & Kitazawa, 2007; Sengul et al., 2012, 2013).

La représentation neuronale de l'espace péripersonnel est encodée par l'interaction multisensorielle de la vision et du toucher dans plusieurs aires dont les cortex sensoriels primaires (Ladavas & Serino, 2008; Schaefer, Heinze, & Rotte, 2012). La vision spécifie la position d'une cible et le toucher transforme cette position en une commande motrice appropriée pour l'atteindre (Rizzolatti et al., 1981a, 1981b). La représentation neuronale de l'espace péripersonnel est très plastique et plusieurs études chez les humains et les primates ont démontré qu'elle peut s'étendre pour inclure des outils (Iriki, Tanaka, & Iwamura, 1996; Maravita, 2006; Maravita & Iriki, 2004). Nos résultats ont démontré que la vision transmet l'information sensorielle au cortex somatosensoriel primaire et que ce dernier module cette information en retour. Dans le cas d'une interface humain-robot, le transfert d'information visuelle se fait dans un sens, mais il n'y a pas de *feedback* tactile

pour moduler cette information. Nos résultats suggéreraient que l'ajout de *feedback* tactile, comme une vibration par exemple, contribuerait à l'immersion de l'utilisateur dans l'environnement à distance et rendrait ces outils plus faciles à intégrer dans l'espace péripersonnel. Une telle perspective de recherche dans la conception des interfaces humain-robot serait à considérer. Par conséquent, la réconciliation des domaines de la neuroscience tels que les neurosciences comportementales et la neuroanatomie est importante pour comprendre tous les aspects de l'espace péripersonnel. Les résultats de notre deuxième étude fournissent des données importantes sur les influences réciproques entre la vision et le toucher au niveau de la partie caudale du champ de tonneaux du cortex somatosensoriel primaire et du cortex visuel primaire, ce qui représente une étape importante de la recherche sur l'utilisation d'outils tels que les robots chirurgicaux et la plasticité de la représentation neuronale de l'espace péripersonnel.

Objectif 3 : Effets de l'énucléation sur les connexions corticocorticales directes et réciproques entre le cortex visuel et somatosensoriel primaire de la souris

Le troisième et dernier objectif de cette thèse était d'étudier l'impact de la perte de la vision sur la microcircuiterie des connexions entre V1 et S1 à l'aide d'un échantillon de souris énucléées à la naissance et de souris intactes. L'étude plus poussée de la structure des connexions entre V1 et S1 a permis de mieux comprendre comment les connexions entre deux cortex sensoriels primaires sont altérées par la perte d'un sens, car peu d'études se sont consacrées aux efférences du cortex visuel vers les aires des autres modalités sensorielles suite à la perte de la vision. En effet, les conséquences de la

cécité sur les modalités intactes est devenu l'objet d'études que récemment (Bavelier & Neville, 2002; Merabet & Pascual-Leone, 2010).

Il était auparavant suggéré que la plasticité intermodale dans les aires déprivées était le résultat du développement de nouvelles projections provenant d'aires des autres modalités ou du démasquage de projections existantes (Rauschecker, 1995). À cette époque, le paradigme dominant en matière d'organisation sensorielle corticale considérait les cortex sensoriels primaires comme étant seulement habileté à traiter les informations de leur propre modalité (Felleman & Van Essen, 1991; Jones & Powell, 1970; Paperna & Malach, 1991). Dans ce contexte, si un cortex sensoriel primaire venait à perdre sa source d'activation, la plasticité intermodale qui s'en suit serait le résultat du développement de nouvelles projections. Cependant, une multitude d'études récentes ont démontré qu'il y a des connexions corticocorticales directes et réciproques entre les cortex sensoriels primaires même lorsque l'ensemble des modalités sensorielles est intact.

C'est pourquoi notre troisième étude s'est intéressée davantage au mécanisme de la réorganisation des circuits corticaux intermodaux de la plasticité intermodale qui implique l'amplification ou la diminution des connexions. Les résultats de notre troisième étude confirment que l'énucléation réduit le poids de la projection de S1 vers V1 tel que démontré précédemment (Charbonneau et al., 2012). De plus, nos résultats démontrent que l'énucléation réduit l'étendue de taille des boutons terminaux et des

axones de la projection du cortex visuel vers le cortex somatosensoriel. La diminution de l'étendue de taille des boutons terminaux dans la projection de V1 vers S1 chez les souris énucléées suggère que l'influence de V1 sur S1 est modifiée par l'énucléation. Notre troisième étude démontre que la cécité entraine des modifications neuroanatomiques dans les connexions corticocorticales intermodales entre le cortex visuel et somatosensoriel primaire chez la souris.

Les effets de la cécité sur le poids des projections

Nos résultats confirment que l'énucléation réduit le poids des projections somatosensorielles vers V1 (Charbonneau et al., 2012), et montrent pour la première fois qu'elle n'a aucun effet sur le poids des projections visuelles vers S1. Cette conséquence de la cécité pourrait être spécifique au toucher étant donné que le nombre de neurones projetant de A1 vers V1 n'était pas significativement différent entre les souris intactes et énucléées (Charbonneau et al., 2012), de même que le nombre de neurones projetant de V1 vers S1 comme le démontrent nos résultats. De même, l'absence d'activité somatosensorielle suivant la coupe des vibrisses durant les cinq premiers jours après la naissance diminue significativement les afférences visuelles vers le cortex somatosensoriel primaire chez le rat (Sieben et al., 2015). Cette étude démontre également une diminution fonctionnelle de cette projection. Des études antérieures ont également démontré une connectivité fonctionnelle diminuée entre le cortex visuel et le cortex somatosensoriel ainsi que le cortex moteur et les aires multisensorielles temporales chez les humains aveugles (Liu et al., 2007; Yu et al., 2008). Les

changements observés chez l'humain au niveau de la connectivité fonctionnelle ne s'expliquent toutefois par nécessairement par des changements anatomiques qui vont dans le même sens.

Nos résultats penchent en faveur de l'hypothèse de la diminution des connexions existantes entre les aires visuelles et les aires des autres modalités sensorielles. Les capacités non visuelles exacerbées chez les aveugles ne peuvent donc pas s'expliquer par une amplification des connexions corticocorticales entre les cortex sensoriels primaires. Les individus aveugles sont pourtant plus performants que les individus voyants pour localiser des sons périphériques (Despres, Candas, & Dufour, 2005; Fieger, Roder, Teder-Salejarvi, Hillyard, & Neville, 2006; Roder et al., 1999; Voss et al., 2004), ou des stimuli monauraux (Gougoux, Zatorre, Lassonde, Voss, & Lepore, 2005; Lessard, Pare, Lepore, & Lassonde, 1998; Voss, Gougoux, Zatorre, Lassonde, & Lepore, 2008). Ils ont aussi une meilleure résolution temporelle de détection des stimuli auditifs (Stevens & Weaver, 2005) et peuvent discriminer plus facilement des variations de fréquence sonore (Gougoux et al., 2004). Quant aux informations somatosensorielles, en plus de posséder une meilleure résolution spatiale pour la détection des stimuli tactiles (Van Boven, Hamilton, Kauffman, Keenan, & Pascual-Leone, 2000) les aveugles détectent plus facilement des stimuli vibrotactiles (Wan, Wood, Reutens, & Wilson, 2010) que les individus voyants. Finalement, ils démontrent aussi des performances améliorées pour la détection (Beaulieu-Lefebvre, Schneider, Kupers, & Ptito, 2011; Cuevas, Plaza, Rombaux, De Volder, & Renier, 2009) et l'identification (Cuevas et

al., 2009; Rosenbluth, Grossman, & Kaitz, 2000) de stimuli olfactifs. Les résultats d'une étude antérieure de Collignon et collègues publiés dans la revue Brain (2013) ont suggéré que les aveugles précoces utilisent des connexions corticocorticales entre les aires sensorielles primaires pour traiter l'information auditive au sein du cortex visuel, alors que les aveugles tardifs utiliseraient plutôt des connexions corticocorticales provenant des aires associatives.

Les effets de la cécité sur la nature des projections

La nature de la projection de S1 vers V1 en termes de la distribution laminaire des neurones rétrogradement marqués (Felleman & Van Essen, 1991; Rouiller & Welker, 1991), a changé pour une distribution beaucoup plus infragranulaire chez les souris énucléées à la naissance. Un mécanisme qui pourrait expliquer la diminution du nombre de neurones dans les couches supragranulaires et leur augmentation dans les couches infragranulaires dans la projection de V1 vers S1 observées chez les cas énucléés pourrait être celui du raffinement des projections reliant les aires corticales grâce à l'élimination sélective des connexions initialement surabondantes (Batardiere et al., 2002; Kennedy, Bullier, & Dehay, 1989). Des études ont testé si l'élimination sélective des connexions joue un rôle fondamental dans la formation de l'organisation hiérarchique du cortex. Chez les primates, la distribution laminaire des neurones des connexions corticocorticales émerge à un stade précoce où il y a un excès de neurones dans les couches supragranulaires. Dans le développement de ces connexions, il y a une augmentation concomitante du nombre de neurones infragranulaires et une diminution

des neurones supragranulaires. Les résultats de notre troisième étude, bien que chez la souris, suggéreraient qu'il y a une diminution excessive du nombre de neurones dans les couches supragranulaires. On aurait donc ici un développement aberrant de la projection de S1 vers V1.

Tel que mentionné précédemment, peu d'études se sont consacrées aux effets de la cécité sur les efférences de V1. Certaines études ont toutefois démontré que l'expérience sensorielle affecte l'organisation des circuits corticaux dans le système visuel et les efférences de V1 vers les aires extrastriées. Il a été démontré chez les rats énucléés à la naissance que l'activité visuelle était nécessaire pour le développement normal des connexions striées-extrastriées. Chez les cas énucléés à la naissance, le schéma de distribution des projections de V1 vers les aires extrastriées était aberrant et la cécité a entrainé un élargissement anormal des champs de projection (Bravo & Inzunza, 1994; Laing, Bock, Lasiene, & Olavarria, 2012; Laramée et al., 2011). Ces résultats mettent en évidence une diminution de la spécificité de la topographie des connexions striées-extrastriées des aveugles. D'autres études de traçage démontrent également une vaste réorganisation des connexions corticocorticales préexistantes entre les cortex sensoriels primaires chez les opossums énucléés (Karlen, Kahn, & Krubitzer, 2006), les souris ayant une déficience visuelle (Larsen et al., 2009) et les humains aveugles (Klinge et al., 2010).

Les effets de la cécité sur la taille des boutons et des axones

Les effets de la déprivation visuelle sur les connexions corticocorticales entre le cortex visuel primaire et le cortex somatosensoriel primaire ont également été observés dans l'étendue de taille des boutons terminaux et des axones. Les gros boutons terminaux observés dans le champ de tonneaux chez les cas intacts ne sont plus présents chez les cas énucléés. Le modèle de la transmission glutamatergique stipule que le transfert de l'information sensorielle dépend des réponses synaptiques de Classe 1 (Covic & Sherman, 2011; Sherman & Guillery, 2013b). Cependant, l'identification des réponses postsynaptiques en tant que Classe 1 ou Classe 2 sur la base de la taille des boutons terminaux doit être faite parcimonieusement. En effet, bien que l'on sache que l'activité sensorielle joue un rôle important dans la détermination de la taille d'une synapse (Harris & Sultan, 1995; Pierce & Lewin, 1994; Schikorski & Stevens, 1997, 1999), l'absence de gros boutons terminaux dans le champ de tonneaux suite à l'énucléation ne signifierait pas systématiquement l'absence de réponses postsynaptiques de Classe 1. En conséquence à l'absence d'activité visuelle dans le cortex visuel primaire, celui-ci ne serait plus en mesure de transmettre de l'information visuelle au cortex somatosensoriel primaire, ce qui pourrait entrainer une diminution de la taille des boutons terminaux associés aux réponses postsynaptiques de Classe 1 sans pour autant signifier leur disparition totale. Si tel est le cas, les résultats de notre troisième étude suggèrent que l'influence inductrice du cortex visuel primaire vers le champ de tonneaux du cortex somatosensoriel primaire est diminuée par l'énucléation et l'absence d'activité visuelle qui en découle dans le cortex visuel primaire.

La déprivation sensorielle n'affecte pas seulement la taille des boutons terminaux, il a également été démontré qu'elle affecte la densité des boutons sur les neurones excitateurs et inhibiteurs du cortex visuel et somatosensoriel (Marik, Yamahachi, McManus, Szabo, & Gilbert, 2010; Marik, Yamahachi, Meyer zum Alten, & Gilbert, 2014). Une augmentation de la densité totale des boutons terminaux a été démontrée sur les neurones excitateurs dans les aires déprivées tandis qu'une diminution de la densité totale des boutons terminaux a été démontrée sur les neurones inhibiteurs dans les aires déprivées. Même si un grand nombre de questions demeurent sur les mécanismes de la transmission synaptique glutamatergique, nos résultats suggèrent que l'activité sensorielle et certaines caractéristiques neuroanatomiques des axones tels que la taille de leurs boutons terminaux sont corrélées.

L'énucléation avait également diminué significativement le diamètre des axones dans S1 suite aux injections dans V1. Le diamètre des axones est une variable importante dans la détermination de la vitesse de conduction. Tout comme la longueur, cette variable détermine les délais de transmission et la synchronisation des impulsions aux différentes cibles d'un axone individuel (Tomasi, Caminiti, & Innocenti, 2012). Autrement dit, plus le diamètre d'un axone est gros, plus les potentiels d'action seront rapidement transmis entre les aires corticales. Les projections corticocorticales comprennent des axones de diamètres différents dépendant de leur source et des aires corticales qu'elles ciblent (Anderson & Martin, 2002; Caminiti, Ghaziri, Galuske, Hof, & Innocenti, 2009; Caminiti et al., 2013; Innocenti et al., 2014; Tomasi et al., 2012). Peu

d'études ont examiné l'effet de l'activité sensorielle sur le diamètre des axones dans les connexions corticocorticales. Nos résultats ont démontré que la cécité peut diminuer le diamètre des axones projetant à partir d'une aire déprivée vers une aire non déprivée et peut augmenter le diamètre des axones projetant à partir d'une aire non déprivée vers une aire déprivée. En d'autres termes, suivant la déprivation visuelle, la projection de V1 vers S1 perdrait beaucoup de sa vitesse de conduction, ce qui est cohérent avec ce qui a été vu dans l'étendue de taille des boutons terminaux chez les cas énucléés. Le Tableau 19 résume les caractéristiques qui différencient les projections entre V1 et S1.

Tableau 19

Résumé des caractéristiques des projections entre V1 et S1

	Projection de V1 vers S1	Projection de S1 vers V1
Caractéristiques anatomiques	Poids relatif plus grand	Poids relatif plus petit
	Projection de type latéral selon le marquage rétrograde	Projection de type *feedback* selon le marquage rétrograde
	Projection de type *feedback* selon le marquage antérograde	Projection de type *feedback* selon le marquage antérograde
	Influence inductrice	Influence modulatrice
	Axones avec un gros diamètre	Axones avec un petit diamètre
	Axones avec une large étendue de taille de boutons terminaux	Axones avec seulement des petits boutons terminaux
Effets de l'énucléation	Aucun effet sur le poids relatif	Diminue le poids relatif
	Diminue la taille des boutons terminaux et des axones	

Conclusion

Les résultats des trois études présentés dans cette thèse ont une signification importante dans le contexte des connaissances actuelles sur les interactions multisensorielles et la hiérarchie des sens. Notre première étude démontre que le traitement effectué dans un cortex sensoriel primaire tel que le cortex somatosensoriel primaire est effectivement plus complexe que ce qui était initialement cru (Felleman & Van Essen, 1991; Jones & Powell, 1970; Mesulam, 1998), et qu'il implique l'information sensorielle provenant des autres modalités et l'information non sensorielle. Sa position à mi-chemin entre les voies sensorielles ascendantes provenant du thalamus et les voies sensorielles descendantes provenant des aires corticales associatives multisensorielles suggérait que ce cortex sensoriel primaire a un rôle clé dans le traitement de l'information axé sur le stimulus et le traitement de l'information sur la tâche.

Nos résultats ont entre autres démontré que les informations des modalités auditives et visuelles atteignent le champ de tonneaux à partir de trois sources. D'une part il y a les connexions thalamocorticales provenant de certains noyaux thalamiques propices aux interactions multisensorielles et il y a les connexions corticocorticales directes provenant du cortex auditif et visuel primaire. D'autre part, il y les connexions corticocorticales de type *feedback* provenant de plusieurs aires associatives et multisensorielles d'ordre supérieur. Dans le premier cas, ces connexions seraient le moyen le plus rapide et le plus

efficace de transmettre les informations sensorielles des autres modalités vers le cortex somatosensoriel primaire (Budinger et al., 2006; Cappe et al., 2009; Kayser et al., 2005; Schroeder et al., 2003; Sieben et al., 2013). Dans le dernier cas, ces connexions permettraient de moduler l'information acheminée par le thalamus dans le cortex somatosensoriel primaire (Bullier, 2001; Tononi & Koch, 2008), et lui conférerait un rôle clé dans le codage prédictif qui est le processus d'appariement du système nerveux entre l'information sensorielle des stimuli acheminée par les signaux ascendants et les attentes envers l'environnement généré à l'interne par les signaux descendants (Grossberg, 1980; Lee & Mumford, 2003; Llinas & Pare, 1991). Ces signaux descendants suffiraient à construire un percept sensoriel consciemment accessible dans le cortex somatosensoriel primaire même en l'absence de stimuli externes provenant des organes sensoriels (Kosslyn, Thompson, Kim, & Alpert, 1995; Kraemer, Macrae, Green, & Kelley, 2005; Le et al., 1993; Yoo, Freeman, McCarthy, III, & Jolesz, 2003; Yoo, Lee, & Choi, 2001).

Notre deuxième étude démontre que les connexions entre les cortex visuel et le cortex somatosensoriel primaires, bien que réciproques, ne sont pas symétriques. En effet, la projection du champ de tonneaux du cortex somatosensoriel primaire vers le cortex visuel primaire est de type *feedback* et a une influence modulatrice prédominante alors que la projection réciproque est de type latéral et a plutôt une influence inductrice. Bien que l'on ait pu supposer que ces deux sensoriels primaires soient au même niveau initial dans la hiérarchie corticale et liée par des connexions réciproques symétriques

(Felleman & Van Essen, 1991), nos résultats démontrent que ce n'est pas le cas. Ces observations suggèrent que les influencent mutuelles entre les sens au niveau des cortex sensoriels primaires ne sont pas équivalente. Chez la souris, la vision serait plus importante pour l'amélioration de l'exploration tactile et que l'information tactile est moins importante pour l'amélioration de l'information visuelle. Comme on l'a vu précédemment, cette asymétrie pourrait refléter la plus grande influence de la vision sur la détection et la navigation tactile médiée par les vibrisses chez la souris, et l'importance relative des différentes modalités sensorielles chez les rongeurs qui dépendent moins des stimuli visuels par rapport aux primates (Whishaw & Kolb, 2004). En effet, le bénéfice des interactions multisensorielles serait plus grand pour certaines modalités sensorielles (Hollensteiner et al., 2015). Cet aspect de la dominance des modalités sensorielles se reflète chez l'humain qui dépend plus des stimuli visuels par rapport aux rongeurs avec la dominance de la vision sur l'audition et le toucher en cas de divergence (Gori et al., 2008, 2012; Shams & Beierholm, 2010). Si nous spéculons, ce serait donc le toucher qui viendrait améliorer la vision chez l'humain.

Notre troisième et dernière démontre l'impact de la cécité sur la microcircuiterie des connexions entre V1 et S1. Nos résultats démontrent que la perte de la vision entraine non seulement la réduction du poids de la projection du cortex visuel primaire vers le cortex somatosensoriel primaire, mais suggèrent aussi que la projection réciproque n'a plus d'influence inductrice. Si l'on se base sur le modèle de la transmission glutamatergique qui stipule que le transfert de l'information sensorielle dépend des

réponses synaptiques inductrices (Covic & Sherman, 2011; Sherman & Guillery, 2013b), l'information visuelle ne serait plus transmise à S1 suivant l'énucléation.

Cette thèse démontre l'originalité de la recherche effectuée dans les trois articles présentés. Notre première étude fait la démonstration qu'un cortex sensoriel primaire comme le cortex somatosensoriel primaire n'est pas limité au traitement unisensoriel. Cette étude se démarque des études antérieures et des projets de grandes envergures avec une analyse plus complète et détaillée sur les afférences du cortex somatosensoriel primaire. Cela est important, car on démontre ainsi que même avec moins de moyens que certains grands laboratoires travaillant dans le même domaine, on arrive à contribuer de manière significative aux connaissances sur la connectivité du cerveau de la souris. Notre deuxième étude fait la démonstration que les modalités sensorielles n'ont pas la même influence au niveau des cortex sensoriels primaires. Cette étude se démarque par l'étude de la morphologie des axones et de leurs boutons terminaux, deux aspects qui n'ont jamais été étudiés dans les connexions corticocorticales intermodales et qui ont permis d'en apprendre davantage sur la fonction de ces connexions. La méthodologie employée pour échantillonner les axones et les boutons terminaux a été conçue en partant de rien et a dû être mise à l'épreuve par essais et erreurs. Notre troisième et dernière étude fait la démonstration que la perte d'un sens entraine des modifications de la structure des connexions corticocorticales intermodales. Cette étude se démarque en étant sans précédent et en démontrant comment les connexions entre deux cortex sensoriels primaires sont altérées par la perte d'un sens. C'est pour toutes ces raisons que

cette thèse contribue de façon originale aux connaissances sur la microcircuiterie, la neuroanatomie, la connectivité entre les cortex sensoriels primaires, les interactions multisensorielles, la perception sensorielle et la cécité.

Références générales

Ahmed, B., Anderson, J. C., Douglas, R. J., Martin, K. A., & Nelson, J. C. (1994). Polyneuronal innervation of spiny stellate neurons in cat visual cortex. *Journal of Comparative Neurology, 341,* 39-49.

Allman, B. L., Keniston, L. P., & Meredith, M. A. (2009). Not just for bimodal neurons anymore: The contribution of unimodal neurons to cortical multisensory processing. *Brain Topography, 21,* 157-167.

Amlot, R., Walker, R., Driver, J., & Spence, C. (2003). Multimodal visual-somatosensory integration in saccade generation. *Neuropsychologia, 41,* 1-15.

Anderson, J. C., & Martin, K. A. (2002). Connection from cortical area V2 to MT in macaque monkey. *Journal of Comparative Neurology, 443,* 56-70.

Angelucci, A., Clasca, F., & Sur, M. (1996). Anterograde axonal tracing with the subunit B of cholera toxin: A highly sensitive immunohistochemical protocol for revealing fine axonal morphology in adult and neonatal brains. *Journal of Neuroscience Methods, 65,* 101-112.

Armel, K. C., & Ramachandran, V. S. (2003). Projecting sensations to external objects: evidence from skin conductance response. *Proceedings of the Royal Society of London: Biological, 270,* 1499-1506.

Bartlett, E. L., & Smith, P. H. (2002). Effects of paired-pulse and repetitive stimulation on neurons in the rat medial geniculate body. *Neuroscience, 113,* 957-974.

Bartlett, E. L., Stark, J. M., Guillery, R. W., & Smith, P. H. (2000). Comparison of the fine structure of cortical and collicular terminals in the rat medial geniculate body. *Neuroscience, 100,* 811-828.

Batardiere, A., Barone, P., Knoblauch, K., Giroud, P., Berland, M., Dumas, A. M. et al. (2002). Early specification of the hierarchical organization of visual cortical areas in the macaque monkey. *Cerebral Cortex, 12,* 453-465.

Bavelier, D., & Neville, H. J. (2002). Cross-modal plasticity: Where and how? *Nature Reviews Neuroscience, 3,* 443-452.

Bear, M. F., Connors, B. W., & Paradiso, M. A. (2007). *Neurosciences: Exploring the brain* (3^{e} éd.). Baltimore, MD: Lippincott Williams & Wilkins.

Beaulieu-Lefebvre, M., Schneider, F. C., Kupers, R., & Ptito, M. (2011). Odor perception and odor awareness in congenital blindness. *Brain Research Bulletin, 84,* 206-209.

Bizley, J. K., & King, A. J. (2008). Visual-auditory spatial processing in auditory cortical neurons. *Brain Research, 1242,* 24-36.

Bizley, J. K., Nodal, F. R., Bajo, V. M., Nelken, I., & King, A. J. (2007). Physiological and anatomical evidence for multisensory interactions in auditory cortex. *Cerebral Cortex, 17,* 2172-2189.

Blomqvist, A., Ericson, A. C., Broman, J., & Craig, A. D. (1992). Electron microscopic identification of lamina I axon terminations in the nucleus submedius of the cat thalamus. *Brain Research, 585,* 425-430.

Blumenfeld, H. (2010). *Neuroanatomy through clinical cases* (2e éd.). Sunderland, MA: Sinauer Associates, Inc.

Botvinick, M., & Cohen, J. (1998). Rubber hands 'feel' touch that eyes see. *Nature, 391,* 756.

Bourassa, J., & Deschenes, M. (1995). Corticothalamic projections from the primary visual cortex in rats: A single fiber study using biocytin as an anterograde tracer. *Neuroscience, 66,* 253-263.

Bourassa, J., Pinault, D., & Deschenes, M. (1995). Corticothalamic projections from the cortical barrel field to the somatosensory thalamus in rats: A single-fibre study using biocytin as an anterograde tracer. *Eur J Neurosci, 7,* 19-30.

Brandt, H. M., & Apkarian, A. V. (1992). Biotin-dextran: A sensitive anterograde tracer for neuroanatomic studies in rat and monkey. *Journal of Neuroscience Methods, 45,* 35-40.

Bravo, H., & Inzunza, O. (1994). Effect of pre- and postnatal retinal deprivation on the striate-peristriate cortical connections in the rat. *Biological Research, 27,* 73-77.

Brodal, P. (2010). *The central nervous system: Structure and function* (4e éd.). Oslo, Norvège: Oxford University Press.

Bruce, C., Desimone, R., & Gross, C. G. (1981). Visual properties of neurons in a polysensory area in superior temporal sulcus of the macaque. *Journal of Neurophysiology, 46,* 369-384.

Budinger, E., Heil, P., Hess, A., & Scheich, H. (2006). Multisensory processing via early cortical stages: Connections of the primary auditory cortical field with other sensory systems. *Neuroscience, 143,* 1065-1083.

Budinger, E., Laszcz, A., Lison, H., Scheich, H., & Ohl, F. W. (2008). Non-sensory cortical and subcortical connections of the primary auditory cortex in Mongolian gerbils: Bottom-up and top-down processing of neuronal information via field AI. *Brain Research, 1220,* 2-32.

Budinger, E., & Scheich, H. (2009). Anatomical connections suitable for the direct processing of neuronal information of different modalities via the rodent primary auditory cortex. *Hearing Research, 258,* 16-27.

Bullier, J. (2001). Integrated model of visual processing. *Brain Research Reviews, 36,* 96-107.

Calvert, G. A., & Thesen, T. (2004). Multisensory integration: Methodological approaches and emerging principles in the human brain. *Journal of Physiology - Paris, 98,* 191-205.

Caminiti, R., Carducci, F., Piervincenzi, C., Battaglia-Mayer, A., Confalone, G., Visco-Comandini, F. et al. (2013). Diameter, length, speed, and conduction delay of callosal axons in macaque monkeys and humans: Comparing data from histology and magnetic resonance imaging diffusion tractography. *Journal of Neuroscience, 33,* 14501-14511.

Caminiti, R., Ghaziri, H., Galuske, R., Hof, P. R., & Innocenti, G. M. (2009). Evolution amplified processing with temporally dispersed slow neuronal connectivity in primates. *Proceedings of the National Academy of Sciences of the United States of America, 106,* 19551-19556.

Campi, K. L., Bales, K. L., Grunewald, R., & Krubitzer, L. (2010). Connections of auditory and visual cortex in the prairie vole (Microtus ochrogaster): Evidence for multisensory processing in primary sensory areas. *Cerebral Cortex, 20,* 89-108.

Cappe, C., Rouiller, E. M., & Barone, P. (2009). Multisensory anatomical pathways. *Hearing Research, 258,* 28-36.

Cardinali, L., Brozzoli, C., & Farne, A. (2009). Peripersonal space and body schema: Two labels for the same concept? *Brain Topography, 21,* 252-260.

Carvell, G. E., & Simons, D. J. (1990). Biometric analyses of vibrissal tactile discrimination in the rat. *Journal of Neuroscience, 10,* 2638-2648.

Castro-Alamancos, M. A. (2002). Properties of primary sensory (lemniscal) synapses in the ventrobasal thalamus and the relay of high-frequency sensory inputs. *Journal of Neurophysiology, 87,* 946-953.

Charbonneau, V., Laramee, M. E., Boucher, V., Bronchti, G., & Boire, D. (2012). Cortical and subcortical projections to primary visual cortex in anophthalmic, enucleated and sighted mice. *European Journal of Neuroscience, 36,* 2949-2963.

Childress, D. S. (1973). Powered limb prostheses: Their clinical significance. *IEEE Transactions on Biomedical Engineering, BME-20,* 200-207.

Chung, S., Li, X., & Nelson, S. B. (2002). Short-term depression at thalamocortical synapses contributes to rapid adaptation of cortical sensory responses in vivo. *Neuron, 34,* 437-446.

Clancy, B., Darlington, R. B., & Finlay, B. L. (2001). Translating developmental time across mammalian species. *Neuroscience, 105,* 7-17.

Colonnier, M., & Guillery, R. W. (1964). Synaptic organization in the lateral geniculate nucleus of the monkey. *Zeitschrift für Zellforschung und mikroskopische Anatomie, 62,* 333-355.

Coogan, T. A., & Burkhalter, A. (1990). Conserved patterns of cortico-cortical connections define areal hierarchy in rat visual cortex. *Experimental Brain Research, 80,* 49-53.

Coogan, T. A., & Burkhalter, A. (1993). Hierarchical organization of areas in rat visual cortex. *Journal of Neuroscience, 13,* 3749-3772.

Corneil, B. D., Van, W. M., Munoz, D. P., & Van Opstal, A. J. (2002). Auditory-visual interactions subserving goal-directed saccades in a complex scene. *Journal of Neurophysiology, 88,* 438-454.

Covic, E. N., & Sherman, S. M. (2011). Synaptic properties of connections between the primary and secondary auditory cortices in mice. *Cerebral Cortex, 21,* 2425-2441.

Craig, A. D., Jr., & Burton, H. (1981). Spinal and medullary lamina I projection to nucleus submedius in medial thalamus: A possible pain center. *Journal of Neurophysiology, 45,* 443-466.

Cuevas, I., Plaza, P., Rombaux, P., De Volder, A. G., & Renier, L. (2009). Odour discrimination and identification are improved in early blindness. *Neuropsychologia, 47,* 3079-3083.

De Pasquale, R., & Sherman, S. M. (2011). Synaptic properties of corticocortical connections between the primary and secondary visual cortical areas in the mouse. *Journal of Neuroscience, 31,* 16494-16506.

De Pasquale, R., & Sherman, S. M. (2012). Modulatory effects of metabotropic glutamate receptors on local cortical circuits. *Journal of Neuroscience, 32,* 7364-7372.

Despres, O., Candas, V., & Dufour, A. (2005). Spatial auditory compensation in early-blind humans: Involvement of eye movements and/or attention orienting? *Neuropsychologia, 43,* 1955-1962.

Diederich, A., Colonius, H., Bockhorst, D., & Tabeling, S. (2003). Visual-tactile spatial interaction in saccade generation. *Experimental Brain Research, 148,* 328-337.

Driver, J., & Noesselt, T. (2008). Multisensory interplay reveals crossmodal influences on 'sensory-specific' brain regions, neural responses, and judgments. *Neuron, 57,* 11-23.

Ehrsson, H. H., Rosen, B., Stockselius, A., Ragno, C., Kohler, P., & Lundborg, G. (2008). Upper limb amputees can be induced to experience a rubber hand as their own. *Brain, 131,* 3443-3452.

Ehrsson, H. H., Spence, C., & Passingham, R. E. (2004). That's my hand! Activity in premotor cortex reflects feeling of ownership of a limb. *Science, 305,* 875-877.

Feig, S., & Harting, J. K. (1998). Corticocortical communication via the thalamus: Ultrastructural studies of corticothalamic projections from area 17 to the lateral posterior nucleus of the cat and inferior pulvinar nucleus of the owl monkey. *Journal of Comparative Neurology, 395,* 281-295.

Felleman, D. J., & Van Essen, D. C. (1991). Distributed hierarchical processing in the primate cerebral cortex. *Cerebral Cortex, 1,* 1-47.

Fieger, A., Roder, B., Teder-Salejarvi, W., Hillyard, S. A., & Neville, H. J. (2006). Auditory spatial tuning in late-onset blindness in humans. *Journal of Cognitive Neuroscience, 18,* 149-157.

Forster, B., Cavina-Pratesi, C., Aglioti, S. M., & Berlucchi, G. (2002). Redundant target effect and intersensory facilitation from visual-tactile interactions in simple reaction time. *Experimental Brain Research, 143,* 480-487.

Frassinetti, F., Bolognini, N., & Ladavas, E. (2002). Enhancement of visual perception by crossmodal visuo-auditory interaction. *Experimental Brain Research, 147,* 332-343.

Frens, M. A., Van Opstal, A. J., & Van der Willigen, R. F. (1995). Spatial and temporal factors determine auditory-visual interactions in human saccadic eye movements. *Attention Perception, & Psychophysics, 57,* 802-816.

Fujii, T., Tanabe, H. C., Kochiyama, T., & Sadato, N. (2009). An investigation of cross-modal plasticity of effective connectivity in the blind by dynamic causal modeling of functional MRI data. *Neurosciences Research, 65,* 175-186.

Ghazanfar, A. A., & Schroeder, C. E. (2006). Is neocortex essentially multisensory? *Trends in Cognitive Sciences, 10,* 278-285.

Giard, M. H., & Peronnet, F. (1999). Auditory-visual integration during multimodal object recognition in humans: A behavioral and electrophysiological study. *Journal of Cognitive Neuroscience, 11,* 473-490.

Goldenberg, G., & Spatt, J. (2009). The neural basis of tool use. *Brain, 132,* 1645-1655.

Gori, M., Del, V. M., Sandini, G., & Burr, D. C. (2008). Young children do not integrate visual and haptic form information. *Current Biology, 18,* 694-698.

Gori, M., Sandini, G., & Burr, D. (2012). Development of visuo-auditory integration in space and time. *Frontiers in Integrative Neurosciences, 6,* 77.

Gougoux, F., Lepore, F., Lassonde, M., Voss, P., Zatorre, R. J., & Belin, P. (2004). Neuropsychology: Pitch discrimination in the early blind. *Nature, 430,* 309.

Gougoux, F., Zatorre, R. J., Lassonde, M., Voss, P., & Lepore, F. (2005). A functional neuroimaging study of sound localization: Visual cortex activity predicts performance in early-blind individuals. *PLoS Biol, 3,* e27.

Graziano, M. S., Cooke, D. F., & Taylor, C. S. (2000). Coding the location of the arm by sight. *Science, 290,* 1782-1786.

Gregory, R. L. (1970). *The Intelligent Eye*. London: Weidenfeld & Nicolson.

Grossberg, S. (1980). How does a brain build a cognitive code? *Psychological Review, 87,* 1-51.

Guénard, H. (1996). *Physiologie humaine* (2e éd.). Paris : Pradel.

Guillery, R. W. (1969). The organization of synaptic interconnections in the laminae of the dorsal lateral geniculate nucleus of the cat. *Zeitschrift für Zellforschung und mikroskopische Anatomie, 96,* 1-38.

Hajdu, F., Hassler, R., & Somogyi, G. (1982). Neuronal and synaptic organization of the lateral geniculate nucleus of the tree shrew, Tupaia glis. *Cell and Tissue Research, 224,* 207-223.

Harrington, L. K., & Peck, C. K. (1998). Spatial disparity affects visual-auditory interactions in human sensorimotor processing. *Experimental Brain Research, 122,* 247-252.

Harris, K. M., & Sultan, P. (1995). Variation in the number, location and size of synaptic vesicles provides an anatomical basis for the nonuniform probability of release at hippocampal CA1 synapses. *Neuropharmacology, 34,* 1387-1395.

Henschke, J. U., Noesselt, T., Scheich, H., & Budinger, E. (2014). Possible anatomical pathways for short-latency multisensory integration processes in primary sensory cortices. *Brain Structure and Function.*

Hilgetag, C. C., O'Neill, M. A., & Young, M. P. (2000). Hierarchical organization of macaque and cat cortical sensory systems explored with a novel network processor. *Philosophical Transactions of the Royal Society of London B: Biological Sciences, 355,* 71-89.

Hoefer, M., Tyll, S., Kanowski, M., Brosch, M., Schoenfeld, M. A., Heinze, H. J. et al. (2013). Tactile stimulation and hemispheric asymmetries modulate auditory perception and neural responses in primary auditory cortex. *Neuroimage, 79,* 371-382.

Hollensteiner, K. J., Pieper, F., Engler, G., Konig, P., & Engel, A. K. (2015). Crossmodal integration improves sensory detection thresholds in the ferret. *PLoS.One., 10,* e0124952.

Hoogland, P. V., Wouterlood, F. G., Welker, E., & Van der Loos, H. (1991). Ultrastructure of giant and small thalamic terminals of cortical origin: A study of the projections from the barrel cortex in mice using Phaseolus vulgaris leuco-agglutinin (PHA-L). *Experimental Brain Research, 87,* 159-172.

Horn, G., & Hill, R. M. (1966). Responsiveness to sensory stimulation of units in the superior colliculus and subjacent tectotegmental regions of the rabbit. *Experimental Neurology, 14,* 199-223.

Huberman, A. D., & Niell, C. M. (2011). What can mice tell us about how vision works? *Trends in Neurosciences, 34,* 464-473.

Hughes, H. C., Reuter-Lorenz, P. A., Nozawa, G., & Fendrich, R. (1994). Visual-auditory interactions in sensorimotor processing: Saccades versus manual responses. *Journal of Experimental Psychology: Human perception and performance, 20,* 131-153.

Ichida, J. M., & Casagrande, V. A. (2002). Organization of the feedback pathway from striate cortex (V1) to the lateral geniculate nucleus (LGN) in the owl monkey (Aotus trivirgatus). *Journal of Comparative Neurology, 454,* 272-283.

Innocenti, G. M., Vercelli, A., & Caminiti, R. (2014). The diameter of cortical axons depends both on the area of origin and target. *Cerebral Cortex, 24,* 2178-2188.

Iriki, A., Tanaka, M., & Iwamura, Y. (1996). Coding of modified body schema during tool use by macaque postcentral neurones. *Neuroreport, 7,* 2325-2330.

Iurilli, G., Ghezzi, D., Olcese, U., Lassi, G., Nazzaro, C., Tonini, R., ... Medini, P. (2012). Sound-driven synaptic inhibition in primary visual cortex. *Neuron, 73,* 814-828.

Jiang, X., Johnson, R. R., & Burkhalter, A. (1993). Visualization of dendritic morphology of cortical projection neurons by retrograde axonal tracing. *Journal of Neuroscience Methods, 50,* 45-60.

Jones, E. G., & Powell, T. P. (1970). An anatomical study of converging sensory pathways within the cerebral cortex of the monkey. *Brain, 93,* 793-820.

Kaas, J. H., & Collins, C. E. (2013). The resurection of multisensory cortex in primates: Connection patterns that integrate modalities. Dans G. A. Calvert, C. Spence, & B. E. Stein (Éds), *The handbook of multisensory processes* (pp. 285-293). Cambridge: The MIT Press.

Karlen, S. J., Kahn, D. M., & Krubitzer, L. (2006). Early blindness results in abnormal corticocortical and thalamocortical connections. *Neuroscience, 142,* 843-858.

Katz, L. C., & Shatz, C. J. (1996). Synaptic activity and the construction of cortical circuits. *Science, 274,* 1133-1138.

Kayser, C., Petkov, C. I., Augath, M., & Logothetis, N. K. (2005). Integration of touch and sound in auditory cortex. *Neuron, 48,* 373-384.

Kayser, C., Petkov, C. I., Augath, M., & Logothetis, N. K. (2007). Functional imaging reveals visual modulation of specific fields in auditory cortex. *Journal of Neuroscience, 27,* 1824-1835.

Kennedy, H., Bullier, J., & Dehay, C. (1989). Transient projection from the superior temporal sulcus to area 17 in the newborn macaque monkey. *Proceedings of the National Academy of Sciences of the United States of America, 86,* 8093-8097.

Kennett, S., Taylor-Clarke, M., & Haggard, P. (2001). Noninformative vision improves the spatial resolution of touch in humans. *Current Biology, 11,* 1188-1191.

Kenngott, H. G., Fischer, L., Nickel, F., Rom, J., Rassweiler, J., & Muller-Stich, B. P. (2012). Status of robotic assistance--a less traumatic and more accurate minimally invasive surgery? *Langenbecks Archives of Surgery, 397,* 333-341.

Kleinfeld, D., Ahissar, E., & Diamond, M. E. (2006). Active sensation: Insights from the rodent vibrissa sensorimotor system. *Current Opinion in Neurobiology, 16,* 435-444.

Klinge, C., Eippert, F., Roder, B., & Buchel, C. (2010). Corticocortical connections mediate primary visual cortex responses to auditory stimulation in the blind. *Journal of Neuroscience, 30,* 12798-12805.

Kobbert, C., Apps, R., Bechmann, I., Lanciego, J. L., Mey, J., & Thanos, S. (2000). Current concepts in neuroanatomical tracing. *Progress in Neurobiology, 62,* 327-351.

Kosslyn, S. M., Thompson, W. L., Kim, I. J., & Alpert, N. M. (1995). Topographical representations of mental images in primary visual cortex. *Nature, 378,* 496-498.

Kraemer, D. J., Macrae, C. N., Green, A. E., & Kelley, W. M. (2005). Musical imagery: Sound of silence activates auditory cortex. *Nature, 434,* 158.

Ladavas, E., & Serino, A. (2008). Action-dependent plasticity in peripersonal space representations. *Cognitive Neuropsychology, 25,* 1099-1113.

Laing, R. J., Bock, A. S., Lasiene, J., & Olavarria, J. F. (2012). Role of retinal input on the development of striate-extrastriate patterns of connections in the rat. *Journal of Comparative Neurology, 520,* 3256-3276.

Lanciego, J. L., & Wouterlood, F. G. (2011). A half century of experimental neuroanatomical tracing. *Journal of Chemical.Neuroanatomy, 42,* 157-183.

Laramée, M. E., Kurotani, T., Rockland, K. S., Bronchti, G., & Boire, D. (2011). Indirect pathway between the primary auditory and visual cortices through layer V pyramidal neurons in V2L in mouse and the effects of bilateral enucleation. *European Journal of Neuroscience, 34,* 65-78.

Larsen, D. D., Luu, J. D., Burns, M. E., & Krubitzer, L. (2009). What are the effects of severe visual impairment on the cortical organization and connectivity of primary visual cortex? *Frontiers Neuroanatomy, 3,* 30.

Le, B. D., Turner, R., Zeffiro, T. A., Cuenod, C. A., Jezzard, P., & Bonnerot, V. (1993). Activation of human primary visual cortex during visual recall: A magnetic resonance imaging study. *Proceedings of the National Academy of Sciences of the United States of America, 90,* 11802-11805.

Lee, C. C., & Sherman, S. M. (2008). Synaptic properties of thalamic and intracortical inputs to layer 4 of the first- and higher-order cortical areas in the auditory and somatosensory systems. *Journal of Neurophysiology, 100,* 317-326.

Lee, C. C., & Sherman, S. M. (2009a). Modulator property of the intrinsic cortical projection from layer 6 to layer 4. *Frontiers in Systems Neuroscience., 3,* 3.

Lee, C. C., & Sherman, S. M. (2009b). Glutamatergic inhibition in sensory neocortex. *Cerebral Cortex, 19,* 2281-2289.

Lee, C. C., & Sherman, S. M. (2010). Topography and physiology of ascending streams in the auditory tectothalamic pathway. *Proceedings of the National Academy of Sciences of the United States of America, 107,* 372-377.

Lee, T. S., & Mumford, D. (2003). Hierarchical Bayesian inference in the visual cortex. *Journal of the Optical Society of America. Part A, Optics, Image Science and Vision, 20,* 1434-1448.

Lessard, N., Pare, M., Lepore, F., & Lassonde, M. (1998). Early-blind human subjects localize sound sources better than sighted subjects. *Nature, 395,* 278-280.

Li, J., Guido, W., & Bickford, M. E. (2003). Two distinct types of corticothalamic EPSPs and their contribution to short-term synaptic plasticity. *Journal of Neurophysiology, 90,* 3429-3440.

Li, J., Wang, S., & Bickford, M. E. (2003). Comparison of the ultrastructure of cortical and retinal terminals in the rat dorsal lateral geniculate and lateral posterior nuclei. *Journal of Comparative Neurology, 460,* 394-409.

Liu, Y., Yu, C., Liang, M., Li, J., Tian, L., Zhou, Y., ... Jiang, T. (2007). Whole brain functional connectivity in the early blind. *Brain, 130,* 2085-2096.

Llinas, R. R., & Pare, D. (1991). Of dreaming and wakefulness. *Neuroscience, 44,* 521-535.

Longo, M. R., Schuur, F., Kammers, M. P., Tsakiris, M., & Haggard, P. (2008). What is embodiment? A psychometric approach. *Cognition, 107,* 978-998.

Lovelace, C. T., Stein, B. E., & Wallace, M. T. (2003). An irrelevant light enhances auditory detection in humans: A psychophysical analysis of multisensory integration in stimulus detection. *Cognitive Brain Research, 17,* 447-453.

Luppi, P. H., Fort, P., & Jouvet, M. (1990). Iontophoretic application of unconjugated cholera toxin B subunit (CTb) combined with immunohistochemistry of neurochemical substances: A method for transmitter identification of retrogradely labeled neurons. *Brain Research, 534,* 209-224.

Luppi, P. H., Sakai, K., Salvert, D., Fort, P., & Jouvet, M. (1987). Peptidergic hypothalamic afferents to the cat nucleus raphe pallidus as revealed by a double immunostaining technique using unconjugated cholera toxin as a retrograde tracer. *Brain Research, 402,* 339-345.

Macaluso, E. (2006). Multisensory processing in sensory-specific cortical areas. *Neuroscientist, 12,* 327-338.

Maravita, A. (2006). *From body in the brain, to body in space: Sensory and intentional aspects of body representation.* New York, NY: Oxford University Press..

Maravita, A., & Iriki, A. (2004). Tools for the body (schema). *Trends in Cognitive Sciences, 8,* 79-86.

Marik, S. A., Yamahachi, H., McManus, J. N., Szabo, G., & Gilbert, C. D. (2010). Axonal dynamics of excitatory and inhibitory neurons in somatosensory cortex. *PLoS Biol, 8,* e1000395.

Marik, S. A., Yamahachi, H., Meyer zum Alten, B. S., & Gilbert, C. D. (2014). Large-scale axonal reorganization of inhibitory neurons following retinal lesions. *Journal of Neuroscience, 34,* 1625-1632.

Markov, N. T., Vezoli, J., Chameau, P., Falchier, A., Quilodran, R., Huissoud, C. et al. (2014). Anatomy of hierarchy: Feedforward and feedback pathways in macaque visual cortex. *Journal of Comparative Neurology, 522,* 225-259.

Masse, I. O., Ross, S., Bronchti, G., & Boire, D. (2016). Asymmetric direct reciprocal connections between primary visual and somatosensory cortices of the mouse. *Cerebral Cortex*.

Merabet, L. B., & Pascual-Leone, A. (2010). Neural reorganization following sensory loss: The opportunity of change. *Nature Reviews Neuroscience, 11,* 44-52.

Meredith, M. A., & Lomber, S. G. (2016). Species-dependent role of crossmodal connectivity among the primary sensory cortices. *Hearing Research, 343,* 83-91.

Mesulam, M. M. (1998). From sensation to cognition. *Brain, 121,* 1013-1052.

Miletic, V., & Coffield, J. A. (1989). Responses of neurons in the rat nucleus submedius to noxious and innocuous mechanical cutaneous stimulation. *Somatosensory and Motor Research, 6,* 567-587.

Moizumi, S., Yamamoto, S., & Kitazawa, S. (2007). Referral of tactile stimuli to action points in virtual reality with reaction force. *Neuroscience Research, 59,* 60-67.

Molholm, S., Ritter, W., Murray, M. M., Javitt, D. C., Schroeder, C. E., & Foxe, J. J. (2002). Multisensory auditory-visual interactions during early sensory processing in humans: A high-density electrical mapping study. *Cognitive Brain Research, 14,* 115-128.

Moller, A. R. (2003). *Sensory systems: Anatomy and physiology* (1re éd.). San Diego, USA: Academic Press.

Morest, D. K. (1975). Synaptic relationships of Golgi type II cells in the medial geniculate body of the cat. *Journal of Comparative Neurology, 162,* 157-193.

Naber, P. A., Witter, M. P., & Lopes da Silva, F. H. (2000). Differential distribution of barrel or visual cortex. Evoked responses along the rostro-caudal axis of the peri- and postrhinal cortices. *Brain Research, 877,* 298-305.

Nieuwenhuys, R., Voogd, J., & Van Juijzen, C. (2008). *The human central nervous system: A symposis and atlas.* (4e éd.) Berlin Heidelberg, Allemagne: Springer-Verlag.

Noesselt, T., Tyll, S., Boehler, C. N., Budinger, E., Heinze, H. J., & Driver, J. (2010). Sound-induced enhancement of low-intensity vision: Multisensory influences on human sensory-specific cortices and thalamic bodies relate to perceptual enhancement of visual detection sensitivity. *Journal of Neuroscience, 30,* 13609-13623.

Octavia, J. R., Raymaekers, C., & Coninx, K. (2011). Adaptation in virtual environments: Conceptual framework and user models. *Multimedia Tools and Applications, 54,* 121-142.

Oztas, E. (2003). Neuronal tracing. *Neuroanatomy, 2,* 2-5.

Paperna, T., & Malach, R. (1991). Patterns of sensory intermodality relationships in the cerebral cortex of the rat. *Journal of Comparative Neurology, 308,* 432-456.

Pascual-Leone, A., & Hamilton, R. (2001). The metamodal organization of the brain. *Progress in Brain Research, 134,* 427-445.

Pavani, F., Spence, C., & Driver, J. (2000). Visual capture of touch: out-of-the-body experiences with rubber gloves. *Psychological Science, 11,* 353-359.

Peeters, R., Simone, L., Nelissen, K., Fabbri-Destro, M., Vanduffel, W., Rizzolatti, G., ... Orban, G. A. (2009). The representation of tool use in humans and monkeys: Common and uniquely human features. *Journal of Neuroscience, 29,* 11523-11539.

Peters, A., & Palay, S. L. (1966). The morphology of laminae A and A1 of the dorsal nucleus of the lateral geniculate body of the cat. *Journal of Anatomy, 100,* 451-486.

Petrof, I., & Sherman, S. M. (2013). Functional significance of synaptic terminal size in glutamatergic sensory pathways in thalamus and cortex. *Journal of Physiology, 591,* 3125-3131.

Pierce, J. P., & Lewin, G. R. (1994). An ultrastructural size principle. *Neuroscience, 58,* 441-446.

Price, D. J., Kennedy, H., Dehay, C., Zhou, L., Mercier, M., Jossin, Y., ... Molnárz, Z. (2006). The development of cortical connections. *European Journal of Neuroscience, 23,* 910-920.

Prusky, G. T., West, P. W., & Douglas, R. M. (2000). Behavioral assessment of visual acuity in mice and rats. *Vision Research, 40,* 2201-2209.

Ralston, H. J., III (1969). The synaptic organization of lemniscal projections to the ventrobasal thalamus of the cat. *Brain Research, 14,* 99-115.

Rassweiler, J., Safi, K. C., Subotic, S., Teber, D., & Frede, T. (2005). Robotics and telesurgery--an update on their position in laparoscopic radical prostatectomy. *Minimally Invasive Therapy & Allied Technologies, 14,* 109-122.

Rauschecker, J. P. (1995). Compensatory plasticity and sensory substitution in the cerebral cortex. *Trends in Neurosciences, 18,* 36-43.

Reichova, I., & Sherman, S. M. (2004). Somatosensory corticothalamic projections: Distinguishing drivers from modulators. *Journal of Neurophysiology, 92,* 2185-2197.

Reid, A. T., Krumnack, A., Wanke, E., & Kotter, R. (2009). Optimization of cortical hierarchies with continuous scales and ranges. *Neuroimage., 47,* 611-617.

Reiner, A., Veenman, C. L., Medina, L., Jiao, Y., Del, M. N., & Honig, M. G. (2000). Pathway tracing using biotinylated dextran amines. *Journal of Neuroscience Methods, 103,* 23-37.

Reyes, A., Lujan, R., Rozov, A., Burnashev, N., Somogyi, P., & Sakmann, B. (1998). Target-cell-specific facilitation and depression in neocortical circuits. *Nature Neuroscience., 1,* 279-285.

Rizzolatti, G., Fadiga, L., Fogassi, L., & Gallese, V. (1997). The space around us. *Science, 277,* 190-191.

Rizzolatti, G., Scandolara, C., Matelli, M., & Gentilucci, M. (1981a). Afferent properties of periarcuate neurons in macaque monkeys. I. Somatosensory responses. *Behavioural Brain Research, 2,* 125-146.

Rizzolatti, G., Scandolara, C., Matelli, M., & Gentilucci, M. (1981b). Afferent properties of periarcuate neurons in macaque monkeys. II. Visual responses. *Behavioural Brain Research, 2,* 147-163.

Rochat, P. (1998). Self-perception and action in infancy. *Experimental Brain Research, 123,* 102-109.

Rockland, K. S., & Pandya, D. N. (1979). Laminar origins and terminations of cortical connections of the occipital lobe in the rhesus monkey. *Brain Research, 179,* 3-20.

Roder, B., Teder-Salejarvi, W., Sterr, A., Rosler, F., Hillyard, S. A., & Neville, H. J. (1999). Improved auditory spatial tuning in blind humans. *Nature, 400,* 162-166.

Rodgers, K. M., Benison, A. M., Klein, A., & Barth, D. S. (2008). Auditory, somatosensory, and multisensory insular cortex in the rat. *Cerebral Cortex, 18,* 2941-2951.

Rosen, J., Hannaford, B., & Satava, R. (2011). *Surgical robotics: Systems applications and visions*. London: Springer.

Rosenbluth, R., Grossman, E. S., & Kaitz, M. (2000). Performance of early-blind and sighted children on olfactory tasks. *Perception, 29,* 101-110.

Rouiller, E. M., & Welker, E. (1991). Morphology of corticothalamic terminals arising from the auditory cortex of the rat: A Phaseolus vulgaris-leucoagglutinin (PHA-L) tracing study. *Hearing Research., 56,* 179-190.

Rouiller, E. M., & Welker, E. (2000). A comparative analysis of the morphology of corticothalamic projections in mammals. *Brain Research Bulletin, 53,* 727-741.

Sawchenko, P. E., & Gerfen, G. R. (1985). Plant lectins and bacterial toxins as tools for tracing neuronal connections. *Trends in Neurosciences, 8,* 378-384.

Schaefer, M., Flor, H., Heinze, H. J., & Rotte, M. (2007). Morphing the body: Illusory feeling of an elongated arm affects somatosensory homunculus. *Neuroimage., 36,* 700-705.

Schaefer, M., Heinze, H. J., & Rotte, M. (2012). Close to you: Embodied simulation for peripersonal space in primary somatosensory cortex. *PLoS One, 7,* e42308.

Scheich, H., Brechmann, A., Brosch, M., Budinger, E., & Ohl, F. W. (2007). The cognitive auditory cortex: Task-specificity of stimulus representations. *Hearing Research., 229,* 213-224.

Schikorski, T., & Stevens, C. F. (1997). Quantitative ultrastructural analysis of hippocampal excitatory synapses. *Journal of Neuroscience, 17,* 5858-5867.

Schikorski, T., & Stevens, C. F. (1999). Quantitative fine-structural analysis of olfactory cortical synapses. *Proceedings of the National Academy of Sciences of the United States of America, 96,* 4107-4112.

Schroeder, C. E., Smiley, J., Fu, K. G., McGinnis, T., O'Connell, M. N., & Hackett, T. A. (2003). Anatomical mechanisms and functional implications of multisensory convergence in early cortical processing. *Int J Psychophysiol, 50,* 5-17.

Sengul, A., Rognini, G., van, E. M., Aspell, J. E., Bleuler, H., & Blanke, O. (2013). Force feedback facilitates multisensory integration during robotic tool use. *Experimental Brain Research, 227,* 497-507.

Sengul, A., van, E. M., Rognini, G., Aspell, J. E., Bleuler, H., & Blanke, O. (2012). Extending the body to virtual tools using a robotic surgical interface: Evidence from the crossmodal congruency task. *PLoS.One., 7,* e49473.

Shams, L., & Beierholm, U. R. (2010). Causal inference in perception. *Trends in Cognitive Sciences, 14,* 425-432.

Sherman, S. M., & Guillery, R. W. (1996). Functional organization of thalamocortical relays. *Journal of Neurophysiology, 76,* 1367-1395.

Sherman, S. M., & Guillery, R. W. (1998). On the actions that one nerve cell can have on another: Distinguishing "drivers" from "modulators". *Proceedings of the National Academy of Sciences of the United States of America, 95,* 7121-7126.

Sherman, S. M., & Guillery, R. W. (2006). *Exploring the thalamus and its role in cortical function.* Cambridge MA: MIT Press.

Sherman, S. M., & Guillery, R. W. (2013a). *Functional connections of cortical areas. A new view from the thalamus.* Cambridge, Massachussetts; London, England: MIT Press.

Sherman, S. M., & Guillery, R. W. (2013b). *Functional connections of cortical areas.* Cambridge, Massachussetts; London, England: MIT Press.

Shimada, S., Fukuda, K., & Hiraki, K. (2009). Rubber hand illusion under delayed visual feedback. *PLoS.One., 4,* e6185.

Sieben, K., Bieler, M., Roder, B., & Hanganu-Opatz, I. L. (2015). Neonatal restriction of tactile inputs leads to long-lasting impairments of cross-modal processing. *PLoS Biol, 13,* e1002304.

Sieben, K., Roder, B., & Hanganu-Opatz, I. L. (2013). Oscillatory entrainment of primary somatosensory cortex encodes visual control of tactile processing. *Journal of Neuroscience, 33,* 5736-5749.

Slater, M., Spanlang, B., Sanchez-Vives, M. V., & Blanke, O. (2010). First person experience of body transfer in virtual reality. *PLoS One, 5,* e10564.

So, K. F., Campbell, G., & Lieberman, A. R. (1985). Synaptic organization of the dorsal lateral geniculate nucleus in the adult hamster. An electron microscope study using degeneration and horseradish peroxidase tracing techniques. *Anatomy and Embryology (Berl), 171,* 223-234.

Stein, B. E., Huneycutt, W. S., & Meredith, M. A. (1988). Neurons and behavior: The same rules of multisensory integration apply. *Brain Research, 448,* 355-358.

Stein, B. E., Meredith, M. A., Huneycutt, W. S., & McDade, L. (1989). Behavioral indices of multisensory integration: Orientation to visual cues is affected by auditory stimuli. *Journal of Cognitive Neuroscience, 1,* 12-24.

Stein, B. E., Stanford, T. R., & Rowland, B. A. (2014). Development of multisensory integration from the perspective of the individual neuron. *Nature Review Neurosciences, 15,* 520-535.

Stevens, A. A., & Weaver, K. (2005). Auditory perceptual consolidation in early-onset blindness. *Neuropsychologia, 43,* 1901-1910.

Stoeckel, K., Schwab, M., & Thoenen, H. (1977). Role of gangliosides in the uptake and retrograde axonal transport of cholera and tetanus toxin as compared to nerve growth factor and wheat germ agglutinin. *Brain Research, 132,* 273-285.

Stone, R. (2000). Haptic feedback: A potted history, from telepresence to virtual reality. *Springer,* 1-7.

Suematsu, Y., & del Nido, P. J. (2004). Robotic pediatric cardiac surgery: Present and future perspectives. *The American Journal of Surgery, 188,* 98S-103S.

Szentagothai, J. (1963). The structure of the synapse in the lateral geniculate body. *Acta Anatomica (Basel), 55,* 166-185.

Tavakoli, M., Aziminejad, A., Patel, R. V., & Moallem, M. (2007). High-fidelity bilateral teleoperation systems and the effect of multimodal haptics. *IEEE Transactions on Systems, Man, and Cybernetics - Part B: Cybernetics, 37,* 1512-1528.

Teder-Salejarvi, W. A., McDonald, J. J., Di, R. F., & Hillyard, S. A. (2002). An analysis of audio-visual crossmodal integration by means of event-related potential (ERP) recordings. *Cognitive Brain Research, 14,* 106-114.

Tomasi, S., Caminiti, R., & Innocenti, G. M. (2012). Areal differences in diameter and length of corticofugal projections. *Cerebral Cortex, 22,* 1463-1472.

Tononi, G., & Koch, C. (2008). The neural correlates of consciousness: An update. *Annals of the New York Academy of Sciences, 1124,* 239-261.

Tsakiris, M., & Haggard, P. (2005). The rubber hand illusion revisited: Visuotactile integration and self-attribution. *Journal of Experimental Psychology: Human Perception and Performance, 31,* 80-91.

Van Boven, R. W., Hamilton, R. H., Kauffman, T., Keenan, J. P., & Pascual-Leone, A. (2000). Tactile spatial resolution in blind braille readers. *Neurology, 54,* 2230-2236.

van den Bos, E., & Jeannerod, M. (2002). Sense of body and sense of action both contribute to self-recognition. *Cognition, 85,* 177-187.

Van Horn, S. C., Erisir, A., & Sherman, S. M. (2000). Relative distribution of synapses in the A-laminae of the lateral geniculate nucleus of the cat. *Journal of Comparative Neurology, 416,* 509-520.

Van Horn, S. C., & Sherman, S. M. (2004). Differences in projection patterns between large and small corticothalamic terminals. *Journal of Comparative Neurology, 475,* 406-415.

Veenman, C. L., Reiner, A., & Honig, M. G. (1992). Biotinylated dextran amine as an anterograde tracer for single- and double-labeling studies. *Journal of Neuroscience Methods, 41,* 239-254.

Vercelli, A., Repici, M., Garbossa, D., & Grimaldi, A. (2000). Recent techniques for tracing pathways in the central nervous system of developing and adult mammals. *Brain Research Bulletin, 51,* 11-28.

Vezoli, J., Falchier, A., Jouve, B., Knoblauch, K., Young, M., & Kennedy, H. (2004). Quantitative analysis of connectivity in the visual cortex: extracting function from structure. *Neuroscientist, 10,* 476-482.

Viaene, A. N., Petrof, I., & Sherman, S. M. (2011a). Synaptic properties of thalamic input to layers 2/3 and 4 of primary somatosensory and auditory cortices. *Journal of Neurophysiology, 105,* 279-292.

Viaene, A. N., Petrof, I., & Sherman, S. M. (2011b). Synaptic properties of thalamic input to the subgranular layers of primary somatosensory and auditory cortices in the mouse. *Journal of Neuroscience, 31,* 12738-12747.

Viaene, A. N., Petrof, I., & Sherman, S. M. (2011c). Properties of the thalamic projection from the posterior medial nucleus to primary and secondary somatosensory cortices in the mouse. *Proceedings of the National Academy of Sciences of the United States of America, 108,* 18156-18161.

Vidnyanszky, Z., Borostyankoi, Z., Gorcs, T. J., & Hamori, J. (1996). Light and electron microscopic analysis of synaptic input from cortical area 17 to the lateral posterior nucleus in cats. *Experimental Brain Research, 109,* 63-70.

Voss, P., Gougoux, F., Zatorre, R. J., Lassonde, M., & Lepore, F. (2008). Differential occipital responses in early- and late-blind individuals during a sound-source discrimination task. *Neuroimage, 40,* 746-758.

Voss, P., Lassonde, M., Gougoux, F., Fortin, M., Guillemot, J. P., & Lepore, F. (2004). Early- and late-onset blind individuals show supra-normal auditory abilities in far-space. *Current Biology, 14,* 1734-1738.

Wallace, M. T., Ramachandran, R., & Stein, B. E. (2004). A revised view of sensory cortical parcellation. *Proceedings of the National Academy of Sciences of the United States of America, 101,* 2167-2172.

Wan, C. Y., Wood, A. G., Reutens, D. C., & Wilson, S. J. (2010). Congenital blindness leads to enhanced vibrotactile perception. *Neuropsychologia, 48,* 631-635.

Wang, Q., & Burkhalter, A. (2007). Area map of mouse visual cortex. *Journal of Comparative Neurology, 502,* 339-357.

Wang, S., Eisenback, M. A., & Bickford, M. E. (2002). Relative distribution of synapses in the pulvinar nucleus of the cat: Implications regarding the "driver/modulator" theory of thalamic function. *Journal of Comparative Neurology, 454,* 482-494.

Welch, R. B., & Warren, D. H. (1986). Intersensory interactions. Dans K. R. Boff, L. Kaufman, & J. P. Thomas (Éds), *Handbook of perception and human performance* (pp. 25-1-25-36). New York, NY: J. Wiley.

Whishaw, I. Q., & Kolb, B. (2004). *The Behavior of the Laboratory Rat: A Handbook with Tests* (1re éd.). New York, NY: Oxford University Press.

Witten, I. B., & Knudsen, E. I. (2005). Why seeing is believing: Merging auditory and visual worlds. *Neuron, 48,* 489-496.

Woolsey, T. A., & Van der Loos, H. (1970). The structural organization of layer IV in the somatosensory region (SI) of mouse cerebral cortex. The description of a cortical field composed of discrete cytoarchitectonic units. *Brain Research, 17,* 205-242.

Wu, H. P., Ioffe, J. C., Iverson, M. M., Boon, J. M., & Dyck, R. H. (2013). Novel, whisker-dependent texture discrimination task for mice. *Behavioural Brain Research, 237,* 238-242.

Yoo, S. S., Freeman, D. K., McCarthy, J. J., III, & Jolesz, F. A. (2003). Neural substrates of tactile imagery: A functional MRI study. *Neuroreport, 14,* 581-585.

Yoo, S. S., Lee, C. U., & Choi, B. G. (2001). Human brain mapping of auditory imagery: Event-related functional MRI study. *Neuroreport, 12,* 3045-3049.

Yu, C., Liu, Y., Li, J., Zhou, Y., Wang, K., Tian, L., ... Li, K. (2008). Altered functional connectivity of primary visual cortex in early blindness. *Human Brain Mapping, 29,* 533-543.

Zakiewicz, I. M., Bjaalie, J. G., & Leergaard, T. B. (2014). Brain-wide map of efferent projections from rat barrel cortex. *Frontiers in Neuroinformatics, 8,* 5.

Zembrzycki, A., Chou, S. J., Ashery-Padan, R., Stoykova, A., & O'Leary, D. D. (2013). Sensory cortex limits cortical maps and drives top-down plasticity in thalamocortical circuits. *Nature Neuroscience, 16,* 1060-1067.

Zingg, B., Hintiryan, H., Gou, L., Song, M. Y., Bay, M., Bienkowski, M. S., ... Dong, H. W. (2014). Neural networks of the mouse neocortex. *Cell, 156,* 1096-1111.